

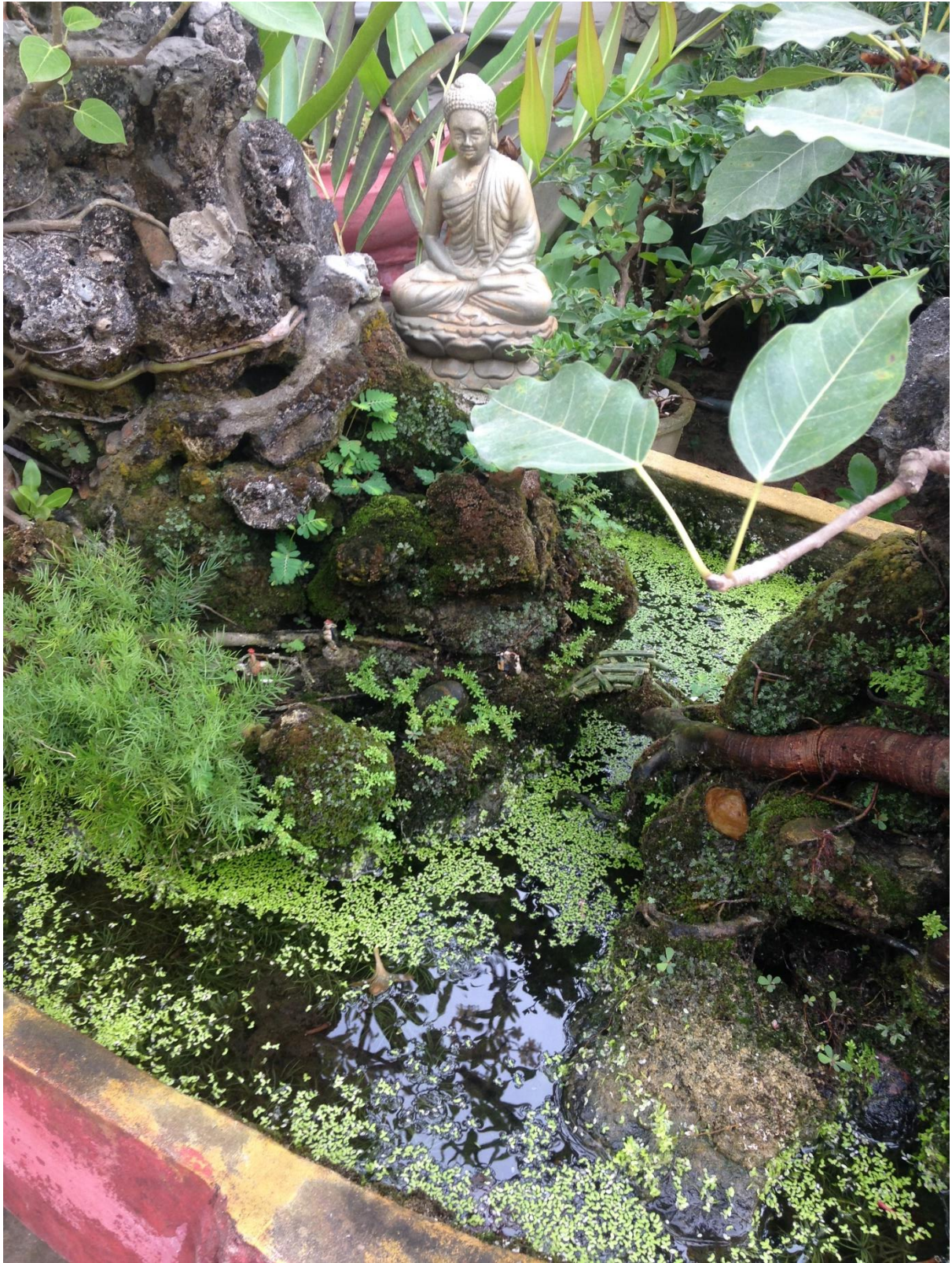
Genetic Control of *Lemna* Growth Rate and Protein Content

Javier Espinosa Montiel, BSc. (Hons), MRSB

Submitted to the University of Hertfordshire in partial fulfilment of the requirements of the degree
of Doctor of Philosophy

School of Life and Medical Sciences, University of Hertfordshire, Hatfield, Hertfordshire, AL10 9AB

December 2024



“An inefficient virus kills its host.

A clever virus stays with it.”

James Lovelock

Abstract

Duckweed (*Lemna* spp.) has emerged as a promising sustainable protein source due to its rapid growth and adaptability to diverse environmental conditions. This thesis investigated the effects of nitrogen availability and temperature on duckweed growth, protein accumulation, and the underlying physiological and molecular mechanisms, aiming to optimize its use for human and animal consumption.

The study began with the establishment of a *Lemna* collection comprising 50 clones sourced globally. A novel method to quantify total nitrogen and nitrate using FT-IR spectroscopy was developed and applied throughout the research. The first experimental phase (Chapter 3) examined how different nitrogen sources—nitrate, Ammonium-Nitrate, Urea-Nitrate, and nitrogen-free—affected growth rate, protein content, and nitrate accumulation. Ammonium treatment significantly reduced growth in some clones due to pH acidification, though clone 7796 maintained higher growth rates under ammonium and Urea-Nitrate treatments. This clone also exhibited the highest protein accumulation across all nitrogen treatments. Expression analysis of eight nitrogen assimilation genes (*NR*, *NiR*, *GS1;1*, *GS1;2*, *GS2*, *CLCa*, *Fd-GOGAT*, and *NADH-GOGAT*) revealed distinct regulation patterns depending on nitrogen source and clone, underscoring the importance of selecting appropriate nitrogen sources to optimize protein yield.

The second experimental phase (Chapter 4) investigated heat stress tolerance in 42 *Lemna* clones (36 *L. gibba* and 6 *L. minor*) collected from diverse geographic regions. Physiological assessments at 20°C and 35°C identified three heat-tolerant clones (6861, 7763, and 7796) and one heat-sensitive clone (8703), with the widely used clone Manor serving as a control. Further testing across a broader temperature range (15°C–35°C) revealed that while all clones exhibited reduced growth at higher temperatures, protein content increased in heat-tolerant clones but declined in the heat-sensitive clone at 35°C.

In the final experimental phase (Chapter 5), transcriptomic analysis provided insights into the molecular mechanisms underlying heat tolerance in the selected five clones. Differential gene expression analyses revealed upregulation of genes involved in photosynthesis (e.g., ATP synthase), zinc ion binding, and stress response pathways in heat-tolerant clones, while these genes were downregulated in the heat-sensitive clone and the control. KEGG and GO pathway enrichment analyses highlighted critical metabolic and regulatory pathways associated with heat resilience.

Together, these findings demonstrate that nitrogen source selection influences duckweed growth and protein accumulation, with clone-specific responses to ammonium availability. Heat-tolerant clones

maintain higher protein levels under elevated temperatures, and their transcriptomic profiles suggest a genetic basis for resilience to heat stress. These results provide valuable insights into optimizing duckweed cultivation under variable environmental conditions, supporting its potential as a sustainable protein source in the context of climate change.

Acknowledgements

First, I would like to thank my supervisory team, a group of three smart scientists who are a clear demonstration of empowered women who can lead the world. Cristina, always kind, trustworthy, welcoming, patient, and always there—anytime and anywhere. I felt like one of the family in her house, a house I miss every day since I left. Yongju, always professional, funny, and positive, a person who always gives you encouraging comments and leads you to improve yourself and become a better person. Alyssa, always supportive, approachable, and humble, creating an atmosphere where you feel comfortable and confident in your work.

I would like to start by thanking my funding bodies, Hertfordshire Local Enterprise and the European Union, for their financial contributions to my research project. I am also grateful to the start-up DryGro for making my placement a wonderful experience. Special thanks to Sean for his leadership and care for his employees, Cawley for his motivation to keep progressing and improving the company, and the plant science team (Conrad, Mary, and Okinji) who helped me understand and love this tiny plant, welcoming me so warmly to the team.

Additionally, I want to thank a group of scientists who showed me how to love science. Javi, the handsome one—not me—whose pure passion for science is unmatched. He was always there to help and one of the most creatively scientific people I will ever meet. A beer talk with him was more inspirational and motivational than 1000 articles. Alla, an incredible mix of botanist and statistician, who always expressed her passion for these fields. Her help during my PhD was key to understanding and organizing my thesis. Bruce, full of knowledge and experience, whose opinion could save you months of work and reveal points you never imagined to be important. I also want to thank the people who gave me the opportunity to start working in the lab and delve deeply into research—Stephan, Cathy, and Gifty. My time working with them was always a pleasure, and I will always miss it. Thanks for giving me the opportunity to start my research career and for your patience and kindness.

I want to thank a key part of my PhD journey—the people who best understood this part of my life, my PhD colleagues. Maca and Gala, who were my best colleagues when starting my PhD journey. Always in a good mood and willing to help me at any time. The best welcoming people I could have ever found in my life that gave me the essentials tips to survive at UH after Covid. Laura, my dear flatmate. Always up for any plan, no matter what. Always there when you need her. I loved cooking for her, and those pizzas at TGF could destroy every stomach in the world. Jacob, my dear bro. I still remember the first time I met him in the Science building. I didn't know then how important he would become in my life. The king of finding alternative plans, I loved how he showed me his childhood through the streets of Kentish Town. Paloma, constantly talking and dreaming, but you just couldn't

stop listening. She has a beautiful and shiny soul that lights up everything around her. Giorgia, one of my first friends when I arrived at UH. She gave me the keys to survive in the building. Always complaining but always helping those she loves.

I would like to thank the members of the University of Hertfordshire Crop and Climate Change research group who provided incredible feedback for my PhD, and the technical team at the Science building who were always there to solve my problems.

A special thanks to the Spanish Researchers Undergraduate Students who came to do their internships with us: Adri, Iskra, María, Lucía, Carlota, Sandra, Celia, Coral, Guille, Sandra, Alejandro, Lucía, Carmen, Antonio, Diego, and Rocío, as well as the students who worked in Cristina's group: Nigel and Nathaniel. They taught me how to teach, and I learned more from them than they did from me. It was a pleasure to welcome you to Hatfield and show you how fun this city could be if you knew where to go.

I want to thank my closest friends now. Antonio, my best friend and the person I miss the most when I'm away. One of the smartest people I've ever met. An example of humility, intelligence, mental strength, critical thinking, a great listener, and an enjoyer of life. Living closer to you now makes my life easier and happier. Leti, my friend since I can remember. Our mums are unaware of the connections they created when my mum saved your brother's life. She is the type of person who always has time to listen and offer perfect advice. She's an example of constant support and a big role model. One of the most charismatic people I've ever met—her LetiPardadas are unique. Eva, pure passion for her loved ones. Always working and busy but always there when called upon. She has a special soul that makes everyone feel comfortable when they are next to her. One of the hardest workers I've ever met, but the one who really knows how to have fun when needed. Maena, I just want to thank her for her incredible knowledge and for showing me how to do everything well. Every drama was minimized with her advice, and she got a piece of my heart in a very short time. I want to thank my London gang, the kindest and funniest people that I met in London. I will always appreciate that I had a plan or a sofa available to me at any time. The Hatfield gang, they were key to my success in my PhD. Always a gate to escape and have fun in Hatfield, and I will always be thankful.

And finally, my family. I just want to give a special thank you to them for always supporting me, while also keeping me humble and teaching me to keep working. Among them, my mum is the most important part of my resilience during the PhD. She is an example of strength and a positive mindset, showing that a solution can always be found and that things are often less problematic than you think. Thanks for giving me life and for keeping me alive all these years.

Lists of Publication and Conferences

Publications

Fat Duckweed (*Lemna gibba*) Might Be Much More Widespread in Hertfordshire Than Previously Thought. Status: Published Co-Authors: Alla Mashanova, Javier Espinosa-Montiel, Cristina Barrero-Sicilia. Journal: Transactions of the Hertfordshire Natural History Society. 54 (1) 2022

International Conference Attendances

II Jornadas Jóvenes Investigadores Barreños – Dec 5th, 2024 – Los Barrios, Spain – Presentation – (Appendices 2A).

I Jornada Jóvenes Investigadores Barreños – Oct 30th, 2023 – Los Barrios, Spain – Presentation – (Appendices 2C).

Sixth International Conference on Duckweed Research and Applications – FT-MIR-PLSR Simultaneous Determination of Total Nitrogen and Nitrate in Duckweeds - May 29th to Jun 1st, 2022 – Gatersleben, Germany – (Appendices 1B), 1C), 3C), and C).

National Conference Attendances

Early career innovators' Forum Conference 2024 – Apr 25th, 2024 – Rothamsted Research, United Kingdom - Attendance.

Association of Applied Biologists Early Career Professional Skills and Science Workshop – Dec 18th and 19th, 2023 – University of Leicester, United Kingdom – Presentation – (Appendices 2B)

Future Agricultural Researchers PhD Conference 2023 – Nov 14th, 2023 – Exeter, United Kingdom – Poster – (Appendices 3A).

SRUK Annual General Assembly 2022 – Jul 3rd, 2022 – Oxford, United Kingdom – Poster – (Appendices 1A).

LMS Annual Research Conference 2022 – Jun 21st, 2022 – Hatfield, United Kingdom – Poster – (Appendices 1D).

Cereals the Arable Event – Jun 8th, 2022 – Duxford, United Kingdom – Attendance – (Appendices 3B).

LMS Annual Research Conference 2022 – Jun 21st, 2022 – Hatfield, United Kingdom – Presentation – (Appendices 2D).

3 Minute Thesis Competition UH – May 5th, 2022 – Hatfield, United Kingdom – Presentation – (Appendices 2E).

University of Hertfordshire Postgraduate Research Conference 2022 – Feb 7th, 2022 – Hatfield, United Kingdom – Presentation – (Appendices 2F).

University of Hertfordshire Postgraduate Research Conference 2021 – Jul 12th, 2021 – Hatfield, United Kingdom – Poster – (Appendices 2G).

Table of Contents

Abstract.....	I
Acknowledgements.....	III
Lists of Publication and Conferences	V
Table of Contents.....	VII
List of Figures	XIII
List of Tables	XVII
List of Equations.....	XVIII
List of Abbreviations	XIX
1. Chapter 1: General Introduction.....	1
1.1. Duckweed, a Tiny Aquatic Plant.....	1
1.1.1. Duckweed Dispersal and Distribution.....	1
1.1.2. Anatomical Features	3
1.1.3. Growth and Reproduction Characteristics.....	8
1.1.4. Genomics of Duckweed	11
1.2. Historical Utilization of Duckweed.....	12
1.3. Duckweed Uses and Biotechnological Applications	14
1.3.1. Duckweed: A Versatile Resource for Biofuel Production.....	14
1.3.2. Environmental Remediation	15
1.3.3. Production of Biopolymers, Biofactories, and Vaccines	16
1.3.4. Implication of Plant Secondary Metabolites.....	17
1.3.5. Human Nutrition and Animal Feed	18
1.4. Duckweed as a Plant-Based Protein Source	19
1.5. Nitrogen Assimilation.....	22
1.6. Environmental Impacts on Duckweed Nutritional Composition	25
1.7. Duckweed Response to Heat Stress.....	27

1.8.	Aims and Objectives of the Project.....	31
2.	Chapter 2: General Materials and Methods	32
2.1.	Plant Materials.....	32
2.1.1.	Establishment of Duckweed Collection at University of Hertfordshire (UH).....	32
2.2.	Nucleic Acids Extraction and Purification	36
2.2.1.	DNA Extraction.....	36
2.2.2.	RNA Extraction	36
2.3.	Nucleic Acid Quantification and Quality Control Checks	37
2.3.1.	Electrophoresis and Visualization of Nucleic Acids in Agarose Gels.....	37
2.3.2.	DNA Contamination Analysis Through PCR Techniques and Visualization in Agarose Gel 37	
2.3.3.	Nanodrop Spectrophotometer	38
2.3.4.	Quantification with Qubit Fluorometer	40
2.3.5.	TapeStation Analysis	40
2.4.	DNA Barcoding – Clone Genotyping	40
2.5.	Duckweed Growth Rate Measurements.....	41
2.6.	Sample Preparation for Total Nitrogen and Nitrate Measurements with FT-MIR Model	41
2.6.1.	Plant Materials from Different Cultivation Treatments.....	41
2.6.2.	Identification of Nitrate-N Peaks in the FTMIR Spectra.....	41
2.6.3.	Total Nitrogen Determination by Dumas Combustion	42
2.6.4.	Total Nitrate Determination by Salicylic Nitration with Spectrophotometric Determination.....	42
2.6.5.	FTIR Spectra Collection	42
2.7.	Statistical Analysis.....	43
3.	Chapter 3. Impacts of Different Nitrogen Sources on Growth Rate, Protein Content, and Gene Expression of Genes Involved in Nitrogen Assimilation in Different Duckweed Clones.....	44
3.1.	Introduction	44
3.2.	Materials and Methods.....	47

3.2.1.	Plant Material and Treatments	47
3.2.2.	Characterization of Major <i>Lemna</i> Genes Related to N Assimilation.....	49
3.2.3.	Phylogenetic Analysis.....	49
3.2.4.	Gene Expression Analysis by RT-qPCR	49
3.2.5.	Statistical Analysis.....	50
3.3.	Results.....	52
3.3.1.	Duckweed Identification	52
3.3.2.	Influence of Nitrogen Sources on Duckweed Growth, pH, Nitrogen, Nitrate, And Protein Levels	52
3.3.3.	<i>In Silico</i> Identification, Genomic Location and Evolutionary Insights of N Assimilation Genes in Duckweed.....	64
3.3.4.	Expression of Nitrogen Assimilation Genes in Duckweed Under Different Nitrogen Sources	81
3.4.	Discussion.....	84
4.	Chapter 4. Physiological Assessments on <i>Lemna</i> Growth Under Heat Stress	92
4.1.	Introduction	92
4.2.	Materials and Methods.....	95
4.2.1.	Plant Materials.....	95
4.2.2.	Growth Rate Assessments	95
4.2.3.	Nitrogen and Nitrate Quantification.....	95
4.2.4.	Degree of Heat Tolerance	97
4.2.5.	Statistical Analysis.....	97
4.3.	Results.....	98
4.3.1.	Growth Rate Analysis	98
4.3.2.	Analysis of the Degree of Heat Tolerance.....	99
4.3.3.	Total Nitrogen Content	102
4.3.4.	Total Nitrate Content	102
4.3.5.	Total Protein Content Analysis.....	105

4.3.6.	Comparative Physiological Responses of <i>Lemna gibba</i> and <i>Lemna minor</i> Clones Under Control and Heat Stress Conditions	107
4.3.7.	Evaluation of Heat Tolerance and Heat Sensitivity Duckweed Clones Using PCA analysis of Physiological Parameters.....	109
4.3.8.	Correlation Analysis of RGR, Chlorophyll, and Protein in Duckweed Clones Under Temperature Stress to Identify Heat Sensitive and Heat Tolerant Clones	111
4.3.9.	Validation of Heat Sensitive and Heat Tolerant Clones Across Different Temperature Conditions	113
4.4.	Discussion.....	116
5.	Chapter 5. Gene Expression Kinetics on <i>Lemna</i> Growth Under Heat Stress	119
5.1.	Introduction	119
5.2.	Materials and Methods.....	121
5.2.1.	Plant Materials	121
5.2.2.	RNA Extraction and Quality Control.....	121
5.2.3.	Library Construction and Sequencing	122
5.2.4.	Bioinformatics Analysis Pipeline	122
5.3.	Results.....	124
5.3.1.	RNA Control Checks	124
5.3.2.	RNA Sequencing Quality Control	128
5.3.3.	Mapping of Sequencing Data.....	130
5.3.4.	Gene Expression Profile Analysis	132
5.3.5.	Differential Gene Expression Analysis Under Heat Stress Conditions	143
5.3.6.	Gene expression levels were quantified and normalized to account for sequencing depth. A statistical model was then applied to identify significant differences between growing conditions. To ensure accuracy, p-values were calculated, and multiple testing corrections were performed to determine false discovery rate (FDR) values (Anders & Huber, 2010).	143
5.3.7.	Functional Analysis of Differentially Expressed Genes in Duckweed Clones.....	147
5.3.8.	Identification and Annotation of Key Genes Associated with Heat Resistance.....	175
5.4.	Discussion.....	177

6. Chapter 6: General Discussion	182
6.1. Impacts of Different Nitrogen Sources on Growth Rate, Protein Content, and Gene Expression of Genes Involved in Nitrogen Assimilation in Different Duckweed Clones.....	182
6.2. Physiological Assessments on <i>Lemna</i> Growth Under Heat Stress.....	186
6.3. Gene Expression Kinetics on <i>Lemna</i> Growth Under Heat Stress	187
6.4. Conclusions	189
References	191
Appendices.....	219
Appendix 1 – Supplementary Materials	219
Appendix 2 – Poster Presentations.....	228
A) SRUK Annual General Assembly 2022 – Ponds to Pounds: Maximising the Potential of Duckweeds to Convert Nitrogen to Protein – Jul 3 rd , 2022 – Oxford, United Kingdom	228
B) Sixth International Conference on Duckweed Research and Applications – FT-MIR-PLSR simultaneous determination of total nitrogen and nitrate in duckweeds - May 29 th to Jun 1 st , 2022 – Gatersleben, Germany	229
C) Sixth International Conference on Duckweed Research and Applications – Biomass, protein and nitrate accumulation in duckweeds supplied with 3 different sources of nitrogen - May 29 th to Jun 1 st , 2022 – Gatersleben, Germany.....	230
D) LMS Annual Research Conference 2021 – Unlocking rapid, inexpensive total nitrogen determination in <i>Lemna</i> using FTIR spectroscopy and PLSR analysis. – Jun 21 st , 2021 – Hatfield, United Kingdom	231
Appendix 3 – Presentations	232
A) II Jornadas Jóvenes Investigadores Barrenos – Inspirando a las Nuevas Generaciones – Dec 5 th , 2024 – Los Barrios, Spain	232
B) Association of Applied Biologists Early Career Professional Skills and Science Workshop – Physiological and Growth Responses of Duckweed to Heat Stress – Dec 18 th and 19 th , 2023 – University of Leicester, United Kingdom	233
C) I Jornada Jóvenes Investigadores Barreños – Inspirando a las Nuevas Generaciones – Oct 30 th , 2023 – Los Barrios, Spain	234

D) LMS Annual Research Conference 2022 – Ponds to Pounds: Maximising the Potential of Duckweeds to Convert N to Protein. – Jun 21 st , 2022 – Hatfield, United Kingdom.....	235
E) 3 Minute Thesis Competition UH - Genetic Control of <i>Lemna</i> growth rate and protein content under heat stress – May 5 th , 2022 – Hatfield, United Kingdom.....	236
F) University of Hertfordshire Postgraduate Research Conference 2022 – Genetic Control of <i>Lemna</i> Growth Rate and Protein Content. – Feb 7 th , 2022 – Hatfield, United Kingdom	237
G) University of Hertfordshire Postgraduate Research Conference 2021 – Genetic Control of <i>Lemna</i> Growth Rate and Protein Content. – Jul 12 th , 2021 – Hatfield, United Kingdom	238
Appendix 4 – Events.....	239
A) Future Agricultural Researchers PhD Conference 2023 – Nov 14 th , 2023 – Exeter, United Kingdom	239
B) Cereals the Arable Event – Jun 8 th , 2022 – Duxford, United Kingdom	240
C) Sixth International Conference on Duckweed Research and Applications – May 29 th to Jun 1 st , 2022 – Gatersleben, Germany	241
Publications.....	242

List of Figures

Figure 1.1. Worldwide distribution of the family of Araceae, subfamily Lemnoideae.....	2
Figure 1.2. Cladogram of duckweed genera within the Lemnoideae subfamily of the Araceae family.	4
Figure 1.3. Fronds of mother (MF) and daughter (DF) <i>Lemna trisulca</i> clones connected at the stipe.	6
Figure 1.4. Microscopic structure of <i>Lemna trisulca</i>	7
Figure 1.5. Vegetative growth cycle of <i>Lemna minor</i> (A) and <i>Lemna trisulca</i> (B).....	9
Figure 1.6. <i>Lemna gibba</i> with flowers represented with red arrows. M, mother frond, D, daughter frond and G, granddaughter frond	10
Figure 1.7. Bayesian consensus tree from the analysis of the combined cpDNA dataset (<i>atpF-atpH</i> and <i>psbK-psbI</i> intergenic spacers) of all Lemnoideae taxa, with <i>Colocasia esculenta</i> as the outgroup.	13
Figure 1.8. Amino acid concentration in different groups of food compared with nutritional requirements in different animals and humans	24
Figure 1.9. Simplified diagram of the nitrogen assimilation pathway in plants	26
Figure 1.10. Transcriptional regulatory network in plant heat stress responses.	30
Figure 2.1. Daughter duckweed frond being born in aseptic conditions.	35
Figure 3.1. Images of the <i>Lemna</i> clones used in this study.....	53
Figure 3.2. Relative Growth Rate (RGR) of duckweed clones (SD, DG4, DG8, 7796) grown under different Nitrogen sources at day 7	55
Figure 3.3. Variation in medium pH for duckweed clones (SD, DG4, DG8, 7796) grown under different Nitrogen sources on day 7	57
Figure 3.4. Total Nitrogen content (%) in duckweed clones (SD, DG4, DG8, 7796) grown under different Nitrogen sources on day 7	59
Figure 3.5. Total Nitrate content (mg NO ₃ ⁻ /kg DW) in duckweed clones (SD, DG4, DG8, 7796) grown under different Nitrogen sources at day 7	61
Figure 3.6. Total Protein content (%) in duckweed clones (SD, DG4, DG8, 7796) grown under different Nitrogen sources at day 7.	63
Figure 3.7. Exon-Intron structures of <i>Spirodela polyrhiza</i> (Sp), <i>Lemna gibba</i> (Lg), and <i>Lemna minor</i> (Lm) Nitrate Reductase (NR) and Nitrite Reductase (NiR) genes.	67
Figure 3.8. Phylogenetic tree of NiR and NR proteins in <i>Lemna gibba</i> and <i>Lemna minor</i> with other representative species	68

Figure 3.9. The Exon-Intron structures of <i>Spirodela polyrhiza</i> , <i>Lemna gibba</i> and <i>Lemna minor</i> Glutamine Synthetase (GS) genes	70
Figure 3.10. Phylogenetic tree of GS proteins in <i>Lemna gibba</i> and <i>Lemna minor</i> with other representative species.	72
Figure 3.11. The Exon-Intron structures of <i>Spirodela polyrhiza</i> , <i>Lemna gibba</i> and <i>Lemna minor</i> Glutamine oxoglutarate aminotransferase-ferredoxin dependent (<i>Fd-GOGAT</i>) and Glutamine oxoglutarate aminotransferase-NADH dependent genes (<i>NADH-GOGAT</i>)	74
Figure 3.12. Phylogenetic tree of Fd-GOGAT and NADH-GOGAT proteins in <i>Lemna gibba</i> and <i>Lemna minor</i> with other representatives species.....	76
Figure 3.13. The Exon-Intron structures of <i>Spirodela polyrhiza</i> , <i>Lemna gibba</i> and <i>Lemna minor</i> of Chloride Channel A genes	78
Figure 3.14. Phylogenetic tree of CLCa proteins in <i>Lemna gibba</i> and <i>Lemna minor</i> with other representative species	80
Figure 3.15. Relative expression of <i>NR</i> , <i>NiR</i> , <i>GS1-1</i> , <i>GS1-2</i> , <i>GS2</i> , <i>CLCa1</i> , <i>Fd-GOGAT</i> , and <i>NADH-GOGAT</i> genes in four duckweed clones.....	83
Figure 4.1. Heat stress on plant physiological changes	93
Figure 4.2. Geographical distribution of the 42 <i>Lemna</i> clones treated in this chapter	96
Figure 4.3. Relative Growth Rate (RGR) of 6 <i>L. minor</i> (left) and 36 <i>L. gibba</i> (right) clones under control (20°C, green) and heat stress (35°C, red) conditions	100
Figure 4.4. Total chlorophyll content (µg/mL) of of 6 <i>L. minor</i> (left) and 36 <i>L. gibba</i> (right) clones under control (20°C, green) and heat stress (35°C, red) conditions.	101
Figure 4.5. Total Nitrogen content (%) of of 6 <i>L. minor</i> (left) and 36 <i>L. gibba</i> (right) clones under control (20 °C, green) and heat stress (35 °C, red) conditions	103
Figure 4.6. Total Nitrate content (mg/kg DW) of of 6 <i>L. minor</i> (left) and 36 <i>L. gibba</i> (right) clones under control (20°C, green) and heat stress (35°C, red) conditions	104
Figure 4.7. Total protein content (%) of of 6 <i>L. minor</i> (left) and 36 <i>L. gibba</i> (right) clones under control (20°C, green) and heat stress (35°C, red) conditions	106
Figure 4.8. The PCA plot illustrates the multivariate analysis of clones' responses to temperature treatments (20 and 35 °C)	110
Figure 4.9. Correlation analysis between RGR, chlorophyll, and protein in duckweed clones under 20°C (control) and 35°C (heat stress).....	112
Figure 4.10. Protein content (A) and RGR (B) of five <i>L. gibba</i> clones (Manor, 6861, 7763, 7796, and 8703) at different temperatures.....	115

Figure 5.1. RNA quality assessment of duckweed samples grown at 35°C (A) and 20°C (B) using agarose gel electrophoresis	127
Figure 5.2. RNA quality assessment of duckweed samples grown at 20°C and 35°C.	129
Figure 5.3. Distribution of gene expression levels across clones and temperature conditions	135
Figure 5.4. Pearson correlation heat map of gene expression levels.....	137
Figure 5.5. Principal Component Analysis of gene expression profiles.....	139
Figure 5.6. Venn diagram displaying the distribution of gene expression across five duckweed clones under two temperature conditions	142
Figure 5.7. Differential gene expression counts across clones between 35°C and 20°C.	144
Figure 5.8. Hierarchical clustering heatmap of Differentially Expressed Genes (DEGs) in heat-sensitive and heat-tolerant duckweed clones at 20°C and 35°C.	146
Figure 5.9. Enrichment analysis of GO terms for differentially expressed genes in five duckweed clones	153
Figure 5.10. Classification of Differentially Expressed Genes (DEGs) by GO terms in five duckweed clones	156
Figure 5.11. Directed Acyclic Graphs (DAGs) of cellular components for differentially expressed genes in duckweed clones	162
Figure 5.12. KEGG pathway enrichment analysis across clones under heat-stressed and control conditions	168
Figure 5.13. Cluster analysis of gene expression patterns for selected GO terms across five clones.	171
Figure 5.14. Cluster analysis of gene expression patterns for selected KEGG pathways across clones.	174
Figure 6.1. Cluster analysis of gene expression patterns for selected DEG in Nitrogen assimilation pathways	185
Figure S.1. Identification and Barcoding of Four <i>Lemna</i> Clones Used in the Study Trough <i>psbK-psbI</i> Intergenic Spacers.....	219
Figure S.2. Identification and Barcoding of Four <i>Lemna</i> Clones Used in the Study Trough <i>atpF-atpH</i> Intergenic Spacers	220
Figure S.3. Relative Growth Rate (RGR) of Duckweed Clones (SD, DG4, DG8, 7796) Grown Under Different Nitrogen Sources at Day 4.....	221
Figure S.4. Variation in Medium pH for Duckweed Clones (SD, DG4, DG8, 7796) Grown Under Different Nitrogen Sources on Day 4.....	222

Figure S.5. Total Nitrogen Content (%) in Duckweed Clones (SD, DG4, DG8, 7796) Grown Under Different Nitrogen Sources on Day 4.....	223
Figure S.6. Total Nitrate Content (mg NO₃⁻/kg DW) in Duckweed Clones (SD, DG4, DG8, 7796) Grown Under Different Nitrogen Sources at Day 4.....	224
Figure S.7. Total Protein Content (%) in Duckweed Clones (SD, DG4, DG8, 7796) Grown Under Different Nitrogen Sources at Day 4.....	225

List of Tables

Table 1.1. Comparison of methionine, threonine, lysine, and histidine composition (% Total Protein) across <i>Lemna</i> , legumes, grains, and green tissues.....	23
Table 2.1. List of duckweed species at UH duckweed collection.....	33
Table 2.2. List of primers used for end-point PCR.....	39
Table 3.1. Nutrient composition of the modified Rorison medium for 4 different Nitrogen sources	48
Table 3.2. RT-qPCR primers for nitrogen assimilation gene expression analysis in <i>L. gibba</i> and <i>L. minor</i> clones.	51
Table 3.3. Gene structure, genomic location, and functional domains of Nitrogen assimilation and transport-related genes in <i>Lemna gibba</i> and <i>Lemna minor</i>	65
Table 4.1. Physiological responses of <i>L. gibba</i> and <i>L. minor</i> clones at 20°C and 35°C	108
Table 5.1. RNA quality and quantity metrics for duckweed clones under different temperature treatments	125
Table 5.2. Sequencing quality statistics for RNA samples.	131
Table 5.3. RNA-seq read counts and mapping statistics for different clones grown at 20 °C and 35 °C.	133
Table 5.4. Summary of gene expression across individual clones (Manor, 6861, 7763, 7796, and 8703) at 20°C and 35°C.	141
Table 5.5. Key genes associated with heat resistance identified in KEGG and GO pathway analyses.	176
Table S.1. List of species, nitrogen assimilation proteins, and their accession numbers.	226
Table S.2. Summary of clone characteristics and physiological data	227

List of Equations.

- 1 $RGR = (\ln X_{t_7} - \ln X_{t_0}) / (t_7 - t_0)$ 41
- 2 Total protein (%) = $6.25 \times (TN - TNO_3^-)$ 47
- 3 $E = (10^{-1/\text{slope}} - 1) * 100$ 50
4. Total chlorophyll ($\mu\text{g/mL}$) = $1.44 \times A_{665} + 24.93 \times A_{652}$ 97

List of Abbreviations

Abbreviation	Definition
2-OG	2-oxoglutarate
<i>A. thaliana</i> / At	<i>Arabidopsis thaliana</i>
AMTs	Ammonium Transporters
ANOVA	Analysis of Variance
APX	Ascorbate Peroxidase
AS	Asparagine Synthetase
Asn	Asparagine
ATP	Adenosine Triphosphate
<i>B. distachyon</i> / Bp	<i>Brachypodium distachyon</i>
BP	Biological Process
BPP	Bayesian Posterior Probabilities
CA	California
CAT	Catalase
CC	Cellular Component
CE	Controlled Environments
CLC	Chloride Channel
cpDNA	Chloroplast DNA
CRISPR/Cas9	Clustered Regularly Interspaced Palindromic Repeats Associated Protein 9
DAG	Directed Acyclic Graph
DEGs	Differentially Expressed Genes
DIw	Deionized water
dNTP	Deoxynucleotide Triphosphate
DREB2A	Dehydration-Responsive Element Binding Protein 2A
DRIFT	Diffuse Reflectance Infrared Fourier Transform
DT	Doubling time
DW	Dry weight
EU	European Union
FAO	Food and Agriculture Organization
Fd-GOGAT	Ferredoxin-dependent GOGAT
FDS	False Discovery Rate
FPKM	Fragments Per Kilobase of transcript sequence per Million base pairs sequenced
fq	FASTQ

FT-MIR	Fourier Transform Mid Infrared
FW	Fresh Weight
GAPDH	Glyceraldehyde-3-Phosphate Dehydrogenase
Gln	Glutamine
Glu	Glutamate
GO	Gene Ontology
GOGAT	Glutamine-2-Oxoglutarate Aminotransferase
GS	Glutamine Synthetase
GSEA	Gene Set Enrichment Analysis
<i>H. vulgare / Hv</i>	<i>Hordeum vulgare</i>
HPP	Histidin-Prolin-Prolin containing Protein
HS	Heat Stress
HsfA1s	Heat Shock Transcription Factor A1s
HSPs	Heat Shock Proteins
HSR	Heat Stress Responses
HTL	Hydrothermal Liquefaction
HTS	High Throughput Screening
HYS	Histidine
IBV	Infectious Bronchitis Virus
KEGG	Kyoto Encyclopedia of Genes and Genomes
<i>L. gibba / Lg</i>	<i>Lemna gibba</i>
<i>L. minor / Lm</i>	<i>Lemna minor</i>
<i>L. trisulca</i>	<i>Lemna trisulca</i>
LYS	Lysine
MBF1C	Multiprotein Bridging Factor 1C
MCT	Mercury Cadmium Telluride
MDA	Malondialdehyde
MET	Methionine
MF	Molecular Function
MPBS	Maximum Parsimony Bootstrap Values
<i>N. nucifera / Nn</i>	<i>Nelumbo nucifera</i>
<i>NADH-GOGAT</i>	NADH-dependent GOGAT
NF-YA2	Nuclear Factor Y, Subunit A2
NH4+	Ammonium

<i>NiR</i>	Nitrite reductase
NO ₃ ⁻	Nitrate
<i>NR</i>	Nitrate reductase
<i>NRTs</i>	Nitrate Transporters
NUE	Nitrogen Use Efficiency
<i>O. sativa / Os</i>	<i>Oryza sativa</i>
OD	Optical Density
PCA	Principal component analysis
PCR	Polymerase chain reaction
PFDs	Photon Flux Densities
PLS	Partial Least-Squares
PPR	Pentatricopeptide repeat
qPCR	quantitative Polymerase Chain Reaction
RGR	Relative Growth Rate
RIN	RNA Integrity Number
RMSE	Root Mean Square Error of Prediction
RMSECV	Root Mean Squared Errors of Cross Validation
RNA-Seq	RNA sequencing
ROS	Reactive Oxygen Species
<i>S. bicolor / Sb</i>	<i>Sorghum bicolor</i>
<i>S. polyrhiza / Sp</i>	<i>Spirodela polyrhiza</i>
SH	Schenk and Hildebrandt
SOD	Superoxide Dismutase
SOPs	Standard Operating Procedures
SSPs	Seed Storage Proteins
TFIIH	The General Transcription Factor IIH
TFs	Transcription Factors
THR	Threonine
UCHs	Ubiquitin Carboxyl-terminal Hydrolases
UCP1	Uncoupling Protein 1
UH	University of Hertfordshire
UK	United Kingdom
USA	United States of America
WHO	World Health Organization

1. Chapter 1: General Introduction

1.1. Duckweed, a Tiny Aquatic Plant

1.1.1. Duckweed Dispersal and Distribution

Water lentils or duckweeds belong to the monocot order of the *Alismatales*. It is enclosed in subfamily Lemnoideae within the family *Araceae*, where duckweed is classified in five genera: *Spirodela*, *Landoltia*, *Lemna*, *Wolffia* and *Wolffiella*. There are 36 species across the five genera. Duckweeds are spread in every continent, except Antarctica (Landolt, 1986), as shown in Figure 1.1. This tiny plant is dispersed by streaming water or occasionally by strong winds. Besides, duckweed can be transported between the feathers of dispersing birds during their migrations (up to 250 km). However, *Wolffia columbiana* was found in the faeces of ducks and swans, indicating plants can survive passage through the guts of some waterfowls (Silva *et al.*, 2018).

High mountains, such as the Himalayas, are considered geographical barriers to the dispersal of duckweed. This was suggested by Xu *et al.*, (2019) through resequencing and comparison of 68 genomes of *Spirodela polyrhiza* clones from Southeast Asia. This hypothesis is further supported by a study of 23 *Spirodela polyrhiza* clones from Hungary, which were identified as unique Hungarian clones. The mountainous borders surrounding Hungary are suggested to contribute to this genetic uniqueness by acting as barriers to the dispersal of the species (Chu *et al.*, 2018).

However, some species can be considered as an alien in some regions. *Lemna minuta*, native in temperate zones of the Americas, is invasive in Eurasia (Ceschin *et al.*, 2018; Lucey, 2003; Mifsud, 2010). Similarly, *Lemna turionifera*, *Lemna valdiviana* and *Wolffia columbiana* are also regarded as invasive in Eurasia (Ardenghi *et al.*, 2017; Iberite *et al.*, 2011), and *Landoltia punctata* is an alien species in both Europe and North America, while six non-native species of duckweed were found in Florida, USA (Ward & Hall, 2010).

Duckweed growth in natural ecosystem can be increased by anthropogenic activities like rising nitrogen and phosphorus level or water temperature in ponds affecting natural ecosystems like phytoplankton (Feuchtmayr *et al.*, 2009; Peeters *et al.*, 2013). Besides, increased temperature reduced the grazing pressure of *Lemna minor* by *Cataclysta lemnata* (natural herbivore of duckweed) (Van Der Heide *et al.*, 2006).

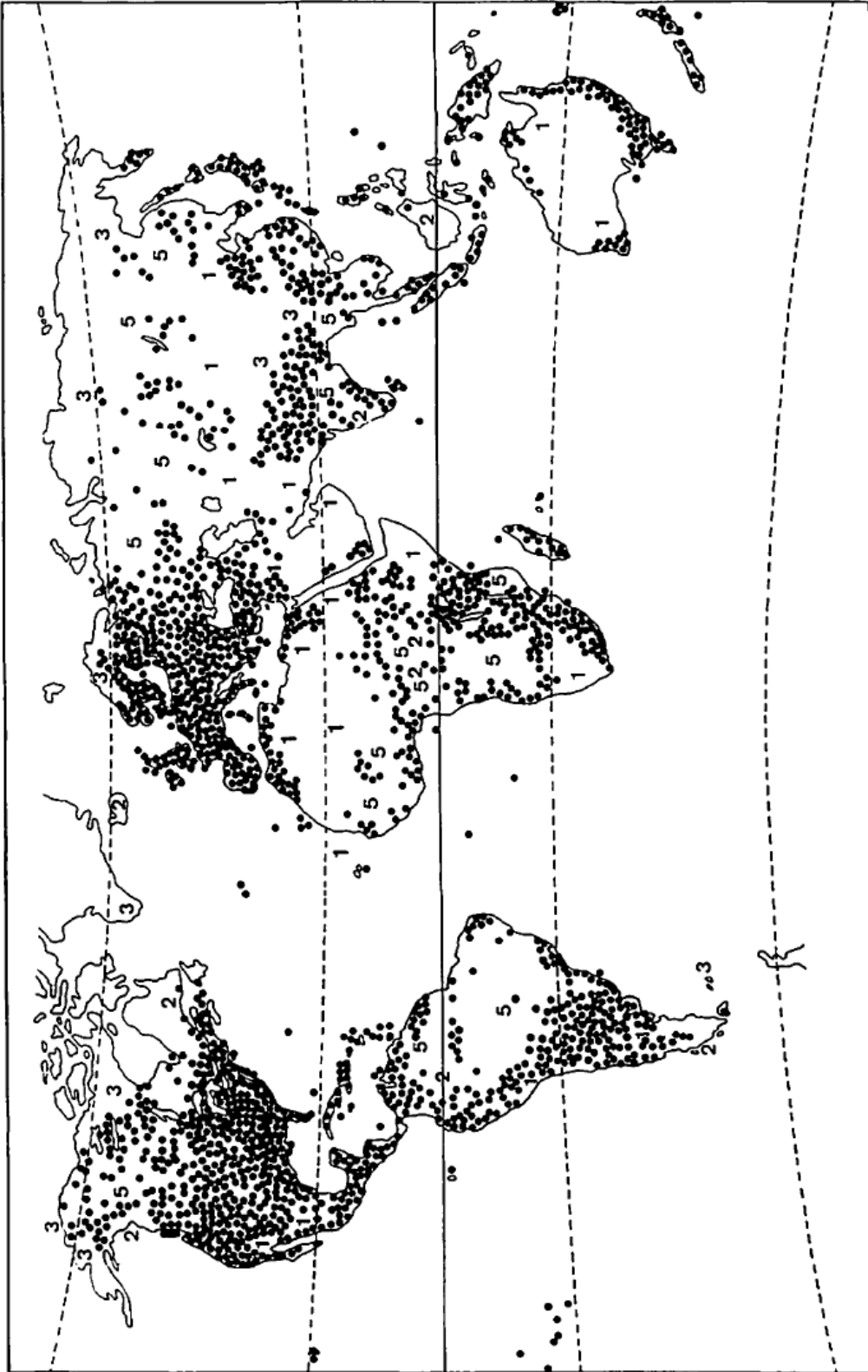


Figure 1.1. Worldwide distribution of the family Araceae, subfamily Lemnoideae. It was reported by Landolt (1986), lack of duckweed species in different regions due to; 1 - too dry, 2- too wet, 3 - too cold and 5- to be deeply explored.

1.1.2. Anatomical Features

The duckweed plants are composed by a leaf-stem structure, called frond, and some genera have roots such as *Spirodela*, *Landoltia* and *Lemna*. Based on phylogenetic analysis *Spirodela* and *Landoltia* genera have been classified closer to the common ancestor than *Lemna*, *Wolffia* and *Wolffiella* (Acosta *et al.*, 2021). This structure has evolved to reduce size and complexity, as observed across different genera, as shown in Figure 1.2, *Spirodela* species have larger fronds and multiple roots. In contrast, *Lemna* species have medium-sized fronds, ranging from 1 to 3 mm, with a single root. *Wolffiella* species are rootless and have small fronds, up to 1 mm in size. The reduction in complexity from *Spirodela* to *Wolffia* reflects a decreasing "degree of primitivity" (Bog *et al.*, 2020; Landolt, 1986).

With such a small size and rapid growth by clonal propagation, duckweed indeed produces high yields. The floating lifestyle facilitates uptake of labelled compounds from the media and interaction with microbial symbionts (Acosta *et al.*, 2020; Hillman, 1976).

Duckweed forms colonies because, after the creation of daughter fronds, they remain attached to the mother fronds. The number of fronds per colony depend on the species. Colonies from *Wolffia* or *Wolffiella* consist of two fronds, except *Wolffiella gladiata* or *Lemna trisulca* in the *Lemna* genera that can be up to 50 fronds. Mother and daughter fronds are held together by the abscission zones on the stipe (two in *S. polyrhiza* and one in *W. microscopica*), which facilitate their eventual separation (Bog *et al.*, 2020; Landolt, 1986). The stipe originates on the ventral side of the mother frond, where cells divide and grow (Figure 1.3). It serves as a channel, providing nutrients from the mother to the daughter frond (Kim, 2016).

Duckweed epidermis is fortified with a transparent waxy cuticle against mechanical injury and solar radiation (Borisjuk *et al.*, 2018). The structure of the cell walls varies across genera: *Spirodela* has a bent structure, *Landoltia* and *Lemna* have undulated cell walls, and *Wolffiella* and *Wolffia* have straight cell walls. The ventral epidermis is involved in nutrient uptake and provides an active surface for interactions with aquatic bacteria (Cedergreen & Madsen, 2002; Duong & Tiedje, 1985).

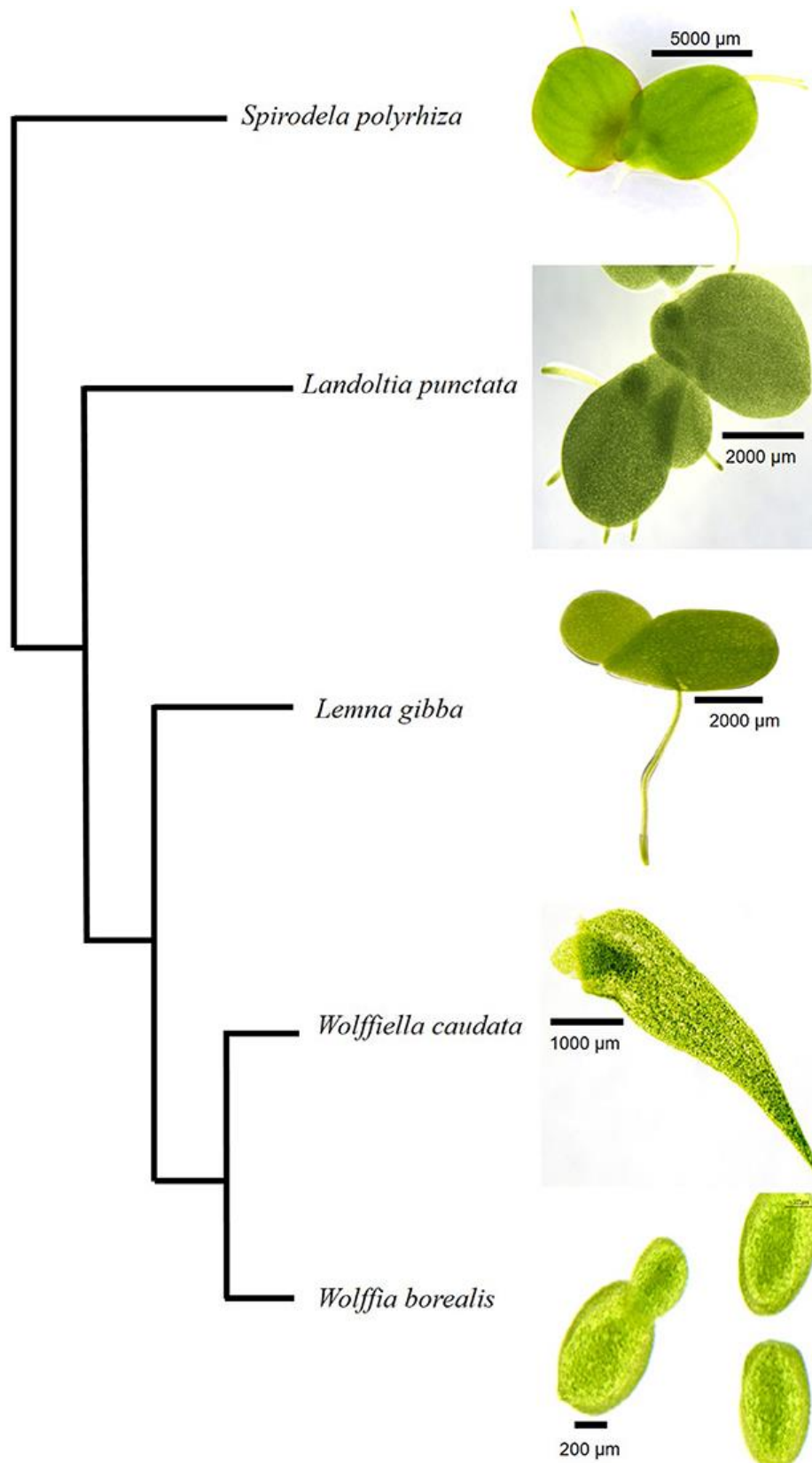


Figure 1.2. Cladogram of duckweed genera within the Lemnoideae subfamily of the Araceae family. The five duckweed species from different genera are presented according to the phylogeny proposed by Tippery *et al.*, (2015). A scale bar (μm) in each photograph indicates the size of the respective specimen. This image was adapted from Pagliuso *et al.*, (2018).

Roots develop on the lower side of the frond, near the budding pouches at the node. They subtended by epidermal sheath at the junction and by the root-cap at the root tip. Roots in duckweed are thought to act like a pendulum, helping to mitigate dynamic loads or wind motion (Acosta *et al.*, 2021). Unlike land plants, which typically regulate stomatal opening, duckweed maintains its stomata open (McLaren & Smith, 1976). However, under unfavourable environmental conditions, some duckweed species can enter a dormant phase by forming specialized structures called turions. During the turion stage, stomata close until conditions such as light, temperature, or nutrient levels become favourable, at which point germination occurs (Borisjuk *et al.*, 2018). Turion cells distinct from frond cells due to their smaller size, the absence of aerenchyma and plasmodesmata, and thicker cell walls (Jacobs, 1947; Kim, 2013).

Most cells in duckweed are parenchyma cells. These cells have a central vacuole, that contains 95% of the water content. The dorsal cell layers have a high density of chloroplasts, functioning as the chlorenchyma (Kwak & Kim, 2008; White & Wise, 1998). Parenchyma cells are modified into aerenchyma, which is made up by spongy tissue that forms spaces or air channels within the leaves (Figure 1.4). Aerenchyma facilitates exchange of gases between the dorsal and ventral parts of the plant and help in flotation by regulating the air space volume within fronds (Landolt & Kandeler, 1987).

Meristem cells are found on the ventral side of the frond body inside the vegetative pouch, where vegetative reproduction happens (Figure 1.4). These cells contain small vacuoles and proplastids with only a few thylakoids (Kim, 2011; McCormac & Greenberg, 1992).

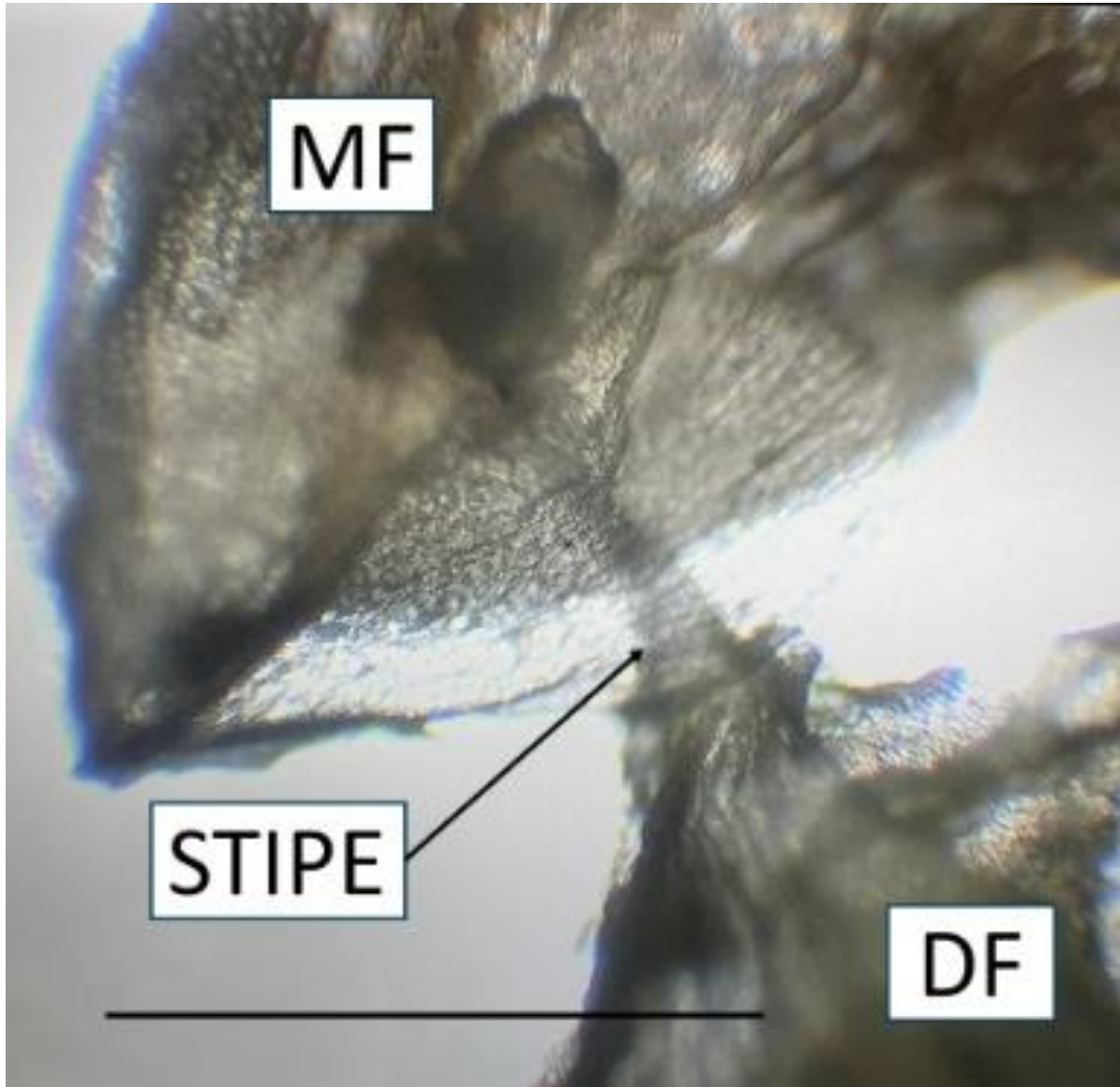


Figure 1.3. Fronds of mother (MF) and daughter (DF) *Lemna trisulca* clones connected at the stipe. The bar corresponds to 1mm.

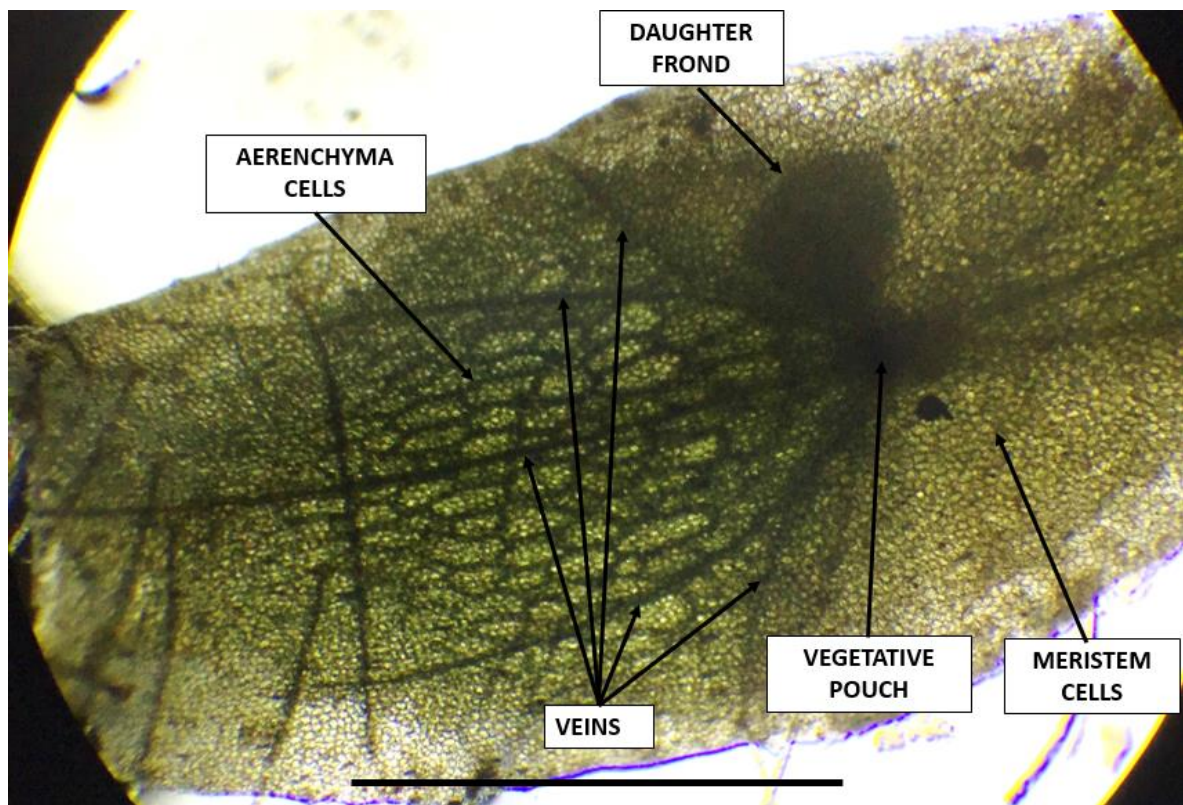


Figure 1.4. Microscopic structure of *Lemna trisulca*. This microscopic image provides insight into the intricate anatomy of *L. trisulca*. Aerenchyma cells, derived from modified parenchyma cells, form a spongy tissue crucial for facilitating air exchange within the plant. The image highlights the presence of meristem cells located within the vegetative pouch, where roots attach, and daughter fronds initiate growth. The central vein of the *Lemna* genus is flanked by two lateral veins, with the potential for additional vein development. The bar corresponds to 1mm.

1.1.3. Growth and Reproduction Characteristics

Under favourable conditions, duckweed can double its weight in less than 24 hours. Vegetative reproduction, through the production of clonal daughter fronds from a mother frond, is the most common mode of duckweed propagation (Ashby, 1948). Duckweed colonies growth includes increases in cell size, the number of individual plants, and the number of daughter fronds produced by each plant. Growth rate can be measured in terms of biomass (fresh or dry weight) or the number of fronds. Ziegler *et al.* (2015) developed a standardized method for determining duckweed growth rates, which can be influenced by abiotic factors such as light and temperature.

Vegetative reproduction implies new daughter fronds bud off from the side pouches of the older mother frond, creating clones of the mother. Depending on the species, the frond can separate as soon as the daughter fronds mature, or they may remain connected. This results in small groups, as seen in *Lemna* species (Figure 1.5 (A)), or longer groups, as in *L. trisulca* (Figure 1.5 (B)). Exponential growth is important for the colonisation of open water surfaces before other aquatic plants can establish themselves (Landolt, 1986). Growth rates are influenced by abiotic factors. For example, *S. polyrrhiza* can grow at 38 °C, whereas some *L. minor* clones are affected by temperature above 32 °C. Contrariwise, some *L. minor* strains can grow at 5 °C, while most of *S. polyrrhiza* described so far are adversely affected by temperatures below 12 °C (Docauer, 1983; Landolt, 1986).

Although the most common form of duckweed reproduction is vegetative clonal division (Bog *et al.*, 2020; Landolt, 1986; Sree *et al.*, 2015), under certain conditions, some duckweed clones produce flowers. These flowers consist of male (androecium) and female (gynoecium) floral organ, without the presence of corolla and calyx (Figure 1.6). Flowering can be induced by abiotic factors or exposure to chemical molecules such as phytohormones, chelators, heavy metal ions and photosynthetic products (Landolt & Kandeler, 1987). For instance, in *W. microscopica*, exposure to low temperature (22 °C) can trigger flowering (Rimon & Galun, 1968).

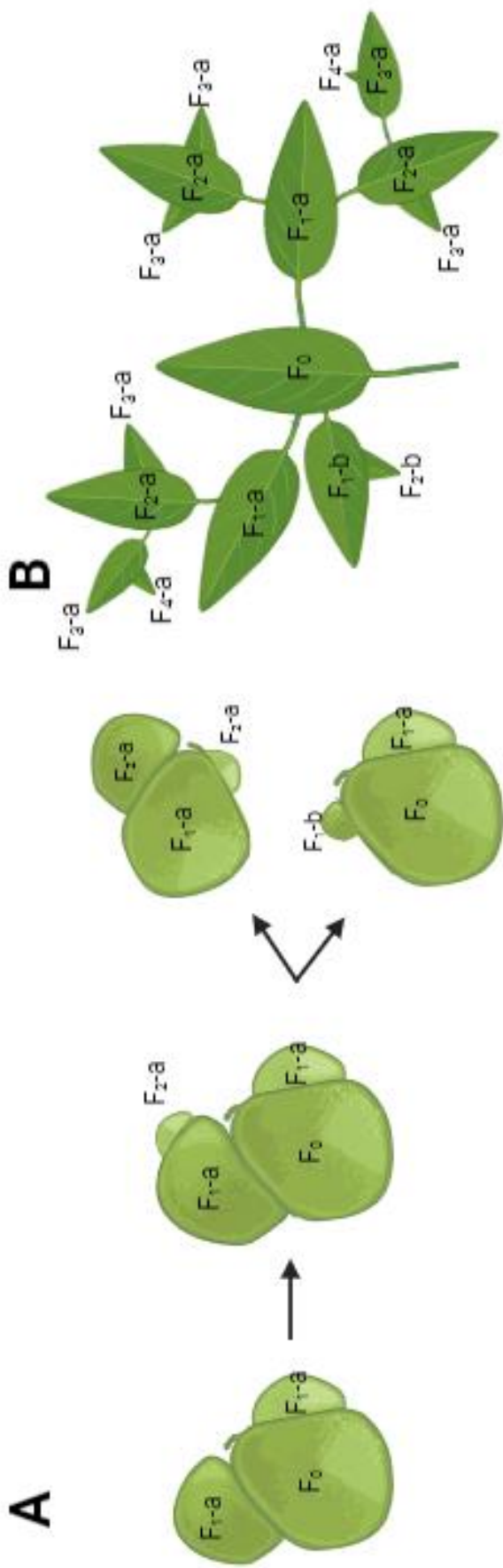


Figure 1.5. Vegetative growth cycle of *Lemna minor* (A) and *Lemna trisulca* (B). Where; F_0 mother frond; F_1 daughter frond of the first generation; F_2 daughter frond of the second generation; a first daughter frond; b second daughter frond.

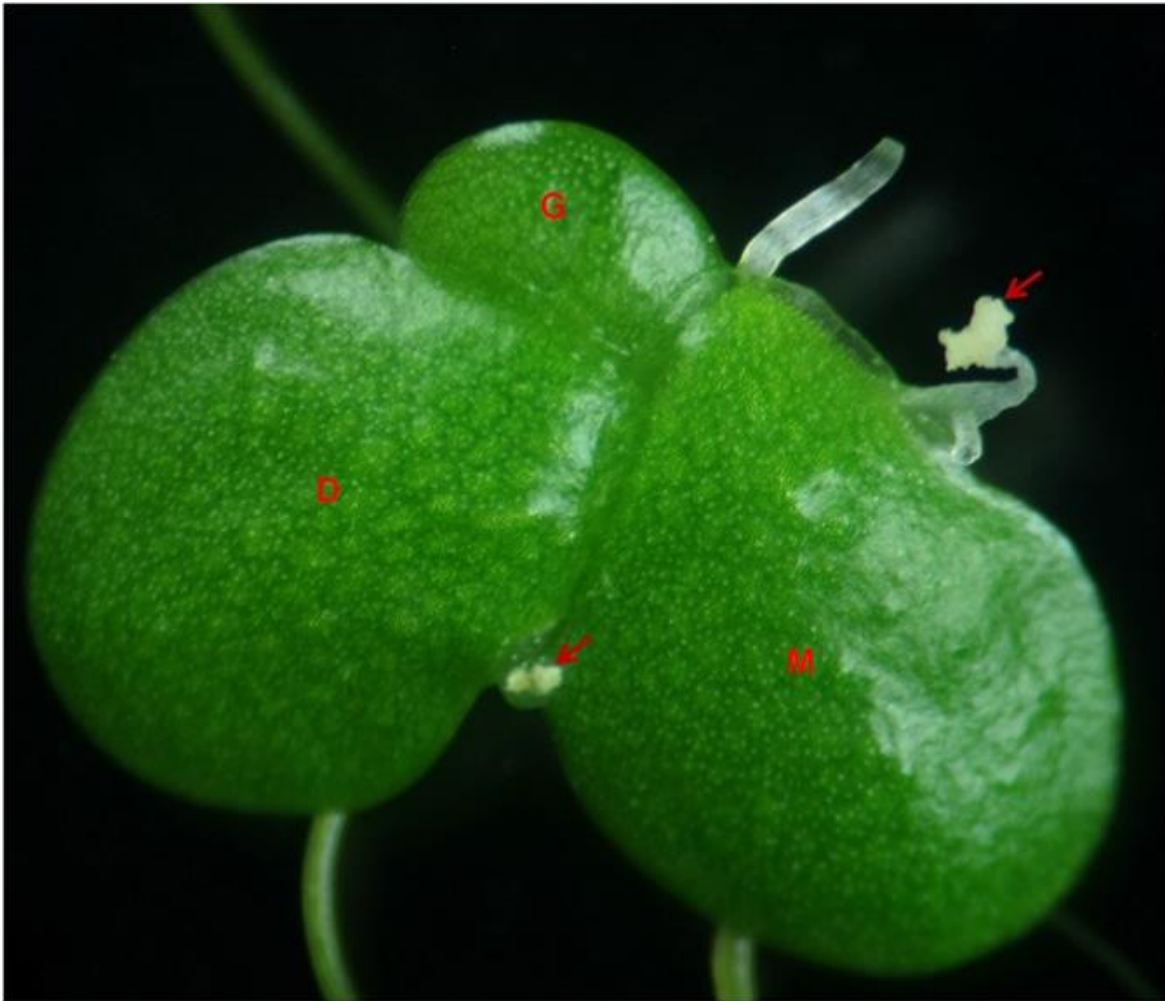


Figure 1.6. *Lemna gibba* with flowers represented with red arrows. M, mother frond, D, daughter frond and G, granddaughter frond. Picture collected from Fu et al., (2017).

1.1.4. Genomics of Duckweed

Since the 1950s, duckweed has been utilised as an experimental system for plant physiology and biochemistry. The first fully sequenced genome of duckweed was *Spirodela polyrhiza*, reported by Blackburn (1933), highlighted the remarkably small size of the chromosomes, with *S. polyrhiza* possessing some of the smallest known chromosomes in flowering plants, measuring just 0.1 x 0.18 μm (Geber, 1989).

Interestingly, there is a negative correlation between genome size and frond size in duckweeds. *S. polyrhiza* has a small genome of approximately 158 Mb, comparable to that of *Arabidopsis* (Bennett *et al.*, 2003; Wang & Messing, 2011). *Landoltia* has a relatively stable genome size of around 380 Mb, while *Lemna* exhibits significant intraspecific and interspecific variation, ranging from 323 to 760 Mb, suggesting that polyploidy may be a major factor in genome size changes (Seagraves, 2017; Soltis *et al.*, 2015; Van De Peer *et al.*, 2017). The genera *Wolffiella* and *Wolffia* possess the largest genomes among duckweeds, with sizes of 973 Mb and 1,881 Mb, respectively (Wang & Messing, 2011).

Chromosome number in duckweed is also highly variable, with the most common diploid chromosome number being 40 (2n) (Hoang *et al.*, 2019). However, *L. aequinoctialis* has been found to have between 20 and 84 chromosomes (Hoang *et al.*, 2019; Wang *et al.*, 2011). Research on some cultured clones suggests that autotetraploidy may be present in species like *L. aequinoctialis* (2n = 42 and 84 chromosomes). This condition could have occurred naturally or been chemically induced, as observed in *Landoltia punctata* 5562, which has 46 and 92 (2n) chromosomes (Hoang *et al.*, 2019; Vunsh *et al.*, 2015).

Due to its small genome size, *S. polyrhiza* 7498 was the first duckweed species to have its genome fully sequenced, using the 454 and Sanger platforms. This sequencing effort revealed a repertoire of 19,623 protein-coding genes (Wang *et al.*, 2014). Following this milestone, other duckweed species were also sequenced. The first *Lemna* species to be fully sequenced was *L. minor* 5500, using Illumina technology, which uncovered a higher gene repertoire than *Spirodela*, with 22,382 protein-coding genes (Van Hoeck *et al.*, 2015). This was followed by the sequencing of *L. minor* 8627 and *L. gibba* 7742a the next year (Ernst & Martienssen, 2016).

In recent years, several additional duckweed species have been fully sequenced, including *S. polyrhiza* 9509, *L. gibba* 7742a, *L. japonica* 7182, *L. japonica* 8627, *L. japonica* 9421, *L. minor* 7210, *L. minor* 9252, *L. turionifera* 9434, and *W. australiana* 8730 that can be found in *Lemna.Org* repository (Ernst *et al.*, 2023).

As shown in the Figure 1.7, the five genera of duckweed exhibit varying degrees of primitivity and complexity, as illustrated by their phylogenetic positions in a Bayesian consensus tree derived from the analysis of a combined cpDNA dataset (*atpF-atpH* and *psbK-psbI* intergenic spacers) of all Lemnoideae taxa, with *Colocasia esculenta* as the outgroup (Borisjuk *et al.*, 2015). In this phylogenetic tree, *Spirodela* and *Wolffiella* are positioned oppositely, with *Lemna* and *Landoltia* sharing one cluster, and *Wolffia* and *Wolffiella* grouped together. *Spirodela* and *Landoltia*, which possess more complex morphological features, have higher nuclear DNA content compared to the simpler *Lemna*, *Wolffiella*, and *Wolffia* (Borisjuk *et al.*, 2015). This pattern suggests that the evolution of duckweed involved a morphological reduction, a strategy likely employed to enhance their adaptation to an aquatic lifestyle (Landolt, 1986).

1.2. Historical Utilization of Duckweed

Duckweed, a seemingly ordinary aquatic plant, boasts a rich historical legacy that spans civilizations and periods. The first recorded mention of duckweed dates to Theophrastus, the renowned botanist of Ancient Greece. Theophrastus not only classified duckweed based on its aquatic habitat but also coined the term “*lemna*” (water plant), laying the foundation for the subfamily *Lemnoideae* (Hort, 1917). However, the influence of duckweed extends far beyond the shores of Greece, it was mentioned in diverse cultures including Chinese, Christian, Greek, Hebrew, Hindu, Japanese, Maya, Muslim, and Roman societies (Edelman *et al.*, 2022).

The medieval era witnessed the emergence of St. Hildegard von Bingen, whose compendium on herbal medicine, “*Causa et Curae*,” documented the medicinal virtues of duckweeds. From alleviating colic to fortifying the immune system, duckweed found its place in the pharmacopoeia of the High Middle Ages (Von Bingen, 1933).

Across ancient rituals and healing practices, duckweed held significance. In Maya society, it was invoked in healing incantations, reflecting its revered status among healers (Doemel, 2013; Knowlton, 2018). Similarly, in Yemenite cultures, duckweed adorned stagnant waters, not merely as flora but as a symbol of purification. Its presence was integral to water conservation, as it curtailed evaporation and safeguarded vital water sources, as the natives expressed “it prevents the wind from taking the water” (Hovden, 2006).

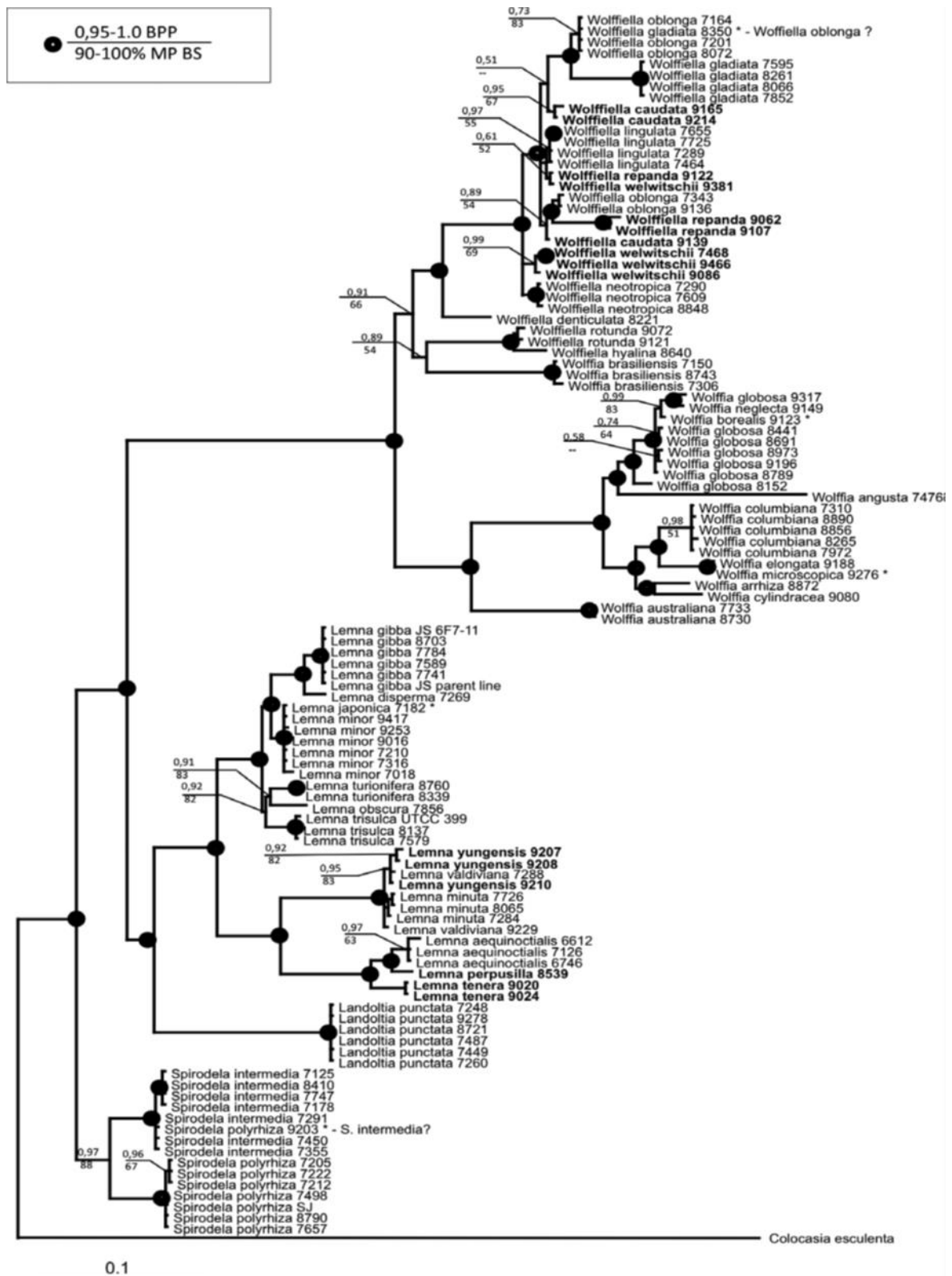


Figure 1.7. Bayesian consensus tree from the analysis of the combined cpDNA dataset (*atpF-atpH* and *psbK-psbI* intergenic spacers) of all Lemnoideae taxa, with *Colocasia esculenta* as the outgroup. Bayesian posterior probabilities (BPP) and maximum parsimony bootstrap values (MPBS) are shown on the branches. Strongly supported clades (MPBS >90% and BPP >0.95) are indicated with black points. Strains with questionable species assignments are marked with asterisks (*). Adapted from Borisjuk *et al.*, (2015).

Though the historical importance of duckweed is unquestionable, its story doesn't conclude in ancient times. The ancient practices involving duckweed propel us towards modern innovation, connecting the wisdom of the past with present-day scientific exploration. As duckweed researchers explore further into the potential of duckweed, we unveil a wealth of opportunities to tackle urgent global issues, ranging from environmental sustainability to advancements in biotechnology and human health.

1.3. Duckweed Uses and Biotechnological Applications

1.3.1. Duckweed: A Versatile Resource for Biofuel Production

The excessive use of fossil fuels is leading to the depletion of reserves, highlighting the urgent need for alternative, sustainable, and carbon-neutral energy sources (Campbell, 2013). Biomass waste from duckweed, which is abundant and diverse in natural environments, provides a promising approach to addressing this challenge (Welfle *et al.*, 2020). Duckweed is an excellent candidate for bioenergy production, as it can be easily converted into various forms of energy, including bio-oil, gas, bioethanol, and high-value industrial precursors through different transformation technologies (Chen *et al.*, 2022).

The accelerated consumption of petroleum necessitates the development of renewable fuels to replace petroleum-based ones. Among these alternatives, bio-oil, which can be directly used as fuel for industrial oil boilers or refined to replace gasoline or diesel, stands out. The optimal production method for bio-oil is thermochemical conversion, specifically pyrolysis and hydrothermal liquefaction (HTL) (Collard & Blin, 2014; Hu *et al.*, 2018). Pyrolysis, which involves thermal cracking of biomass in the absence of oxygen at temperatures between 400–600°C (Xu *et al.*, 2021), has been effectively used to produce bio-oil from duckweed. For instance, Muradov *et al.*, (2010) explored the pyrolysis of duckweed, showed that while the reaction temperature had minimal effect on the final product distribution, it significantly influenced the relative quantities of individual products. Campanella & Harold (2012) demonstrated that fast pyrolysis of duckweed in a nitrogen atmosphere yielded 44.9 wt% bio-oil at 500°C. Additionally, Campanella *et al.*, (2012) compared the pyrolysis of microalgae and duckweed, noting that the feedstock composition and heating rate were critical factors influencing the bio-oil's composition, which is complex due to numerous cross-linking reactions during pyrolysis.

Gases, another crucial bioenergy product, can be generated from duckweed through anaerobic digestion, fermentation, and pyrolysis. Methane, a renewable energy source produced by anaerobic digestion, is not only an ideal fuel but also a raw material for various industrial chemicals (Chen *et al.*,

2022). Gaur & Suthar (2017) investigated the impact of mixing duckweed biomass with waste activated sludge and acclimatized anaerobic granular sludge on methane production, highlighting duckweed's potential due to its high cellulose and low lignin content. Hydrogen, recognized for its clean, high-energy-density properties, is another gas produced during duckweed pyrolysis, although the yield is relatively low, and the process is energy-intensive (Chen *et al.*, 2022). The main gaseous products from duckweed pyrolysis include H₂, CO, CO₂, CH₄, and a small amount of C₂H₆, with CO₂ being the predominant component (Muradov *et al.*, 2010).

Bioethanol, a renewable fuel that can reduce carbon dioxide emissions by more than 50% compared to traditional fossil fuels, is primarily produced from high-starch biomass feedstocks like corn, sugarcane, and wheat (Green *et al.*, 2015; Mishima *et al.*, 2008; Sun *et al.*, 2014). Duckweed, particularly *L. punctata*, has been studied as a feedstock for bioethanol production. Chen *et al.*, (2012) used pectinase to treat duckweed, significantly enhancing sugar release and resulting in an ethanol yield of 2.20 g L⁻¹ h⁻¹ with an ethanol concentration of 30.8 ± 0.8 g L⁻¹. Ge *et al.*, (2012) found that using *L. minor* and two yeast strains for enzymatic hydrolysis resulted in a higher ethanol yield of 24.0 g L⁻¹ for the ATCC 24859 strain. Cultivation of a high-starch duckweed (*S. polyrhiza*) in a pilot-scale culture pond, achieving an annual starch yield of 9.42 × 10³ kg ha⁻¹. After fermentation, the bioethanol yield reached 6.42 × 10³ L ha⁻¹, approximately 50% higher than that of maize-based fermentation (Xu *et al.*, 2011).

Overall, duckweed's versatility in producing bioenergy and its potential for environmental remediation underscore its importance as a sustainable resource in addressing both energy needs and environmental challenges.

1.3.2. Environmental Remediation

The need to reduce anthropogenic nutrients in aquatic ecosystems to prevent water eutrophication has been widely recognized (Conley *et al.*, 2009). One promising approach for addressing this issue is the cultivation of aquatic plants, which offer an eco-friendly method for restoring eutrophic water bodies by removing nutrients, bioaccumulating toxic substances, and regulating oxygen balance (Dhote & Dixit, 2009). Among these aquatic plants, duckweeds stand out due to their specific physiology, high growth rates, multiple options for biomass usage, simple maintenance, and easy harvesting (Ekperusi *et al.*, 2019).

Eutrophication is primarily driven by the excessive use and runoff of agrochemical fertilizers containing nitrogen (N) and phosphorus (P) (Hilton *et al.*, 2006). Duckweeds have shown potential as

a low-cost solution for wastewater treatment, efficiently removing excess N and P (Cui & Cheng, 2015; Zhou *et al.*, 2018; Zimmo *et al.*, 2004). For example, a study by Zhou *et al.*, (2018) demonstrated that within 15 days, four duckweed species removed over 93% of total N and P from municipal wastewater.

In addition to nutrient removal, duckweeds are also valuable for addressing other environmental contaminants. With the growing demand for food and the extensive use of agrochemicals, herbicides, and other toxic substances are increasingly introduced into ecosystems (Zhou *et al.*, 2023). Duckweeds generally tolerate low concentrations of agrochemicals but can be inhibited at higher levels. For instance, Wilson & Koch, (2013) found that while *L. minor* was severely inhibited by the herbicide norflurazon, it rapidly recovered after the contaminant was removed from the environment.

Duckweeds are also being explored for the phytoremediation of pharmaceuticals, which pose significant toxicity risks to plants (Zhang *et al.*, 2023). Studies have shown that both live and inactivated duckweeds—duckweeds that have been treated to eliminate their biological activity while retaining their physical structure—can effectively remove pharmaceuticals such as fluoxetine and ibuprofen from wetland systems (Reinhold *et al.*, 2010). Interestingly, duckweeds can even use some pharmaceutical compounds, like sucralose, as a carbon source, enhancing their photosynthetic capacity, though other compounds like fluoxetine can negatively impact their growth (Amy-Sagers *et al.*, 2017).

Heavy metal contamination is another significant environmental concern, particularly from mining and industrial activities (Zhou *et al.*, 2023). Traditional remediation methods for heavy metals are often costly and time-consuming (Dhaliwal *et al.*, 2020). However, duckweeds have demonstrated significant potential in monitoring and remediating heavy metals, effectively absorbing them from wastewater. For instance, Chen *et al.*, (2013) found that the lead ion (Pb^{2+}) adsorption capacity of dried powder from *L. aequinoctialis* exceeded 57 mg/g. Similarly, Nie *et al.*, (2015) compared the removal rate of uranium ions (U^{4+}) by live *L. punctata* and its dry powder, finding that 1.25 g/L of dry powder removed nearly 96% of 5 g/L U^{4+} at pH 5, outperforming the live plant's removal rate of 79%. These findings underscore duckweed's potential as an effective tool for environmental cleanup, particularly in heavy metal remediation.

1.3.3. Production of Biopolymers, Biofactories, and Vaccines

Duckweed, a small and fast-growing aquatic plant, has gained recognition as a promising bioreactor for producing a variety of biological products due to its high biomass yield, simple processing, and

cost-effectiveness. Its potential spans across fields such as biopolymers, biofactories, and vaccine production (Yang *et al.*, 2021).

One of the key advantages of duckweed is its ability to produce a wide range of biological products, including vaccines, antibodies, proteins for the pharmaceutical uses, and industrial enzymes. This capability is largely attributed to its high biomass yield and straightforward processing requirements (Liu *et al.*, 2021; Yang *et al.*, 2021). For instance, duckweed has been successfully utilized to produce recombinant biopharmaceuticals, such as the hemagglutinin antigen of the H5N1 virus, demonstrating its potential for low-cost vaccine production (Thu *et al.*, 2015). Additionally, duckweed has been used to produce chicken interleukin-17B (chIL-17B), an immunoadjuvant that significantly enhances immune responses in chickens against infectious bronchitis virus (IBV) (Tan *et al.*, 2022).

Overall, duckweed holds significant promise as a bioreactor for producing biopolymers, biofactories, and vaccines. Its rapid growth, ease of genetic transformation, and ability to produce high-value biological products make it an attractive candidate for various biotechnological applications. Continued research and development in this area are likely to enhance its utility and efficiency in producing a wide range of bioproducts.

1.3.4. Implication of Plant Secondary Metabolites

Plant secondary metabolites are organic compounds that are produced by plants, playing an important role in plant defence against herbivores, pathogens, and environmental stresses (Ashraf *et al.*, 2018). Secondary metabolites derived from duckweed (*L. minor*) have demonstrated significant potential as biostimulants in agriculture, offering a sustainable means to enhance plant growth, nutrient uptake, and resistance to environmental stresses (Mrid *et al.*, 2021). Duckweed extracts, rich in bioactive phytochemicals like phenolics and glucosinolates, are particularly effective in promoting these benefits (Del Buono *et al.*, 2022; Regni *et al.*, 2021).

In practical applications, duckweed extracts have been shown to improve various growth parameters in crops such as maize and olive trees. For example, a 0.50% concentration of duckweed extract was found to be most effective in enhancing germination, biomass, leaf area, pigment content, and vigour index in maize (Del Buono *et al.*, 2022). Similarly, in olive trees, these extracts improved leaf net photosynthesis, stomatal conductance, chlorophyll content, and overall plant biomass production (Regni *et al.*, 2021).

The stimulatory effects of duckweed extracts are partly due to their ability to enhance the assimilation of essential nutrients. In maize, the extracts boosted the uptake of nitrogen (N), phosphorous (P),

potassium (K), calcium (Ca), magnesium (Mg), sodium (Na), iron (Fe), and copper (Cu) (Del Buono *et al.*, 2022). In olive trees, the extracts facilitated increased absorption of nitrogen (N), potassium (K), calcium (Ca), magnesium (Mg), iron (Fe), and zinc (Zn) (Regni *et al.*, 2021).

These benefits are further supported by the presence of signalling compounds, phytohormones, phenolics, and glutathione in duckweed extracts, which collectively contribute to their biostimulant properties (Del Buono *et al.*, 2022; Regni *et al.*, 2021). Additionally, secondary metabolites in these extracts play a crucial role in enhancing plant resilience against both abiotic and biotic stresses.

Duckweed extracts have gained attention as promising biostimulants in agriculture, offering a sustainable and eco-friendly approach to enhancing crop productivity and resilience. These extracts are rich in bioactive secondary metabolites, such as phenolics and glucosinolates, which play a key role in improving plant growth, nutrient assimilation, and stress tolerance. Studies have shown that biostimulant treatments with duckweed extracts can enhance physiological parameters, including chlorophyll content, photosynthetic efficiency, and overall biomass production in various crops, highlighting their potential as a versatile tool for sustainable agricultural practices (Mrid *et al.*, 2021; Panfili *et al.*, 2019).

1.3.5. Human Nutrition and Animal Feed

Lemna and *Wolffia* genera have been granted Generally Recognized as Safe Status by the US Food and Drug Administration. In fact, duckweed has been traditionally consumed in Southeast Asian countries such as Thailand, Laos or Cambodia (Bhanthumnavin & Mcgarry, 1971). Duckweed grows very fast, it can produce a total biomass of up to 50 g in 7 days with an initial biomass of 1 g under ideal conditions (Sree *et al.*, 2015).

Duckweed species are recognized for their high protein content, ranging from 20% to 45.5% per dry weight, positioning them as a significant protein source (Appenroth *et al.*, 2017; Duangjarus *et al.*, 2022; Mbagwu & Adeniji, 1988). The amino acid profile of duckweed closely aligns with the World Health Organization (WHO) recommendations, featuring substantial levels of essential amino acids such as lysine (4.8%), methionine + cysteine (2.7%), and phenylalanine + tyrosine (7.7%) (Appenroth *et al.*, 2017). Notably, *W. globosa* provides all nine essential amino acids, making it a complete protein source (Kaplan *et al.*, 2019). Similarly, *L. minor*, when cultured with different fertilizers, has demonstrated high levels of lysine and phenylalanine, with essential amino acids comprising 44.8% to 50% of the total amino acids (Opiyo *et al.*, 2023). In addition to its protein content, duckweed species exhibit a fat content ranging from 4% to 7% per dry weight, with a significant proportion of

polyunsaturated fatty acids (48% to 71%) and a favourable n6/n3 ratio of 0.5 or less (Appenroth *et al.*, 2017). Furthermore, while the starch content in duckweed typically ranges from 4% to 10% per dry weight under normal conditions (Appenroth *et al.*, 2017), *L. punctata* has been shown to achieve a remarkable starch content of 72.2% under conditions of nutrient limitation and CO₂ elevation treatment (Fang *et al.*, 2023). Some duckweed genera like *Spirodela*, *Landoltia* and *Lemna* have significant levels of calcium oxalate which can cause health issues like kidney stones, while *Wolffia* and *Wolffiella* does not produce calcium oxalate (Landolt, 1986).

Duckweed has been extensively studied as a potential feed ingredient for various animals. In poultry, its inclusion in broiler diets showed mixed results, with higher levels negatively affecting production parameters but lower levels showing promise, especially in terms of body weight gains (Ahammad *et al.*, 2003; Haustein *et al.*, 1992, 1994; Kabir *et al.*, 2005). For laying hens, duckweed inclusion improved feed conversion ratios and egg quality, indicating its potential as a protein source (Anderson *et al.*, 2011; Chowdhury & Akter, 2011; Witkowska *et al.*, 2012). Ducks fed with diets containing duckweed exhibited improved growth performance compared to controls, albeit with variation depending on supplementation levels (Khanum *et al.*, 2005; Ngamsaeng *et al.*, 2004). In pigs, duckweed inclusion in diets showed promising results, with higher levels positively impacting body weight gains (Du, 1998; Gutiérrez *et al.*, 2001; Moss, 1999; Rojas *et al.*, 2014; Van *et al.*, 1997). Similarly, in ruminants, duckweed demonstrated potential as a protein source, improving nitrogen retention and showing comparable nutritional value to soybean meal (Babayemi *et al.*, 2006; Damry *et al.*, 2001; Huque *et al.*, 1996; Reid, 2004). In aquaculture, duckweed inclusion in fish and shrimp diets showed potential for growth enhancement and improved protein efficiency, suggesting its suitability as a feed ingredient (Effiong *et al.*, 2009; El-Shafai *et al.*, 2004; Flores-Miranda *et al.*, 2014; Flores-Miranda *et al.*, 2015; Tavares *et al.*, 2008). While further research is needed to optimize inclusion levels and assess long-term effects, duckweed presents itself as a viable and sustainable alternative feed source across various animal species.

1.4. Duckweed as a Plant-Based Protein Source

As the global population continues to rise, the need for sustainable, nutritious, and environmentally friendly food options is becoming more critical, driving investment in alternative protein sources (Fasolin *et al.*, 2019). Plant-based proteins, insects, algae, and fungi offer a lower environmental footprint compared to traditional animal-based proteins, making them more sustainable choices (Fasolin *et al.*, 2019; Grossmann & Weiss, 2021; López-Martínez *et al.*, 2022; Moura *et al.*, 2022; Sawicka *et al.*, 2020; Van Der Heijden *et al.*, 2023). Given its rapid growth rate and significant protein

accumulation, duckweed stands out as a promising candidate for novel protein sources in this evolving landscape.

Over the last decades, several companies have suggested that products derived from *Lemna* and *Wolffia* species could be used as a protein source for food due to their high protein contents (Appenroth *et al.*, 2017). Duckweed is an aquatic plant that can be grown in artificial ponds built on unproductive lands, absorbing nutrients such as nitrogen from wastewater. The use of wastewater can increase the growth rate and protein content of the duckweed, while reducing nutrients and water lost during irrigation and reduce the subsequent contamination of ground and surface waters (Cheng & Stomp, 2009). In addition, duckweed can accumulate up to 50% starch on a dry-weight basis, and their cell walls contain low content of lignin making the cell wall carbohydrates more accessible and easily be converted in fermentable sugars compared with other plants, which make duckweed a potential feedstock for bioenergy production (Ma *et al.*, 2018). Nutritional composition in plants is strongly affected by the cultivation conditions, such as light and temperature, and also the components of the culture media (Y. Yin *et al.*, 2015). Under favourable cultivation conditions, starch content can be reduced up to 4% whereas protein concentration can increase up to 45% on a dry-weight basis in *L. minor*, being rich in polyunsaturated n³ fatty acids and phytosterols (Appenroth *et al.*, 2017). Most importantly, the content of essential amino acids in duckweed is similar to other vegetable sources such as grains or soybean, according to the WHO recommendations (Edelman & Colt, 2016).

To assess how different food sources, meet the amino acid requirements of animals and humans, the amino acid content of duckweed was compared with that of cereal seeds, legume seeds, and green leaf tissues commonly used for animal feed and human consumption, based on data from various studies. Specifically, the amino acid profiles of *L. gibba* and *L. minor* were compared with various legumes, cereals, and green leaves, as detailed in Table 1.1.

The comparison focused on amino acids that are typically limiting in grains and legumes, such as lysine and methionine, respectively (K. J. Appenroth *et al.*, 2017, 2018; Cheng & Stomp, 2009; Edelman & Colt, 2016; Jahreis *et al.*, 2016). Additionally, threonine was included due to its common deficiency in poultry diets (FAO, 2004), and histidine was considered because it is often present in low concentration in many feed sources. The amino acid requirements for chicken at different ages (FAO, 2004), tilapia-fish (FAO, 2020; Santiago & Lovell, 1988) and humans (WHO, 2007) were then compared with the amino acid concentrations (g amino acid per 100g protein) in *Lemna*, legumes, cereals and green leaves as shown in Figure 1.8.

The results of the comparison indicate that both *Lemna* species meet the nutritional requirements for threonine, histidine, and lysine for animals and humans. However, the concentration of methionine in *Lemna*, like that in legumes, may be insufficient if used as the sole feedstock. The observed differences in amino acid profiles can be attributed to the predominant types of proteins in these sources. In grains and legumes, the most abundant proteins are seed storage proteins (SSPs), which are typically low in lysine and methionine. In contrast, green leaves contain Rubisco (ribulose 1,5-bisphosphate carboxylase/oxygenase) as the major protein, which has a better balance of essential amino acids (Edelman & Colt, 2016).

A balanced amino acid profile and high protein content make duckweed a promising novel protein source for animals and humans. Consuming 100g of duckweed protein per day can meet the essential threonine and lysine nutritional requirements for both animal feed and human consumption. For example, chickens fed with a diet deficient in lysine showed reduced body and tissue wet weights, as well as lower protein and RNA content, compared to those on a diet with a balanced amino acid profile (Tesseraud *et al.*, 1996). Studies have indicated that if threonine intake falls below 75% of the required amount in chickens, broilers begin to lose weight, which could seriously affect poultry health (Ayasan *et al.*, 2009; Duarte *et al.*, 2012). While duckweed has a lower histidine concentration compared to other food sources, it still meets all nutritional requirements. Furthermore, the methionine concentration in duckweed is higher than that found in legumes (Figure 1.8), which is beneficial since methionine is limited in some species. Methionine is crucial for protein synthesis due to its sulphur content, making it an essential amino acid (Baker, 2006; Finkelstein, 1990).

Rubisco (ribulose-1,5-bisphosphate carboxylase/oxygenase) is the main protein found in green leaves. It retains its structure across all green leafy plants and fulfils essential amino acid requirements, as recognized by the Food and Agriculture Organization (FAO) (Kung & Tso, 1978). Rubisco is present in cyanobacteria, chemoautotrophic bacteria, and eukaryotes such as algae and higher plants, comprising up to 50% of the total soluble protein in the plant leaf or inside the microbe (Ellis, 1979). It plays a crucial role in photosynthetic carbon reduction and photorespiratory carbon oxidation. However, its catalytic functions can be influenced by abiotic factors. For instance, high levels of oxygen and low levels of carbon dioxide stimulate the photorespiratory pathway, leading to the production of glycolate, a precursor for amino acid synthesis (Hofmann *et al.*, 2013). Furthermore, the availability of nitrate enhances nitrate assimilation and photorespiration rates, which in turn support Rubisco carboxylation, highlighting the significant impact of nitrogen availability on Rubisco activity and overall plant growth (Guilherme *et al.*, 2019).

1.5. Nitrogen Assimilation

The nitrogen assimilation in plants involves several key steps and enzymes (Figure 1.9). Nitrogen, as an essential element for protein and nucleotide synthesis, is absorbed by plant roots from the soil in inorganic forms, primarily as nitrate or ammonium. Nitrate transporters (NRTs) and ammonium transporters (AMTs) facilitate the uptake of these ions (Krapp, 2015; Masclaux-Daubresse *et al.*, 2010). Once absorbed, nitrate is transported to the shoots, where it undergoes reduction to nitrite by nitrate reductase in the cytoplasm. Subsequently, nitrite is further reduced to ammonium by nitrite reductase in the plastids, and ammonium is assimilated via glutamine synthetase (GS), present in both the plastids and cytoplasm (Lam *et al.*, 1996).

Ammonium, either taken up directly through AMTs or produced from nitrate reduction, is incorporated into amino acids through the GS/glutamine-2-oxoglutarate aminotransferase (GOGAT) cycle. The GS isoenzymes, GS1 and GS2, function in different cellular compartments: cytosolic GS1 is primarily involved in NH_4^+ assimilation in roots, especially during protein degradation and amino acid catabolism, while chloroplastic GS2 assimilates NH_4^+ released during photorespiration or from NO_2^- reduction during NO_3^- conversion. GOGAT enzymes also vary, with ferredoxin-dependent GOGAT (Fd-GOGAT) utilizing ferredoxin for electron transfer, and NADH-dependent GOGAT (NADH-GOGAT) using NADH (Zhou *et al.*, 2022).

Table 1.1. Comparison of methionine, threonine, lysine, and histidine composition (% Total Protein) across *Lemna*, legumes, grains, and green tissues. The table presents a comparison of amino acid composition sourced from various articles, as indicated in the species column with studies by ¹ Appenroth *et al.*, (2017), ² Jahreis *et al.*, (2016), ³ Edelman & Colt, (2016), ⁴ Cheng & Stomp, (2009).

Groups	Species	Amino acid (%total protein)			
		Methionine	Threonine	Lysine	Histidine
<i>Lemna</i>	<i>L. minor</i> ¹	1.6	4	5	1.5
	<i>L. gibba</i> ^{1,4}	1.6	4	4.2	1.6
Legumes	Soya ^{2,3,4}	1.3-1.7	3.9-4.1	6-6.8	2.6-2.9
	Chickpea ^{2,3}	1.4-1.6	3.8-3.9	6.9-7	2.7-2.9
	Lupin ²	0.7	4.2	4.9	2.8
	Green pea ²	0.9	4.2	7.2	2.5
	Lentil ³	0.9	3.9	7.6	3.1
	Peanut ⁴	1	1.6	3	2.1
Grains	Wheat ³	1.6	2.7	2.2	2.4
	Corn ^{3,4}	2.1-2.35	3-3.8	1.85-2.8	2.1-3.1
	Rice ^{3,4}	2.3-3	3.6-3.8	3.2-3.6	1.7-2.3
Green tissues	Spinach ³	2.1	4.9	7	2.6
	Broccoli ³	1.8	3.9	7.4	2.5
	Green grass ⁴	2.5	5.4	5.5	2

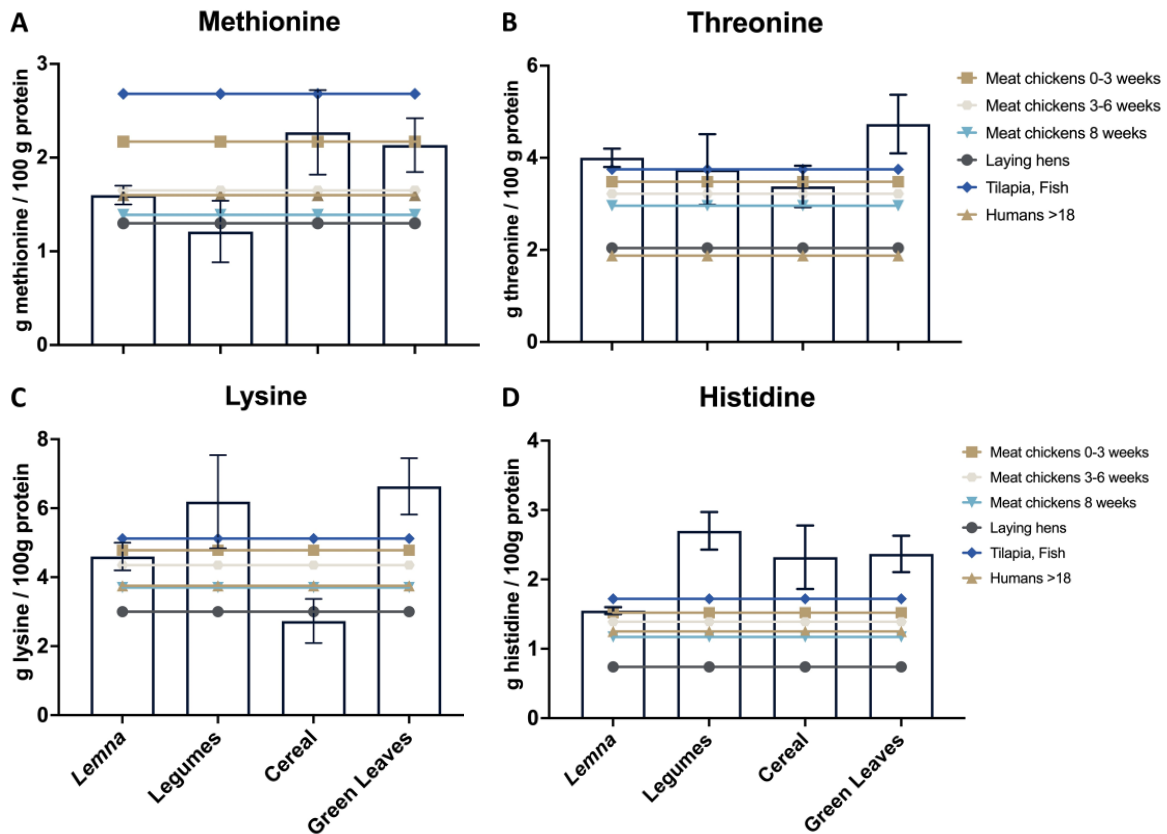


Figure 1.8. Amino acid concentration in different groups of food compared with nutritional requirements in different animals and humans. Amino acids concentration is represented as g amino acids per 100 g total protein while the nutritional requirements are measured like g amino acids per day required by that diet. Each amino acid is explained in different graphs. A) Methionine, B) Threonine, C) Lysine and D) Histidine. White bars represent four different food groups: *Lemna*, legumes, cereals, and green tissues. The different coloured lines are nutritional requirements for different animals: Light brown line with square dots for meat chickens from 0 to 3 weeks, grey line for meat chicken from 3 to 6 weeks, light blue line for meat chickens at 8 weeks old, dark brown line for laying hens (FAO, 2004), dark blue line for tilapia (fish) (FAO, 2020; Santiago & Lovell, 1988) and light brown line with triangle dots for humans over 18 years old (WHO, 2007).

Aminotransferases then catalyse the transfer of the amino group from glutamate (Glu) to form various amino acids. Asparagine synthetase (AS) is responsible for synthesizing asparagine (Asn) and glutamate from aspartate and glutamine, respectively. During the senescence stage of leaves, nitrogen is stored within their structure, but as senescence progresses, nitrogen is remobilized to support the development of new seeds (Lam *et al.*, 1996). Notably, up to 95% of the seed protein is derived from amino acids released from protein degradation in senescing leaves (Taylor *et al.*, 2010).

Unlike many higher plants, duckweed does not frequently produce seeds. Primarily consisting of leaf structures, it contains a significant amount of Rubisco (ribulose 1,5-bisphosphate carboxylase/oxygenase) which makes up about 50% of its protein content. This enzyme complex is crucial for its photosynthetic activity (Kawashima & Wildman, 1970).

In duckweed, nitrogen assimilation occurs in both roots and leaves, where NRTs and AMTs are present (Zhou *et al.*, 2022). This dual-site uptake enhances nitrogen use efficiency (NUE), enabling up to 68 kg of biomass per kg of nitrogen absorbed (Guo *et al.*, 2020). The plant's simple morphology and widespread transporters optimize nutrient absorption and utilization.

1.6. Environmental Impacts on Duckweed Nutritional Composition

Environmental factors and growth conditions significantly impact the nutritional composition of duckweed, affecting its contents of proteins, lipids and carbohydrates. For instance, Stewart *et al.*, (2021) demonstrated that *L. gibba* could maintain a high growth rate across a broad range of photosynthetic photon flux densities (PFDs), from as low as 50 $\mu\text{mol photons m}^{-2}\text{s}^{-1}$ to as high as 1000 $\mu\text{mol photons m}^{-2}\text{s}^{-1}$. In contrast, Ishizawa *et al.*, (2017) found that co-cultivating *L. minor* with bacterial communities from various aquatic environments resulted in significant variations in duckweed growth, with changes ranging from -24% to +14% compared to aseptic controls.

Additionally, environmental stressors such as heavy metals impact duckweed's nutritional profile. Sree & Appenroth, (2014) reported that cadmium ions induced starch accumulation in duckweed after four days of treatment at concentrations that almost completely suppressed growth. Hou *et al.*, (2007) observed that exposure to copper and cadmium ions led to a decrease in soluble protein content, with more pronounced effects at higher concentrations. Similarly, Su *et al.*, (2019) noted that the presence of aluminium in the growth medium reduced protein content by 43% compared to duckweeds grown without aluminium.

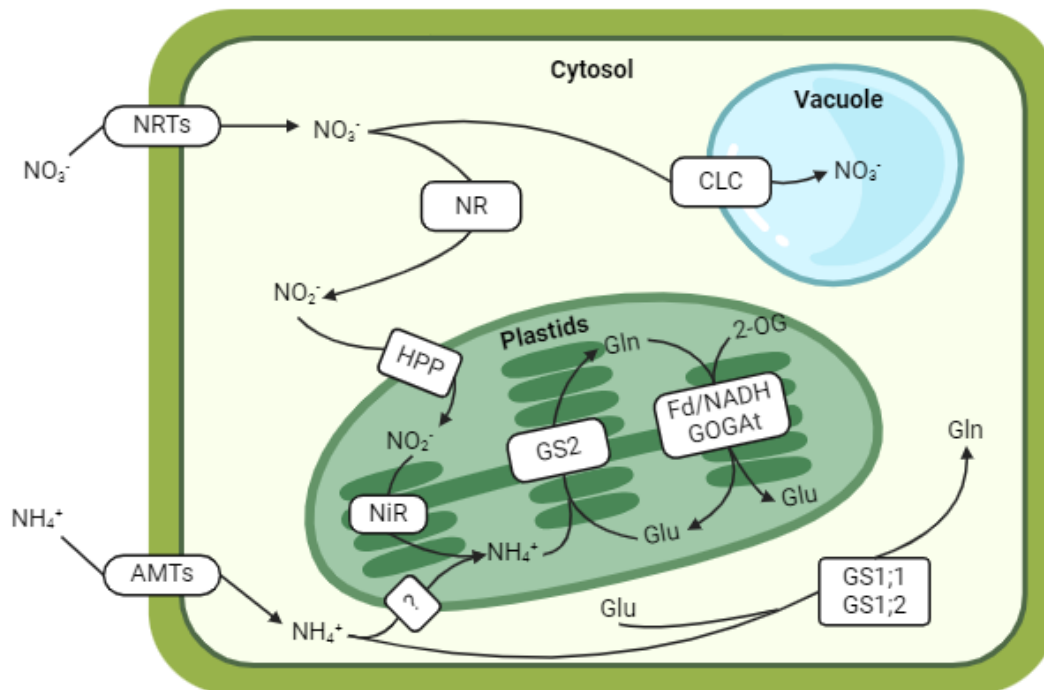


Figure 1.9. Simplified diagram of the nitrogen assimilation pathway in plants. Nitrate enters the cell via Nitrate Transporters (**NRTs**), while ammonium is taken up through Ammonium Transporters (**AMTs**). Nitrate Reductase (**NR**) converts nitrate into nitrite, which is then transported into plastids by Histidine-Proline-Proline (**HPP**). Inside the plastids, Nitrite Reductase (**NiR**) reduces nitrite to ammonium. The resulting ammonium is assimilated by cytosolic glutamine synthetase isoforms (**GS1;1** and **GS1;2**) and chloroplastic glutamine synthetase (**GS2**), along with Ferredoxin-dependent glutamate-oxoglutarate aminotransferase (**Fd-GOGAT**) and NADH-dependent glutamate-oxoglutarate aminotransferase (**NADH-GOGAT**), to form glutamate (Glu) and glutamine (Gln), which serve as precursors for amino acid biosynthesis. Excess nitrate is stored in the vacuole and transported across the membrane via the chloride channel (**CLC**).

Furthermore, Ullah *et al.*, (2021) highlighted that low salinity levels promote higher protein content in duckweed, while increased salinity leads to a reduction in lipid content and a decrease in carbohydrate levels. The study revealed that the highest carbohydrate percentages were obtained at moderate salt concentrations, whereas higher salt levels resulted in significant reductions in both growth and carbohydrate content.

A crucial factor in duckweed's nutritional profile is nitrogen source in the growth medium. NH_4^+ and NO_3^- are commonly used as nitrogen fertilizers in agriculture (Coskun *et al.*, 2017). Research by Zhou *et al.* (2022) indicates a preference for NH_4^+ over NO_3^- . Nitrate assimilation is more energy-intensive because NO_3^- must be converted to NH_4^+ before it can be used for protein synthesis. However, excess NH_4^+ accumulation can lead to toxicity, causing chlorosis and reduced growth rates (Britto & Kronzucker, 2013), primarily due to the increase of reactive oxygen species (ROS), which triggers oxidative damage and results in cell death (Wang *et al.*, 2016). Regardless of this, duckweed demonstrates higher resistance to NH_4^+ stress compared to other plants (Huang *et al.*, 2013; Tian *et al.*, 2021).

1.7. Duckweed Response to Heat Stress

A positive environment is crucial for plant development, as plants are sessile organisms unable to move or relocate. Their growth rate, yield, and overall evolution are intricately tied to environmental conditions (Lippmann *et al.*, 2019). With the rise in global temperatures due to global warming, future plant generations are increasingly at risk of heat stress (HS), which can have severe, and sometimes lethal, impacts on their health and productivity (Hedhly *et al.*, 2009).

Heat stress disrupts critical plant processes such as growth, germination, development, reproduction, and yield (Hasanuzzaman *et al.*, 2013), since high temperatures can damage essential physiological functions including photosynthesis, respiration, transpiration, and cell structure (Ben-Asher *et al.*, 2008). To combat these challenges, plants have evolved intricate and multifaceted systems known as Heat Stress Responses (HSR). Among the key components of these responses are heat shock proteins (HSPs) and reactive oxygen species (ROS)-scavenging enzymes, which play crucial roles in mitigating heat-induced damage and maintaining cellular stability under stress conditions (Ohama *et al.*, 2017).

Heat shock proteins (HSPs) play a vital role in protecting plants from heat stress (HS) by acting as molecular chaperones that help regulate protein quality. Key HSPs include HSP100, HSP90, HSP70, HSP60, and small heat shock proteins (sHSPs). These proteins are essential for renaturing denatured proteins caused by heat stress, ensuring proper protein folding and function (Kotak *et al.*, 2007; Qu *et*

al., 2013). They are well-established targets of HS-responsive transcription factors (TFs) and are upregulated during heat stress responses.

In addition to HSPs, reactive oxygen species (ROS)-scavenging enzymes such as ascorbate peroxidase (APX) and catalase (CAT) play a critical role in mitigating oxidative damage during heat stress. ROS, including hydrogen peroxide (H₂O₂), superoxide anions (O₂⁻), and singlet oxygen (1O₂), are generated under stress conditions and can enhance HS-responsive pathways as well as contribute to cell death if not adequately managed (Baxter *et al.*, 2014; Suzuki & Mittler, 2006).

As presented in the Figure 1.10, heat stress transcriptional networks involve a complex array of transcriptional regulators. HEAT SHOCK TRANSCRIPTION FACTOR A1s (HsfA1s) serve as 'master regulators' in these networks, crucial for activating various heat stress-responsive genes (Liu *et al.*, 2011; Mishra *et al.*, 2002). HsfA1s are known to directly regulate the expression of genes encoding other important HS-responsive TFs, such as DEHYDRATION-RESPONSIVE ELEMENT BINDING PROTEIN 2A (DREB2A), HsfA2, HsfA7a, HsfBs, and MULTIPROTEIN BRIDGING FACTOR 1C (MBF1C) (Yoshida *et al.*, 2011). DREB2A itself induces the expression of HsfA3 as a direct target gene with a coactivator complex of NUCLEAR FACTOR Y, SUBUNIT A2 (NF-YA2), NF-YB3, and DNA POLYMERASE II SUBUNIT B3-1 (DPB3-1)/NF-YC10. DREB2A, in particular, induces the expression of HsfA3 as a direct target gene, often in coordination with a coactivator complex that includes NUCLEAR FACTOR Y, SUBUNIT A2 (NF-YA2), NF-YB3, and DNA POLYMERASE II SUBUNIT B3-1 (DPB3-1)/NF-YC10 (Sato *et al.*, 2014). These transcriptional regulators collectively enhance thermotolerance or long-term adaptation to heat stress (Ohama *et al.*, 2017).

Research on high-temperature stress has been extensively documented for vegetables (Hu *et al.*, 2021), fruits (Almeida *et al.*, 2021), and other crops worldwide (Sah & Sherpa, 2020). In aquatic plants, exposure to high temperatures triggers various physiological and molecular mechanisms that help them survive under stress. For example, *Ipomoea aquatica* shows that heat stress negatively affects photosynthesis and increases oxidative stress, activating specific genes involved in thermal adaptation (Guo *et al.*, 2020). Similarly, studies in *Potamogeton* species highlight how thermotolerant species produce heat shock proteins (HSPs) and transcription factors, offering protection against thermal damage (Amano *et al.*, 2012). Invasive species like *Gracilaria vermiculophylla* also exhibit heat resistance traits, which have been key for their colonization in new thermal environments (Hammann *et al.*, 2016). Research on *Elodea nuttallii* further supports the idea that gradual heat exposure enhances plant protective mechanisms more effectively than abrupt heat shocks, demonstrating the diversity of responses in aquatic species (De Silva & Asaeda, 2018).

A transcriptomic study on *Pyropia haitanensis* found that a heat-tolerant strain expressed genes related to HSPs, antioxidant defences, and energy metabolism more efficiently than heat-sensitive strains, protecting its cells from heat damage (Wang *et al.*, 2018). These insights are crucial for improving *Pyropia* cultivation under rising global temperatures (Wang *et al.*, 2018).

In the case of duckweed, Shang *et al.*, (2022) focused on the physiological and transcriptional responses of *S. polyrhiza* under heat stress. The researchers observed that superoxide dismutase (SOD) levels initially increased before declining, whereas malondialdehyde (MDA) content consistently rose, indicating oxidative damage. Additionally, they identified fourteen differentially expressed transcription factors (TFs) involved in heat stress responses, including those from the HSF, ERF, WRKY, and GRAS families.

Despite significant advances, there remains a gap in understanding how different duckweed clones respond to heat stress, particularly regarding protein content. Previous research on *Spirodela polyrhiza* has shown that heat stress induces oxidative damage and fluctuating antioxidant responses, affecting overall plant health. However, its impact on protein levels, particularly under different temperature regimes, has not been thoroughly explored. In *Spirodela*, heat-responsive genes, including those involved in oxidative stress regulation and protein metabolism, have been identified, suggesting that protein levels may be closely linked to thermotolerance. This study aims to build on these findings by investigating how heat stress specifically influences protein content across multiple *Lemna* clones, shedding light on the genetic factors controlling protein synthesis and degradation under environmental stresses.

To achieve stable, protein-rich duckweed production for human and animal consumption, it is crucial to investigate the effect of abiotic stresses, particularly heat stress and nitrogen sources, on duckweed's protein content. Results of previous studies show that heat stress can significantly influence duckweeds biochemical composition, including protein levels (Shang *et al.*, 2022) and the nitrogen removal efficiency and protein yield of duckweed are influenced by nitrogen levels (Zhou *et al.*, 2022). Therefore, both heat stress and nitrogen levels play a pivotal role in determining the protein yield in duckweed, which needs further investigation to optimize production for nutritional use. Understanding and managing these abiotic stress factors can lead to more consistent and higher-quality protein production in duckweed, which is vital for its use as a sustainable food source.

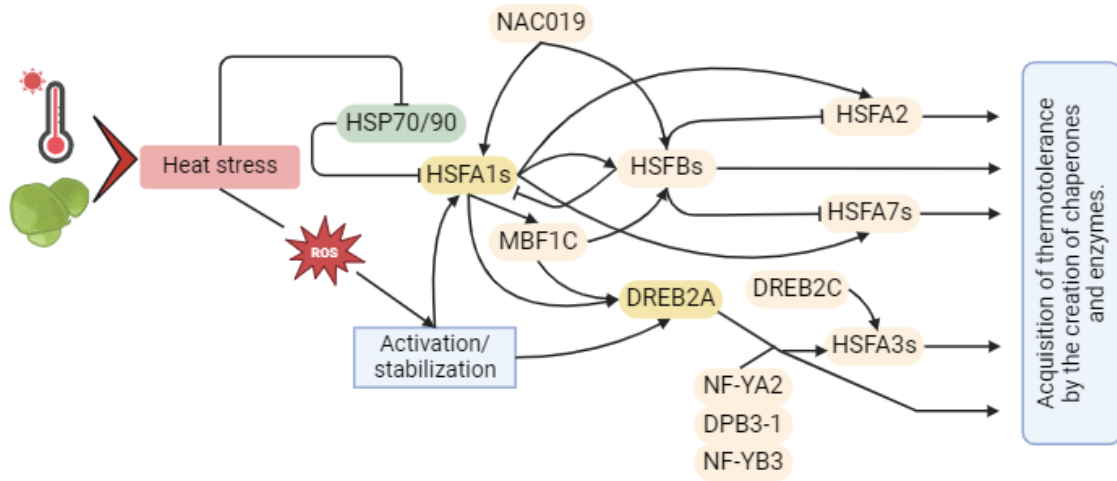


Figure 1.10. Transcriptional regulatory network in plant heat stress responses. Heat stress induces the generation of reactive oxygen species (ROS), triggering a cascade of regulatory events. HSF1 proteins act as central regulators, activating transcription factors like HSF2, HSF3, HSF7, HSFBs, and DREB2A, which regulate downstream heat-responsive genes. Proteins such as HSP70/90 stabilize HSF1s and assist in maintaining protein homeostasis. Additional transcription factors, including NAC019, MBF1C, and NF-Y family members, integrate stress signals to enhance thermotolerance by activating chaperones and enzymes. This network highlights the intricate interplay between transcription factors, heat shock proteins, and co-regulators in acquiring heat tolerance in plants.

1.8. Aims and Objectives of the Project

This project aims to investigate the impact of heat and nitrogen source on duckweed growth and protein content. By exploring these two critical environmental factors, this research will help us to understand how nitrogen availability and temperature variations impact both the biochemical composition and overall productivity of different duckweed clones. The findings will contribute to optimizing duckweed's use as a sustainable protein source for human and animal consumption. The project has three objectives, each corresponding to a dedicated experimental chapter:

- Objective 1: To explore the influence of different nitrogen sources on protein yield across distinct clones of *Lemna minor* and *Lemna gibba* and examine the differences in expression of nitrogen assimilation genes in these species (Chapter 3).
- Objective 2: To distinguish heat-tolerant and heat-sensitive *Lemna* clones based on their physiological responses to heat stress. Differences in traits such as growth, chlorophyll content, and nitrogen levels were analysed to determine variations in heat tolerance among clones (Chapter 4).
- Objective 3: To assess changes in protein content among heat-tolerant and heat-sensitive clones under different temperature conditions and identify differential gene expression patterns among the clones through transcriptomic analysis (Chapter 5).

2. Chapter 2: General Materials and Methods

2.1. Plant Materials

2.1.1. Establishment of Duckweed Collection at University of Hertfordshire (UH)

To maintain the collection, standard operating procedures (SOPs) for collection, growing, sterilization and identification needed to be produced since this is the first project on duckweed at the UH. When conditions for duckweed collected from Hertfordshire were set, *L. gibba* clones were purchased from Rutgers Duckweed Cooperative Stock (Rutgers Duckweed Stock Cooperative - Retrieved on 18/12/2024). The number of clones maintained at UH was 50.

In this thesis, 20 duckweed clones were collected from local ponds in Hertfordshire, UK, and 30 clones were purchased from the Rutgers Duckweed Stock Cooperative. The clones were listed on Table 2.1, where ID number, species and location is explained.

2.1.1.1. Field Sampling, Processing, and Morphological Identification of Duckweed

Duckweeds were collected from the pond surface with a net, trying to not disturb the aquatic environment. Other vegetative or animal organisms were removed from the sample and then duckweed samples were saved in labelled plastic zip-lock bags. Besides, pH of the pond water was measured with a portable pH meter and ammonia, nitrate and nitrite concentration were measured with a test kit (JNW Direct, 9 in 1 Aquarium Test Strips). Pond location was noted to trail different duckweed clones collected for geographic analysis.

Promptly, samples were transported to the lab for a deep clean. Samples were placed on a 2mm mesh strainer where duckweed were cleaned with tap water until all non-duckweed materials (small sticks, leaves, etc.) were removed. Then, it was finally washed with deionized water (DIW, <15mΩ). Half of the samples were dried at 60°C for 48 hours for protein quantification analysis, and the remaining samples were stored at 4°C in 50 ml Falcon tubes until further use.

To visualise duckweed morphological features for duckweed identification, chlorophyll was removed from duckweed tissues by 1 hour incubation series from 50 to 100% ethanol at room temperature in dark conditions (Miazek & Ledakowicz, 2013). After removing chlorophyll, samples were stored in 75% ethanol at 4°C in dark conditions.

Table 2.1. List of duckweed species at UH duckweed collection. It is composed by clones purchased at Rutgers Duckweed Stock Cooperative and collected in local ponds. Last eight *Lemna* samples were not taxonomically identified by barcoding identification.

ID	Species	Continent	Country	City
5615	<i>L. gibba</i>	Asia	Israel	Soreq National Park, Palmachim
6861	<i>L. gibba</i>	Europe	Italy	Toscana, Lagodi, Massaciuccoli
7021	<i>L. gibba</i>	Europe	Spain	Andalusia, Cordoba
7245	<i>L. gibba</i>	Africa	South Africa	Cape, Stellenbosch, Jonkershoek
7263	<i>L. gibba</i>	Europe	Greece	Thessalia, Trikala
7532	<i>L. gibba</i>	Europe	Eire	Carlow Co., Barrow R.
7537	<i>L. gibba</i>	Africa	Spain	Tenerife, Puerto de la Cruz
7641/7582	<i>L. gibba</i>	Asia	Israel	Hadera, Kirket Batih
7705	<i>L. gibba</i>	Asia	India	Gujarat, Khaira, Anand
7749	<i>L. gibba</i>	Europe	Belgium	Liege, Terwagne
7763	<i>L. gibba</i>	Europe	UK	Wales, Cardiff, Wentlooge level
7784	<i>L. gibba</i>	Africa	Ethiopia	Shoa, 30 km E of Addis Abeba
7796/G3	<i>L. gibba</i>	Europe	Italy	Sicilia, Catania, Bot. Garden
7798	<i>L. gibba</i>	America	Peru	Lima, Laguna de Villa
7805	<i>L. gibba</i>	Europe	France	Camargue, La Tourdu Vallat
8124	<i>L. gibba</i>	America	USA	Arizona, Pima Co., Arivaca
8428	<i>L. gibba</i>	Europe	Switzerland	Aargau, Koblenz
8655	<i>L. gibba</i>	America	Argentina	Cordoba, Rio Cuarto, Gigena-Elena
8678	<i>L. gibba</i>	Asia	India	Kashmir, Srinagar
8682	<i>L. gibba</i>	Asia	Saudi-Arabia	Asir-Baha, 2020m
8703	<i>L. gibba</i>	Asia	Japan	Honshu Aichi
8738	<i>L. gibba</i>	America	Argentina	Rio Negro, General Roca
9248	<i>L. gibba</i>	Europe	Italy	Alto Adige, Trento
9255	<i>L. gibba</i>	Europe	Finland	Uusimaa, Pukila
9435	<i>L. gibba</i>	Europe	Albania	Lashnja, Distr. Lushnjy, Saveri
9481	<i>L. gibba</i>	Europe	Denmark	Mon
9532	<i>L. gibba</i>	Europe	Germany	Marburg
9583	<i>L. gibba</i>	Europe	Poland	Topilo
9591	<i>L. gibba</i>	Europe	Hungary	Szarvas, Arboretum, river Körös
9619	<i>L. gibba</i>	Europe	Albania	Pogradeci
Manor	<i>L. gibba</i>	Europe	UK	Harpenden
SD	<i>L. minor</i>	Europe	UK	Harpenden
DG4/7868	<i>L. minor</i>	Europe	Ireland	Dublin, Ballsbridge
DG8/9441	<i>L. minor</i>	Europe	Germany	Marburg St.
DG9/8292	<i>L. minor</i>	Asia	Iran	Mazandaran, Ghassem Abbath
DG10/7766	<i>L. minor</i>	Pacific	NZ	Southern Island
DG12	<i>L. minor</i>	Europe	UK	
Colour	<i>L. gibba</i>	Europe	UK	Hackney Wick, London
Jen Young	<i>L. gibba</i>	Europe	UK	Clifton Road, London
O. Wood	<i>L. gibba</i>	Europe	UK	Hatfield, Hertfordshire
S. Grove	<i>L. gibba</i>	Europe	UK	Hertford, Hertfordshire
The pond	<i>L. gibba</i>	Europe	UK	Hatfield, Hertfordshire
Pinetum	<i>Lemna</i>	Europe	UK	Hertford, Hertfordshire
Hatfield	<i>Lemna</i>	Europe	UK	Hatfield, Hertfordshire
HG	<i>Lemna</i>	Europe	UK	Hertford, Hertfordshire
Ashridge	<i>Lemna</i>	Europe	UK	Welwyn Garden City, Hertfordshire
Cambridge	<i>Lemna</i>	Europe	UK	Cambridge, Cambridgeshire
Tewimbury	<i>Lemna</i>	Europe	UK	Welwyn Garden City, Hertfordshire
D. Lake	<i>Lemna</i>	Europe	UK	Welwyn Garden City, Hertfordshire
D. Pond	<i>Lemna</i>	Europe	UK	Welwyn Garden City, Hertfordshire

2.1.1.2. Duckweed Sterilization

To store the clones under aseptic conditions, duckweed plants were sterilised following the method established by Appenroth *et al.* (2015). Plants were washed 4 times with 7.5% NaOCl for 3-, 4-, 5- and 6-min. Fronds were rinsed gently with water after each bleach-bath. After bleach bath, samples were transferred into 50 ml Falcon Tubes containing sterilized Schenk and Hildebrandt (SH) medium with the following composition 0.68 mM CaCl₂·2H₂O, 12.4 mM KNO₃, 0.81 mM MgSO₄·7H₂O, 1.3 mM (NH₄)H₂PO₄, 30 μM MnSO₄·H₂O, 40 μM H₃BO₃, 1.74 μM ZnSO₄·7H₂O, 3.0 μM KI, 0.4 μM CuSO₄·5H₂O, 0.21 μM Na₂MoO₄·2H₂O, 0.21 μM CoCl₂·6H₂O, 27.0 μM FeNaEDTA, 2.74 μM Na₂EDTA·2H₂O (Schenk & Hildebrandt, 1972; Ziegler *et al.*, 2015), containing sugar (50 mM glucose or 25 mM sucrose) for 2 weeks. The pH was adjusted to 5.5 with 0.5 mM HCl. After sterilization process, the mother frond died but seven days later, the daughter grown from the meristematic pockets in completely aseptic conditions as shown in Figure 2.1. After 14 days, if the medium remained clear, the sterilization was successful. Afterwards, clones were stored in CE cabinets at 15°C in 300 ml Erlenmeyer flasks containing 100 ml sterile SH nutrient medium, with continuous white light at 30 μmol·m⁻²·s⁻¹ (photosynthetically active radiation) from fluorescent tubes TLD 36W/86 (Philips, Eindhoven, the Netherlands).

2.1.1.3. Pre-cultivation and Cultivation

For pre-cultivation phase, plants were acclimated for two weeks keeping the plant young with a high relative growth rate to ensure reproducible results. When samples were cleaned, they were cultivated in Controlled Environment (CE) cabinets at 20°C in magenta vessels containing 300 ml sterile nutrient medium under continuous white light at 100 μmol·m⁻²·s⁻¹ (photosynthetically active radiation) from fluorescent tubes TLD 36W/86 (Philips, Eindhoven, the Netherlands) following the protocol ISO 20079, (2005). To avoid nutrient limitation, medium was refreshed every week. Schenk and Hildebrandt medium was employed with the composition explained in section 0.

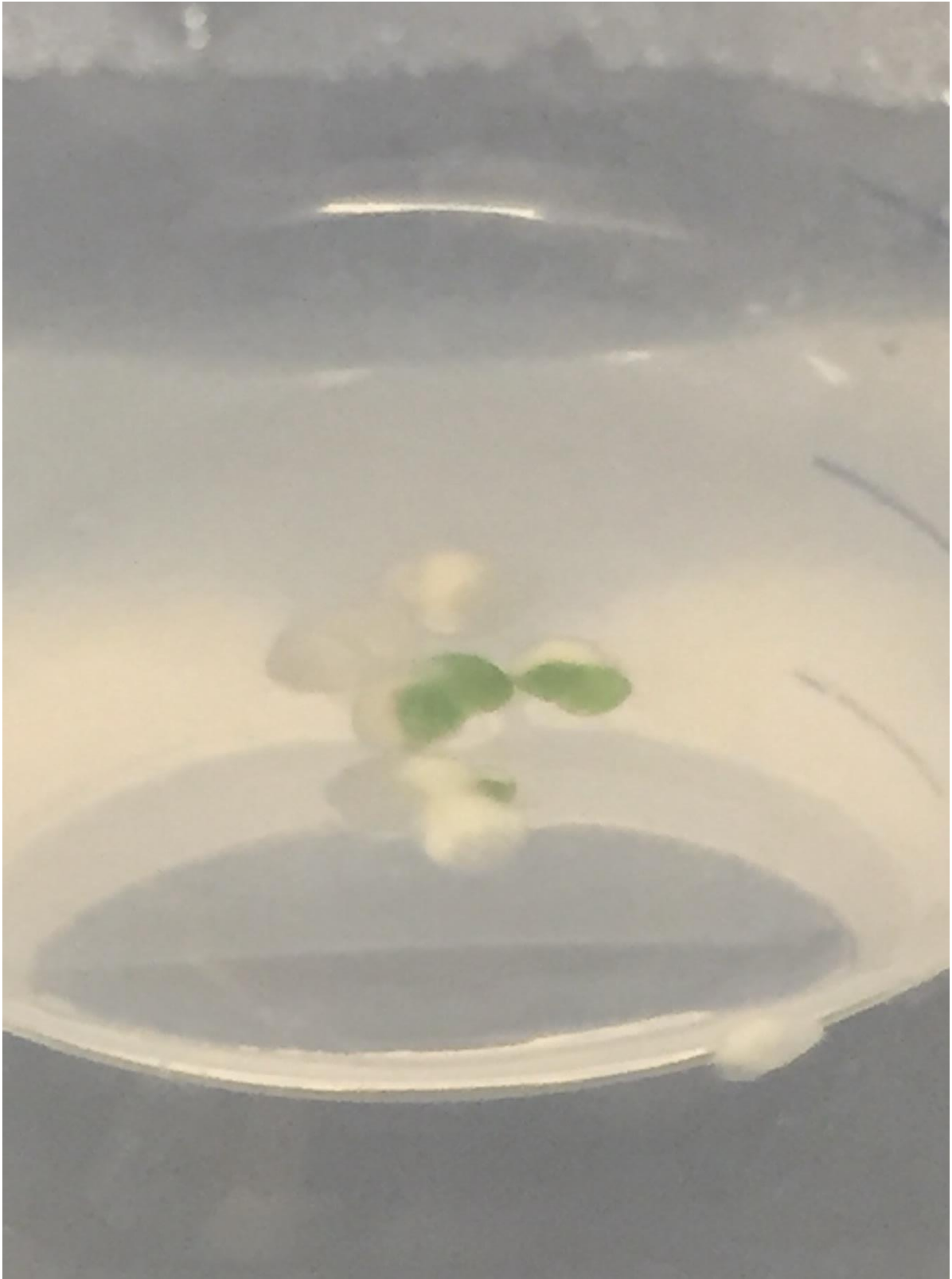


Figure 2.1. Daughter duckweed frond being born in aseptic conditions.

2.2. Nucleic Acids Extraction and Purification

2.2.1. DNA Extraction

DNA extraction from duckweed clones was conducted using a modified protocol from the DNeasy Plant Mini Kit (Qiagen, Valencia, CA, USA). Fresh duckweed tissue (80 mg) was prepared by removing excess water and placing the sample in a 2 ml Eppendorf tube with stainless steel bead 0.5 cm. The tissue was disrupted using a TissueLyser (Tissuelyser II) at 12,000 rpm for 30 seconds, ensuring complete homogenization.

For cell lysis and RNA removal, 400 μ l of Buffer AP1 and 4 μ l of RNase A were added to the homogenized tissue. The mixture was briefly vortexed and incubated at 65°C for 10 min, with occasional gentle inversions to facilitate the process. After lysis, 130 μ l of Buffer P3 was added to precipitate proteins, followed by incubation on ice for 5 min. The lysate was then centrifuged at 14,000 rpm for 5 min to separate proteins from nucleic acids.

The supernatant was transferred into a QIAshredder spin column and centrifuged for 2 min at 14,000 rpm. The flow-through was collected into a new tube, and 1.5 volumes of Buffer AW1 were added and mixed thoroughly. The mixture was then transferred to a DNeasy Mini spin column and centrifuged at 8,000 rpm for 1 min. This step was repeated with the remaining sample.

For the wash steps, the spin column was placed in a clean collection tube, and 500 μ l of Buffer AW2 was added, followed by centrifugation at \geq 8,000 rpm for 1 min. A second wash was performed with an additional 500 μ l of Buffer AW2, centrifuged at 14,000 rpm for 2 min to ensure complete removal of contaminants.

To elute the DNA, the spin column was transferred to a new 1.5 ml microcentrifuge tube, and 100 μ l of Buffer AE was added. The column was incubated at room temperature (15–25°C) for 5 min before centrifuging at 8,000 rpm for 1 min. The purified DNA was subsequently stored at -20°C for future use in downstream applications.

2.2.2. RNA Extraction

RNA extraction from duckweed plants was carried out using a modified protocol from the E.Z.N.A.[®] Plant RNA Kit Protocol (Norcross, Georgia, USA). Fresh green leaves (80 mg) were harvested from plants cultivated under various experimental conditions. The tissue samples were immediately frozen in liquid nitrogen and ground with ceramic beads in a TissueLyser (Tissuelyser II) at 12,000 rpm for 30

sec. The resulting powder was lysed by adding 500 μ L of RB Buffer containing 2-mercaptoethanol, followed by thorough vortexing to ensure complete mixing and prevent clump formation.

To remove cell debris and homogenize the lysate, the samples were centrifuged at 12,000 x rpm for 5 min. The supernatant was then transferred to a new tube, and one volume of 70% ethanol was added to the lysate, mixed, and transferred to a HiBind[®] RNA Mini Column. This column, inserted into a collection tube, facilitated RNA binding during a 1-min centrifugation at 11,000 rpm. DNA contaminants were eliminated by adding a DNase I solution directly to the column membrane and incubating at 37°C for 30 min. The column was then washed with RNA Wash Buffers I and II, followed by a drying spin to remove residual ethanol. Finally, RNA was eluted with 50 μ L of preheated nuclease-free water, and the purified RNA was stored at -70°C for further analyses.

2.3. Nucleic Acid Quantification and Quality Control Checks

2.3.1. Electrophoresis and Visualization of Nucleic Acids in Agarose Gels

Nucleic acid samples were visualised through an agarose gel with TAE buffer (40 mM Tris-Acetate; 1mM EDTA; pH 8) with GelRed[®] Nucleic Acid Gel Stain 0.1 %(p/v) from Biotium. The agarose gel concentration varies depending on the length of the nucleic acid. A 1.2% agarose gel was used, as lower concentrations (e.g., 0.8%) are suitable for larger DNA fragments, while higher concentrations (e.g., 2%) improve resolution for smaller fragments. For nucleic acids size determination, 1Kb and 100 bp ladder was added to the gel. Nucleic acid bands were visualised by ultraviolet camera where picture was taken. For RNA samples, RNA denaturalization step preceded the loading. Samples were heated at 65°C for 5 min to denature the RNA. After heating, samples were placed on ice for 2 min to ensure cooling and stability. 1 kb and 100 bp ladders were added in the gel.

2.3.2. DNA Contamination Analysis Through PCR Techniques and Visualization in Agarose Gel

To check for DNA contamination in the RNA samples, a polymerase chain reaction (PCR) was conducted using primers specific to the reference gene Glyceraldehyde-3-phosphate dehydrogenase (GAPDH). The primers used for this assay are listed in Table 2.2. The PCR protocol was designed to amplify any genomic DNA present in the RNA samples. The thermal cycling conditions included an initial denaturation at 94°C for 3 min, followed by 30 cycles of denaturation at 94°C for 45 sec, annealing at 55°C for 30 sec, and extension at 72°C for 1 min. The process concluded with a final extension step at 72°C for 10 min.

Subsequently, a final extension step was conducted at 72°C for 10 min to ensure thorough amplification. The PCR reaction setup included 2.5 µL of 10x PCR buffer containing 0.75 µL of 50 mM MgCl₂, 0.5 µL of 10 mM dNTP Mix, 1.25 µL each of 10 µM forward and reverse primers designed using Benchling (Table 2.2), and 0.1 µL of Taq DNA Polymerase (1 unit), which was sourced from Invitrogen. The reaction mixture was prepared using nuclease free water to reach a final volume of 25 µL.

After PCR amplification, the products were analysed via gel electrophoresis (see previous section 2.3.1). The presence of bands corresponding to the expected size of the GAPDH PCR product (98 bp) on the gel would indicate DNA contamination in the RNA samples. Conversely, the absence of such bands would confirm the absence of DNA contamination, thereby verifying the purity of the RNA samples.

2.3.3. Nanodrop Spectrophotometer

The concentration and purity of the nucleic acids were determined by measuring UV absorbance at 260 nm using the Nanodrop® ND 1000 Spectrophotometer. An optical density (OD) unit at 260 nm corresponds to 40 µg/mL for RNA and 50 µg/mL for DNA. A 260/280 ratio of 1.8-2.0 indicates good DNA purity, while a ratio of 2.0 suggests pure RNA. In contrast, a ratio of approximately 0.6 indicates protein contamination. Additionally, a 260/230 ratio of 2.0-2.2 signifies high nucleic acid purity; deviations from these values may suggest contamination with substances absorbing at 230 nm, such as carbohydrates or phenol.

To proceed with the analysis, the Nanodrop spectrophotometer software was launched, and the appropriate analysis tab (e.g., "Nucleic Acid" for DNA or RNA concentration measurement) was selected. With the sampling arm open, 1.5 µL of nuclease-free water was pipetted onto the lower measurement pedestal to establish a blank baseline. Following this, 1.5 µL of the RNA sample was applied to the lower pedestal, and the sampling arm was closed. The spectral measurement was initiated through the software on the connected PC, and the sample column was automatically positioned between the upper and lower pedestals for measurement. Upon completion, the sampling arm was opened, and both the upper and lower pedestals were carefully cleaned with a soft laboratory wipe to prevent cross-contamination.

After the final measurement, all surfaces were thoroughly cleaned with deionized water to ensure the instrument's cleanliness and maintain its integrity for subsequent uses.

Table 2.2. List of primers used for end-point PCR.

Marker	Primer sequence	Amplicon size	T ^a optimum
<i>GAPDH</i>	Forward: 5' -CCTCCACCATTGACTCCTCGTT- 3'	98 bp	62 °C
	Reverse: 5' -CACCCGTTGACTGTATCCCCAT- 3'		
<i>atpF-atpH</i>	Forward: 5' -ACTCGCACACACTCCCTTTCC- 3'	675 bp	53 °C
	Reverse: 5' -GCTTTTATGGAAGCTTTAACAAT- 3'		
<i>psbK-psbI</i>	Forward: 5' -TTAGCATTTGTTTGGCAAG- 3'	544 bp	51 °C
	Reverse: 5' -AAAGTTTGAGAGTAAGCAT- 3'		

2.3.4. Quantification with Qubit Fluorometer

To determine the concentration of nucleic acids, the Qubit® 4 Fluorometer from Invitrogen Life Technologies was employed. The procedure began with the preparation of the Qubit® Working Solution for Broad Range by diluting the Qubit® RNA BR Assay Kit reagent in Qubit® buffer at a 1:200 ratio. For each standard and user sample, 200 µL of the Working Solution was prepared. Specifically, 190 µL of the Working Solution was combined with 10 µL of the standard kit, and 198 µL of the Working Solution was mixed with 2 µL of each sample, resulting in a total volume of 200 µL per assay.

The samples were then vortexed for 2-3 seconds to ensure thorough mixing. Following this, they were incubated at room temperature for 2 min in the dark to protect the fluorescent dye from light exposure. After the incubation period, the samples were placed into the Qubit® Fluorometer, and the nucleic acid concentrations were measured according to the device's protocol.

2.3.5. TapeStation Analysis

The Agilent TapeStation system is an automated electrophoresis solution for the sample quality control of DNA and RNA samples. Samples quality was measured using 4150 TapeStation System from Agilent. The diluted ladder solution was prepared by adding 10 µL of RNase-free water to the High Sensitivity RNA Ladder vial. Solution was mixed thoroughly. One µL of High Sensitivity RNA Sample Buffer with 2 µL of RNA ladder was mixed. RNA samples were mixed 1 µL of High Sensitivity RNA Sample Buffer with 2 µL of RNA sample. Samples were spin down, then vortexed using an IKA vortexer and adaptor at 2000 rpm for 1 min. Samples were centrifuged to ensure they were collected at the bottom of the tube. Ladder and samples were heated at 72°C for 3 min to ensure denaturation. Then, the ladder and samples were placed on ice for 2 min. Prepared samples were loaded into the 2200 Agilent TapeStation instrument for analysis where data were obtained.

2.4. DNA Barcoding – Clone Genotyping

Only the clones used for future experiments from the UH duckweed collection were taxonomically classified by DNA barcoding, following the method described by (Wang *et al.*, 2010). These clones were SD, DG4 and DG8 which were classified as *L. minor* and Manor, Colour factory, Jen Young, Oxley's Wood, Sailor's Grove and Pond clone which were classified as *L. gibba*. Two chloroplast markers, atpF-atpH and psbK-psbI, were amplified using specific primers (Table 2.2) based on reference sequences

from duckweed. Clones obtained from the Rutgers collection were not subjected to DNA barcoding, as they had already been classified as *Lemna gibba* by the provider.

2.5. Duckweed Growth Rate Measurements

To measure growth rate of duckweed under different conditions, initial weight and final weight were weighted in a balance removing the excess of water to get an exact value. Growth rate was measured with these formulas where the weight at day 0 and day 7 were normalised and divided by the time (Ziegler *et al.*, 2015).

Relative growth rate (d^{-1}) for two-point measurements (day 0 and day 7):

$$1 \quad RGR = (\ln X_{t7} - \ln X_{t0}) / (t_7 - t_0)$$

X = Weight, t = time.

2.6. Sample Preparation for Total Nitrogen and Nitrate Measurements with FT-MIR Model

2.6.1. Plant Materials from Different Cultivation Treatments

Duckweed samples from different treatments were collected with a sieve whilst excess of water was removed with tissues. Leaves were immediately put into a 2 ml Eppendorf tubes and dried in an oven at 60 °C for 48 h. When samples were completely dried, three stainless steel balls of 0.5 cm were added into the tube and samples were milled using TissueLyser at 12,000 rpm for 3 min (Tissuelyser II). Subsequently, samples were centrifuged employing Fisherbrand™ Microcentrifuges, Micro 17/17R, to remove duckweed powder located in the tube walls. Stainless steel balls were collected from the tubes and cleaned in 10% sodium hypochlorite solution for re-use. Samples were stored in the 2 ml Eppendorf tubes in dry conditions and room temperature until further analysis.

2.6.2. Identification of Nitrate-N Peaks in the FTMIR Spectra

Two sets of samples were prepared to identify organic and inorganic nitrogen peaks (i.e. nitrate, nitrite and ammonium). One set was composed by 1 g of cellulose aliquots with 1 ml of NO₃-N standard solutions (Nitrate standard solution, 1198110500, Merck Millipore) prepared to give final concentrations of 10,000, 5,000, 1,000 and 100 mg/kg NO₃-N in the plant sample after drying. The second set was composed by 1 g of duckweed standard sample called Ma-STD, collected in Harpenden, United Kingdom, with the same sample preparation. Both the amount of sample and the volume of

the NO₃-N standard solutions were carefully chosen after several weight to volume ratio checks to ensure that the sample would be entirely and homogeneously wet with the spiking solution. Both set of samples were dried at 60 °C for 48 h and thoroughly mixed before FTMIR scanning.

2.6.3. Total Nitrogen Determination by Dumas Combustion

Total-N (TN) in food is traditionally measured by Dumas combustion (Liu et al., 2025). For that reason, TN was determined according to the procedure of Dumas using a LECO CN628 Combustion Analyser (LECO Corporation, St Joseph, Michigan, USA). Dried 100 mg of plant material is combusted, and the N₂ is measured with a thermal conductivity sensor. For this method, all nitrogen forms were combusted and then analysed. This analysis gives the sum of organic, nitrate, nitrite and ammonium nitrogen. Quality analyses were done with the addition of plant references standards of certified Total-N content (NIST-Spinach, NIST-Tomato, NIST-Peach, Wepal IPE-100, Wepal IPE 154) and an in-house grass standard. Besides, one repeat sample was included every ten samples for additional quality analysis.

2.6.4. Total Nitrate Determination by Salicylic Nitration with Spectrophotometric Determination

Nitrate nitrogen (NO₃-N) measurement was developed by Cataldo *et al.* (1975). This method determines nitrate content in plants based on nitration with salicylic acid. Dried 25 mg sample was used to extract NO₃-N with 1 ml of 18 MΩ-cm ultrapure water at 70 °C for 60 min. Samples were centrifuged at 15850 g, then 0.1 ml of supernatant was mixed with 0.4 ml of a 5% (w/v) solution of salicylic acid in concentrated H₂SO₄. After 30 min of reaction, 9.5 ml of 8% NaOH was added developing a yellow colour that was measured spectrophotometrically at 410 nm (NanoDrop™ 2000/2000c Spectrophotometers). Standard calibration set was prepared with 0.7 mM KNO₃ solution with 0, 10, 20, 30, 40, 60, 80, 100 and 120 mg/L of NO₃-N concentration. Each sample was analysed in triplicate and each batch of samples included blanks and different plant IPE standards of known reference NO₃-N value (Zhao & Wang, 2017).

2.6.5. FTIR Spectra Collection

All samples were further sieved to pass through a 210 µm mesh. For each sample, three replicate subsamples of approximately 0.1 g each were scanned. Reference samples of an in-house standard *Lemna* sample (Ma-STD) and blanks (clean holes) were measured in each run for quality control.

Analysis was conducted with a TENSOR II benchtop FT-IR (Fourier-Transform Infrared) spectrometer (Bruker, Berlin, Germany). This has a spectral range of 8000–340 cm^{-1} , a KBr broadband beam-splitter and window, and an MCT (mercury cadmium telluride) mid-band detector cooled by liquid nitrogen. Diffuse Reflectance Infrared Fourier Transform (DRIFT) spectra were collected. A background spectrum was taken with a gold-plated reference cap. The high throughput screening accessory (HTS-XT), which scans 95 samples in one plate, was used. The spectral resolution was 4 cm^{-1} and scan time was 32 s per sample. Absorbance data in the spectral range 4000–600 cm^{-1} were obtained. All the data were obtained and processed using the Bruker OPUS-QUANT II software (Bruker, Berlin, Germany). Corrections of the raw data were made using the first derivative, with 8 smoothing points using the Savitsky–Golay algorithm and mean centred vector normalization. CO_2 peaks at 2361 and 2339 cm^{-1} were removed from the data.

Mid-infrared chemometric models were built using PLS (partial least-squares) modelling with OPUS-QUANT II software. A matrix is formed from the spectral data of the calibration samples of known composition. The matrix is transformed by the PLS algorithm into a result matrix consisting of eigenvectors (factors). The predictive reliability of the chemometric model strongly depends on the choice of the rank (the correct number of factors needed). In this case, a Cross Validation (leave one out) system is used to calculate the optimum rank by looking at the root mean square error of prediction (RMSE) with the minimum potential for over-fitting. Assessments of model predictive performance are made with calculations of the correlation coefficient (a measure of relative precision and closeness to the line of best fit), the coefficient of determination (R^2 , gives the percentage of variance present in the true component values, which is reproduced in the prediction), the RMSECV (root mean squared errors of cross validation), the residual prediction deviation for the rank (RPD = SD/SECV), which allows comparison of model performance across different data sets, and the bias (mean value of deviation, also called “systematic error”). Additionally, the wavenumbers with the highest coefficient explaining the most variation in TN (VIP scores) were identified.

2.7. Statistical Analysis

Statistical analyses were performed on data collected from different experiments. Data were analysed using RStudio software (R version 3.6.0+) (RStudio Team, 2022), employing appropriate statistical tests to evaluate differences between different treatments. For data visualization, including the creation of plots and graphs, GraphPad Prism software (version Prism 10.2.2) was used. This ensured clear and accurate representation of the results.

3. Chapter 3. Impacts of Different Nitrogen Sources on Growth Rate, Protein Content, and Gene Expression of Genes Involved in Nitrogen Assimilation in Different Duckweed Clones

3.1. Introduction

Nitrogen, which constitutes about 78% of the Earth's atmosphere (Bloom, 2015), undergoes various transformations into organic nitrogen, ammonium (NH_4^+), and nitrate (NO_3^-) through natural processes, which plants utilize for growth and metabolism (Britto & Kronzucker, 2013). This element is essential to the formation of macromolecules such as proteins, nucleic acids, and hormones, playing a pivotal role in plant development and signalling (Krapp, 2015). However, nitrogen is one of the most limiting nutrients in agriculture, directly influencing crop yields (Leghari *et al.*, 2016; Robertson & Vitousek, 2009). To address this, nitrogen fertilizers are widely used to enhance productivity, yet their overuse has contributed to serious environmental challenges (Liu *et al.*, 2021).

In modern agriculture, plants only absorb about 50% of the nitrogen applied through fertilizers, with the rest escaping into the environment via processes like volatilization, runoff, and leaching (Billen *et al.*, 2013). This nitrogen loss contributes to several environmental issues, including soil acidification, air pollution, and water eutrophication, primarily due to nitrate (NO_3^-) and ammonium (NH_4^+) (Camargo & Alonso, 2006; Martínez-Dalmau *et al.*, 2021). There is a growing need for sustainable solutions that can mitigate these negative impacts, and one promising approach is the use of duckweed for nitrogen detoxification.

Duckweed is increasingly recognized for its ability to absorb excess nutrients like nitrogen and phosphorus from water, making it a promising candidate for wastewater treatment (Cheng & Stomp, 2009; Iatrou *et al.*, 2019; Soñta *et al.*, 2019). In addition to its role in nutrient remediation, duckweed's high protein content, exceeding 45% in dry weight, makes it an attractive source of protein for livestock and even human consumption (Appenroth *et al.*, 2017, 2018). These dual functionalities of nutrient absorption and protein production highlight the potential of duckweed as both an environmental and nutritional resource.

Given the importance of nitrogen in both environmental and agricultural contexts, understanding how different nitrogen sources influence duckweed's physiological and molecular responses is critical. Research suggests that various nitrogen sources, such as ammonium or nitrate can influence duckweed's physiological responses. For instance, certain nitrogen sources may alter protein accumulation rates and overall growth performance (Devlamynck *et al.*, 2020; Petersen *et al.*, 2021; Ullah *et al.*, 2022). These nitrogen sources may also change gene expression patterns related to

nitrogen metabolism and protein synthesis, further affecting overall growth performance and protein accumulation (Zhou *et al.*, 2022).

As illustrated in Figure 1.9, in terrestrial plants, nitrate and ammonium from the ground are transported into the cell by nitrate transporters (*NRTs*) or ammonium transporters (*AMTs*). Nitrate undergoes reduction to nitrite through the action of cytosolic nitrate reductase (*NR*), after which the nitrite is transported to the plastids by histidin-prolin-prolin (*HPP*) transporters (Maeda *et al.*, 2014). Within the plastids, nitrite is further reduced to ammonium by plastidic nitrite reductase (*NiR*) (Liu *et al.*, 2022). Ammonium assimilation involves the conversion of inorganic nitrogen to organic nitrogen through the glutamate synthase (*GS*)/glutamine-2-oxoglutarate aminotransferase (*GOGAT*) cycle. In this cycle, *GS* catalyses the incorporation of a molecule of ammonium into glutamate (Glu) in an ATP-dependent manner, while *GOGAT* generates two molecules of Glu through the transfer of the amide group from glutamine (Gln) to 2-oxoglutarate (2-OG) (Liu *et al.*, 2022). *GS* exists in different cellular locations, including cytosolic *GS1* and plastidic *GS2*, while two types of *GOGAT*, nicotinamide adenine dinucleotide (*NADH*)-*GOGAT* and ferredoxin (*Fd*)-*GOGAT*, are present in plastids (Krapp, 2015; Liu *et al.*, 2022; Zhou *et al.*, 2022).

In the shoot of a plant, nitrate is first converted to nitrite by *NR* in the cytoplasm, and then further reduced to ammonium by *NiR* in the plastids. Glutamine synthetase (*GS*) plays a vital role in nitrogen assimilation, with two major enzyme classes encoded in plant nuclear genomes: cytoplasmic *GS1* and chloroplastic *GS2* (Krapp, 2015; Xu *et al.*, 2012). Most plants possess a small family of three to five genes encoding cytosolic *GS1* isoforms and a single gene for *GS2* (Bernard & Habash, 2009; James *et al.*, 2018). The two isoforms of *GOGAT*, *Fd-GOGAT* and *NADH-GOGAT*, function across different cellular compartments, with chloroplastic *Fd-GOGAT* predominantly involved in leaves, while cytosolic *NADH-GOGAT* participates in various tissues including roots, vascular bundles, and reproductive organs, enabling efficient nitrogen utilization (Kojima *et al.*, 2014; Krapp, 2015).

Glutamate also acts as an amino group donor in the synthesis of other amino acids through transamination reactions catalysed by aminotransferases. These enzymes transfer the amino group from glutamate to keto acids, producing various amino acids and alpha-ketoglutarate (Crump *et al.*, 1990). Mechanistically, the transamination reaction proceeds through the transfer of an amino group to pyridoxal phosphate, forming a 2-ketoacid by-product and an enzyme-bound pyridoxamine phosphate intermediate, which then transfers the amino group to a 2-ketoacid acceptor, regenerating the pyridoxal phosphate cofactor (Crump *et al.*, 1990).

Nitrate can also be transported into the vacuole through Chloride Channels (*CLC*), with Chloride Channels A *CLCa* acting as a $2\text{NO}_3^-/1\text{H}^+$ exchanger involved in vacuolar nitrate storage (Liang & Zhang,

2020; Zifarelli & Pusch, 2009). Mutations in the *CLCa* gene disrupt water homeostasis and nitrate accumulation, adversely affecting nitrogen use efficiency and plant development (Hodin *et al.*, 2023). For example, plants with *AtCLC-a* mutations exhibit lower nitrate storage and impaired growth, underscoring the role of *CLCa* in maintaining optimal nitrate levels (Geelen *et al.*, 2000). In *Arabidopsis*, seven *CLC* genes have been identified, including *CLCa* and *CLCb*, which function as NO_3^-/H_1 antiporters in vacuolar nitrate storage (De Angeli *et al.*, 2006; Von Der Fecht-Bartenbach *et al.*, 2010).

Nitrate is a key nutrient for plants, and its accumulation and transport are fundamental for growth and nitrogen use efficiency. Proper function of *NRTs*, *AMTs*, *GS/GOGAT*, and *CLC* channels enables plants to effectively assimilate and store nitrogen, ensuring resilience under varying environmental conditions (Liang & Zhang, 2020).

Understanding the impact of different nitrogen sources on protein yield in duckweed is crucial for optimizing cultivation methods and harnessing its potential as a sustainable solution for environmental and nutritional challenges. By investigating how various nitrogen sources influence protein accumulation in duckweed, researchers can explore strategies to increase its protein yield while preserving its efficacy in wastewater treatment and nutrient absorption. Furthermore, understanding duckweed responses to nitrogen sources across different clones and species is necessary to gain valuable insights into the genetic basis of nitrogen assimilation. This understanding can aid in identifying strains with favourable traits for protein production and environmental remediation. This comprehensive understanding highlights the significance of duckweed as a versatile and sustainable plant species with multifaceted applications in environmental remediation and protein synthesis.

This study aimed to investigate how different nitrogen sources (Nitrate, Nil, Ammonium-Nitrate, and Urea-Nitrate) affect duckweed's physiological responses, specifically focusing on protein and nitrate accumulation and growth rate. In addition to these physiological assessments, the study also sought to explore the expression patterns of eight homologous genes involved in nitrogen assimilation. These genes, identified through *in silico* analysis in *L. gibba* and *L. minor*, were analysed via qPCR to determine how different nitrogen treatments impact their expression. By exploring these responses across different duckweed clones, this research hopes to provide deeper insights into optimizing duckweed for both environmental and nutritional applications.

3.2. Materials and Methods

3.2.1. Plant Material and Treatments

Clones used for this study were SD (*L. minor*), DG4 (*L. minor*), DG8 (*L. minor*), and 7796 (*L. gibba*), sourced from the University of Hertfordshire collection. The selection of these clones was based on specific characteristics and research considerations. The SD clone was chosen due to its previously demonstrated high nitrate content and notably longest root system in prior experiments. Clones DG4 and DG8 were included at the request of the collaborating company, who expressed specific interest in these particular *L. minor* variants. The 7796 clone of *L. gibba* was selected as it serves as the reference clone widely recognized in duckweed research, providing a standard point of comparison for the study. Clones were treated and sterilised as explained in the Section 0. The taxonomic classification of the UH duckweed collection was performed using DNA barcoding, following the method described by Wang *et al.*, 2010. Two chloroplast markers, *atpF-atpH* and *psbK-psbI*, were amplified with specific primers explained in Section 2.4.

Experiments were carried out in a Controlled Environment (CE) cabinet at 20 °C, continuous white light at 100 $\mu\text{mol}\cdot\text{m}^{-2}\cdot\text{s}^{-1}$ (photosynthetically active radiation) from fluorescent tubes TLD 36W/86 (Philips, Eindhoven, the Netherlands). For the acclimation process, 50 mg of fresh weight from each clone was cultivated in 400 ml beakers with transparent lids. A modified Rorison medium (Hewitt, 1966) was used for this experiment, as shown in Table 3.1. Plants were acclimated in Rorison medium in Nitrate form for 2 weeks. The experimental treatments consisted of four distinct nitrogen sources: Nitrate (positive control), Nil (negative control), Ammonium-Nitrate, and Urea-Nitrate. After acclimation, six samples per treatment and per clone were grown for one week, and the plants were collected for future analysis.

Growth rate assessments were conducted following the methodology described in Section 2.5 (Ziegler *et al.*, 2015), using at least three biological replicates for each analysis.

Total nitrogen (TN) and nitrate (TNO_3^-) levels were quantified using Fourier-transform mid-infrared (FT-MIR) spectroscopy, following the protocol outlined in Section 2.6 (Espinosa-Montiel *et al.*, 2022). Each analysis included a minimum of three biological and three technical replicates.

The total protein content (%) was calculated using the equation:

$$2 \quad \text{Total protein (\%)} = 6.25 \times (\text{TN} - \text{TNO}_3^-)$$

Table 3.1. Nutrient composition of the modified Rorison medium for 4 different Nitrogen sources. Nitrate (4mM N), Nil (0mM N), Ammonium-Nitrate (4 mM N) and Urea-Nitrate (4 mM N).

Stock	Chemicals	g/l	Nitrate (4 mM N)	Nil (0 mM N)	Ammonium – Nitrate (4 mM N)	Urea – Nitrate (4 mM N)
			ml/l	ml/l	ml/l	ml/l
A	Ca(NO ₃) ₂ ·4H ₂ O	23.616	20	-	-	10
B	CaSO ₄ ·2H ₂ O	1.7212	0	200	100	100
C	NH ₄ NO ₃	8.004	-	-	20	-
D	CH ₄ N ₂ O`	3.0028	-	-	-	10
S1	MgSO ₄ ·7H ₂ O	24.65	10	10	10	10
S2	FeNaEDTA	1.98	10	10	10	10
	Na ₂ EDTA	0.204				
S3	MnSO ₄ ·4H ₂ O	1	5	5	5	5
	H ₃ BO ₃	0.5				
	KI	0.1				
	ZnSO ₄ ·7H ₂ O	0.1				
	CuSO ₄ ·5H ₂ O	0.02				
	Na ₂ MoO ₄ ·2H ₂ O	0.01				
CoCl ₂ ·6H ₂ O	0.01					
S4	K ₂ HPO ₄	22.77	10	10	10	10

3.2.2. Characterization of Major *Lemna* Genes Related to N Assimilation

The genes involved in Nitrogen assimilation in *L. gibba* and *L. minor* (described in **Error! Reference source not found.**) include, nitrate reductase (*NR*), nitrite reductase (*NiR*), glutamine synthetase (*GS*), NADH-dependent glutamate synthase (*NADH-GOGAT*), and ferredoxin-dependent glutamate synthase (*Fd-GOGAT*). These genes were identified using the reference sequences from *Spirodela polyrhiza* as the initial queries in tBLASTn searches against the *L. gibba* and *L. minor* genomes obtained from CoGe (Lyons *et al.*, 2008; Lyons & Freeling, 2008). The reference sequences included SpNR (OL421561), SpNiR (OL421562), SpGS1;1 (MZ605906), SpGS1;2 (MZ605907), SpGS1;3 (MZ605908), SpGS2 (MZ605909), SpFd-GOGAT (MZ605910), SpNADH-GOGAT (OL421563), as reported by Zhou *et al.*, 2022. Additionally, for the *CLCa* gene, two reference sequences from *Arabidopsis thaliana* - AtCLCa1 (NP_198905.1) and AtCLCa1 (NP_001031990.1) – were retrieved from the NCBI database (<https://www.ncbi.nlm.nih.gov/>).

The intron/exon structure of the genes was determined by comparing them with the homologous genes of *S. polyrhiza* available in GenBank (*National Center for Biotechnology Information*, n.d.). The exon-intron structures were designed and visualized using *Benchling [Biology Software]*, (2024), and further analysed and modelled using *WormWeb.Org*.

3.2.3. Phylogenetic Analysis

Mature protein sequences from monocots and dicots species were obtained from public libraries hosted by the *National Center for Biotechnology Information* (retrieved on 12/08/2024). The monocot species included in the study were *Brachypodium distachyon*, *Hordeum vulgare*, *Oryza sativa*, *Sorghum bicolor*, and *Spirodela polyrhiza*, while the dicot species included *Arabidopsis thaliana* and *Nelumbo nucifera*. Accession numbers of the proteins used in the phylogenetic tree can be found in Table S.1.. Protein alignment were created using *Phylogeny.Fr*, n.d. “A La Carte” analysis workflow, employing MUSCLE for multiple alignment, Gblocks for alignment curation, ProtDist/FastDist + BioNJ for distance-based phylogeny. The resulting phylogenetic tree was customised using the *Interactive Tree Of Life* (iTOL) platform.

3.2.4. Gene Expression Analysis by RT-qPCR

The expression levels of eight target genes (*NR*, *NiR*, *GS1;1*, *GS1;2*, *GS2*, *CLCa1*, *Fd-GOGAT*, and *NADH-GOGAT*) in the four clones were quantified using reverse transcription quantitative PCR (RT-qPCR).

Gene-specific primers were designed based on deduced exon sequences (as detailed in Table 3.2). These primer design process was conducting using *Benchling [Biology Software].*, (2024). Retrieved from <https://benchling.com>.

Total RNA was extracted from 80 mg of fresh duckweed fronds collected after a week of treatment, using the E.Z.N.A.® Plant RNA Kit protocol (Norcross, Georgia, USA). The quality and integrity of the isolated total RNA were evaluated using a Nanodrop® ND 1000 Spectrophotometer (Thermo Fisher Scientific, USA), a Qubit 4 Fluorometer, and 1.5% agarose gel electrophoresis. After treating the RNA samples with DNAase, 100 ng/μl of total RNA was used for reverse transcription, which was carried out with the SuperScript™ IV RT Reaction Kit (Invitrogen, USA), following the manufacturer's instructions.

The qPCR reactions were performed using the Agilent Technologies Stratagene Mx30005P instrument (Agilent, USA), with SYBR Green real-time PCR master mix (Thermo Fisher Scientific, USA). The cycling conditions consisted of an initial denaturation at 95 °C for 10 min, followed by 40 cycles of 15 seconds at 95 °C and 60 seconds at 60 °C. Fluorescence of SYBR Green I was monitored after the annealing step, and the unique-product amplification was validated through a thermal denaturation cycle, ensuring only single-peak results were included. Primer amplification efficiency was calculated using a 10-fold serial dilution, and the efficiency (E) was determined using the formula:

$$3 \quad E = (10^{-1/\text{slope}} - 1) * 100$$

where the slope was obtained from the standard curve generated from the serial dilutions (Pfaffl, 2001).

Relative expression levels were determined using the $2^{-\Delta\Delta C_t}$ method, with *GADPH* serving as the housekeeping gene (Pfaffl, 2001). All samples were run in three replicates. Data analysis was performed using the MxPro QPCR program (Agilent, USA), Microsoft® Excel® for Microsoft 365 MSO (Version 2402) software and GraphPad Prism 10.1.2 for representation.

3.2.5. Statistical Analysis

Statistical analyses were performed using GraphPad Prism software (version Prism 10.2.2). A one-way ANOVA analysis were employed to evaluate potential statistically significant differences between the Nitrate treatment (control) and the alternative treatments: Nil, Ammonium-Nitrate, and Urea-Nitrate. The analysis encompassed two primary sets of variables, the physiological values and the qPCR expression. Statistical significance was defined at $p \leq 0.05$, with data presented as mean \pm standard deviation (SD).

Table 3.2. RT-qPCR primers for nitrogen assimilation gene expression analysis in *L. gibba* and *L. minor* clones.

Gene		Sequence	Product size (bp)	Efficiency (%)
<i>NR</i>	Fw	5' -GTGCTGGTGCTTCTGGTCCGTC- 3'	113	98.2
	Rv	5' -AGATGAGCTTGTCGGGCTGGGT- 3'		
<i>NiR</i>	Fw	5' -CTACTCGTGGAGCGCTTTGGGG- 3'	85	94.6
	Rv	5' -GTCAAGAGCGAAGGCGTCTGGC- 3'		
<i>GS1;1</i>	Fw	5' -CGCGAGACAGAGCAAAACGGGA- 3'	108	105.3
	Rv	5' -CCAAAGGATGGTGGTCTCGGCA- 3'		
<i>GS1;2</i>	Fw	5' -CTCTCGTTGCACCCCAAGCCAA- 3'	119	100.1
	Rv	5' -CATCCGGCACC GTTCCAGTCAC- 3'		
<i>GS2</i>	Fw	5' -TGTTGCCAACC GTGTTGCTCC- 3'	83	106.1
	Rv	5' -CGGGGCGGCGATCTTCCATGTA- 3'		
<i>Fd-GOGAT</i>	Fw	5' -GCACAAAGGGGGCCACCATTCT- 3'	99	109.7
	Rv	5' -CGCTGGCTTCGGGAGTGTCTTC- 3'		
<i>NADH-GOGAT</i>	Fw	5' -ATGAGAACGGCGCGGTCAAAGG- 3'	92	98.9
	Rv	5' -GCCAGCGACTTCTGGAAGTGG- 3'		
<i>CLCa1</i>	Fw	5' -GAGGGCGGAAAACATTCTCAGC- 3'	101	96.1
	Rv	5' -TCTGCAGCATCGTGATGAGCTA- 3'		
<i>GAPDH</i>	Fw	5' -CCTCCACCATTGACTCCTCGTT- 3'	98	98.3
	Rv	5' -CACCCGTTGACTGTATCCCAT- 3'		

3.3. Results

3.3.1. Duckweed Identification

Before setting up the experiment, four different *Lemna* clones were sterilised and identified by DNA barcoding. The identification was achieved by sequencing the *atpF-atpH* and *psbK-psbI* intergenic spacers and comparing the resulting sequences with those compiled in the CoGe sequence database. The analysis revealed that clones DG4, DG8 and SD belonged to *Lemna minor*, while clone 7796 was identified as *Lemna gibba* (Figure 3.1). The detailed sequence data used for identification are provided in the appendices (Figure S.1 and Figure S.2).

3.3.2. Influence of Nitrogen Sources on Duckweed Growth, pH, Nitrogen, Nitrate, And Protein Levels

The effects of various nitrogen sources on key parameters in duckweed performance, such as Relative Growth Rate (RGR), Medium pH, Total Nitrogen Content (TN), Nitrate Levels (TNO_3^-), and Protein Concentration (TP), were studied. Measurements were conducted on both Day 4 and Day 7 of the experiment. The results from Day 7 were represented in the main text, as they provide a more comprehensive understanding of the longer-term effects of the treatments. Data from Day 4, which represent the initial responses of duckweed to the treatments, were presented in Appendices (RGR (Figure S.3), pH Medium (Figure S.4), TN (Figure S.5), TNO_3^- (Figure S.6) and TP (Figure S.7.)).

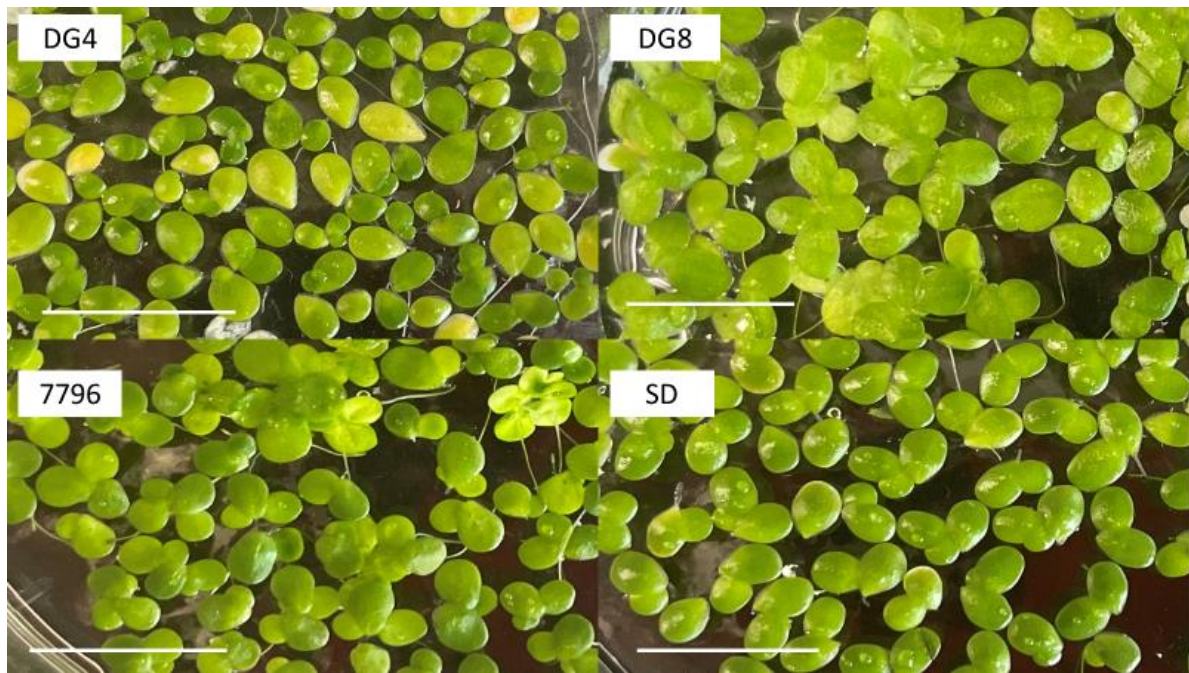


Figure 3.1. Images of the *Lemna* clones used in this study. Based on the sequence of the *atpF-atpH* and *psbK-psbI* intergenic spacers, clones SD, DG4, and DG8 identified as *Lemna minor*, and clone 7796 as *Lemna gibba*. The scale bar represents 1 cm.

3.3.2.1. Relative Growth Rate (RGR)

Different medium compositions for four different nitrogen treatments (Table 3.1) significantly affected the growth rate of duckweed clones (Figure 3.2). The results show that RGR varied across clones and treatments, reflecting the combined effects of genetic and nutrient availability.

For the clone SD, the RGR was consistently low under Nil, Ammonium, and Urea treatments compared to the Nitrate treatment by Day 7. This indicates that Nitrate is the most effective nitrogen source for promoting growth in this clone, highlighting its specific preference for this nutrient over others.

Clone DG4, however, displayed a particularly strong response to nitrogen supplementation. Under both Ammonium and Urea treatments, it exhibited significantly higher RGR by Day 7, suggesting a superior ability to utilize these nitrogen sources for growth. This clone's enhanced growth under these treatments indicates that it may possess a genetic advantage in efficiently utilizing Ammonium and Urea, making it particularly well-suited for environments where these forms of nitrogen are prevalent.

In contrast, the clone DG8 demonstrated no significant differences in RGR between nitrogen treatments, although Nil consistently resulted in significantly lower growth compared to the control Nitrate treatment (Figure 3.2). This indicates a uniform growth response when nitrogen is present, with minimal variation in growth depending on the nitrogen source. It suggests that DG8 may not exhibit a strong preference for a nitrogen form but instead grows well in the presence of any nitrogen source.

Clone 7796 displayed uniformly low RGR across all treatments, with Urea yielded marginally higher values. This suggests that 7796 has limited responsiveness to different nitrogen sources and maintains a relatively consistent growth rate, regardless of the nutrient provided. The clone's ability to grow at a similar rate in both nitrogen-supplemented and Nil conditions suggests a degree of nitrogen independence or an inefficient nitrogen uptake mechanism.

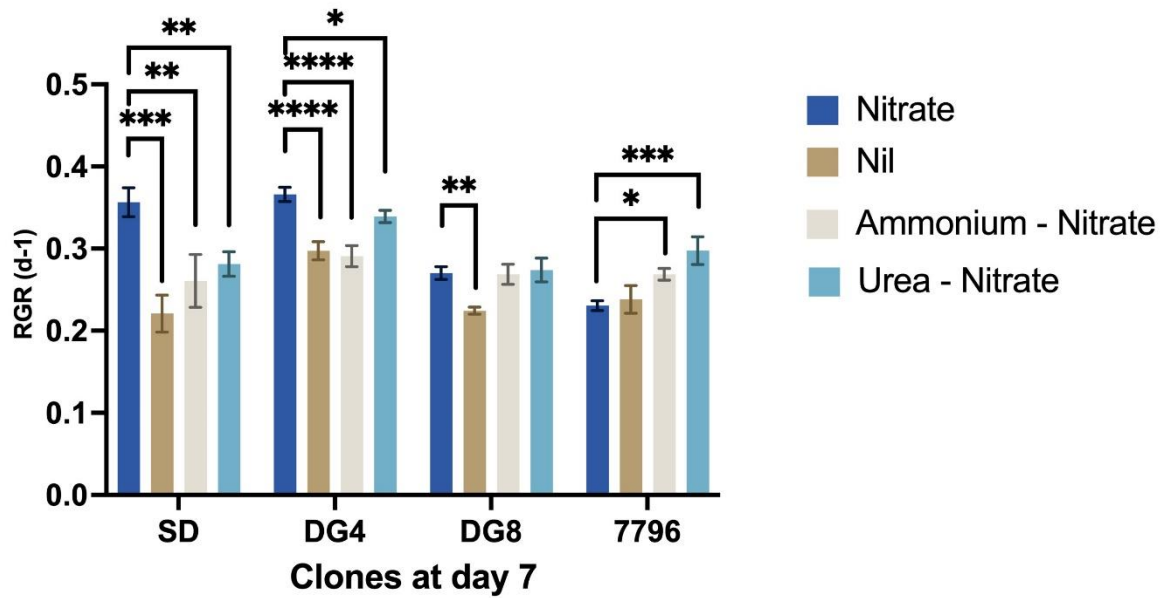


Figure 3.2. Relative Growth Rate (RGR) of duckweed clones (SD, DG4, DG8, 7796) grown under different Nitrogen sources at day 7. Bars represent the mean RGR of three biological replicates, with standard errors shown. Asterisks denote significant differences compared to the control (Nitrate), as determined by One-way Anova: * $p < 0.05$, ** $p < 0.01$, *** $p < 0.001$, **** $p < 0.0001$. The four nitrogen conditions tested were Nitrate (control), Nil (negative control with no nitrogen), Ammonium Nitrate, and Urea Nitrate.

3.3.2.2. Medium pH

The pH of the medium was carefully monitored throughout the experiment, with an initial pH of 6 at the start of the experiment. The pH measurements were taken on Day 4 and Day 7, with only the Day 7 values presented in Figure 3.3. Across all clones, similar trends in pH changes were observed in response to different nitrogen treatments (Figure 3.3), indicating a general pattern that holds regardless of the specific genetic background of the clones.

Notably, treatments with Nitrate (controls) and Urea-Nitrate resulted in an increase in pH by Day 7. This pH rise could be associated with the uptake of these nitrogen forms, possibly due to the production of hydroxide ions during nitrogen assimilation or the depletion of acidic by-products. In contrast, Nil-nitrogen and Ammonium-Nitrate treatments led to a decrease in pH, with the pH dropping significantly to 4 by Day 7 in the Ammonium-Nitrate treatment. This marked decrease in pH suggests that the presence of Ammonium, which is known to acidify the medium as it is assimilated by plants, may have contributed to a more acidic environment.

The observed pH reduction could have influenced the growth responses of the clones. As seen in Figure 3.2, clones exposed to Ammonium-Nitrate treatment showed growth rates similar to those in the Nil-nitrogen treatment, where nitrogen supplementation was absent. This suggests that the lower pH in the Ammonium-Nitrate medium could have had an inhibitory effect on growth, possibly due to the increased acidity impeding optimal nutrient uptake or enzymatic activity.

While Ammonium-Nitrate and Nil treatments resulted in a significant pH reduction by Day 7, the control and Urea-Nitrate treatment resulted in a more stable pH (Figure 3.3). The pH decline was most pronounced in the Nil-nitrogen and Ammonium-Nitrate treatments, with a more moderate decrease observed under the Urea-Nitrate treatment. These pH shifts highlight the dynamic interplay between nitrogen source, nutrient uptake, and pH regulation, and further suggest that extreme changes in pH, especially those leading to more acidic conditions, could negatively affect plant growth.

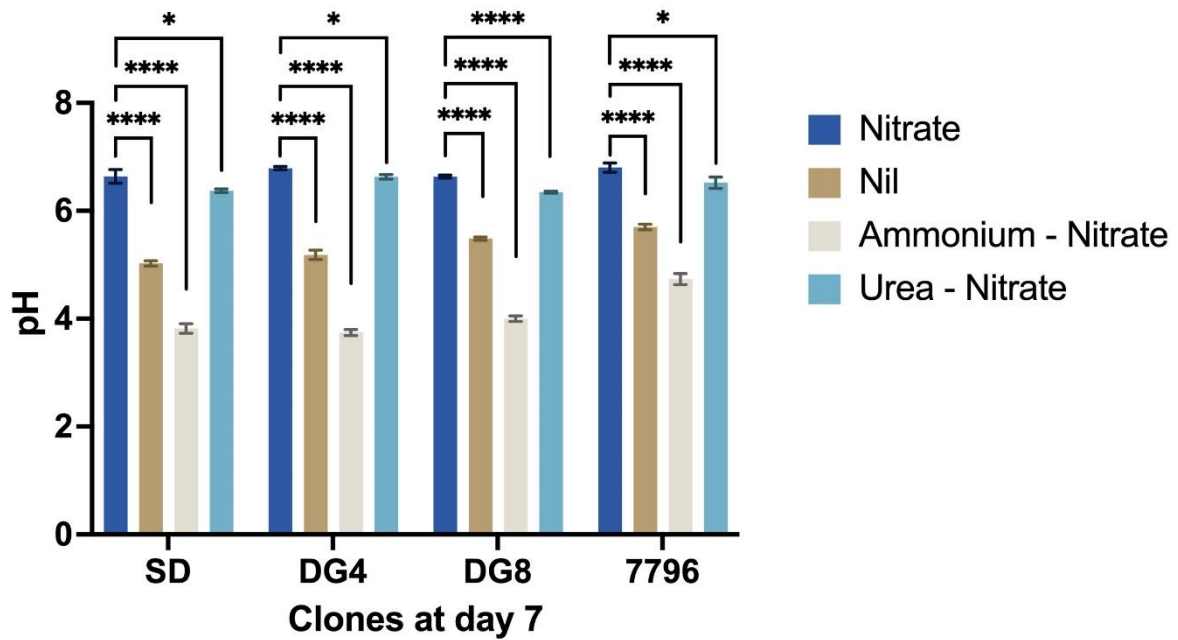


Figure 3.3. Variation in medium pH for duckweed clones (SD, DG4, DG8, 7796) grown under different Nitrogen sources on day 7. Bars represent the mean pH values of the growth medium from three biological replicates, with standard error (SE) shown. Asterisks denote significant differences compared to the control (Nitrate), as determined by One-way Anova: * $p < 0.05$, ** $p < 0.01$, *** $p < 0.001$, **** $p < 0.0001$. The four nitrogen conditions tested were Nitrate (control), Nil (negative control with no nitrogen), Ammonium-Nitrate, and Urea-Nitrate.

3.3.2.3. Total Nitrogen Content (TN)

Total nitrogen content (TN%) was quantified using FT-IR spectroscopy at Day 4 and Day 7. At Day 4, differences in TN% were observed among all clones (Figure S.5), likely reflecting the plants' initial acclimation to the nitrogen sources. By Day 7, however, these initial differences diminished, suggesting that the plants had adjusted their nitrogen uptake mechanisms over time. This adaptation highlights the duckweed clones' ability to optimize nitrogen acquisition as they acclimate to different nutrient conditions.

By day 7, distinct trends in TN% were observed across clones (Figure 3.4). For clone SD, there were no significant differences between nitrogen treatments, although the Nil treatment consistently exhibited much lower TN%. This suggests that, while SD may be less responsive to changes in nitrogen sources, it still requires supplementation for optimal nitrogen content. Similarly, clone DG4 showed a comparable pattern, with nitrogen treatments yielding similar TN% values by Day 7, except for the Nil treatment, which remained significantly lower in nitrogen content. This indicates that DG4 also benefits from nitrogen supplementation but does not display a preference for a specific nitrogen source.

Clone DG8 presented a slightly different pattern, with Ammonium-Nitrate treatment resulting in a marginally but significant higher TN% than Nitrate treatment, suggesting a shift in nitrogen uptake efficiency in response to Ammonium. This implies that DG8 may prefer Ammonium under certain conditions, or it may be able to utilize it more effectively than Nitrate in this experiment.

For Clone 7796, TN% was relatively consistent across treatments, with only a small significant decrease observed under Ammonium treatment. This indicates that Clone 7796 demonstrates a stable nitrogen uptake mechanism across different nitrogen sources, showing resilience and efficient nitrogen acquisition, even under varying nutrient conditions.

These results underscore the critical role of nitrogen supplementation in sustaining healthy growth and nitrogen content in duckweed. The observed variation in total nitrogen percentage (TN%) among clones highlights the genetic diversity in nitrogen uptake efficiency. For instance, clone 7796 demonstrated consistently higher total nitrogen content across various nutrient conditions compared to other clones. In contrast, other clones exhibited relatively stable nitrogen content across treatments, with reductions observed under nitrogen-deficient conditions and variability in response to Ammonium-Nitrate.

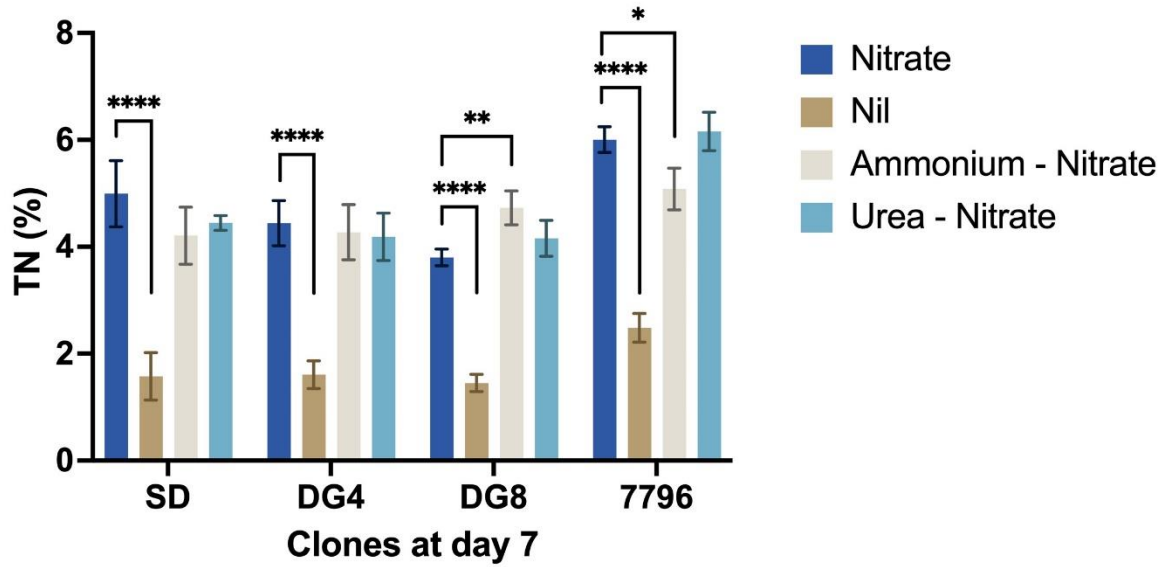


Figure 3.4. Total Nitrogen content (%) in duckweed clones (SD, DG4, DG8, 7796) grown under different Nitrogen sources on day 7. Bars represent the mean total nitrogen content from three biological replicates, with standard error (SE) shown. Asterisks denote significant differences compared to the control (Nitrate), as determined by One-way Anova: * $p < 0.05$, ** $p < 0.01$, *** $p < 0.001$, **** $p < 0.0001$. The four nitrogen conditions tested were Nitrate (control), Nil (negative control with no nitrogen), Ammonium-Nitrate, and Urea-Nitrate.

3.3.2.4. Total Nitrate Content (TNO₃⁻)

Total nitrate content (mg/kg DW) was measured using FT-IR spectroscopy at Day 4 and Day 7. At Day 4, significant variability in nitrate accumulation was observed across the clones, likely due to the initial acclimation phase of the plants to the different nitrogen sources (Figure S.6). By Day 7, however, as the plants adapted to the nutrient conditions, differences in nitrate accumulation patterns became more consistent across the clones (Figure 3.5), reflecting the plants' adjustment to the nitrogen sources and their ability to optimize nitrate uptake.

Clone SD demonstrated the strongest affinity for nitrate, with the Nitrate treatment consistently yielding the highest nitrate accumulation. This suggests that SD is the most efficient at nitrate storage, utilizing Nitrate as its primary nitrogen source for growth and nutrient accumulation. Similarly, Clone DG4 although it showed higher nitrate accumulation in the control, the treatment significantly influenced in their capacity of nitrate storage.

Clone DG8 exhibited similar nitrate accumulation between the Nitrate and Urea-Nitrate treatments, while both Nil and Ammonium-Nitrate treatments resulted in lower nitrate levels. This suggests that DG8 can initially utilize Urea as a nitrogen source and may rely more on nitrate accumulation once the nitrate source becomes available. It highlights DG8's flexibility in nitrogen utilization, particularly under varying nutrient conditions.

Clone 7796 showed the lowest nitrate accumulation in the Nil treatment at both Day 4 and Day 7, reinforcing the importance of nitrogen supplementation for optimal nitrate content. However, by Day 7, the Urea-Nitrate treatment led to the significant highest nitrate content in 7796 when compared with the nitrate source control (Figure 3.5), indicating a dynamic response to nitrogen sources like that of DG8. This suggests that 7796 can effectively utilize Urea-Nitrate for nitrate accumulation, showcasing its ability to adapt to different nitrogen sources over time.

The findings reinforce the idea that nitrate supplementation plays a crucial role in nitrate accumulation and overall plant nutrition. However, clones showed varying levels of nitrate uptake efficiency depending on the nitrogen source. While SD exhibited the highest nitrate affinity, other clones like DG4 showed reduced nitrate accumulation when non-nitrate sources were provided, highlighting the importance of specific nitrogen forms for different genetic backgrounds. Clones like DG8 and 7796 demonstrated more flexibility in utilizing different nitrogen sources, with Urea-Nitrate leading to higher nitrate accumulation in 7796 by Day 7. These results underscore the importance of considering both the genetic variability of the clones and the available nitrogen sources for optimizing nitrate uptake and growth.

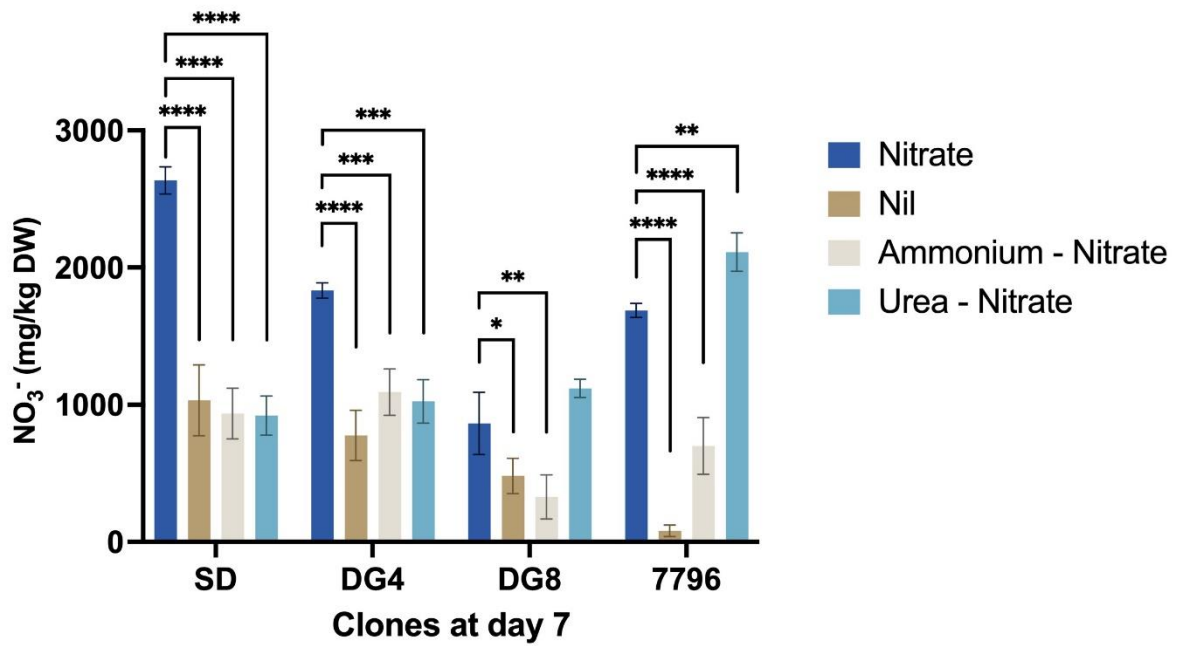


Figure 3.5. Total Nitrate content (mg NO₃⁻/kg DW) in duckweed clones (SD, DG4, DG8, 7796) grown under different Nitrogen sources at day 7. Bars represent the mean total nitrate content from three biological replicates, with standard error (SE) shown. Asterisks denote significant differences compared to the control (Nitrate), as determined by One-way Anova: *p < 0.05, **p < 0.01, ***p < 0.001, ****p < 0.0001. The four nitrogen conditions tested were Nitrate (control), Nil (negative control with no nitrogen), Ammonium-Nitrate, and Urea-Nitrate.

3.3.2.5. Total Protein Content (TP)

Total protein content (%) was calculated by multiplying the difference between total nitrogen content and total nitrate content by 6.25. At Day 4, significant variability in protein content was observed across different clones and nutrient conditions (Figure S.7), likely due to the plants' early adaptation to the nitrogen sources. However, by Day 7, protein levels stabilized across clones (Figure 3.6). This suggests that the initial variability was a result of acclimation, and over time, the plants became more efficient at utilizing the available nitrogen sources for protein synthesis.

For Clones SD and DG4, similar protein content values were observed in the Nitrate, Ammonium-Nitrate, and Urea-Nitrate treatments, with a significant decrease in protein content for the treatment without nitrogen (Nil). This suggests that nitrogen supplementation is essential for maintaining protein accumulation in these clones. Clone DG8 showed similar protein values between the Nitrate and Urea-Nitrate treatments, but significantly higher values when comparing Nitrate with Ammonium-Nitrate sources. This indicates that DG8 may be able to utilize Ammonium more effectively for protein synthesis than other nitrogen sources.

In contrast, Clone 7796 consistently showed higher protein values across all treatments and time points, suggesting that this clone has a greater adaptability or inherent advantage in protein synthesis under different nutrient conditions. The negative control (Nil) consistently exhibited the lowest protein content across all clones, reinforcing the necessity of nitrogen supplementation for optimal protein accumulation.

Interestingly, while 7796 had lower protein content at Day 4 under Nil treatment, statistical analysis revealed no significant differences in the values obtained for this clone compared to the nitrogen forms of other clones. This finding suggests that 7796 might possess a more robust mechanism for protein synthesis, even when nitrogen is limited. The lack of statistical differences indicates a certain resilience of the 7796 clone in nutrient-limited environments, potentially highlighting its adaptive capabilities under nitrogen-deficient conditions.

Additionally, total protein (Figure 3.6) and total nitrogen content (Figure 3.4) exhibited similar trends across different nitrogen sources and clones. Notably, higher nitrate content in the plants did not correspond to a decrease in protein content, suggesting that the plants were able to efficiently convert available nitrogen into protein, regardless of nitrate levels.

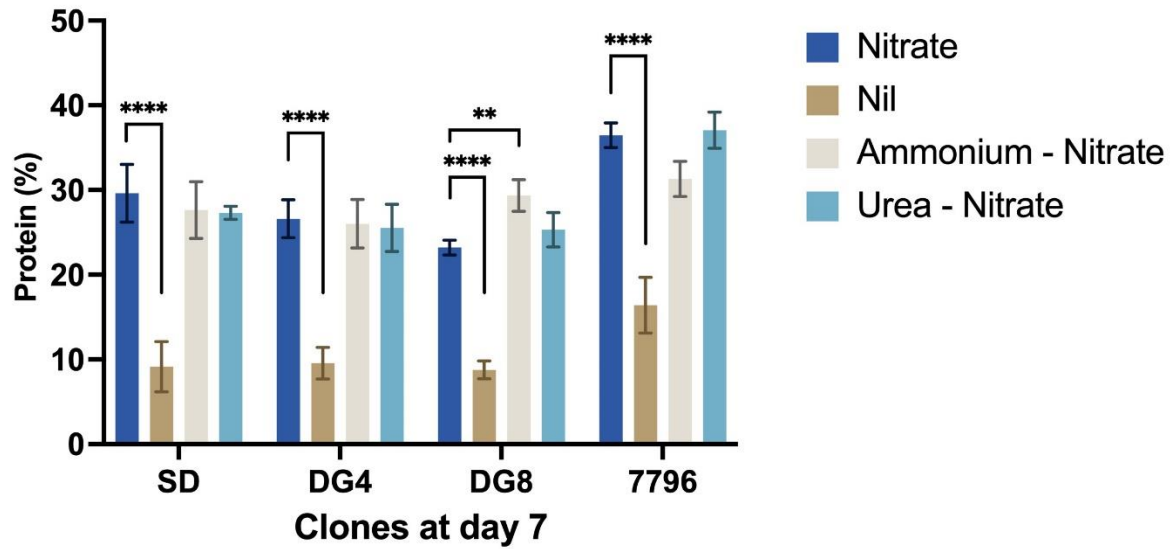


Figure 3.6. Total Protein content (%) in duckweed clones (SD, DG4, DG8, 7796) grown under different Nitrogen sources at day 7. Bars represent the mean total protein content from three biological replicates, with standard error (SE) shown. Asterisks denote significant differences compared to the control (Nitrate), as determined by One-way Anova: * $p < 0.05$, ** $p < 0.01$, *** $p < 0.001$, **** $p < 0.0001$. The four nitrogen conditions tested were Nitrate (control), Nil (negative control with no nitrogen), Ammonium-Nitrate, and Urea-Nitrate.

3.3.3. *In Silico* Identification, Genomic Location and Evolutionary Insights of N Assimilation Genes in Duckweed

The results of analysis to characterize the genomic features and functional domains of nitrogen assimilation and transport-related genes (*NR*, *NiR*, *GS1;1*, *GS1;2*, *GS2*, *Fd-GOGAT*, *NADH-GOGAT* and *CLCa*) in *Lemna gibba* and *Lemna minor* were presented in Table 3.3. For each gene, the information on gene structure, such as the number of amino acids, exons, and introns, as well as chromosomal location and genomic start and finish positions, was presented. The catalytic domains were identified through InterPro analysis, accompanied by their functional descriptions. This information provides a comprehensive overview of the genetic architecture and potential functional roles of these genes in nitrogen metabolism.

3.3.3.1. Structural and Evolutionary Analysis of Nitrate and Nitrite Reductase Genes

To explore the evolutionary dynamics of duckweed species, the genomic locations of the *Nitrate Reductase (NR)* and *Nitrite Reductase (NiR)* genes in *L. gibba* clone 7742a (7796 in USA collection) (Lg) and *L. minor* clone 7210 (Lm) were analysed. The *NR* and *NiR* genes in both species were found to be co-localized on chromosome 11. This co-localization suggests that these genes may have originated from a common ancestor following a duplication event, potentially explaining for their conserved genomic positions across these two duckweed species.

The genomic organization of *NR* genes in *L. gibba* and *L. minor* was compared with the well-annotated duckweed species *S. polyrhiza (Sp)*, as shown in Figure 3.7. The *NR* structure is consistent across all three species, consisting of four exons and three introns. However, differences were observed in amino acid sequence length and chromosomal positioning (Table 3.3):

- *SpNR* is located on chromosome 18 (positions 2,446,426 to 2,449,628) and encodes a protein of 903 amino acids.
- *LgNR* is located on chromosome 11 (positions 9,613,697 to 9,617,305) and encodes 882 amino acids.
- *LmNR* is also located on chromosome 11 (positions 7,817,313 to 7,820,783) and encodes 882 amino acids.

Despite these differences, the catalytic and functional domains remain highly conserved, including key domains such as the cytochrome b5-like heme/steroid binding domain (IPR001199) and oxidoreductase FAD/NAD(P)-binding domain (IPR001433). This conservation suggests a crucial role in maintaining nitrate reductase functionality across species.

Table 3.3. Gene structure, genomic location, and functional domains of Nitrogen assimilation and transport-related genes in *Lemna gibba* and *Lemna minor*. Columns include gene names, amino acid (AA) number, number of exons and introns, chromosomal location, genomic start and finish positions, identified catalytic domains (with InterPro accession IDs), and functional descriptions.

Gene	AA number	Exons	Introns	Chromosome	Start finish	Catalytic domain	Description
<i>LgNR</i>	882	4	3	11	9613697 - 9617305	IPR001199	Cytochrome b5-like heme/steroid binding domain
						IPR001433	Oxidoreductase FAD/NAD(P)-binding
						IPR001709	Flavoprotein pyridine nucleotide cytochrome reductase
						IPR005066	Molybdenum cofactor oxidoreductase, dimerization
						IPR017927	FAD-binding domain, ferredoxin reductase-type
<i>LmNR</i>	882	4	3	11	7817313 - 7820783	IPR000572	Oxidoreductase, molybdopterin-binding domain
						IPR008333	Flavoprotein pyridine nucleotide cytochrome reductase-like, FAD-binding domain
<i>LgNIR</i>	586	3	2	11	10714277-10716247	IPR006067	Nitrite/sulphite reductase 4Fe-4S domain.
<i>LmNiR</i>	592	3	2	11	8399636-8401606	IPR005117	Nitrite/Sulfite reductase ferredoxin-like domain
<i>LgGS1;1</i>	356	12	11	15	13857966 - 13861284	IPR008146	Glutamine synthetase, catalytic domain
<i>LmGS1;1</i>	356	12	11	15	10462922 – 10466358	IPR008147	Glutamine synthetase, N-terminal domain
<i>LgGS1;2</i>	356	13	12	11	5789297 - 5791241	IPR008146	Glutamine synthetase, catalytic domain
<i>LmGS1;2</i>	356	12	11	11	5320487 - 5322507	IPR008147	Glutamine synthetase, N-terminal domain
<i>LgGS2</i>	424	13	12	1	30797493-30802011	IPR008146	Glutamine synthetase, catalytic domain
<i>LmGS2</i>	423	13	12	1	22489655-22494918	IPR008147	Glutamine synthetase, N-terminal domain
<i>LgFD</i>	1592	33	32	1	32543357 - 32562115	IPR017932.	Glutamine amidotransferase type 2 domain
<i>LmFD</i>	1489	33	32	1	23855540 - 23875394	IPR002489	Glutamate synthase, alpha subunit, C-terminal
						IPR006982	Glutamate synthase, central-N
						IPR002932	Glutamate synthase domain
<i>LgNADH</i>	2203	22	21	6	16377495 - 16386050	IPR017932	Glutamine amidotransferase type 2 domain
						IPR002489	Glutamate synthase, alpha subunit, C-terminal.
						IPR028261	Dihydropyrimidine dehydrogenase domain II
						IPR006982	Glutamate synthase, central-N.
<i>LmNADH</i>	2203	22	21	6	11803706 - 11812244	IPR023753	FAD/NAD(P)-binding domain.
						IPR002932	Glutamate synthase domain
<i>LgCLCa</i>	822	4	3	21	6378711-6384350	IPR001807	Chloride channel, voltage gated
<i>LmCLCa1</i>	848	4	3	21	4939808-4943394	IPR002251	Chloride channel CLC-plant
						IPR051280	Voltage-gated chloride channel/antiporter

The *NiR* genes in *L. gibba* and *L. minor* also share a similar genomic organization with *S. polyrhiza*, consisting of three exons and two introns. Notably, these species exhibit a fusion of the third and fourth exons, reducing the total exon count compared to the typical four found in other plant species (Figure 3.7). Nevertheless, differences were observed in amino acid sequence length and chromosomal positioning (Table 3.3):

- *SpNiR* is located on chromosome 18 (positions 2,029,327 to 2,032,054) and encodes a protein of 604 amino acids.
- *LgNiR* is located on chromosome 11 (positions 10,714,277 to 10,716,247) and encodes a protein of 586 amino acids.
- *LmNiR* is located on chromosome 11 (positions 8,399,636 to 8,401,606) and encodes a protein of 592 amino acids.

Despite minor variations in sequence length and location, the *NiR* functional domain remain conserved. All three *NiR* proteins contain a chloroplast transfer peptide with differing confidence scores (0.8323 for *S. polyrhiza*, 0.7625 for *L. gibba*, and 0.5527 for *L. minor*). Additionally, essential functional domains, such as the nitrite/suphite reductase 4Fe-4S domain (IPR006067) and the nitrite/sulphite reductase ferredoxin-like domain (IPR005117), are preserved across species.

To explore the phylogenetic relationships of the *NR* and *NiR* genes in different species, the protein sequences from *L. gibba* clone 7742a and *L. minor* clone 7210 were compared with those from *S. polyrhiza* (a well characterized duckweed species), monocot species like *Brachypodium distachyon* (Bd), *Oryza sativa* (Os), *Sorghum bicolor* (Sb) and dicot species like *Arabidopsis thaliana* (At) and *Nelumbo nucifera* (Nn).

The phylogenetic tree (Figure 3.8) revealed two distinct clusters of orthologous genes, corresponding to *NiR* and *NR*. The *NiR* sequences from *L. gibba* and *L. minor* grouped together within the monophyletic clade of monocot *NiRs*, indicating their evolutionary affinity with monocots. In contrast, the *NR* sequences from *L. gibba* and *L. minor* aligned more closely with the *NR* clade of dicotyledonous plants, highlighting a divergence in the evolutionary trajectories of these two gene families.

The phylogenetic analysis also revealed that only a single *NR* gene sequence is present in the three duckweed species analysed (*L. gibba*, *L. minor*, and *Spirodela polyrhiza*). This differs markedly from other monocot and dicot species included in the study, which have two or more copies of *NR* genes. Notably, *Oryza sativa* and *Sorghum bicolor* have three distinct *NR* gene copies.

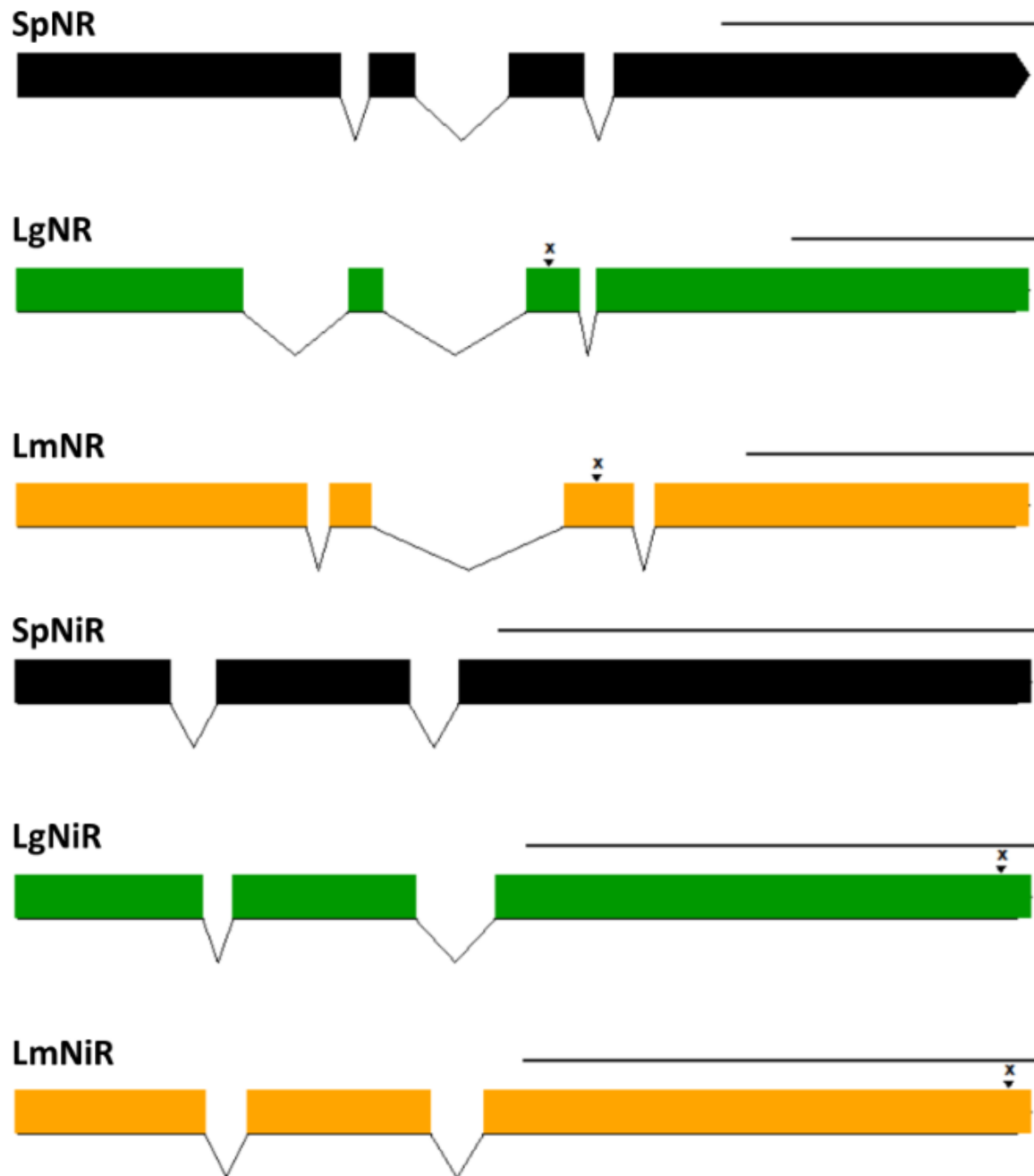


Figure 3.7. Exon-Intron structures of *Spirodela polyrhiza* (Sp), *Lemna gibba* (Lg), and *Lemna minor* (Lm) Nitrate Reductase (NR) and Nitrite Reductase (NiR) genes. The exon-intron structures of *L. gibba* and *L. minor* NR and NiR genes were compared with *S. polyrhiza* (NR: OL421561; NiR: OL421562). The coloured boxes are coding sequences, and the black lines are introns. The X marks the primer binding sites used for RT-qPCR gene expression analysis. The scale bar represents 1 kb of DNA sequence.

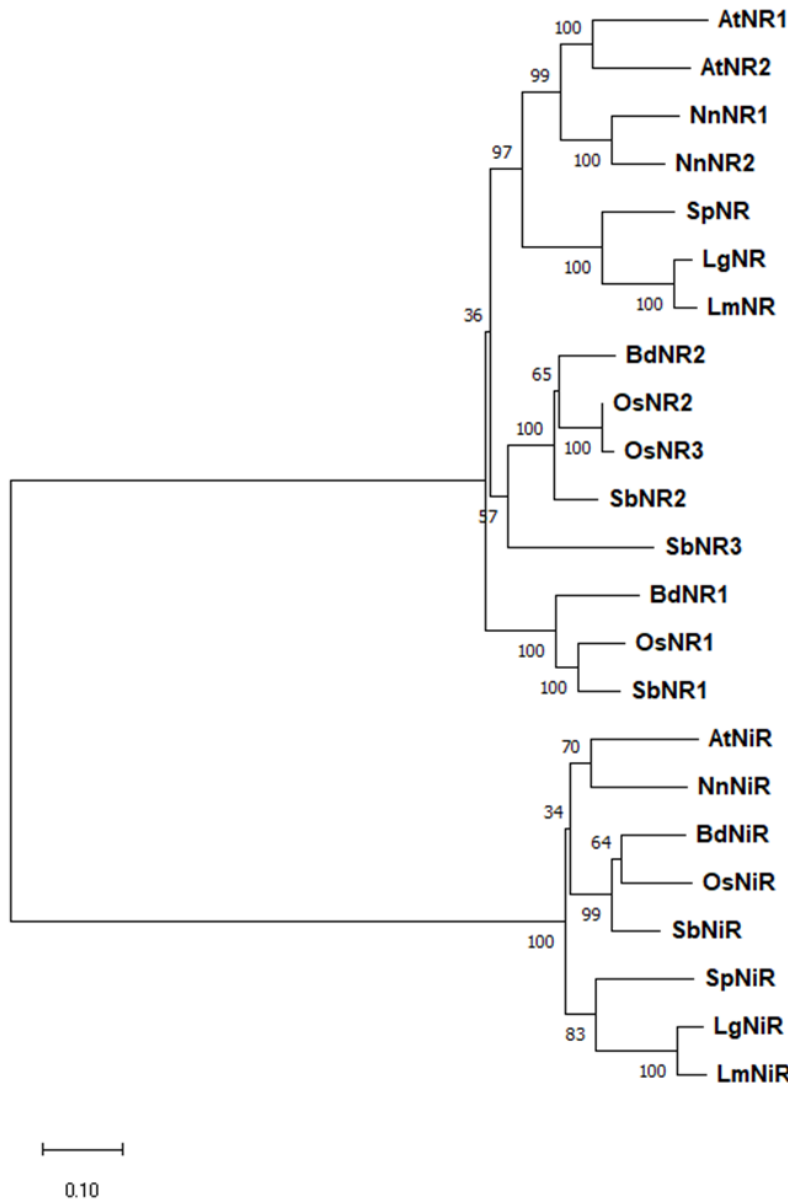


Figure 3.8. Phylogenetic tree of NiR and NR proteins in *Lemna gibba* and *Lemna minor* with other representative species. The phylogenetic tree highlights the relationships of nitrite reductase (NiR) and nitrate reductase (NR) proteins from *L. gibba* (LgNiR, LgNR) and *L. minor* (LmNiR, LmNR) with those from other monocot and dicot species. Branch lengths are proportional to evolutionary distances, with the mean branch length scale indicated at the bottom of the tree. Numbers on the nodes represent bootstrap values, providing statistical support for the clustering of the proteins.

NiR proteins: AtNiR (*A. thaliana* - NP_179164); BdNiR (*B. distachyon* - XP_003570568); NnNiR (*N. nucifera* - XP_010263547); OsNiR (*O. sativa* - NP_001388488.1); SbNiR (*S. bicolor* - XP_002454602); SpNiR (*S. polyrhiza* - sequence translated from Acc. ID OL421562); LgNiR (*L. gibba*_Chr11); LmNiR (*L. minor*_Chr11).

NR proteins: AtNR1 and AtNR2 (*A. thaliana* - NP_177899.1 and NP_174901.1); BdNR1 and BdNR2 (*B. distachyon* XP_003570548.1 and XP_003574607.1); NnNR1 and NnNR2 (*N. nucifera* - XP_010246478 and XP_010245911); OsNR1, OsNR2 and OsNR3 (*O. sativa* - XP_015622710.1, XP_015650300.1, - XP_015650643.1); SbNR1, SbNR2 and SbNR3 (*S. bicolor* - XP_002454625.1, XP_002444490.1 and XP_002454083.1), SpNR (*S. polyrhiza* - sequence translated from Acc. ID OL421561); LgNR (*L. gibba*_Chr11), LmNR (*L. minor*_Chr11).

3.3.3.2. Structural and Evolutionary Analysis of *Glutamine Synthetase* Genes

In contrast to *S. polyrhiza*, which possesses three *GS1* isoforms, *L. gibba* and *L. minor* exhibit only two *GS1* isoforms, designated as *GS1;1* and *GS1;2*. This difference indicates a reduction in *GS1* isoform diversity in *Lemna* species.

The *GS1;1* gene in *S. polyrhiza* (*SpGS1;1*) span 13 exons and 12 introns (Figure 3.9), located on chromosome 7 (position 6306673 - 6309664). It encodes the Glutamine Synthetase, catalytic domain (IPR008146) and N-terminal domain (IPR008147). In contrast, *L. gibba* (*LgGS1;1*) and *L. minor* (*LmGS1;1*) have a more conserved gene structure with 12 exons and 11 introns, located on chromosome 15 (positions 13857966 - 13861284 and 10462922 - 10466358, respectively). Despite these structural and genomic differences, all three species share the same functional domains, suggesting conservation of key enzymatic functions in *Lemna* species (Table 3.3).

The *GS1;2* gene in *S. polyrhiza* (*SpGS1;2*) maintains a structure of 13 exons and 12 introns on chromosome 18 (position 1351512 - 1353850) (Figure 3.9). Similarly, *L. gibba* (*LgGS1;2*) and *L. minor* (*LmGS1;2*), exhibit identical exon-intron structures (13 exons, 12 introns), located on chromosome 11 (positions 5789297 - 5791241 for *L. gibba* and 5320487 – 5322507 for *L. minor*). These structural similarities across species and the retention of conserved catalytic and N-terminal domains highlight evolutionary conservation (Table 3.3).

Both *Lemna* species and *S. polyrhiza* share a single *GS2* isoform, which is consistent with other plant species. The *GS2* gene comprises 13 exons and 12 introns and it is located on chromosome 1 in all three species. The catalytic and N-terminal domains are also conserved, underscoring functional stability across these species despite genomic differences (Figure 3.9, Table 3.3).

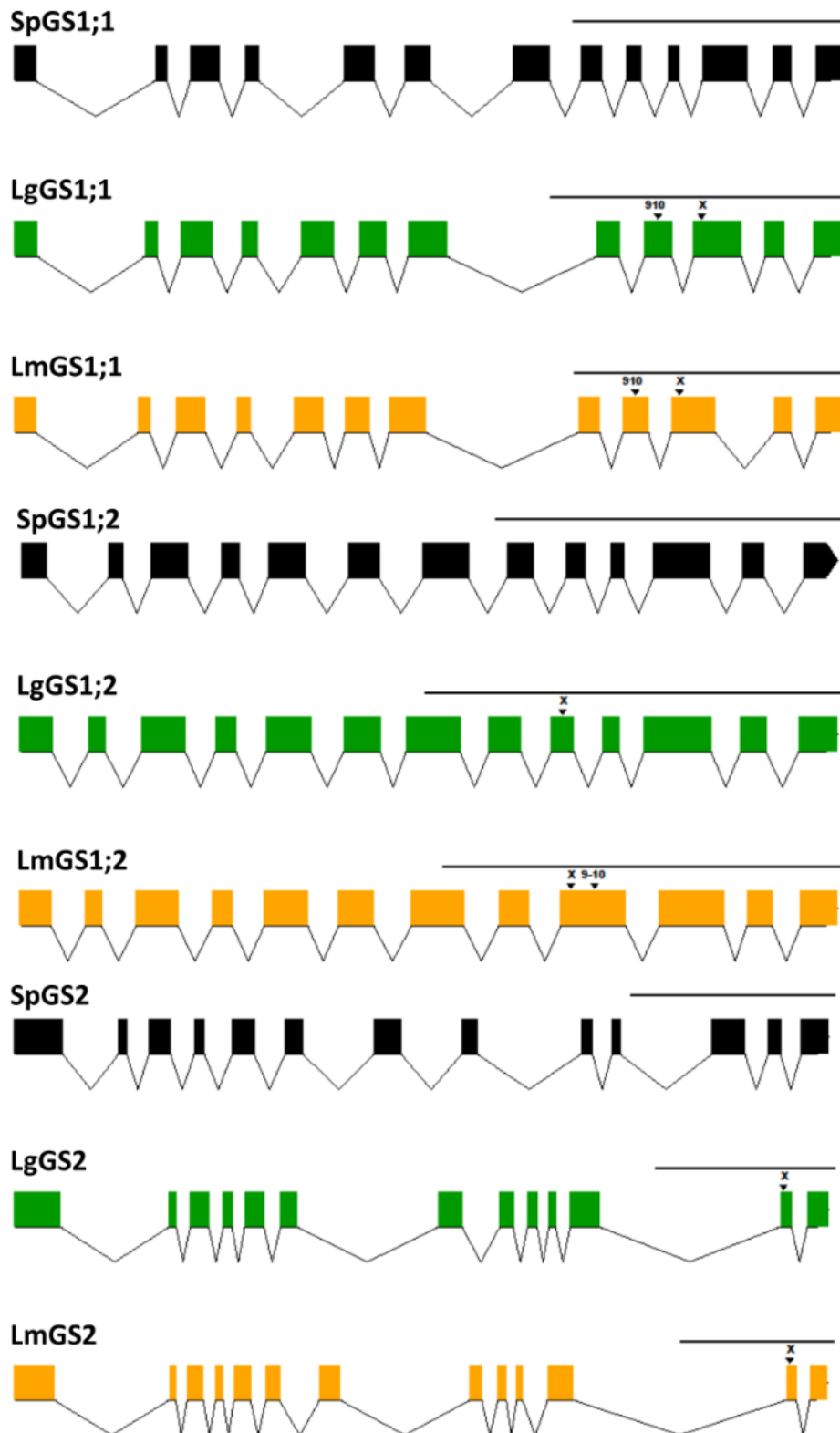


Figure 3.9. The Exon-Intron structures of *Spirodela polyrhiza*, *Lemna gibba* and *Lemna minor* Glutamine Synthetase (GS) genes. The exon-intron structures of the *L. gibba* and *L. minor* GS genes (*GS1;1*, *GS1;2* and *GS2*) are compared with those of *Spirodela polyrhiza* (*GS1;1*: MZ605906, *GS1;2*: MZ605907, and *GS2*: MZ605909). Coding sequences are represented by *GS1;1*, *GS1;2* and *GS2* coloured boxes, and introns are depicted as black lines. The X marks the primer binding sites used for RT-qPCR-based gene expression analysis. The scale bar represents 1 kb of DNA sequence.

The phylogenetic tree of glutamine synthetase (*GS*) genes revealed distinct evolutionary patterns among different plant species, particularly in the duckweed lineages (*L. gibba*, *L. minor*, and *S. polyrhiza*; Figure 3.10).

The *GS1;1* sequence from duckweed species cluster closely with those from monocot species, including *O. sativa*, *S. bicolor* and *B. distachyon*. This grouping suggests a common ancestral origin for these sequences. However, the node representing this cluster has a bootstrap support value of 0.46, indicating a lower confidence level in the precise evolutionary relationship. This lower confidence suggests possible genetic divergence of incomplete lineage sorting within this group, reflecting complex evolutionary dynamics.

The *GS1;2* sequences from duckweed species forms an external node, signifying a distinct evolutionary trajectory compared to other species. Interestingly, these cluster with *Arabidopsis thaliana* *GS1;4* (*AtGS1;4*), highlighting a unique genetic composition. This pattern suggests that the *GS1;2* isoform in duckweed has a separate evolutionary history, potentially driven by specific ecological adaptations or selective pressures unique to their aquatic environment.

The *GS2* sequences from duckweed appear to diverge earlier than the *GS2* sequences of both monocots and dicots, clustering before the major monocot-dicot split. This early divergence indicates that the genetic differentiation of *GS2* in duckweed species occurred prior to the evolutionary split of these plant groups. Such clustering suggests that significant evolutionary changes in *GS2* set the duckweed lineage apart early on, potentially reflecting unique functional adaptations in nitrogen metabolism specific to the duckweed ecological niche.

The phylogenetic tree highlights both conserved and divergent evolutionary pathways in *GS* genes among duckweed and other plant species. The patterns observed suggest that while duckweed shares some ancestral genetic features with monocots, unique evolutionary pressures have shaped their *GS* isoforms, particularly *GS1;2* and *GS2*, leading to distinct adaptations in the duckweed lineage.

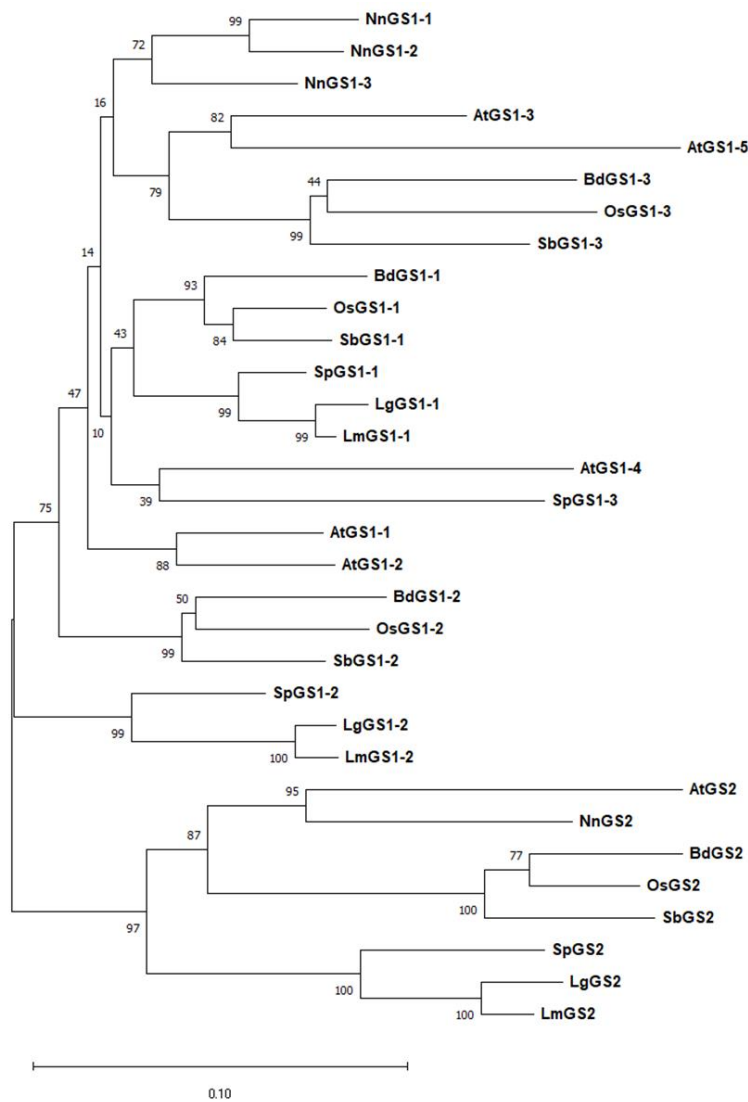


Figure 3.10. Phylogenetic tree of GS proteins in *Lemna gibba* and *Lemna minor* with other representative species. The phylogenetic tree highlights the relationships of nitrite reductase *GS1;1*, *GS1;2*, and *GS2* from *L. gibba* (*LgGS1;1*, *LgGS1;2* and *LgGS2*) and *L. minor* (*LmGS1;1*, *LmGS1;2* and *GS2*) with those from other monocot and dicot species. Branch lengths are proportional to evolutionary distances, with the mean branch length scale indicated at the bottom of the tree. Numbers on the nodes represent bootstrap values, providing statistical support for the clustering of the proteins.

GS1 proteins: AtGln1;1, AtGln1;2, AtGln1;3, AtGln1;4 and AtGln1;5 (*A. thaliana* - NP_198576.1, NP_176794.1, NP_188409.1, NP_001331815.1, and NP_175280.1); BdGS1;1, BdGS1;2 and BdGS1;3 (*B. distachyon* - XP_010236151.1, XP_003560727.2 and XP_003558466.1); NnGS1;1, NnGS1;2 and NnGS1;3 (*N. nucifera* - XP_010271383.1, XP_010271347.1 and XP_010250142.1), OsGS1;1, OsGS1;2 and OsGS1;3 (*O. sativa* - XP_015626102.1, XP_015631679.1 and XP_015628694.1); SbGS1;1, SbGS1;2 and SbGS1;3 (*S. bicolor* - XP_021313946.1, XP_002465624.1 and XP_021306978.1); SpGS1;1, SpGS1;2 and SpGS1;3 (*S. polyrhiza*- sequence translated from Acc. ID MZ605906, MZ605907 and MZ605908); LgGS1;1, LgGS1;2 (*L. gibba*_Chr15 and *L. gibba*_Chr11); LmGS1;1 and LmGS1;2 (*L. minor*_Chr15 and *L. minor*_Chr11).

GS2 proteins: AtGS2 (*A. thaliana* – NP_001031969.1); BdGS2 (*B. distachyon* – XP_003580719.1); HvGS2 (*H. vulgare* – P13564.2); NnGS2 (*N. nucifera* - XP_010255852.1); OsGS2 (*O. sativa* - XP_015635322.1); SbGS2 (XP_021319069.1); SpGS2 (*S. polyrhiza*- sequence translated from Acc. ID MZ605909); LgGS2 (*L. gibba*_Chr1); LmGS2 (*L. minor*_Chr1).

3.3.3.3. Structural and Evolutionary Analysis of *Glutamine Oxoglutarate Aminotransferase* Genes

The *Fd-GOGAT* gene in *S. polyrhiza* (*SpFD-GOGAT*) spans 33 exons and 32 introns (Figure 3.11), located on chromosome 1 (positions 4454784 - 4484474). It encodes a protein of 1623 amino acids, containing critical catalytic domains, including the glutamine aminotransferase type 2 domain (IPR017932), glutamate synthase alpha subunit C-terminal domain (IPR002489), and glutamate synthase domain (IPR002932). In *Lemna gibba* (*LgFD-GOGAT*) and *Lemna minor* (*LmFD-GOGAT*), the *Fd-GOGAT* gene shows an identical exon-intron structure, preserving these catalytic domains (Table 3.3).

The *NADH-GOGAT* gene maintains a consistent exon-intron structure of 22 exons and 21 introns across the species. It is located on chromosome 8 in *S. polyrhiza* (*SpNADH*: 4978991 - 4990379 bp) and chromosome 6 in *L. gibba* (*LgNADH*: 16377495 - 16386050 bp) and *L. minor* (*LmNADH*: 11803706 - 11812244 bp). The catalytic domains shared across species include the glutamine aminotransferase type 2 domain (IPR017932), glutamate synthase alpha subunit C-terminal domain (IPR002489), glutamate synthase central-N domain (IPR006982), FAD/NAD(P)-binding domain (IPR023753), and glutamate synthase domain (IPR002932) (Table 3.3).

Both *Fd-GOGAT* and *NADH-GOGAT* genes display strong structural conservation across *Spirodela* and *Lemna* species, with shared catalytic domains emphasizing their functional importance. However, differences in genomic length and chromosomal positioning highlight evolutionary nuances within the duckweed lineage.

The conservation of exon-intron structures and catalytic domains across these genes underscores their essential role in nitrogen assimilation and suggests evolutionary stability with adaptations specific to the aquatic environment (Figure 3.11).

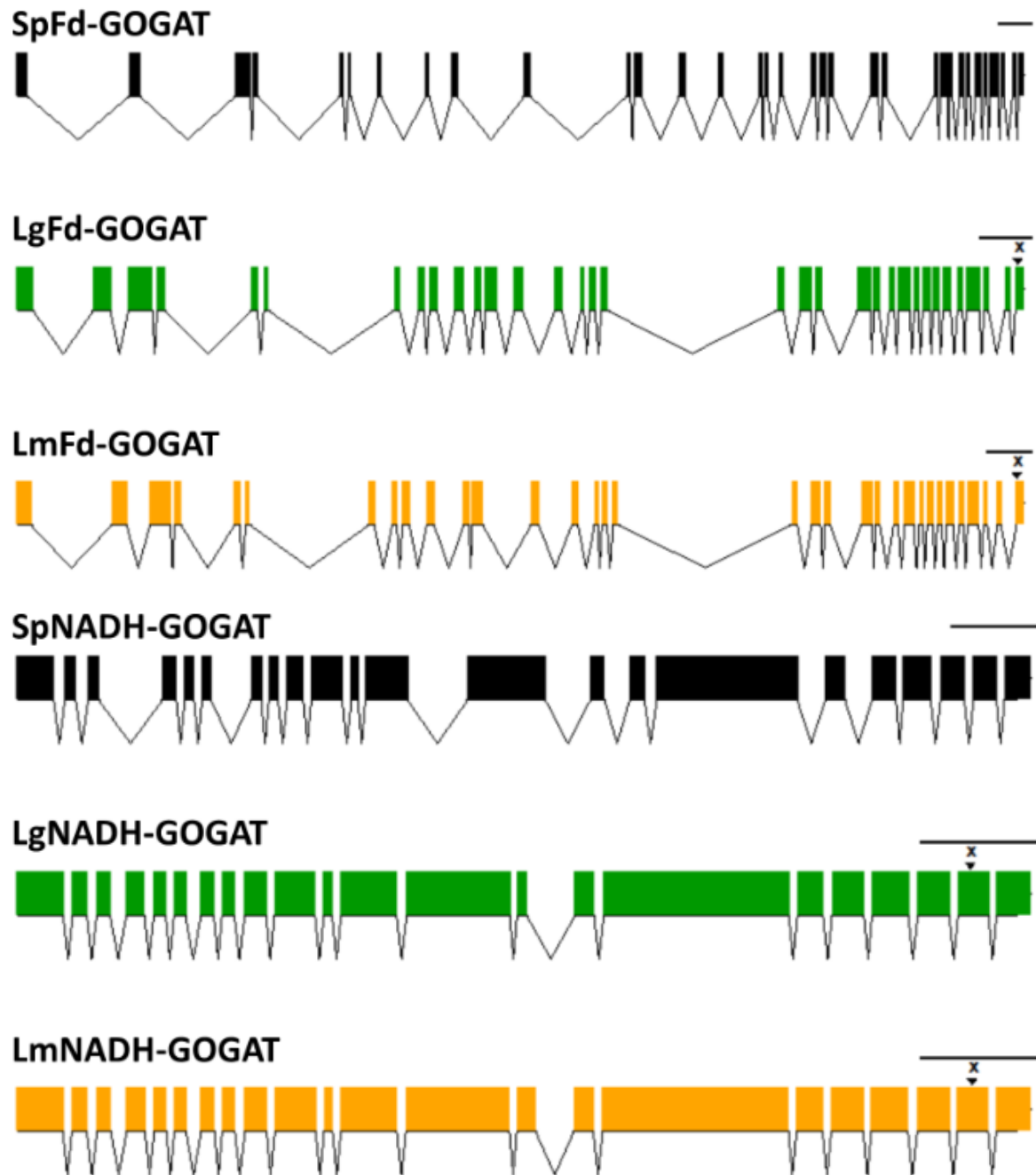


Figure 3.11. The Exon-Intron structures of *Spirodela polyrhiza*, *Lemna gibba* and *Lemna minor* Glutamine oxoglutarate aminotransferase-ferredoxin dependent (*Fd-GOGAT*) and Glutamine oxoglutarate aminotransferase-NADH dependent genes (*NADH-GOGAT*). The exon-intron structure of the *L. gibba* and *L. minor* *Fd-GOGAT* and *NADH-GOGAT* genes are compared with those of *Spirodela polyrhiza* (*Fd-GOGAT*: MZ605910 and *NADH-GOGAT*: OL421563). Coding sequences are represented by coloured boxes, and introns are depicted as black lines. The X marks the primer binding sites used for RT-qPCR-based gene expression analysis. The scale bar represents 1 kb of DNA sequence.

The phylogenetic tree comparing the amino acid sequences of *Fd-GOGAT* and *NADH-GOGAT* genes across various plant species, including duckweed species (*L. gibba* and *L. minor*), reveals distinct evolutionary relationships (Figure 3.12). Two well-differentiated clusters were observed, with *Fd-GOGAT* and *NADH-GOGAT* genes forming separate groups. Each cluster reflects orthologous relationships among the analysed species.

The *Fd-GOGAT* cluster contains a single gene copy in all species studied, except for *Arabidopsis thaliana*, which possesses two copies. Within this cluster, two major sub-clusters were identified. One sub-cluster groups crop such as *Sorghum bicolor*, *Oryza sativa* (rice), and the closely related *Brachypodium distachyon*. Interestingly, despite being classified as monocots, the *Fd-GOGAT* genes from duckweed species (including *L. gibba* and *L. minor*) group within the dicot cluster, alongside species such as *A. thaliana*. Similar clustering patterns were previously reported by Zhou *et al.* (2022) in their analysis of *Fd-GOGAT* genes from *Spirodela*. This clustering suggests that *Fd-GOGAT* genes in duckweed species share a closer evolutionary relationship with dicots than monocots, indicating possible functional or evolutionary convergence with dicot species.

In the *NADH-GOGAT* cluster, most species analysed, except duckweed and *Arabidopsis thaliana*, have two copies of the gene. These copies form sub-clusters in different groups in monocots, indicating that the gene duplication occurred prior to the diversification of the monocot species included in this study. Like the *Fd-GOGAT* cluster, the *NADH-GOGAT* genes from duckweed species group were in the dicot cluster, alongside species such as *A. thaliana* and *N. nucifera*. However, *N. nucifera* had two gene copies that cluster together, suggesting a recent duplication event within the species. The high similarity in *NADH-GOGAT* genes between duckweed and dicot species underscores strong evolutionary conservation, likely due to the critical role of this gene in amino acid biosynthesis.

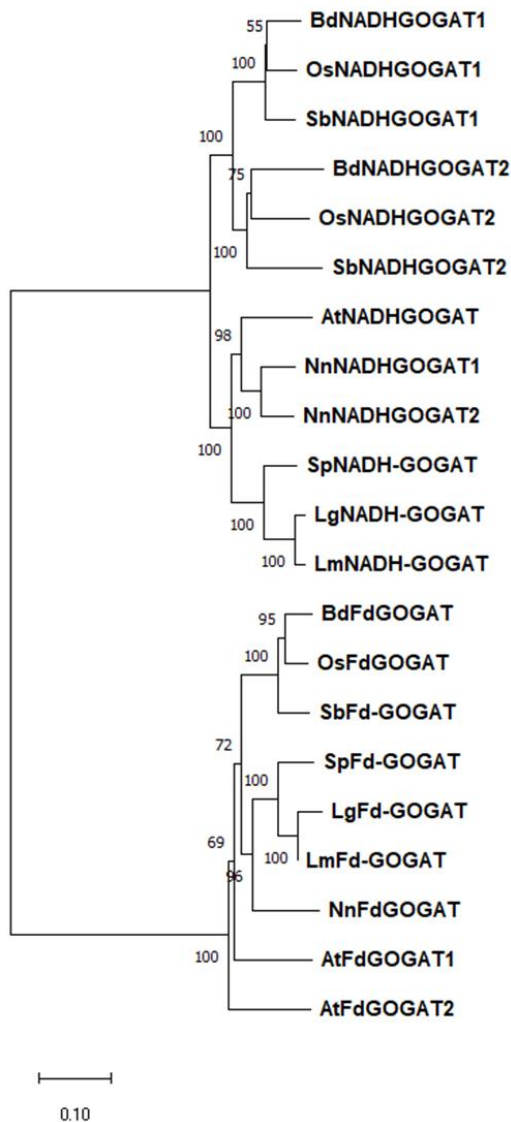


Figure 3.12. Phylogenetic tree of Fd-GOGAT and NADH-GOGAT proteins in *Lemna gibba* and *Lemna minor* with other representative species. The phylogenetic tree highlights the relationships between Fd-GOGAT and NADH-GOGAT for *L. gibba* (*LgFd-GOGAT* and *LgNADH-GOGAT*) and *L. minor* (*LmFd-GOGAT* and *LmNADH-GOGAT*) with those from other monocot and dicot species. Branch lengths are proportional to evolutionary distances, with the mean branch length scale indicated at the bottom of the tree. Numbers on the nodes represent bootstrap values, providing statistical support for the clustering of the proteins.

Fd-GOGAT proteins: AtFd-GOGAT1 and AtFd-GOGAT2 (*A. thaliana* - NP_850763.1 and NP_181655.1); BdFd-GOGAT (*B. distachyon* - XP_003559858.1); NnFd-GOGAT (*N. nucifera* - XP_010276670); OsFd-GOGAT (*O. sativa* - XP_015646712.1); SbFd-GOGAT (*S. bicolor* - XP_002463318.2), SpFdGOGAT (*S. polyrhiza*, sequence translated from Acc. ID MZ605910); LgFd-GOGAT (*L. gibba*_Chr1) and LmFd-GOGAT (*L. minor*_Chr1).

NADH-GOGAT proteins: AtNADH-GOGAT (*A. thaliana* - NP_200158.2), BdNADH-GOGAT1 and BdNADHGOGAT2 (*B. distachyon* - XP_003566997.1 and XP_024315185.1); NnNADH-GOGAT1 and NnNADH-GOGAT 2 (*N. nucifera* - XP_010261570.1 and XP_010266511.1), OsNADH-GOGAT1 and OsNADH-GOGAT2 (*O. sativa* XP_015649242.1 and XP_015640407.1); SbNADH-GOGAT1 and -SbNADH-GOGAT2 (*S. bicolor* - XP_002458326.1 and XP_021302649.1), SpNADH-GOGAT (*S. polyrhiza* - sequence translated from Acc. ID OL421563); LgNADH-GOGAT (*L. gibba*_Chr6) and LmNADH-GOGAT (*L. minor*_Chr6).

3.3.3.4. Structural and Evolutionary Analysis of *Chloride Channel A* Gene

The *Chloride Channel* gene (*CLC*) encodes *Chloride Channel A* (*CLCa*), showed evolutionary conservation and structural similarities among *S. polyrhiza*, *L. gibba*, and *L. minor.*, despite slight differences in amino acid length and chromosomal location (Table 3.3). In all three species, the gene is composed of four exons and three introns, highlighting a highly conserved exon-intron structure (Figure 3.13).

This gene in *L. gibba* (*LgCLCa*) is located on chromosome 21 (positions 6378711-6384350 bp) and encodes a protein of 822 amino acids. In *L. minor* (*LmCLCa1*), this gene is also situated on chromosome 21, spanning positions 4,939,808 to 4,943,394 base pairs, but encoding a slightly longer protein of 848 amino acids. In comparison with *S. polyrhiza* (*SpCLCa*), this gene is located on chromosome 7 (spanning positions 4,214,664 to 4,218,179 base pairs) and producing a shorter protein of 732 amino acids (Table 3.3).

Despite these minor variations in size and genomic location, all three species shared the same critical catalytic and voltage-gated domains essential for chloride channel function. These domains include the chloride channel voltage-gated domain (IPR001807), the CLC-plant domain (IPR002251), and the voltage-gated chloride channel/antiporter domain (IPR051280). The conserved presence of these domains underscores the functional importance of the *CLCa* gene in ion transport and its role in maintaining chloride ion balance within plant cells.

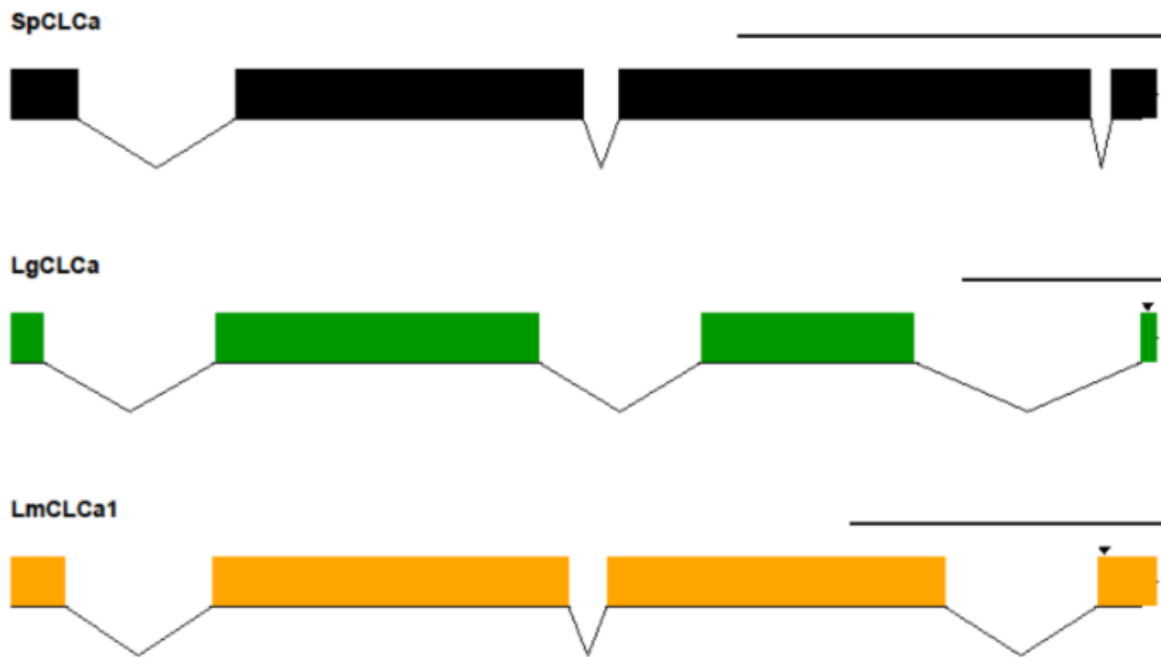


Figure 3.13. The Exon-Intron structures of *Spirodela polyrhiza*, *Lemna gibba* and *Lemna minor* of Chloride Channel A genes. The exon-intron structures of CLCa in *L. gibba* and *L. minor* are compared with those of *Spirodela polyrhiza*. Coding sequences are represented by coloured boxes, and introns are depicted as black lines. The X marks the primer binding sites used for RT-qPCR-based gene expression analysis. The scale bar represents 1 kb of DNA sequence.

The evolutionary relationships between different plant species were shown in the phylogenetic tree for comparing amino acid sequences of *CLCa* genes from *Lemna gibba*, *Lemna minor*, *Spirodela polyrhiza* and other species (Figure 3.14).

Duckweed species (*L. gibba*, *L. minor*, and *S. polyrhiza*) form a cohesive cluster, underscoring their close evolutionary proximity and shared lineage. Within the duckweed group, *L. gibba* and *L. minor* cluster together more closely, indicating greater similarity between these two species compared to *S. polyrhiza*. Interestingly, the tree reveals a closer relationship between duckweed species and other monocots than with dicots, suggesting that the evolution of chloride channels in aquatic monocots may have been influenced by unique ecological pressures.

Further analysis of the tree revealed two major clusters. One cluster included *Lemna* species, which are distinctly separated from all other species analysed, suggesting specialized evolutionary adaptations within the *Lemna* genus. In *L. minor*, two copies of the *CLCa1* gene were observed, similar to the gene duplication seen in *Arabidopsis thaliana*. This duplication may represent an adaptation to the specific physiological needs of these species.

The second major cluster included non-aquatic plants, with a clear division between monocot and dicot species. *S. polyrhiza* was placed within this cluster but formed a distinct subgroup, separated from both monocot and dicot plants. This placement suggests that while *S. polyrhiza* shares some evolutionary characteristics with non-aquatic plants, it retains unique features likely shaped by its aquatic habitat.

The phylogenetic tree highlights the robust and conserved nature of the *CLCa* gene across plant species, maintaining essential functions while adapting to diverse ecological contexts. The clear separation of *Lemna* species and the distinct clustering of *S. polyrhiza* reflect evolutionary diversification among aquatic plants, likely driven by their specialized environments and physiological demands.

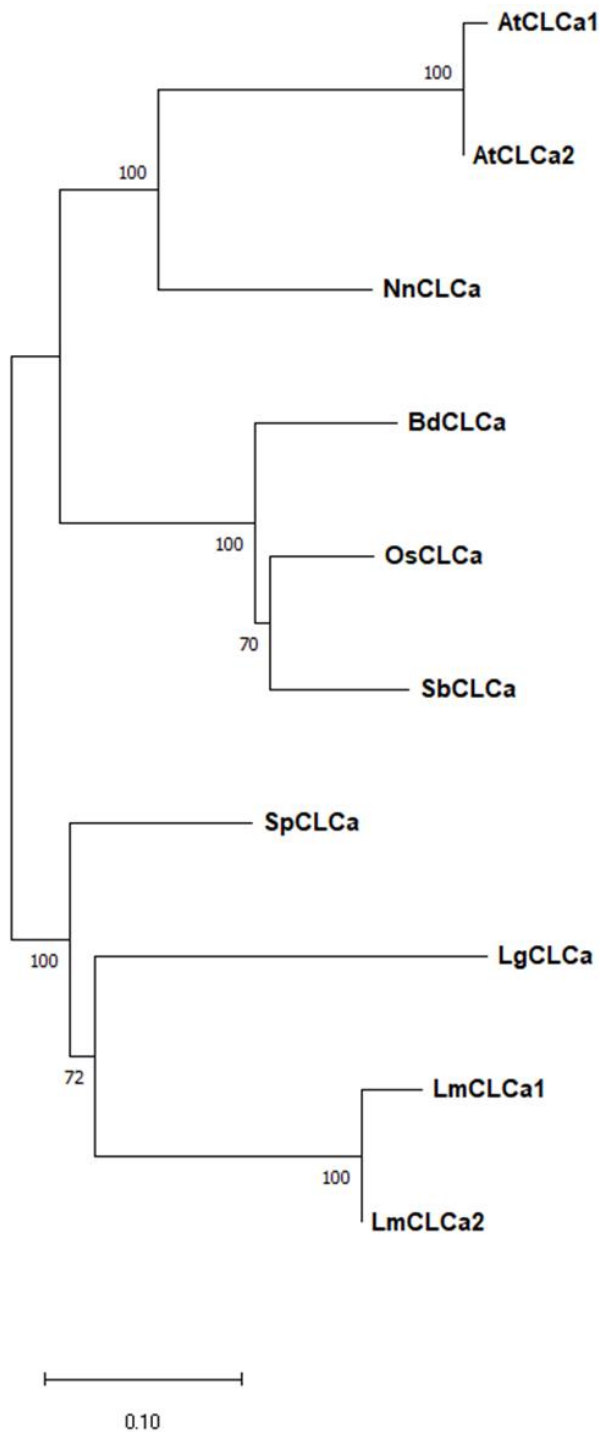


Figure 3.14. Phylogenetic tree of CLCa proteins in *Lemna gibba* and *Lemna minor* with other representative species. The phylogenetic tree shows the relationships between *L. gibba* (LgCLCa) and *L. minor* (LmCLCa) with those from other monocot and dicot species in CLCa proteins. Branch lengths are proportional to evolutionary distances, with the mean branch length scale indicated at the bottom of the tree. Numbers on the nodes represent bootstrap values, providing statistical support for the clustering of the proteins.

CLCa proteins: AtCLCa1 (*A. thaliana* - NP_198905.1), AtCLCa2 (*A. thaliana* - NP_001031990.1), BdCLCa (*B. distachyon* - XP_003576525.1), NnCLCa (*N. nucifera* - XP_010276208), OsCLCa (*O. sativa* - XP_015620662.1), SbCLCa (*S. bicolor* - XP_002438781.1), SpCLCa (*S. polyrhiza* - Spipo7G0046500), LgCLCa (*L. gibba*_Chr21), LmCLCa (*L. minor*_Chr21).

3.3.4. Expression of Nitrogen Assimilation Genes in Duckweed Under Different Nitrogen Sources

The genes analysed in this study were: *NR* (nitrate reductase), *NiR* (nitrite reductase), *GS1-1* (glutamine synthetase 1), *GS1-2* (glutamine synthetase 2), *GS2* (glutamine synthetase 2), *CLCa1* (chloride channel), *Fd-GOGAT* (ferredoxin-dependent glutamate synthase), and *NADH-GOGAT* (NADH-dependent glutamate synthase).

The expression of the *NR* gene exhibited a clear trend across the four clones. In all clones, *NR* expression level was very low (downregulated) under Ammonium-Nitrate treatment (*NR*, Figure 3.15), which is consistent with a reduced need for nitrate reduction when ammonium, a form of nitrogen directly available for assimilation, is present. Statistically significant reductions in *NR* expression under Ammonium-Nitrate were observed compared to the control (Nitrate) treatment, with p-values < 0.05. These results indicate that ammonium as a nitrogen source potentially represses *NR* to limit unnecessary nitrate reduction.

In contrast, under the Nil treatment (absence of nitrogen), clones DG4 and 7796 displayed significant upregulation of *NR* expression, especially when compared to the Nitrate treatment ($p < 0.01$), suggesting that these clones may mobilize internal nitrate reserves to support growth under nitrogen starvation. Clone DG8, however, exhibited less responsiveness overall, showing lower *NR* expression under Ammonium-Nitrate, which may reflect its more efficient use of ammonium as a nitrogen source.

The *NiR* gene, which encodes nitrite reductase, showed considerable variability, particularly in clone 7796 (*NiR*, Figure 3.15). This clone exhibited upregulation under both Nil and Urea-Nitrate treatments, with statistically significant increases in expression ($p < 0.01$) compared to the Nitrate treatment. This suggests that 7796 adjusts its nitrite reduction capacity based on the nitrogen source, with Urea-Nitrate and nitrogen starvation prompting a higher expression of *NiR*.

For clone DG8, significant upregulation of *NiR* expression was observed under Urea-Nitrate ($p < 0.05$), indicating a preference for organic nitrogen sources in this clone. These findings suggest that 7796 and DG8 may utilize different nitrogen assimilation strategies, with 7796 being more responsive to both nitrogen starvation and urea treatments, while DG8 shows a preference for urea-derived nitrogen.

The *GS1-1* gene showed downregulation under Ammonium-Nitrate treatment in SD, DG4, and DG8 (*GS1-1*, Figure 3.15), suggesting that these clones reduce the activity of glutamine synthetase 1 when ammonium is available. In 7796, however, *GS1-1* was upregulated under both Nil and Ammonium-Nitrate treatments ($p < 0.05$), indicating that this clone may rely more on *GS1-1* for nitrogen assimilation, even under conditions of nitrogen starvation. Despite its lower overall expression of *GS1-*

1, 7796 was able to achieve high protein content, suggesting that other genes or pathways may compensate for this reduced expression in nitrogen assimilation.

Similarly, *GS1-2* was generally downregulated under Ammonium-Nitrate and Urea-Nitrate treatments in SD and DG8 (*GS1-2*, Figure 3.15), consistent with reduced reliance on glutamine synthetase activity when nitrogen is readily available. By contrast, 7796 exhibited upregulation of *GS1-2* under Nil and Urea-Nitrate conditions ($p < 0.05$), indicating that *GS1-2* may play a significant role in facilitating nitrogen assimilation under organic nitrogen sources, particularly urea. These findings suggest that 7796 utilizes a more versatile nitrogen assimilation strategy than other clones, possibly favouring organic nitrogen sources like urea when nitrate is not available.

The *GS2* gene was downregulated in DG8 under both Ammonium-Nitrate and Urea-Nitrate treatments (*GS2*, Figure 3.15), which may indicate a reduced reliance on glutamine synthetase 2 activities in these conditions. In contrast, DG4 showed increased *GS2* expression under Urea-Nitrate, suggesting an enhanced capacity for assimilating organic nitrogen. This differential expression of *GS2* reflects the clones' varying ability to utilize nitrogen from different sources.

The expression of *CLCa1*, a chloride channel, was upregulated in the Nil treatment for DG4, DG8, and 7796 (*CLCA1*, Figure 3.15), suggesting its role in maintaining ion balance during nitrogen starvation. However, DG8 exhibited a significant downregulation of *CLCa1* under Ammonium-Nitrate and Urea-Nitrate treatments, which could indicate its sensitivity to these nitrogen treatments. Statistically, these changes were significant ($p < 0.01$) when comparing Nil treatment to other nitrogen sources, emphasizing the role of *CLCa1* in maintaining cellular homeostasis under nitrogen stress conditions.

The expression of *Fd-GOGAT* was significantly reduced in DG8 under urea treatment ($p < 0.05$) (*Fd-GOGAT*, Figure 3.15), reflecting a lower need for ferredoxin-dependent glutamate synthesis when organic nitrogen sources, like urea, are abundant. Similarly, *NADH-GOGAT* was downregulated in SD and DG4 under both Ammonium-Nitrate and Urea-Nitrate treatments, suggesting that this pathway plays a lesser role under these nitrogen conditions. The statistical analysis showed that the reductions in expression were significant, with p -values < 0.05 for both clones compared to the control (nitrate).

Across all clones, distinct regulatory patterns for nitrogen assimilation genes were observed, highlighting the genetic diversity in nitrogen utilization strategies among those clones. The clone 7796 stood out in particular, showed high protein content despite lower *GS1-1* expression, possibly relies more on *NiR* and other pathways to compensate for reduced glutamine synthetase activity. These findings underscore the importance of nitrogen source in regulating nitrogen assimilation pathways and emphasize the flexibility of duckweed in adapting to various nitrogen conditions.

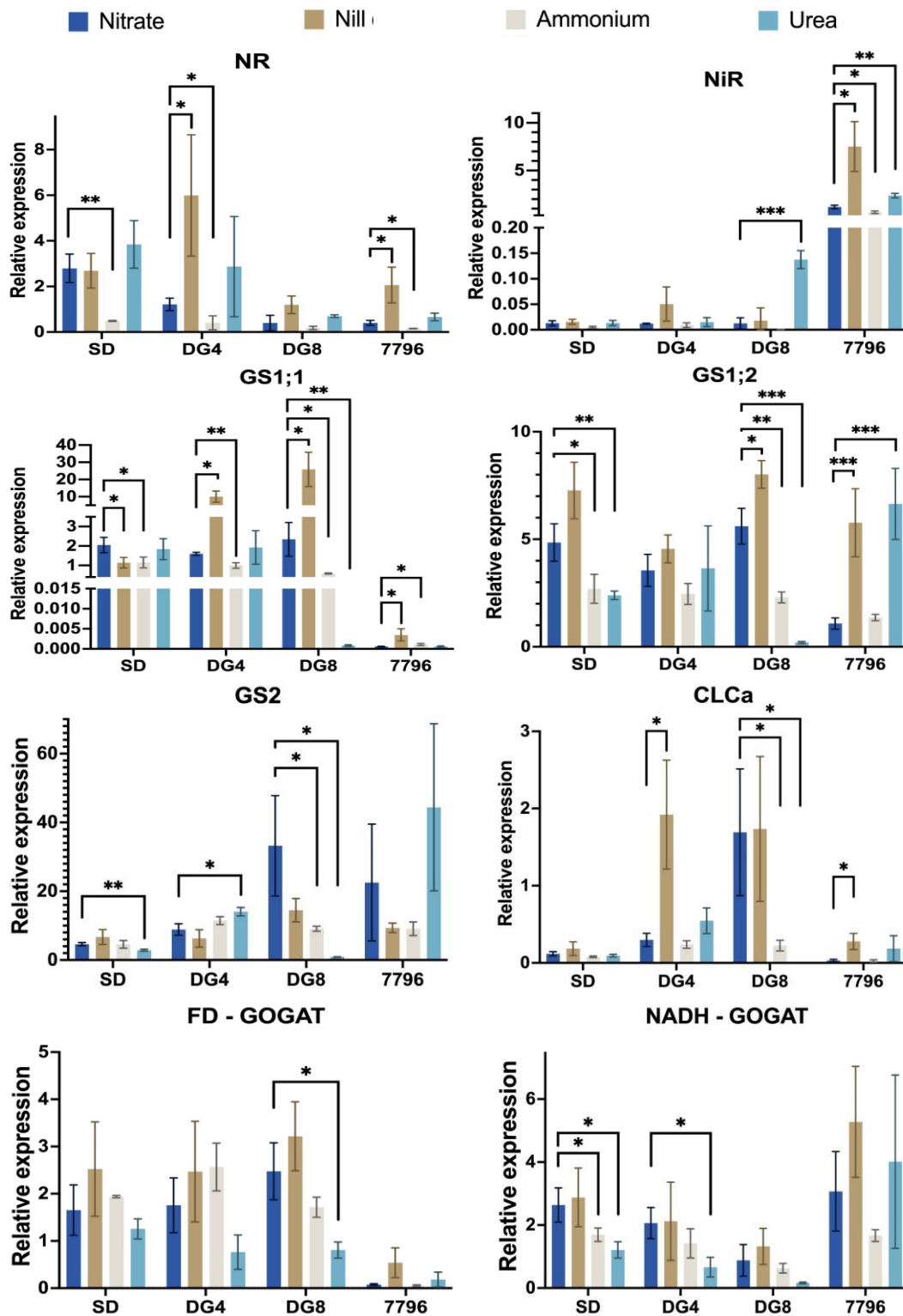


Figure 3.15. Relative expression of *NR*, *NiR*, *GS1-1*, *GS1-2*, *GS2*, *CLCa1*, *Fd-GOGAT*, and *NADH-GOGAT* genes in four duckweed clones. The clones analysed were *Lemna minor* SD, *Lemna minor* DG4, *Lemna minor* DG8, and *Lemna gibba* 7796. These clones were grown under four Nitrogen treatments: Nitrate (control), Nil, Ammonium-Nitrate, and Urea-Nitrate, with gene expression assessed at Day 7. The relative gene expression relative to *GADPH* was determined by RT-qPCR and is presented as fold change relative to the nitrate control. Bars represent the mean expression level from three biological replicates, with standard error (SE) shown. Asterisks (*) indicate significant differences compared to the control (nitrate) based on One-way ANOVA ($p < 0.05$).

3.4. Discussion

The study aimed to investigate the effects of four nitrogen sources (Nitrate, Nil nitrogen, Ammonium-Nitrate, and Urea-Nitrate) on the growth and nitrogen assimilation of four duckweed clones—three *Lemna minor* (SD, DG4, and DG8) and one *Lemna gibba* (7796). Comparative genomics and phylogenetic analyses of nitrogen assimilation genes were done to investigate the evolutionary relationships between duckweed and other monocot and dicot species. Key physiological parameters, including Relative Growth Rate (RGR), medium pH, total nitrogen, total nitrate, and total protein content, were assessed at two time points (day 4 and day 7). Additionally, the expression of eight nitrogen assimilation genes (*NR*, *NiR*, *GS1-1*, *GS1-2*, *GS2*, *Fd-GOGAT*, *NADH-GOGAT*, and *CLCa1*) was analysed via RT-qPCR to understand the regulatory mechanisms underlying nitrogen metabolism in these clones.

The growth patterns observed in response to different nitrogen sources demonstrated clear clone-specific preferences. Relative growth rates (RGR) varied significantly among the clones, with SD and DG4 showed a strong preference for Nitrate treatment since they showed the highest RGR under this condition. This aligns with previous findings that nitrate supports optimal growth in plants, as it serves as a major nitrogen source for many species (Devlamynck *et al.*, 2020). On the other hand, clone 7796, *Lemna gibba*, exhibited better growth under Urea-Nitrate treatment, suggesting that this clone has a distinct metabolic adaptation that favours the use of urea as a nitrogen source. This result supports previous studies that have found urea to be beneficial for certain aquatic plant species, potentially due to its rapid uptake and assimilation by the roots and fronds (Garnica *et al.*, 2010).

Ammonium-Nitrate treatments led to a reduction in growth rates across all clones, with a notable decline observed by day 7. This reduction was correlated with a significant drop in the medium pH to approximately 4, which is known to create acidic conditions that can inhibit plant growth (Körner *et al.*, 2001). These findings are consistent with those of previous studies, which reported that ammonium-based fertilizers, especially when not properly buffered, can suppress plant growth due to acidification of the surrounding environment (Wang *et al.*, 2016). In addition, the Nil nitrogen treatment resulted in a significant decrease in growth for all clones, likely due to nitrogen starvation, which is expected to impede the normal metabolic processes essential for growth.

Protein content, a critical indicator of Nitrogen Use Efficiency (NUE), was different between different clones. Clone 7796 consistently exhibited the highest protein content compared to the other clones under all treatments. This finding highlights the superior NUE of this clone, particularly under Urea-Nitrate and nitrate conditions, where protein synthesis is optimized in response to nitrogen availability. This result is consistent with previous studies that have linked high protein content with

efficient nitrate assimilation (Xu *et al.*, 2023; Zhou *et al.*, 2022). The ability of clone 7796 to achieve high protein levels despite potentially lower nitrogen input or under varying nitrogen conditions suggests that it has adapted robust mechanisms for nitrogen assimilation and storage, further underlining its suitability for agricultural applications, particularly in systems where protein yield is of paramount importance.

In contrast, protein content was relatively consistent across the treatments within each clone, indicating that duckweed plants can adjust their protein synthesis according to the nitrogen forms available in the environment. This highlights the flexibility of duckweed in adjusting its metabolism to optimize nitrogen use, even when nitrogen availability is limited or varied. Clones SD and DG4, which exhibited high growth rates under Nitrate treatment, also demonstrated efficient protein synthesis, suggesting that they rely on nitrate as their preferred nitrogen source.

Nitrate accumulation varied across clones and nitrogen treatments. Clones SD and DG4 accumulated the highest levels of nitrate when grown under Nitrate treatment, which is consistent with previous reports showing that Nitrate treatments directly increase nitrate levels in plants (Bassioni *et al.*, 1980; Ochieng' *et al.*, 2021). On the other hand, clones DG8 and 7796 showed comparable nitrate levels in nitrate and Urea-Nitrate treatments. This suggests that these clones may possess enhanced pathways for nitrate uptake and assimilation, particularly in the presence of urea, which can stimulate nitrate assimilation in some plant systems (Garnica *et al.*, 2010).

Interestingly, clones SD and DG4 demonstrated the highest nitrate accumulation under Nitrate treatment, highlighting their preference for this nitrogen source. This suggests that these clones may have evolved efficient nitrate uptake systems, allowing them to thrive in environments rich in nitrate. In contrast, clones DG8 and 7796 displayed comparable nitrate levels under both nitrate and Urea-Nitrate treatments, indicating that they may have developed more versatile nitrogen assimilation pathways, capable of utilizing both nitrate and urea efficiently.

The comparative genomics and phylogenetic analysis of nitrogen assimilation genes in duckweed revealed a blend of both conserved and divergent genes, providing insights into its evolutionary history. Key genes involved in nitrogen metabolism, such as Nitrate Reductase (*NR*) and Nitrite Reductase (*NiR*), exhibited distinct patterns of evolutionary alignment when compared to other plant species. The *NiR* genes from *L. gibba* and *L. minor* clustered closely with those of monocot species, indicating a shared evolutionary origin, likely due to early adaptation to aquatic environments. This is consistent with findings from previous studies that observed similar patterns of evolutionary alignment in other aquatic species, such as *Spirodela polyrhiza* (Zhou *et al.*, 2022). The *NR* genes,

however, aligned more closely with dicot clades, suggesting a divergence within the Lemnoideae subfamily that might be driven by ecological pressures specific to each lineage's habitat.

A notable divergence in the nitrogen assimilation pathway was the absence of the *GS1-3* isoform in *Lemna* species, a characteristic that distinguishes them from *S. polyrhiza*, another member of the Lemnoideae subfamily (Zhou *et al.*, 2022). This divergence highlights how different species within the same family have adapted to their unique ecological niches. While *S. polyrhiza* retains the *GS1-3* isoform, *Lemna* species rely on the *GS1-1* and *GS1-2* isoforms for efficient nitrogen assimilation. This absence of *GS1-3* in *Lemna* may reflect a more streamlined adaptation to specific environments, where nitrogen metabolism is optimized for efficiency and rapid growth in nutrient-rich aquatic systems.

Further analyses of the amino acid sequences of these genes suggest divergence in nitrogen assimilation strategies among these species. The divergence in the *GS* isoforms and other key nitrogen metabolism genes supports the hypothesis that evolutionary divergence is driven by ecological demands. The ability of *Lemna* species to utilize *GS1-1* and *GS1-2* isoforms for nitrogen assimilation enables them to thrive in a variety of aquatic environments, further emphasizing their specialized adaptation to nutrient-rich waters.

However, the conservation of other nitrogen assimilation genes, such as *Fd-GOGAT* and *NADH-GOGAT*, across monocot and dicot species highlights the fundamental importance of these pathways for plant survival. These genes have remained largely conserved due to their essential role in nitrogen assimilation, providing the flexibility necessary for plants to survive in different nitrogen availability conditions. Duckweed's ability to cluster with dicots in these pathways is particularly significant, as it suggests a deep evolutionary adaptability that has enabled the plant to thrive in a wide range of environments, from nutrient-poor to nutrient-rich aquatic ecosystems. This adaptability allows duckweed to efficiently utilize available nitrogen, making it a promising candidate for both agricultural and ecological applications.

Overall, the balance between the conservation and divergence of nitrogen assimilation genes illustrates how duckweed has evolved to thrive in aquatic ecosystems. The maintenance of essential metabolic functions while adapting to specific ecological niches highlights duckweed's remarkable evolutionary flexibility (Barbosa Neto *et al.*, 2019). These findings provide a deeper understanding of the molecular mechanisms that underlie duckweed's efficient nitrogen metabolism and its potential use in sustainable agricultural and environmental applications.

The expression of eight key nitrogen assimilation genes (*NR*, *NiR*, *GS1-1*, *GS1-2*, *GS2*, *Fd-GOGAT*, *NADH-GOGAT*, and *CLCa1*) was analysed to understand the molecular basis of nitrogen metabolism in the four duckweed clones under different nitrogen treatments. The results revealed distinct patterns of gene expression across clones and treatments, highlighting the genetic diversity and regulatory strategies employed by each clone in response to nitrogen availability.

The *NR* gene, which encodes nitrate reductase, was consistently downregulated in response to Ammonium-Nitrate treatment across all clones. This downregulation reflects a reduced need for nitrate reduction when ammonium is available, as ammonium can directly provide nitrogen for amino acid synthesis and other metabolic processes. Clone 7796 exhibited increased *NR* expression under nitrogen starvation (Nil treatment), suggesting a strategy of mobilizing internal nitrate reserves to support metabolic activity under nitrogen-deficient conditions. This strategy is commonly observed in nitrogen-starved plants, where nitrate reserves are remobilized to sustain essential metabolic processes (X. M. Yin et al., 2014). *NiR*, the gene encoding nitrite reductase, displayed variability across clones. Clone 7796 exhibited significant upregulation of *NiR* under both Nil and Urea-Nitrate treatments, suggesting a preference for organic nitrogen sources, which is consistent with other reports in aquatic plants (Azab & Soror, 2020).

The expression of glutamine synthetase (*GS*) genes, including *GS1-1*, *GS1-2*, and *GS2*, revealed a highly dynamic and complex regulatory network that varied across different clones and treatment conditions. In general, *GS1-1* was downregulated in response to Ammonium-Nitrate treatment in clones SD, DG4, and DG8. This downregulation under nutrient-sufficient conditions suggests that *GS1-1* is primarily involved in nitrogen remobilization, a process that becomes more critical when nitrogen availability is low. Notably, under nitrogen starvation (Nil treatment), *GS1-1* showed upregulation in these same clones, indicating its role in remobilizing ammonium (NH_4^+) derived from protein degradation during nitrogen stress. This pattern aligns with the findings of Hörtensteiner & Feller, (2002) and Masclaux *et al.*, (2000) who proposed that *GS1-1* plays a crucial role in the recycling of nitrogen during periods of low nitrogen availability, helping the plant maintain metabolic functions when external nitrogen sources are limited or senescence.

Clone 7796 displayed an interesting deviation from this pattern, exhibiting low *GS1-1* expression despite maintaining high protein content across all treatments. This observation suggests that clone 7796 may rely on alternative nitrogen assimilation pathways or a more efficient nitrogen use strategy to cope with nitrogen deficiency, enabling it to achieve robust growth and maintain protein synthesis even under limiting nitrogen conditions. This indicates a potential adaptive mechanism that enables clone 7796 to handle nitrogen stress differently from the other clones.

In contrast to *GS1-1*, the expression of *GS1-2* was more variable across the different clones and treatments. In SD and DG8, *GS1-2* expression was downregulated under Ammonium-Nitrate and Urea-Nitrate treatments, suggesting that its role is less prominent under conditions where ammonium and nitrate are readily available. However, *GS1-2* was upregulated under Nil and Urea-Nitrate conditions in clone 7796, pointing to its critical involvement in nitrogen assimilation when nitrate or ammonium availability is limited. This observation supports the idea that *GS1-2* plays a central role in the nitrogen assimilation network, particularly under nitrogen-limiting conditions, possibly by facilitating the assimilation of ammonium released during photorespiration (Zhou *et al.*, 2022).

GS2 expression, which is typically involved in supporting the nitrogen assimilation process in chloroplasts, also demonstrated varying patterns across the clones. In DG8, *GS2* was downregulated under both Ammonium-Nitrate and Urea-Nitrate treatments, while in DG4, *GS2* expression was enhanced under Urea-Nitrate conditions, suggesting a clone-specific regulation of *GS2* activity. This variation in *GS2* expression further supports the hypothesis that different clones exhibit unique strategies for nitrogen assimilation depending on their environmental conditions. The regulation of *GS2*, particularly in response to Urea-Nitrate, might indicate an adaptation that allows certain clones to more effectively utilize available nitrogen sources.

These findings are consistent with studies on other monocot crops, such as barley (Goodall *et al.*, 2013) and rice (Yamaya & Kusano, 2014), where *GS1-2* plays a dominant role in primary ammonium assimilation in roots, complementing *GS2* activity in green tissues by assimilating ammonium produced during photorespiration (Ferreira *et al.*, 2019). The results of this study suggest that a similar mechanism in duckweed, with *GS1-2* and *GS2* working in tandem to optimize nitrogen assimilation and support the plant's rapid growth rate and biomass accumulation. The clone-specific regulation of these *GS* genes reflects the diverse strategies employed by duckweed to manage nitrogen assimilation in response to varying environmental conditions, highlighting the plant's remarkable adaptability.

Overall, the differential expression patterns of *GS* genes across clones and treatments emphasize the complexity of nitrogen metabolism in duckweed and its ability to fine-tune its nitrogen assimilation pathways based on environmental cues as has been described in other plants (Elsanosi *et al.*, 2024). This adaptability is key to duckweed's success in nutrient-variable aquatic environments, enabling it to maintain high growth rates and biomass accumulation even under nitrogen stress.

The expression of *Fd-GOGAT* and *NADH-GOGAT*, genes involved in the assimilation of ammonium into glutamate, revealed further diversity in nitrogen assimilation pathways. *Fd-GOGAT* was significantly downregulated in DG8 under Urea-Nitrate treatment, suggesting a reduced need for ferredoxin-dependent glutamate synthesis under these conditions. Similarly, *NADH-GOGAT* expression was

downregulated in SD and DG4 under Ammonium-Nitrate and Urea-Nitrate treatments, suggesting that this pathway plays a lesser role in nitrogen assimilation under these conditions.

The findings of this study offer significant implications for environmental and agricultural applications, particularly in optimizing nitrogen use efficiency (NUE) in duckweed cultivation. Understanding the nitrogen metabolism of different duckweed clones provides crucial insights into how these plants respond to varying nitrogen sources, and how these responses impact growth rates, protein production, and overall nitrogen assimilation. Notably, clone 7796 exhibited superior protein content and efficient nitrogen utilization, making it a strong candidate for applications where high protein yield is prioritized, such as sustainable feed or food systems. The ability of duckweed to efficiently assimilate nitrogen makes it an appealing candidate for such applications, and by tailoring cultivation practices to specific clones and nitrogen conditions, NUE in duckweed-based systems can be significantly enhanced.

Duckweed, due to its remarkable adaptability and high nitrogen uptake potential, serves a dual purpose as both a nutrient remediator and a protein source (Devlamynck *et al.*, 2020). Its ability to thrive in nutrient-rich environments such as those found in wastewater systems, makes it an effective tool for nitrogen remediation, particularly in environments with excess nitrogen. The variability observed among duckweed clones, especially their differing preferences for nitrogen sources like nitrate or Urea-Nitrate, further highlights their potential for targeted applications. For instance, clones with a high capacity for nitrate uptake, such as SD, are particularly well-suited for wastewater treatment projects, where their ability to absorb and recycle nitrogen from the water can help reduce nutrient pollution. On the other hand, clones like 7796, which demonstrate robust growth and high protein production, could be better suited to support sustainable feed or food production systems, where efficient nitrogen assimilation is crucial for maintaining growth and protein yield.

The genetic and physiological diversity observed among duckweed clones opens new possibilities for broader applications in sustainable agriculture. Integrating duckweed into nutrient management systems could help recycle nitrogen in agricultural runoff, thus minimizing the environmental impact of excess nitrogen. Duckweed's ability to absorb and assimilate nitrogen efficiently means it could play a pivotal role in mitigating nitrogen pollution in agricultural settings. Additionally, by producing valuable biomass in the process, duckweed can contribute to the circular bioeconomy. The versatility of different clones, with varying levels of nitrogen assimilation efficiency and growth traits, further highlights the plant's potential to meet diverse needs across agricultural and environmental sectors. Utilizing these traits not only enhances sustainability but also supports efforts to balance food production with environmental conservation.

Moreover, this study contributes to our understanding of duckweed's potential as a versatile crop in circular bioeconomy initiatives. Duckweed can be integrated into nutrient recycling systems where it not only helps reduce nitrogen runoff but also produces biomass that can be used as a feedstock for biogas production or even as a renewable protein source. Its rapid growth and high nitrogen use efficiency make it an ideal candidate for these applications, offering an environmentally friendly solution for nutrient recovery while also providing a source of valuable biomass.

While the experiments provided valuable insights into the nitrogen metabolism of duckweed, certain limitations should be acknowledged. The controlled laboratory conditions, though essential for maintaining experimental consistency, may not fully capture the complexities of natural environments, where factors such as microbial interactions, fluctuating temperatures, and variable light intensities could significantly affect plant growth and nitrogen assimilation. Furthermore, the study focused on four specific nitrogen sources and eight nitrogen assimilation genes, which limits the scope of its findings. Expanding the analysis to include a broader range of nitrogen forms, such as organic nitrogen compounds or commonly used agricultural fertilizers, could provide a more comprehensive understanding of duckweed's metabolic flexibility. This could also help optimize duckweed cultivation for different agricultural and environmental contexts.

In addition to broadening the range of nitrogen sources tested, future research could benefit from exploring other aspects of nitrogen metabolism in duckweed, such as the regulatory pathways that control the expression of key nitrogen assimilation genes under different environmental conditions. Moreover, while this study focused on four duckweed clones, expanding the genetic pool to include a wider variety of species and clones could provide insights into whether the observed trends are universally applicable to all duckweed species or if they are unique to specific clones. Comparative studies involving different species within the Lemnoideae subfamily, such as *Spirodela* or *Wolffia*, could further expand our understanding of nitrogen metabolism in these plants and provide insights into how evolutionary divergence has shaped their nitrogen assimilation strategies.

Field-based studies will be essential for evaluating the adaptability of duckweed clones in real-world conditions, such as those found in wastewater treatment systems or agricultural runoff environments. Long-term experiments could also help determine how sustained exposure to varying nitrogen treatments influences duckweed biomass quality, nutrient cycling efficiency, and overall ecosystem health. Additionally, incorporating advanced genetic tools to optimize nitrogen use efficiency in duckweed—particularly through the targeted manipulation of key nitrogen assimilation genes—holds great potential for enhancing the plant's utility in both environmental remediation and agricultural systems.

This study explored the impact of four nitrogen sources (Nitrate, Nil nitrogen, Ammonium-Nitrate, and Urea-Nitrate) on the growth and nitrogen assimilation of four duckweed clones, revealed significant clone-specific differences in nitrogen utilization and gene expression. Clone 7796 stood out as the most efficient in nitrogen use, had the highest protein content and growth rates, particularly under Urea-Nitrate and Nitrate treatments. These findings not only enhance our understanding of nitrogen metabolism in duckweed but also highlight the potential of specific clones for targeted agricultural and environmental applications. The results reinforce the idea that different duckweed clones exhibit diverse nitrogen assimilation strategies, and these differences can be leveraged to optimize growth and nutrient uptake in both controlled and natural systems. Overall, results of this research show that duckweed is a promising candidate for sustainable nitrogen management, wastewater treatment, and biomass production, with numerous potential applications in the circular bioeconomy.

4. Chapter 4. Physiological Assessments on *Lemna* Growth Under Heat Stress

4.1. Introduction

Duckweeds, known for their small size and incredibly fast growth, recently have become quite popular in plant research. Their unique growth characteristics make them ideal for experiments requiring quick results and serve as a valuable model for studying plant responses to environmental stresses (Oláh *et al.*, 2010; Scherr *et al.*, 2007; Strzałek & Kufel, 2021). Among these stresses, heat stress stands out due to its increasing prevalence with rising global temperatures. Heat stress significantly affects plants at multiple levels (Figure 4.1): it reduces photosynthetic efficiency by degrading chlorophyll, Rubisco, and other photosynthetic pigments and impairs the function of photosystem II (Hasanuzzaman *et al.*, 2013; Perdomo *et al.*, 2017; Song *et al.*, 2014). Growth and development are also affected, with smaller leaf areas, reduced plant growth, and changes in seed germination and nutritional quality (Zhang *et al.*, 2013). On a cellular level, heat stress triggers the overproduction of reactive oxygen species (ROS), causing oxidative damage (Nosaka & Nosaka, 2017). It also interferes with nutrients uptake (Mishra *et al.*, 2023) and reduces water uptake efficiency, further exacerbating plant stress (Liu *et al.*, 2020). Additionally, it weakens cellular integrity by increasing membranes fluidity and permeability (Wang *et al.*, 2016). Given the challenges posed by climate change, understanding plant responses and adaptations to heat stress is more critical than ever.

Researchers have explored various strategies to help plants cope with heat stress, ranging from protective chemicals to selective breeding for heat-tolerant crop varieties (Akter & Islam, 2017; Wahid *et al.*, 2007). Despite these efforts, high temperatures continue to disrupt essential plants processes, such as growth and protein synthesis, by breaking down proteins, destabilizing membranes, and impairing enzyme functions (Huang & Xu, 2008; Divya *et al.*, 2023). These effects result in reduced biomass, lower crop yields, and declined protein content, although stress-induced proteins such as heat shock proteins are often upregulated (Huang & Xu, 2008).

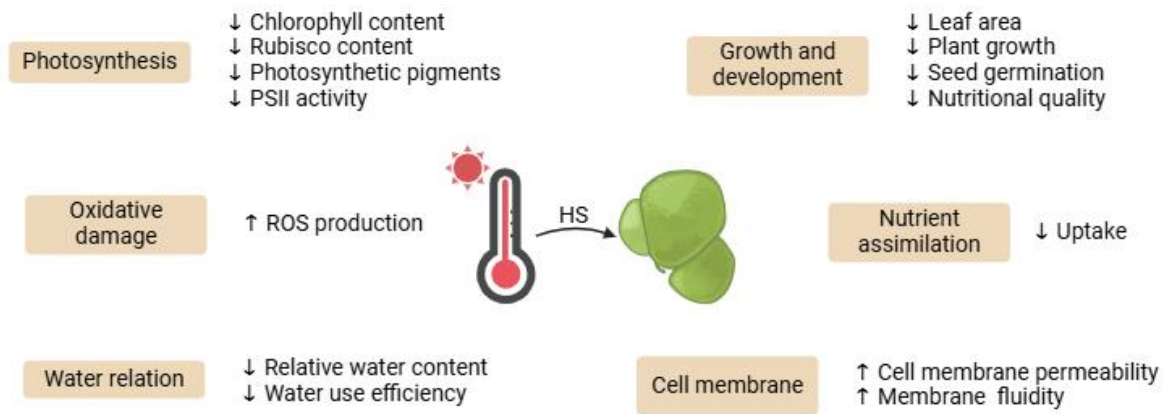


Figure 4.1. Heat stress on plant physiological changes: Upward arrows (↑) indicate upregulation, while downward arrows (↓) represent downregulation.

Not all plants respond to heat stress in the same way, as genotypic differences within species influence their tolerance. For example, in Creeping Bentgrass (*Agrostis stolonifera*), heat-tolerant genotypes showed higher expression of genes associated with chlorophyll metabolism and antioxidant activity, reducing oxidative damage and delaying leaf senescence (Li *et al.*, 2021). Similarly, heat-tolerant *Cucurbita moschata* outperformed heat-sensitive *Cucurbita maxima* by showing lower oxidative stress and increased activity of antioxidant enzymes such as SOD, APX, CAT, and POD (Ara *et al.*, 2013). Wild rice species like *Oryza australiensis* demonstrated heat tolerance through stable of Rubisco activase, which preserved Rubisco activity and sustained photosynthesis under high temperatures (Scafaro *et al.*, 2016). Aquatic plants such as *Potamogeton* species showed species-specific heat tolerant strategies, underscoring the importance of acquired heat acclimation (Amano *et al.*, 2012).

In *Spirodela polyrhiza*, a common duckweed species, adaptation to heat stress involves both physiological and molecular mechanisms. Under extreme temperatures (45°C), enzymatic antioxidants like SOD initially increase but later decline, while rising MDA levels indicate persistent oxidative stress. Transcriptomic analysis reveals the upregulation of thousands of genes, including transcription factors like HSF, ERF, WRKY, and GRAS, which are linked to heat tolerance (Shang *et al.*, 2022). These adaptations enable *S. polyrhiza* to enhance antioxidant defences, maintain energy balance, and preserve cell membrane integrity. However, the specific effects of heat stress on growth rate and protein content in different duckweed species (e.g. *L. gibba* and *L. minor*) remains poorly understood. This study aims to address this knowledge gap.

It is hypothesized that heat stress generally reduces growth rates and protein content of *Lemna* species, but some clones may demonstrate greater resilience due to their genetic adaptations. To test this hypothesis, this study investigated the impact of heat stress on the growth rate and protein content of 42 *Lemna* clones, focusing on two species, *L. gibba* and *L. minor*. The 42 clones, selected from a geographically diverse collection, represent varied environmental conditions, reflecting potential differences in heat stress responses due to evolutionary adaptations and genetic variability. By comparing physiological responses under control (20°C) and heat stress (35°C) conditions, the study aimed to identify heat-tolerant or heat-sensitive clones.

The identified heat-tolerant or heat-sensitive clones were further tested across a broader temperature range (15°C, 20°C, 25°C, 30°C, and 35°C) to investigate at which temperature their growth will be significantly affected. The identified heat-tolerant or heat-sensitive clones were further investigated to understand the molecular mechanisms underlying the different temperatures responses in Chapter 5.

Results of this investigation will enhance our understanding of plant stress related to physiological changes that enable certain *Lemna* clones to withstand high temperatures, contributing valuable knowledge to the development of heat-resilience in plant systems.

4.2. Materials and Methods

4.2.1. Plant Materials

A total of 42 duckweed clones from five continents were selected for this study, comprising 36 clones identified as *L. gibba* (black points in Figure 4.2) and 6 as *L. minor* (red points in Figure 4.2) as illustrated in Figure 4.2 and detailed data were explained in Table S.2. Clones classified as *L. minor* were SD, DG4, DG8, DG9, DG10 and DG12. Each clone was cultured in Schenk and Hildebrandt (SH) medium (nutrient composition provided in Section 0) under constant light conditions at 100 $\mu\text{mol}\cdot\text{m}^{-2}\cdot\text{s}^{-1}$ (photosynthetically active radiation) from fluorescent tubes TLD 36W/86 (Philips, Eindhoven, the Netherlands) at temperatures 20°C (control) or 35°C (heat stress), following protocols outlined in Section 2.1. Fresh weight samples (50 mg per clone) were placed in Magenta vessels containing 300 ml of SH medium.

Based on the results of 42 clones tested at 20°C and 35°C, five clones were selected (Manor, 6861, 7763, 7796 and 8703) and were regrown at temperatures 15, 20, 25, 30 or 35°C for one week to evaluate their responses under these varied thermal conditions.

4.2.2. Growth Rate Assessments

Growth rate assessments were performed using methods detailed in Section 2.5 (Ziegler *et al.*, 2015). A minimum of three biological replicates were used for the analysis.

4.2.3. Nitrogen and Nitrate Quantification

Total nitrogen (TN) and nitrate (TNO_3^-) levels were quantified using Fourier-transform mid-infrared (FT-MIR) spectroscopy, as outlined in Section 2.6 (Espinosa-Montiel *et al.*, 2022). A minimum of three biological and three technical replicates were used for the analysis.

4.2.4. Degree of Heat Tolerance

The degree of heat tolerant was investigated by measuring chlorophyll content, following the method described by Amano *et al.*, (2012). Hundred mg of fresh weight were immersed in 1 ml of 100% methanol after heat treatment. Samples were stored at 4°C for 24 h in darkness, the chlorophyll extracted from the leaves was measured using a spectrophotometer at 665 nm and 652 nm. Total chlorophyll content was calculated using the following formula:

$$4. \quad \text{Total chlorophyll } (\mu\text{g/mL}) = 1.44 \times A_{665} + 24.93 \times A_{652}$$

4.2.5. Statistical Analysis

Statistical data analysis was conducted using R Studio (RStudio Team, 2022). All experiments were done in triplicate to ensure reliability. The data were summarized with independent variables being the clone and temperature, while the dependent variables included chlorophyll content, relative growth rate (RGR) and total protein content. Samples were categorized into control and treatment groups, with controls grown at 20°C and treated grown at 35°C for one week. A ratio was then calculated for RGR, chlorophyll content, and total protein content to differentiate more heat tolerant clones (ratio > 1) from those less heat tolerant (heat sensitive; ratio < 1). Various statistical analyses, including analysis of variance (ANOVA), principal component analysis (PCA), and regression analysis, were performed to evaluate the effects of heat stress on growth rate, protein content, and chlorophyll content across the 42 *Lemna* clones. Visualizations, such as plots, were generated to facilitate interpretation of the results using R Studio (RStudio Team, 2022).

4.2.5.1. Comparative Physiological Responses of *Lemna gibba* and *Lemna minor* Clones Under Control and Heat Stress Conditions

To assess differences in chlorophyll content, growth rate (RGR), total nitrogen, total nitrate, and total protein under control (20°C) and heat stress (35°C) conditions, a comparison was performed between 36 clones of *Lemna gibba* and 6 clones of *Lemna minor* (SD, DG4, DG8, DG9, DG10, and DG12). Statistical significance was determined using two-way ANOVA to analyse species- and temperature-dependent effects, with post hoc Tukey's HSD tests applied for pairwise comparisons.

Principal component analysis (PCA) was conducted to explore the variation in physiological traits between species. The PCA biplot helped visualize the relationship between physiological parameters

and stress conditions, with eigenvalues determining the contribution of each parameter to the principal components.

4.2.5.2. Evaluation of Heat Tolerant and Heat Sensitive Duckweed Clones Using PCA Analysis of Physiological Parameters

PCA analysis was performed to rank the clones' responses to elevated temperature (35°C). The analysis included values for RGR, chlorophyll content, total nitrogen, total protein, and total nitrate. A two-dimensional PCA biplot was generated to visualize how the physiological parameters correlated with each principal component. The positioning of clones along the principal axes was used to infer their relative stress tolerance.

4.2.5.3. Correlation Analysis of RGR, Chlorophyll, and Protein in Duckweed Clones Under Temperature Stress to Identify Heat Sensitive and Heat Tolerant Clones

A Pearson correlation analysis was performed to assess the relationships among RGR, protein, and chlorophyll content under control and heat-stress conditions. Linear regression models were fitted to examine how these physiological traits varied across the 42 clones. The coefficient of determination (R^2) was calculated to evaluate the strength of correlations.

Three scatter plots were generated: (1) RGR vs. Protein content, (2) RGR vs. Chlorophyll content, and (3) Protein vs. Chlorophyll content. The statistical distribution of data points was analysed, and clones demonstrating extreme values were identified as potential heat-tolerant (high RGR, protein, and chlorophyll) or heat-sensitive (low values for these parameters).

4.3. Results

4.3.1. Growth Rate Analysis

The impact of heat stress on the growth rate of 42 *Lemna* clones was assessed by analysing the relative growth rate (RGR) under control conditions (20°C) compared to heat stress conditions (35°C). RGR was determined for three biological replicates, and the results are illustrated in Figure 4.3.

Under control conditions, most clones exhibited RGR values exceeding 0.2, with clones 7245 and 9583 displaying notably higher values above 0.25. However, the application of heat stress significantly affected the growth rates of all clones analysed. In general, clones that had a RGR above 0.2 under

normal conditions showed a substantial reduction in growth rate when subjected to heat stress, with RGR values dropped by approximately half (Figure 4.3). This decrease was particularly pronounced in certain clones, such as 9583 and Pond, which experienced the most drastic declines from 0.27 to 0.07 (d^{-1}) and 0.25 to 0.05 (d^{-1}) respectively. Conversely, clone 6861 demonstrated resilience, maintaining an RGR above 0.15 under heat stress conditions, making it the only clone to exhibit this level of growth under the applied thermal stress.

4.3.2. Analysis of the Degree of Heat Tolerance

Chlorophyll content in plants is closely related to their response to heat stress, as heat stress can directly impact on chlorophyll biosynthesis and disrupt photosynthesis processes (Aleem *et al.*, 2021; Dutta *et al.*, 2009; Fahad *et al.*, 2017). This section aims to explore if chlorophyll content can be used as predictor of heat tolerance in *Lemna* clones by analysing changes in chlorophyll levels in clone's growth under control and heat-stress conditions.

The degree of heat tolerance of *Lemna* clones was investigated by measuring the chlorophyll content. Under optimal conditions (20°C), chlorophyll content in all clones ranged between 500 to 600 $\mu\text{g/mL}$, indicating consistent chlorophyll levels in a non-stressful environment. However, after 7 days of heat exposure, a significant reduction in chlorophyll content was observed across all clones, with varying degrees of decline among them. Clones such as 7798, and 8703 showed the most pronounced reductions in chlorophyll levels 520.65 to 96.6 (p value<0.001) and 546.34 to 61.09 (p value<0.0001) ($\mu\text{g/ml}$) respectively, indicating an increase sensitivity to heat stress in these genotypes. By contrast, clones 9591, 6861, 8428 and 8678 displayed a smaller decrease in chlorophyll content, with no significant differences observed between the control and treatment temperatures. This indicates a relatively higher tolerance to elevated temperatures (Figure 4.4).

This variation in chlorophyll degradation suggests that chlorophyll content could serve as an indicator of heat stress tolerance among *Lemna* clones, with lower declines potentially correlating with higher heat tolerance.

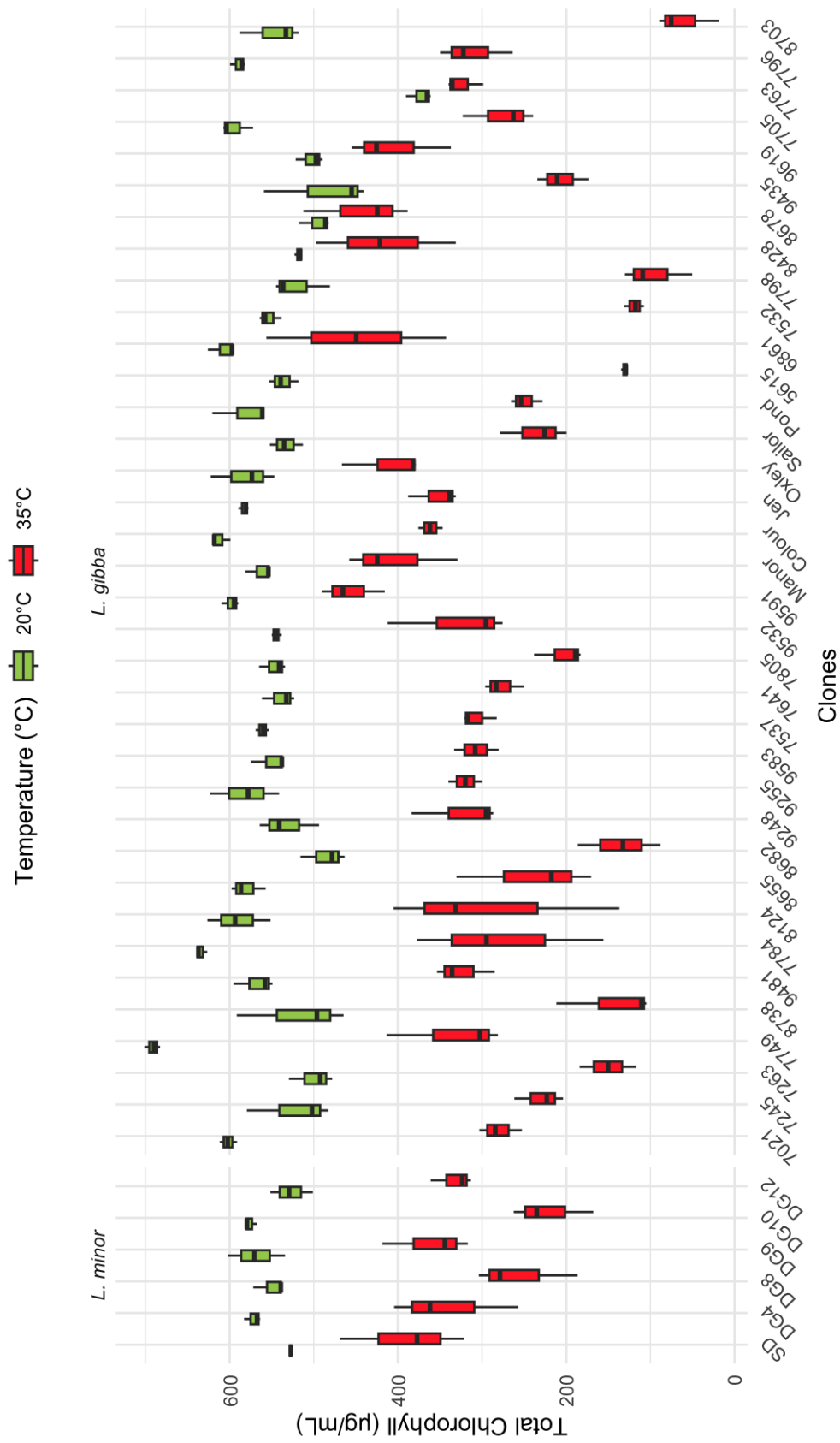


Figure 4.4. Total chlorophyll content (µg/mL) of 6 *L. minor* (left) and 36 *L. gibba* (right) clones under control (20°C, green) and heat stress (35°C, red) conditions. Chlorophyll values are displayed as box plots, with each clone represented by three biological replicates. The line inside each box denotes the median Chlorophyll content, while the box edges indicate the interquartile range (IQR). The whiskers extend to the minimum and maximum observed values.

4.3.3. Total Nitrogen Content

Heat stress is a critical environmental factor that significantly influences nitrogen assimilation in plants, thereby affecting their growth and physiological processes. Elevated temperatures can disrupt nitrogen uptake, assimilation, and incorporation into essential compounds, ultimately impacting overall nitrogen metabolism (Giri *et al.*, 2017). This study evaluated the effects of temperature on nitrogen assimilation in duckweed by screening 42 distinct clones under optimal (20 °C) and heat stress (35 °C) conditions for one week.

As shown in Figure 4.5, total nitrogen ranged from 6% to 7.3% under optimal conditions across the analysed clones, with clone 7763 having the lowest levels (6.01 %) and clone 9591 the highest (7.26%). Under heat stress, total nitrogen levels decreased in most clones. However, notable exceptions were observed in clones 6861 (20°C: 6.77%, 35°C: 6.73%), 9619 (20°C: 6.71%, 35°C: 6.59%), 7796 (20°C: 6.57%, 35°C: 6.77%), and 7763 (20°C: 6.01%, 35°C: 6.32%), which either maintained consistent nitrogen levels or exhibited slight increases under elevated temperatures showing no statistically differences (p value=ns). These clones demonstrated superior heat tolerant compared to the rest. By contrast, clones such as 7784, DG10, 7705, and 8703 exhibited the most significant decline in total nitrogen content, with total nitrogen levels falling below 4% under heat stress conditions.

4.3.4. Total Nitrate Content

Heat stress significantly affects nitrogen metabolism in plants, including nitrate accumulation, by disrupting the activity of key enzymes involved in nutrient assimilation. Previous studies have shown that elevated temperatures can impair enzymes such as nitrate reductase, which plays a central role in nitrate and ammonium assimilation, leading to a notable reduction in nitrate content (Ru *et al.*, 2022).

Under control conditions (20°C), the nitrate contents of the 42 clones ranged from 3000 to 5700 mg/kg DW, as shown in Figure 4.6. However, after one week of heat stress (35°C), most clones exhibited a marked decline in nitrate levels. Clones 9532, SD, DG4, and Jen experienced the most dramatic decreases in nitrate accumulation from 5733.4 to 2006.47 (p value<0.001), 5152.27 to 1111.06 (p value<0.0001), 5009.8 to 1233.1 (p value<0.001) and 4373.02 to 512.98 (p value<0.001) (mg/Kg DW) respectively, suggesting a higher sensitivity to heat stress in these genotypes. By contrast, clones 5615 (2935.13 to 2207.5 (mg/Kg DW)) and 7798 (3165 to 2586 (mg/Kg DW)) showed no significant reductions in nitrate content under heat stress, indicating a degree of resilience in nitrate assimilation pathways.

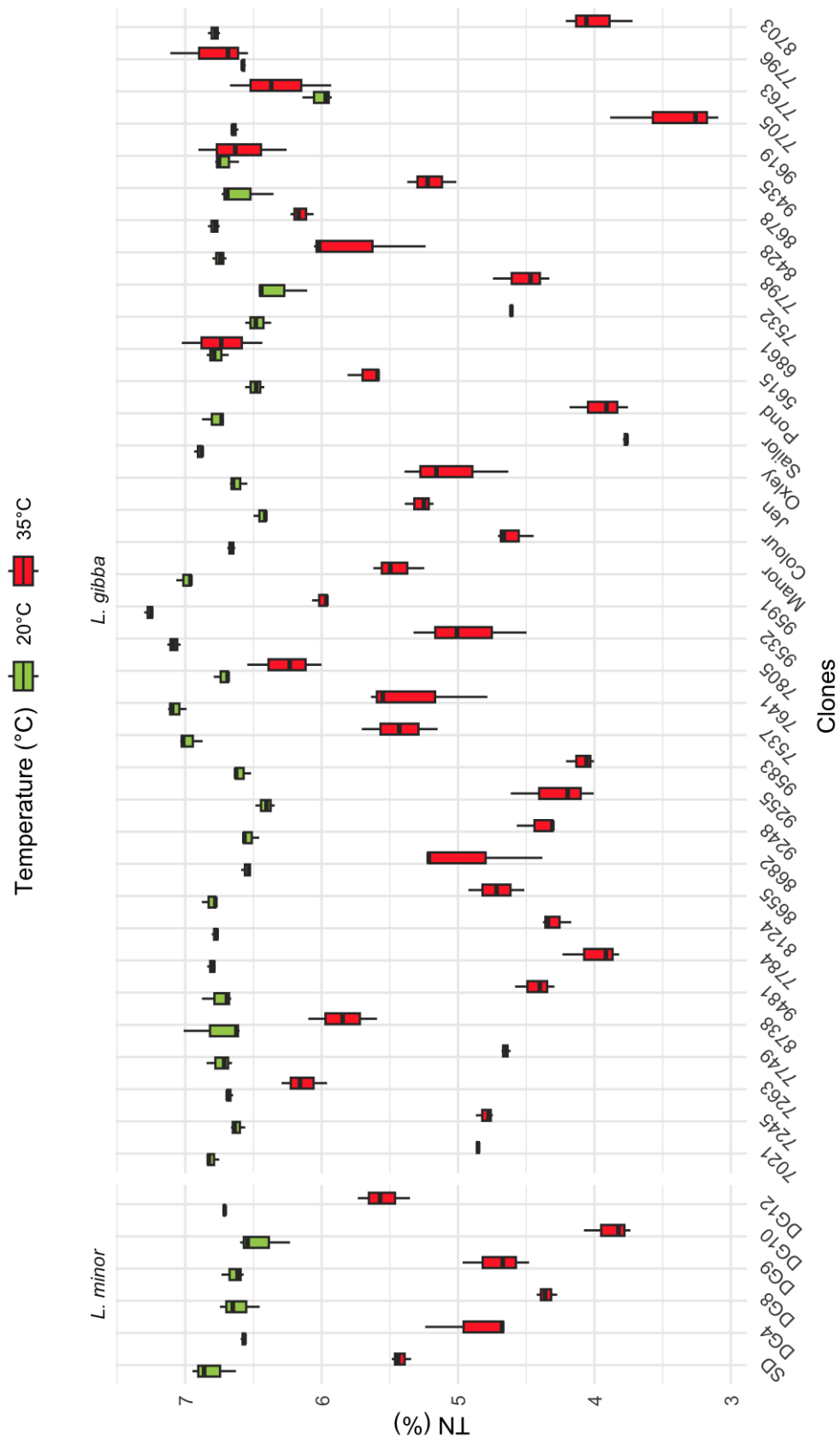


Figure 4.5. Total Nitrogen content (%) of 6 *L. minor* (left) and 36 *L. gibba* (right) clones under control (20 °C, green) and heat stress (35 °C, red) conditions. Nitrogen values are displayed as box plots, with each clone represented by three biological replicates. The line inside each box denotes the median Nitrogen content, while the box edges indicate the interquartile range (IQR). The whiskers extend to the minimum and maximum observed values.

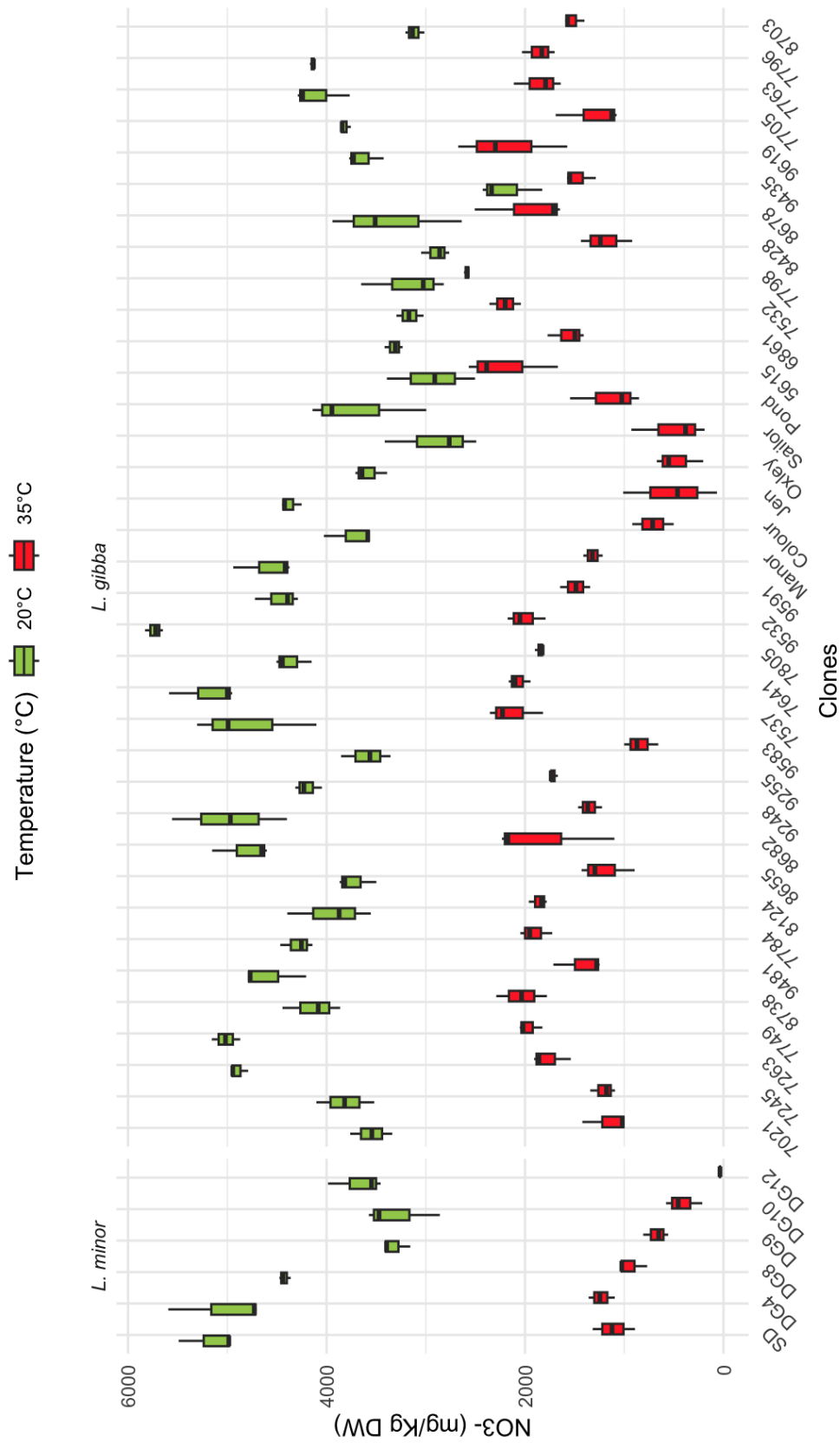


Figure 4.6. Total Nitrate content (mg/kg DW) of 6 *L. minor* (left) and 36 *L. gibba* (right) clones under control (20°C, green) and heat stress (35°C, red) conditions. Nitrate values are displayed as box plots, with each clone represented by three biological replicates. The line inside each box denotes the median Nitrate content, while the box edges indicate the interquartile range (IQR). The whiskers extend to the minimum and maximum observed values.

4.3.5. Total Protein Content Analysis

As can be seen in Figure 4.7, there were changes in total protein levels in duckweed clones at 20 °C compared to one week at 35°C (heat stress) without accounting for nitrate levels. Under control conditions (20 °C), most clones exhibited total protein content ranging between 30–40%, with an average of 39.33%. However, upon exposure to 35 °C for one week, the clones displayed diverse responses. Some clones, such as 7784, DG10, Sailor, Pond, 7705, and 8703, experienced a dramatic decline in protein levels below 25%. By contrast, other clones, such as 7263 (38.67 to 37.25 (p value=ns) (%)) and 7805 (39.28 to 37.97 (p value=ns) (%)), showed no significant changes, while a few, including 6861 (40.24 to 41.1 (p value=ns) (%)), 9619 (39.68 to 39.87 (p value=ns) (%)), 7796 (38.48 to 41.21 (p value=ns) (%)), and 7763 (35.02 to 38.37 (p value=ns) (%)), exhibited increased protein accumulation under heat stress. These latter clones were identified as heat tolerant.

Overall, significant differences in protein accumulation were observed among the clones. As illustrated in Figure 4.7, the heat tolerant clones maintained or even increased protein levels after seven days of heat stress, demonstrating higher resilience to heat stress compared to the other clones.

4.3.6. Comparative Physiological Responses of *Lemna gibba* and *Lemna minor* Clones Under Control and Heat Stress Conditions

To assess differences in chlorophyll content, growth rate (RGR), total nitrogen, total nitrate, and total protein under control (20°C) and heat stress (35°C) conditions, a comparison was performed between 36 clones of *Lemna gibba* and 6 clones of *Lemna minor* (SD, DG4, DG8, DG9, DG10, and DG12); as summarized in Table 4.1. No significant differences were found between the two species for most physiological parameters. However, some notable trends emerged.

At 20°C, both species displayed similar chlorophyll levels, with *L. gibba* averaging 553.26 µg/ml and *L. minor* 553.5 µg/ml (Table 4.1). Under heat stress (35°C), chlorophyll content declined substantially in both species ($p < 0.0001$) but *L. minor* retained marginally higher levels (316.83 µg/ml) compared to *L. gibba* (282.59 µg/ml).

Growth rates showed a similar trend. At 20°C, *L. minor* and *L. gibba* demonstrated comparable relative growth rates (RGR) of 0.24 d⁻¹ and 0.23 d⁻¹, respectively, with no significant differences detected. At 35°C, both species experienced a pronounced decline in growth ($p < 0.0001$), yet no statistically significant differences were observed between them.

For total nitrogen and protein content, both species demonstrated reduction under heat stress, with *L. gibba* maintaining slightly higher levels at both temperatures but the differences were not significantly different. The most pronounced difference between *L. gibba* and *L. minor* was observed in total nitrate content. Under heat stress (35°C), *L. minor* clones displayed significantly lower nitrate levels (734.77 mg/kg DW) than *L. gibba* (1565.23 mg/kg DW) (Table 4.1). These results suggest a potential species-specific difference, though the limited *L. minor* clones analysed (n=6) may have influenced these findings.

In summary, while most physiological traits showed no significant differences between *L. gibba* and *L. minor*, the marked disparity in nitrate content under heat stress warrants further investigation. Expanding the sample size for *L. minor* clones could provide more conclusive insights.

Table 4.1. Physiological responses of *L. gibba* and *L. minor* clones at 20°C and 35°C. Chlorophyll content, relative growth rate (RGR), total nitrogen (TN), total nitrate, and protein content are included.

Species*	T ^a (°C)	Chlorophyll (µg/ml)	RGR (d ⁻¹)	TN (%)	NO ₃ ⁻ (mg/kg DW)	Protein (%)
<i>L. gibba</i>	20	553.26 ± 53.87	0.23 ± 0.02	6.7 ± 0.23	3965.23 ± 768.13	39.4 ± 1.37
<i>L. minor</i>	20	553.5 ± 21.9	0.24 ± 0.01	6.64 ± 0.12	4145.27 ± 832.45	38.88 ± 0.7
<i>L. gibba</i>	35	282.59 ± 104.8	0.09 ± 0.02	5.09 ± 0.9	1565.23 ± 528.38	30.83 ± 5.52
<i>L. minor</i>	35	316.83 ± 64.22	0.08 ± 0.01	4.8 ± 0.63	734.77 ± 453.21	29.51 ± 3.99

*Measurements for *L. gibba* were mean of 36 clones and for *L. minor* were mean of 6 clones.

4.3.7. Evaluation of Heat Tolerance and Heat Sensitivity Duckweed Clones Using PCA analysis of Physiological Parameters

The PCA analyses conducted aimed to rank the clone's responses to elevated temperature (35°C). To determine whether clones treated at the same temperature are grouped together, a PCA plot was utilized using the values for RGR (Figure 4.3), chlorophyll (Figure 4.4), total nitrogen (Figure 4.5), total nitrate (Figure 4.6) and total protein (Figure 4.7). In this PCA plot, a distinct separation between the clones treated at 20°C and those at 35°C was observed (Figure 4.8), highlighting the impact of temperature on the physiological parameters measured. Clones treated at 20°C form a tight cluster, indicating uniform and stable responses with minimal stress. This suggests these clones are well-adapted to the optimal growing conditions provided by 20°C. Conversely, the clones treated at 35°C exhibited a broader distribution, reflecting varied responses to heat stress and suggesting differential heat tolerance among the clones. Notably, the spread along the axes representing total protein and total nitrogen suggests that clones projecting further in these directions may have enhanced mechanisms to maintain or increase protein and nitrogen levels under heat stress, indicating better heat tolerance.

The arrows in the PCA plot, representing RGR, total nitrate, total nitrogen, total chlorophyll, and total protein, indicate the correlation of these variables with the principal components. The strong correlation of total protein and total nitrogen with PC1 suggests these factors are significant in differentiating the clones' responses to temperature stress.

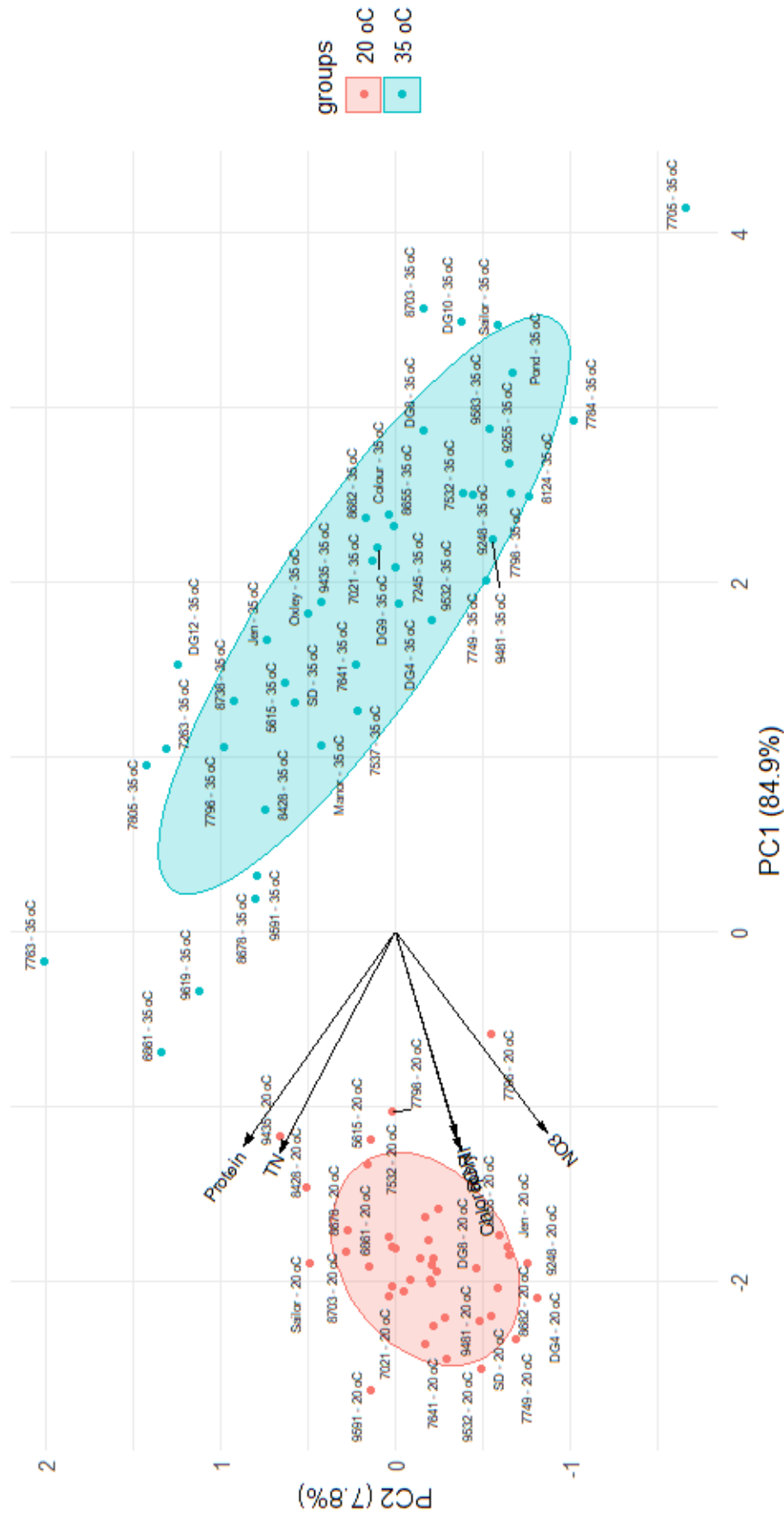


Figure 4.8. The PCA plot illustrates the multivariate analysis of clones' responses to temperature treatments (20 and 35 °C). Arrows represent variables correlated with principal components (PCs): Relative Growth Rate (RGR), Total Nitrate (NO₃-), Total Nitrogen (TN), Total Chlorophyll, and Total Protein. The direction and length of each arrow indicate the correlation and contribution of these variables to sample clustering. Variables pointing similarly are positively correlated and contribute similarly to data variation.

4.3.8. Correlation Analysis of RGR, Chlorophyll, and Protein in Duckweed Clones Under Temperature Stress to Identify Heat Sensitive and Heat Tolerant Clones

For the RGR against the protein content (Figure 4.9A), the R^2 value is 0.553, indicating a good correlation between RGR and protein. Clones 6861, 7763, and 7796 are positioned in the top right, indicating high RGR and protein values. This suggests that these clones maintain or increase their growth rate and protein synthesis under heat stress, showing strong heat tolerance. Conversely, other samples were located at the bottom left, making it less clear to identify a heat sensitive clone based solely on this plot.

For the RGR against the chlorophyll content (Figure 4.9B), clones 6861, 7763, and 7796 again show high RGR and chlorophyll values, suggesting that these clones maintain good growth rates and chlorophyll content, indicative of efficient photosynthesis under heat stress and strong heat tolerant. However, 8703 is positioned alone in the bottom left, showing low values for both RGR and chlorophyll, indicating that this clone struggles with growth and maintaining chlorophyll levels under heat stress, thus being heat sensitive.

For the protein content against the chlorophyll content (Figure 4.9C), clones 6861, 7763, and 7796 showed high values for both protein and chlorophyll, indicating that these clones can maintain or increase these critical components under heat stress, signifying robust stress response mechanisms and strong heat tolerant. The clone 8703 is again positioned alone in the bottom left, confirming its inability to cope with heat stress.

From the analysis of the three correlations, clones 6861, 7763, and 7796 exhibited high heat tolerant, maintaining or increasing their growth rate, protein synthesis, and chlorophyll content under heat stress. Because there was a good correlation between RGR and Protein ($R^2 = 0.553$) and the clones 6861, 7763, and 7796 were positioned in the top right of the plot (Figure 4.9A). In contrast, the clone 8703, was consistently positioned alone in the bottom left of the relationships for RGR vs chlorophyll (Figure 4.9B) or protein vs chlorophyll (Figure 4.9C), indicating high heat sensitivity.

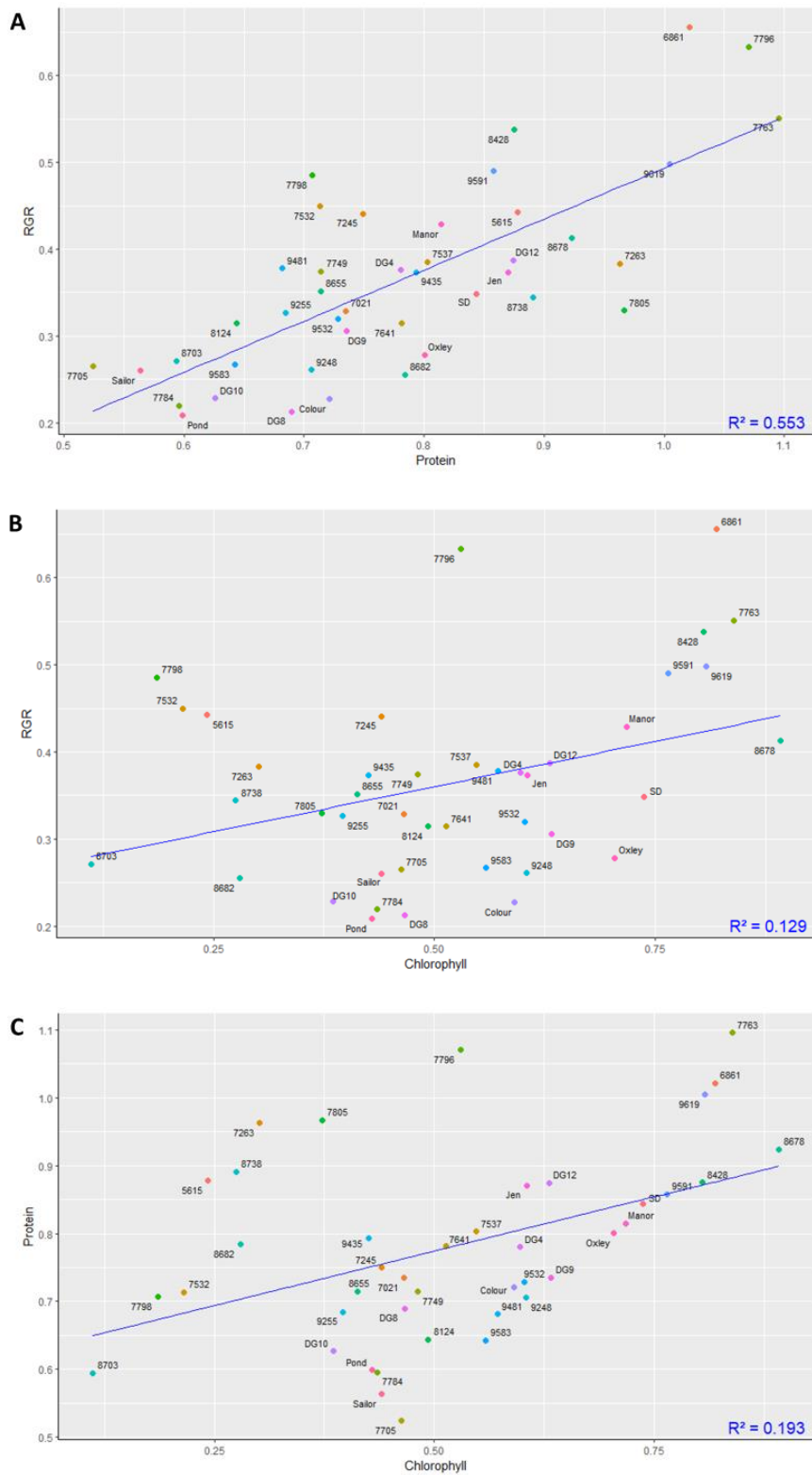


Figure 4.9. Correlation analysis between RGR, chlorophyll, and protein in duckweed clones under 20°C (control) and 35°C (heat stress). These plots analyse the relationship between Relative Growth Rate (RGR), Chlorophyll and Protein contents in 42 duckweed clones treated at 20°C (control) and 35°C (heat stress). Ratios above 1 indicate heat tolerant, while ratios below 1 indicate heat sensitive. A) RGR vs Protein B) RGR vs Chlorophyll C) Protein vs Chlorophyll.

4.3.9. Validation of Heat Sensitive and Heat Tolerant Clones Across Different Temperature Conditions

To further investigate the heat sensitivity of the clones based on results tested at 20 °C and 35°C, five *L. gibba* clones were selected —6861, 7763, and 7796 as heat tolerant, 8703 as heat sensitive, and Manor as the control. Manor was chosen as the control because it was used to establish the duckweed standard for nitrogen and nitrate FT-MIR calibration and exhibited intermediate results in terms of growth rate and protein content. These five clones were grown at five different temperatures (15, 20, 25, 30, and 35°C) for a week to assess the changes in protein content and growth rate under these conditions.

In terms of protein content (Figure 4.10A), the heat sensitive clone 8703 exhibited a clear decline as temperatures increased over 25°C, with the most substantial decrease occurring at 35°C. This sharp reduction at high temperatures indicates a significant loss of protein content under heat stress. In contrast, the heat tolerant clones 6861, 7763, and 7796 maintained more stable protein levels across the temperature range, particularly at 30°C and 35°C. These clones even showed a slight increase in protein content at higher temperatures, which confirms their classification as heat tolerant. The control clone, Manor, displayed minor fluctuations in protein content but remained relatively stable across the tested temperatures, showing no significant changes in response to heat stress. No significant differences were observed between the control clones and the rest at 15, 20, and 25°C. At 30°C, the heat-tolerant clones showed no significant difference compared to the control clones, but the heat-sensitive clone displayed a notable decrease ($p < 0.01$). At 35°C, all clones exhibited statistically significant differences when compared to the control clone Manor. The heat-tolerant clones recorded higher values ($p < 0.001$ for clones 6861 and 7763, and $p < 0.0001$ for clone 7796), whereas the heat-sensitive clone showed a marked reduction ($p < 0.0001$ for clone 8703).

Regarding RGR (Figure 4.10B), all clones reached their peak growth at 25°C, except for the control clone Manor, which exhibited its highest growth rate at 20°C but also performed well at 25°C. As temperatures increased from 25°C to 35°C, RGR decreased for all clones. The heat-sensitive clone 8703 experienced a particularly sharp decline, with a marked drop at 30 and 35°C, confirming its sensitivity to elevated temperatures. In contrast, the heat-tolerant clones 6861, 7763, and 7796 showed more gradual reductions in RGR as temperatures increased, maintaining relatively higher growth rates under heat stress conditions. Interestingly, while Manor reached its peak at 20°C, it still displayed good growth at 25°C and followed a similar trend to the heat-tolerant clones, with a gradual decrease at higher temperatures.

Notably, at 15°C, both Manor and 8703 showed higher growth rates compared to the heat tolerant clones (p value<0.0001). This suggests that these clones may prefer lower temperatures, with 8703 performed better in cooler conditions, further highlighting its sensitivity to heat stress. These results underscore the differences in thermal response between heat tolerant and heat sensitive clones, with the heat tolerant group maintaining better protein content and RGR at higher temperatures, while 8703 and Manor displayed improved growth performance at lower temperatures.

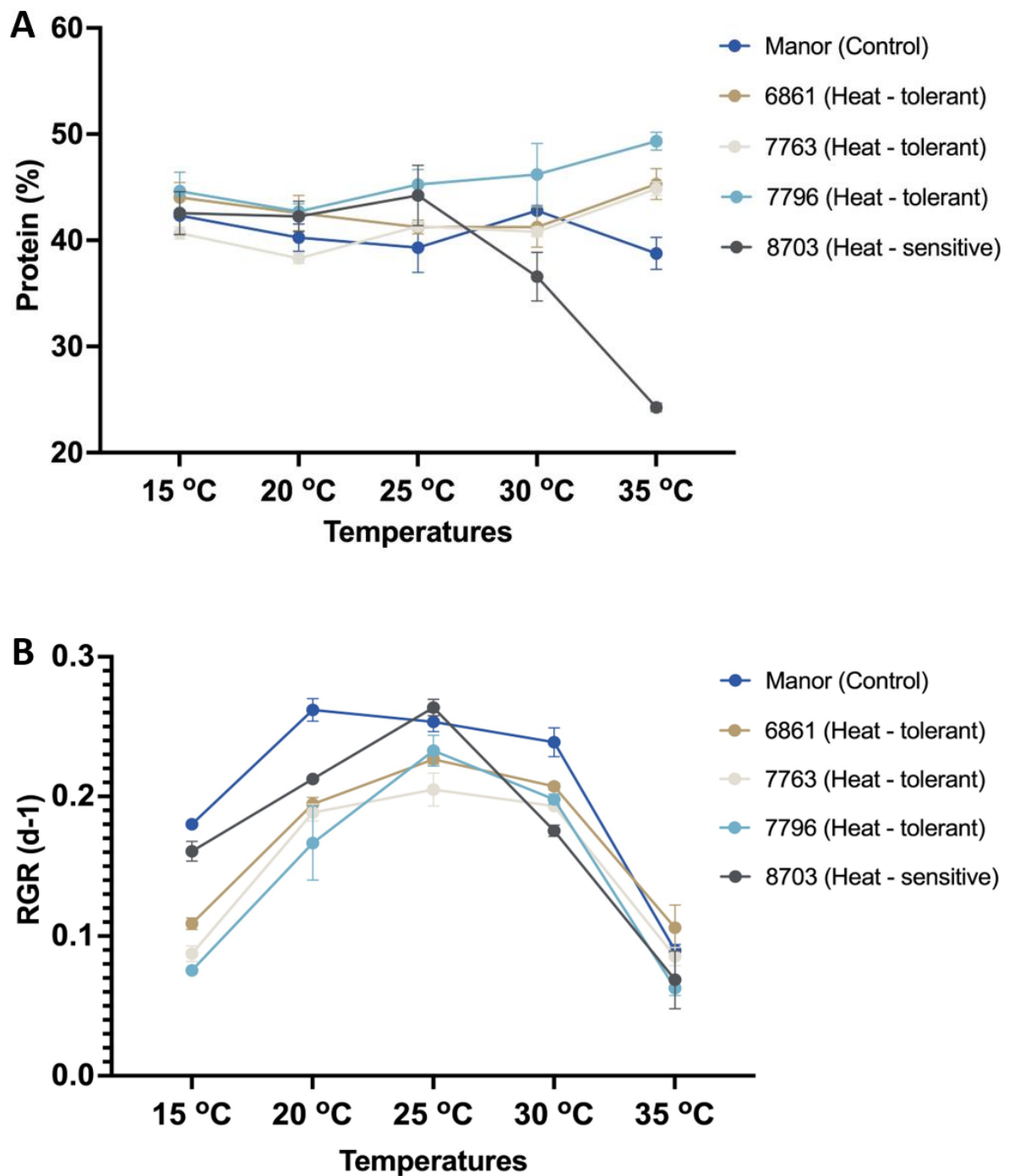


Figure 4.10. Protein content (A) and RGR (B) of five *L. gibba* clones (Manor, 6861, 7763, 7796, and 8703) at different temperatures. Clones were treated to 15, 20, 25, 30 and 35 °C.

4.4. Discussion

The research aimed to determine whether certain *Lemna* clones exhibit greater heat tolerance than others when exposed to increased temperatures. This hypothesis was based on the assumption that different genotypes within the *Lemna* species would exhibit distinct responses to heat stress, as observed in other plant species (Hu *et al.*, 2021; Li *et al.*, 2021; Scafaro *et al.*, 2016). The screening of 42 clones under control conditions (20°C) and heat stress conditions (35°C) effectively distinguished heat-tolerant clones and heat sensitive ones.

This study has identified heat tolerant and heat sensitive *Lemna* clones. Both the protein content and relative growth rate (RGR) of the clone 8703 decreased significantly when the temperature increased over 25°C, suggesting this clone is heat sensitive. This decline likely reflects protein denaturation and disruption of critical metabolic processes, aligning with previous studies documenting protein degradation patterns under heat stress (Wahid *et al.*, 2007). In contrast, the protein levels of clones 6861, 7763, and 7796 maintained stable or slightly increased across temperatures ranged from 15°C to 35°C, suggesting they are more heat-tolerant clones and they may have mechanisms that preserve protein stability, because previous research highlighted the role of heat shock proteins in protecting cellular function during heat stress (Huang & Xu 2008; Amano *et al.*, 2012; Hu *et al.*, 2020).

Interestingly, the control clone Manor showed similar growth rate as the heat sensitive clone 8703 at lower temperatures but maintained more stable growth rates under heat stress. This variable mirrors findings in duckweed, such as those observed by Strzałek & Kufel, (2021), and emphasizes the diverse responses of *Lemna* clones to environmental stress.

This study highlights the importance of understanding the physiological mechanisms driving heat tolerance in *Lemna*. The heat tolerance observed in clones 6861, 7763, and 7796 may be attributed to several physiological and molecular adaptations. One key mechanism is the enhanced synthesis and stability of crucial proteins, which support cellular function under elevated temperatures. Similar findings in wild rice suggest that proteins like Rubisco activase contribute to maintaining photosynthesis under heat stress (Bita & Gerats, 2013 Scafaro *et al.*, 2016).

Results of this study suggest that environmental exposure alone could not determine heat tolerance. For example, despite different climatic backgrounds, clones such as 6861 and 7796 from Italy and 7763 from the UK both demonstrated significant heat tolerance. Similar patterns have been documented in other aquatic plants like *Potamogeton* spp., where heat acclimation varies widely among species and is not strictly tied to geographic or climatic origins (Amano *et al.*, 2012). Such genetic plasticity

not only supports *Lemna's* evolutionary potential but also underpins its capacity to adapt to environmental changes, including rising global temperatures.

The findings of this study hold significant promise for sustainable agriculture and environmental management. Heat tolerant clones, such as 6861, 7763, and 7796, demonstrate resilience under high-temperature conditions, making them valuable resources for regions increasingly affected by global warming. Their ability to sustain growth and maintain protein stability at elevated temperatures highlights their potential for practical applications in biomass production, nutrient cycling, and water purification systems. These traits not only underscore the adaptability of *Lemna* but also position it as an effective tool in addressing the challenges posed by rising global temperatures.

Moreover, this research advances our understanding of plant stress physiology by emphasizing the intricate relationship between genetic diversity and physiological adaptability in coping with environmental challenges. By leveraging the resilience of these clones, we can explore innovative solutions such as breeding programs for stress-resistant crops, optimizing cultivation strategies to improve growth under extreme temperatures, and developing biotechnological approaches to enhance plant resilience. These strategies can help mitigate the impacts of climate change while enhancing productivity and ecological sustainability.

The variation in heat tolerance among clones highlights the critical role of clone diversity in shaping plant responses to heat stress. In *Lemna*, genetic variability likely provides a selective advantage, enabling populations to adapt to fluctuating temperatures over time. This adaptability ensures certain clones thrive under heat stress, while others remain more vulnerable. By elucidating these dynamics, this study contributes to a greater understanding of *Lemna's* resilience and adaptability to environment. Both clone and geographic factors are shown to play complementary roles in defining plants' responses to climate change. For instance, the heat tolerance observed in clones 6861, 7763, and 7796 exemplifies how physiological adaptations can transcend geographic differences, underscoring their potential for broader applications in sustainable agricultural practices.

This study also reinforces the importance of clone diversity in plant science. It demonstrates that even within a single species, physiological and clone factors can vary widely, allowing for differential responses to heat stress. These findings align with existing research that highlights the need for genetic and adaptive diversity to ensure resilience to climate stressors (Mijatović et al., 2013). By shedding light on mechanisms such as protein stability and growth rate, this research contributes to a growing body of knowledge and provides a foundation for identifying specific adaptive traits that enhance crop resilience.

However, there are limitations in this study. While stable protein content and growth rate act as a potential mechanism for heat tolerance, molecular validation is necessary. Future research should include transcriptomic studies to identify differentially expressed genes and confirm the roles of specific stress-related genes or transcription factors. Such validation will provide deeper insights into the molecular mechanisms underpinning heat tolerance and support efforts to translate these findings into practical applications.

In conclusion, this study demonstrates significant variation in heat tolerance among *Lemna* clones, with 6861, 7763, and 7796 exhibiting heat resilience under high-temperature conditions. These clones maintained higher protein content and stable growth rates at 35°C, unlike the heat sensitive clone 8703. The results suggest that these clones possess inherent physiological adaptations, such as enhanced protein stabilization and antioxidant activity, that mitigate the adverse effects of heat stress. By exploring the connections between clone diversity, and heat tolerance, this research improves our understanding of plant resilience and their adaptability to climate change. The findings also lay a foundation for future studies to uncover the molecular mechanisms of heat tolerance and foster sustainable agricultural practices in an era of global warming.

5. Chapter 5. Gene Expression Kinetics on *Lemna* Growth Under Heat Stress

5.1. Introduction

Duckweed's rapid growth and straightforward structure make it an excellent model for examining plant stress responses. Its ability to propagate clonally ensures the quick production of large populations, facilitating its use in experimental studies (Acosta *et al.*, 2021). This aquatic plant has proven valuable in research, such as exploring how factors like temperature, light intensity, and nutrient availability, including nitrogen (N) and phosphorus (P), affect its starch and protein content (Li *et al.*, 2016). Additionally, recent investigations have highlighted its potential for studying variations in growth rate under different environmental conditions (Pasos-Panqueva *et al.*, 2024).

Heat stress impacts plants at all stages of their life cycle, from seed germination to maturity, reducing photosynthetic efficiency, disrupting respiration and water balance, and lowering crop yields. Morphological changes like leaf wilting and reduced leaf area further limit light capture and photosynthesis (B. Huang & Xu, 2008; Wahid *et al.*, 2007). High temperatures damage key components of photosynthesis, including chlorophyll and Calvin cycle enzymes, while also disrupting respiration pathways, leading to metabolic imbalances (Wang *et al.*, 2018; Yu *et al.*, 2017). Protein metabolism is similarly affected, with heat shock proteins (HSPs) protecting damaged proteins and preventing the accumulation of dysfunctional ones (B. Huang & Xu, 2008). Strategies to mitigate heat stress include developing heat-tolerant crops through genetic approaches like marker-assisted breeding and transgenic technologies (Wahid *et al.*, 2007).

Comprehending how plants physiologically respond to elevated temperatures is essential, particularly as climate change continues to intensify (Okamoto *et al.*, 2022). These responses can involve intricate interactions, including hormonal regulation (Li *et al.*, 2021), molecular adaptations (Haider *et al.*, 2021) and symbiotic relationships with microbes. The effects are also observable at the ecosystem level, where broader interactions amplify the consequences of heat stress (Li *et al.*, 2021). Such complexity necessitates detailed analysis of the genetic and molecular pathways underpinning these responses.

Transcriptomic analyses have played a vital role in uncovering the genes and pathways involved in plant stress responses, including thermotolerance. For example, in *Arabidopsis*, the protein phosphatase RCF2 and its partner NAC019 were identified as key regulators of heat shock factors (HSFs) and heat shock proteins (HSPs), which are essential for thermotolerance (Guan *et al.*, 2014). Similar transcriptomic studies on tomato seedlings revealed genotype-specific changes in mRNA levels during heat stress, with genes related to hormonal signalling and RNA regulation correlating with

thermotolerance (Hu *et al.*, 2020). These analyses also provide insights into the genes and pathways that regulate variability in thermotolerance across plant genotypes.

Heat stress profoundly impacts photosynthesis, a process essential for plant growth and productivity. It alters key components such as Photosystem II, the Calvin cycle, and photosynthesis-antenna proteins responsible for light capture and energy production (Chen & Li, 2017; Wang *et al.*, 2017). Studies in maize and *Brachypodium distachyon* have shown that genes like *PsaD* and *PsaN* are sensitive to high-temperature, highlighting the vulnerability of photosynthetic pathways to heat stress (Jagtap *et al.*, 2023). Zinc ion binding also plays a pivotal role in stress responses, supporting biological processes through proteins with zinc finger domains, which act as transcription factors regulating stress-related genes (Chaddad *et al.*, 2023). Additionally, zinc-binding proteins contribute to protein stability during the unfolded protein response (UPR) and enhance antioxidant defences. In heat-tolerant clones, genes linked to photosynthesis and zinc ion binding are notably upregulated, enabling adaptation to high-temperature environments. Genes encoding ATP synthase proteins, crucial for photosynthetic efficiency and energy production, show increased expression under heat stress (Hozain *et al.*, 2012; Liu *et al.*, 2021; Zha *et al.*, 2023). Similarly, zinc ion binding-related genes, such as Pentatricopeptide repeat protein, Ubiquitin carboxyl-terminal hydrolase, and the general transcription factor IIH subunit 2, are significantly upregulated, supporting transcription regulation, protein stability, and cellular stress responses (Liu *et al.*, 2019; Yousefi *et al.*, 2022; Zhang *et al.*, 2019).

Five duckweed clones were identified as heat tolerance or heat sensitive in Chapter 4, laying a solid foundation for further analysis. Among the studied clones, 6861, 7763, and 7796 were identified as heat-tolerant, displaying higher growth rates and stable protein content under elevated temperatures. In contrast, 8703 exhibited heat-sensitive traits, with significant reductions in growth rate and protein content when subjected to the same conditions. Clone Manor served as the control, showing intermediate responses that did not indicate pronounced thermotolerance or sensitivity. These distinct physiological adaptations indicate underlying differences in genetic and molecular mechanisms, making these clones ideal candidates for transcriptomic analyses to identify key genes and pathways associated with thermotolerance.

This chapter aimed to explore the genetic variations within *Lemna gibba* species, with a focus on differences in gene expression between heat-tolerant and heat-sensitive clones. By identifying and interpreting the functions of these genes, the study investigated their roles in heat stress responses and their broader implications. Ultimately, outcomes of this work will contribute to our understanding of the genetic mechanisms underlying thermotolerance, offering potential applications in developing

resilient crops and improving agricultural and ecological management strategies in the face of climate change.

5.2. Materials and Methods

5.2.1. Plant Materials

For this chapter, five duckweed clones were selected based on the temperature screening results presented in Chapter 4. These included three heat-tolerant clones (6861, 7763, and 7796), one heat-sensitive clone (8703), and one control clone (Manor). The heat-tolerance of the clones were characterized by their ability to maintain higher growth rates and stable protein content under elevated temperatures, while the heat sensitive clone exhibited significant reductions in these parameters. The control clone displayed intermediate responses, serving as a baseline for comparison.

Fresh weight samples (50 mg per clone) were placed in Magenta vessels containing 300 mL of Schenk and Hildebrandt (SH) medium (nutrient composition detailed in Section 2.1.1.3) under constant light $100 \mu\text{mol}\cdot\text{m}^{-2}\cdot\text{s}^{-1}$ (photosynthetically active radiation) from fluorescent tubes TLD 36W/86 (Philips, Eindhoven, the Netherlands) at 20°C (control) or 35°C (heat stress) for seven days, following the protocols outlined in Section 2.1. All clones were growth in three biological replicates. After seven days of growth under the assigned temperature conditions, 100 mg of each biological samples were frozen and stored at -80°C until RNA extraction.

5.2.2. RNA Extraction and Quality Control

RNA was extracted from the five different clones grown at 20°C (control temperature) and 35°C (heat stress) following the protocols outlined in Section 2.2.2. Quality control measurements were conducted to ensure the quality of the RNA sample employing methods described in Section 2.3.

- Nanodrop spectrophotometry was used to measure the concentration and purity, based on absorbance readings at 260 nm and the 260/280 and 260/230 nm ratios.
- Agarose gel electrophoresis was performed to visualize the integrity and size distribution.
- Qubit fluorometry provided accurate quantification of RNA concentration.
- TapeStation analysis offered detailed information on RNA integrity and size distribution.

The RNA samples were sequenced using Illumina platforms at Novogene, employing the sequencing-by-synthesis (SBS) mechanism.

5.2.3. Library Construction and Sequencing

All sequencing and initial data processing were carried out by Novogene, including RNA quality assessment, library construction, and sequencing. The following sections describe the procedures undertaken by the sequencing provider.

5.2.3.1. Sample Quality Control

The quality and quantity of RNA samples were assessed by Novogene prior to library construction.

5.2.3.2. Library Construction, Quality Control and Sequencing

Total RNA was purified to isolate messenger RNA using poly-T oligo-attached magnetic beads. After fragmentation, first-strand cDNA synthesis was performed with random hexamer primers, followed by second-strand cDNA synthesis. Directional library construction used dUTP, whereas non-directional library employed dTTP.

For non-directional libraries, the process included end repair, A-tailing, adapter ligation, size selection, amplification, and purification. Meanwhile, directional libraries underwent an additional USER enzyme digestion step after size selection, following amplification and purification.

Library quality was assessed through quantification using Qubit and real-time PCR, with size distribution determined via a bioanalyzer. Once quantified, libraries were pooled based on effective concentration and data requirement before sequencing.

Sequencing was performed on the Illumina NovaSeq platform using a paired-end 150 bp (PE150) sequencing strategy, generating short reads. The sequencing depth for each sample was ≥ 20 million read pairs, ensuring sufficient coverage for downstream transcriptomic analyses.

5.2.4. Bioinformatics Analysis Pipeline

5.2.4.1. Data Quality Control

The first step of the bioinformatics analysis pipeline involved processing raw data (raw reads) in FASTQ format using in-house Perl scripts. This process aimed to obtain clean data (clean reads) by filtering out reads containing adapters, poly-N sequences, and low-quality reads from the raw datasets. Simultaneously, metrics such as Q20, Q30, and GC content were calculated to evaluate data quality.

Clean, high quality data were then used for subsequent analyses, ensuring the accuracy and reliability of downstream processes.

5.2.4.2. Mapping Reads to the Reference Genome

The reference genome used for mapping was *Lemna gibba* 7742a from Lemna.org (Ernst *et al.*, 2023). The reference genome was constructed using HISAT2 v2.0.5 and the paired-end clean reads were aligned to the reference genome with the same HISAT2 version. The HISAT2 (Mortazavi *et al.*, 2008) was selected as the mapping tool due to its ability to generate a splice junction database from the gene model annotation file, providing superior mapping results compared to non-splice mapping tools.

5.2.4.3. Prediction of Novel Transcripts

Mapped reads from each sample were assembled using StringTie v1.3.3b (Pertea *et al.*, 2015) in a reference-based manner. StringTie uses a novel network flow algorithm combined with an optional de novo assembly step to assemble and quantify full-length transcripts representing multiple splice variants for each gene locus.

5.2.4.4. Quantification of Gene Expression Level

FeatureCounts v1.5.0-p3 (Liao *et al.*, 2014) was used to count the number of reads mapped to each gene. Gene expression levels were then quantified using the Fragments Per Kilobase of transcript sequence per Millions base pairs sequenced (FPKM) metric. FPKM accounts for both sequencing depth and gene length, making it a widely adopted for estimating gene expression levels.

5.2.4.5. Differential Expression Analysis

For analyses involving biological replicates, DESeq2 v1.20.0 (Love *et al.*, 2014) was used. The DESeq2 performs differential expression analysis using a model based on the negative binomial distribution (Anders & Huber, 2010). To control the false discovery rate, the resulting p-values were adjusted using the Benjamini and Hochberg method (Benjamini & Hochberg, 1995). Genes with an adjusted p-value ≤ 0.05 were considered as differentially expressed.

5.2.4.6. Enrichment Analysis of Differentially Expressed Genes in GO and KEGG Pathways

The clusterProfiler R package was used for Gene Ontology (GO) enrichment analysis of differentially expressed genes, with adjustments correction for gene length bias (Young *et al.*, 2010). GO terms with corrected p-values < 0.05 were considered significantly enriched. Additionally, KEGG pathway enrichment analysis was performed using the clusterProfiler R package to evaluate the statistical enrichment of differentially expressed genes in KEGG pathways (Kanehisa & Goto, 2000).

5.3. Results

5.3.1. RNA Control Checks

A total of 30 RNA extractions were performed, with each sample assigned a unique identifier for simplification (Table 5.1). The quality and quantity of RNA were assessed using Qubit and Nanodrop measurements, with additional evaluation of RNA integrity through the RNA Integrity Number (RIN). These analyses revealed variation in RNA concentration and quality across samples, reflecting the biological responses of duckweed clones to different temperature treatments.

Notably, sample 8703 exhibited a marked decrease in RNA concentration when grew at 35°C, consistent with findings presented in Chapter 4, which identified this clone as highly sensitive to heat stress. This observation highlights the physiological impact of elevated temperatures on RNA yield in thermosensitive clones.

The Nanodrop 260/280 and 260/230 absorbance ratios provided insights into RNA purity. While the 260/280 ratios were generally within the acceptable range (indicating minimal protein contamination), the 260/230 ratios were inconsistent and not reliably calibrated in our measurements. Despite this limitation, subsequent checking by Novogene confirmed that RNA quality was sufficient, with 260/230 ratios falling within the expected range of 1.8 to 2. This finding reinforces the adequacy of our RNA preparations for downstream applications.

The RIN values further validated RNA integrity, ensuring the suitability of the extracted RNA for sequencing. Table 5.1 provides a comprehensive summary of the RNA quality and quantity metrics for all samples, categorized by sample number, clone identity, temperature treatment (T^a), and analytical method.

Table 5.1. RNA quality and quantity metrics for duckweed clones under different temperature treatments. Summary of the RNA quality and quantity metrics for 30 samples extracted from duckweed clones grown at 20°C (control) or 35°C (heat stress). Each sample is identified by an assigned identity number (N°) and treatment temperature (T°). RNA concentration (ng/μL) was measured using both Qubit and Nanodrop methods. RNA purity was assessed through Nanodrop absorbance ratios (260/280 and 260/230), while RNA integrity was evaluated using the RNA Integrity Number (RIN). Variations in RNA quality and quantity reflect the physiological responses of the clones to temperature stress.

N°	Clones	T° (°C)	Qubit (ng/μL)	Nanodrop (ng/μL)	260/280	260/230	RIN	N°	Clones	T° (°C)	Qubit (ng/μL)	Nanodrop (ng/μL)	260/280	260/230	RIN
31	Manor	35	181	170.9	2.14	1.26	5.9	46	Manor	20	652	586.8	2.15	2	8
32	Manor	35	144	218.2	2.16	1.27	7	47	Manor	20	598	582.1	2.17	2.22	8.1
33	Manor	35	200	188	2.15	0.63	6.4	48	Manor	20	524	464.9	2.13	2.29	8.2
34	6861	35	351	294.4	2.13	0.57	8	49	6861	20	666	726.1	2.17	2.23	7.6
35	6861	35	145	150.7	2.15	0.34	7.4	50	6861	20	596	589.9	2.16	2.3	7.9
36	6861	35	620	620.8	2.15	2.13	8.4	51	6861	20	436	420.7	2.14	1.53	7.5
37	7763	35	299	267.9	2.14	2.13	8.1	52	7763	20	468	493.2	2.18	2.4	7.9
38	7763	35	126	125	2.15	0.65	7.2	53	7763	20	612	590.1	2.16	2.4	7.4
39	7763	35	445	404	2.1	2.28	6.4	54	7763	20	672	665.3	2.15	2.34	7.8
40	7796	35	142	141.7	2.15	0.83	6.3	55	7796	20	784	660.6	2.17	2.34	7.8
41	7796	35	199	217.7	2.14	0.92	6.5	56	7796	20	490	515.4	2.14	0.89	6.7
42	7796	35	91.8	106.7	2.08	0.7	6.9	57	7796	20	351	346.9	2.14	1.81	7.1
43	8703	35	90.9	87.6	2.09	0.75	6.4	58	8703	20	242	204.6	2.24	1.28	8.3
44	8703	35	40.9	46.2	2.02	1.18	5.6	59	8703	20	492	390.2	2.12	2.39	8
45	8703	35	39.6	42.6	1.96	0.4	6.9	60	8703	20	476	523.4	2.16	2.38	-

The integrity of the RNA samples was also assessed using agarose gel electrophoresis, with the results shown in Figure 5.1. The gel images demonstrate consistent RNA quality across all samples, as evidenced by the presence of distinct and well-defined bands corresponding to the 28S and 18S rRNA. However, RNA extracted from clone 8703 grown at 35°C exhibited the lowest concentration among the samples. Despite this lower concentration, the RNA bands, including the rRNA bands, remained visible, indicating that the RNA from sample 8703 maintained relatively good integrity even under heat stress. This suggests that, although the concentration was reduced, the overall RNA quality was still suitable for downstream applications.

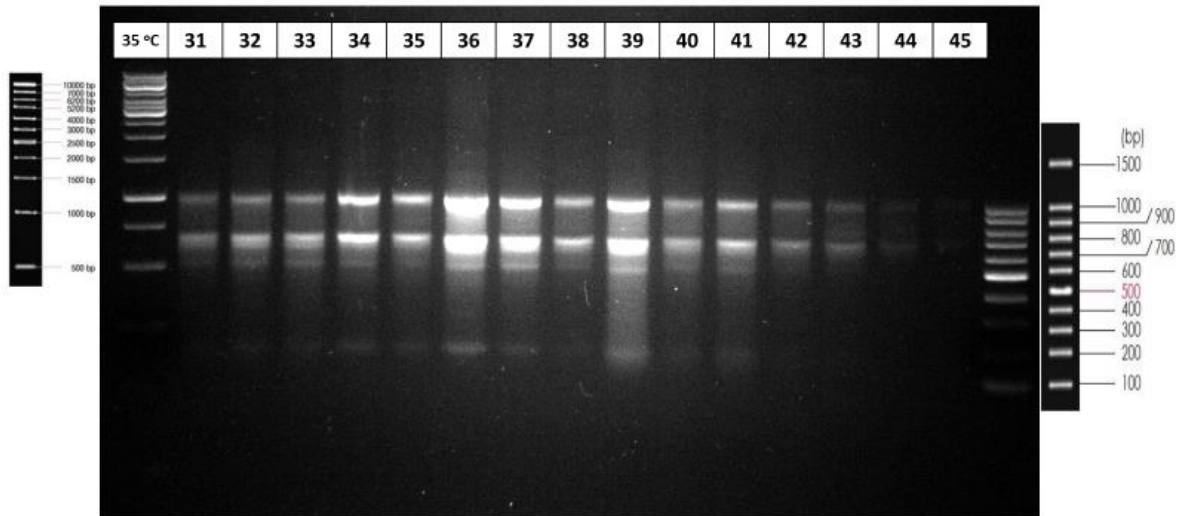
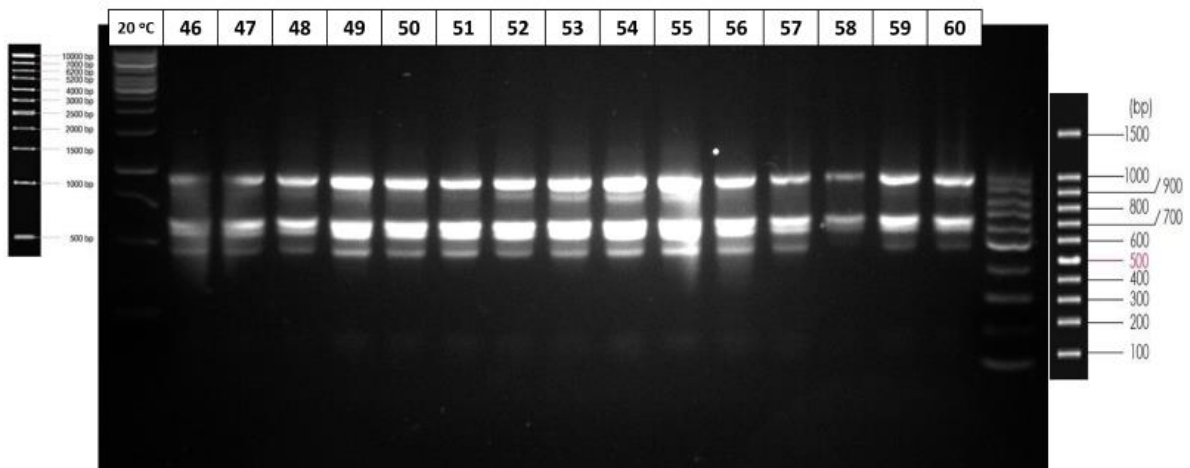
A**B**

Figure 5.1. RNA quality assessment of duckweed samples grown at 35°C (A) and 20°C (B) using agarose gel electrophoresis. Each gel includes a 1Kb ladder on the left side and a 100bp ladder on the right side for size reference.

In addition, the RNA samples were run on a TapeStation to confirm their quality and integrity. Figure 5.2 presents the TapeStation analysis results for RNA samples extracted from duckweeds grown at 20°C and 35°C. The profiles demonstrate good overall RNA quality under both temperature conditions, with well-defined peaks and consistent patterns indicative of high RNA integrity. Notably, sample number 60 did not yield a valid RNA Integrity Number (RIN) due to issues during the TapeStation analysis, however the bands showed in the image confirm that the RNA was not degraded, and the bands were clear. Despite this exception, the remaining samples produced reliable RIN values, reinforcing the overall integrity and quality of the RNA samples. These results confirm the suitability of the RNA samples obtained from both temperature treatments for downstream applications, providing confidence in the experimental outcomes.

5.3.2. RNA Sequencing Quality Control

5.3.2.1. RNA Sequencing Data Generation and Quality Control for Accurate Gene Expression Analysis

The initial step in data processing involved converting original image data files obtained from high-throughput sequencing platforms, such as Illumina, into sequenced reads, termed Raw Data or Raw Reads, using CASAVA base recognition (Illumina, 2024). These raw data were then saved in FASTQ (fq) format files, containing sequences of reads and associated base quality information. Each read was represented by four descriptive lines:

- Line 1: Begins with the at sign (@), followed by sequence identifiers and optional description, like a FASTA header.
- Line 2: Consists of the base sequences representing the raw reads, including adenine (A), guanine (G), cytosine (C), and thymine (T).
- Line 3: Commences with a plus sign (+), optionally followed by the same Illumina sequence identifiers and description information as Line 1.
- Line 4: Provides quality values for each base, corresponding to the data presented in Line 2.

To ensure the accuracy and reliability of gene expression analysis, several quality control measures were applied using FastQC (Andrews, 2020) and Trimmomatic (Bolger *et al.*, 2014) to assess the sequencing data and mitigate potential biases or errors. These analyses confirmed that the results accurately represented the biological conditions of the study.

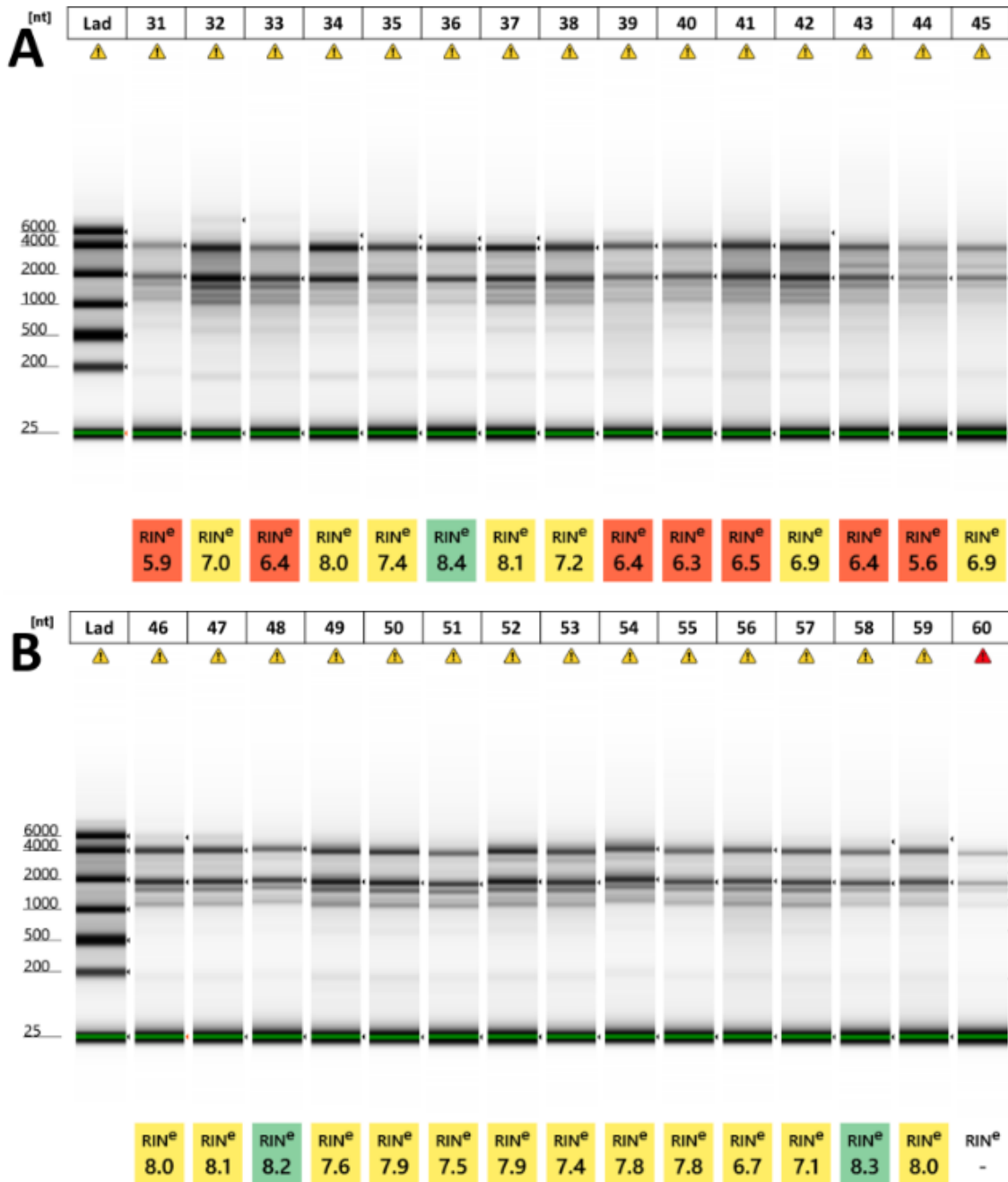


Figure 5.2. RNA quality assessment of duckweed samples grown at 20°C and 35°C. Panel A displays the RNA integrity for samples grown at 35°C, while Panel B presents the RNA integrity for samples grown at 20°C. Each analysis features a ladder in the first column for size reference, followed by the sample identification numbers. RNA Integrity Numbers (RIN) are indicated below each sample line. RNA Integrity Numbers (RIN) are indicated below each sample line, with color-coded rankings: green for high-quality RNA (RIN ≥ 8), yellow for moderate-quality RNA (RIN 5–8), and red for poor-quality RNA (RIN < 5).

The sequencing error rate was first examined, calculated using the Phred score ($Q_{\text{phred}} = -10\log_{10}(e)$), where "e" denotes the error rate. As shown in Table 5.2, Phred scores remained consistently high across all bases, with an error rate below 1%, indicating high sequencing quality.

Next, GC content distribution analysis was conducted to check for any AT and GC content separation, as imbalances can affect accurate gene expression quantification. As expected, GC and AT content showed a balanced distribution overall, with slight variation at the initial bases, as seen in Table 5.2.

A final data filtering step was applied to eliminate low-quality reads, reads contaminated with adapters, and those with over 10% ambiguous nucleotides or where more than half of the bases fell below a Phred score of 5. Following these stringent criteria, over 97% of the data consisted of high-quality, clean reads, as seen in Table 5.2, ensuring a robust dataset for downstream analysis.

5.3.3. Mapping of Sequencing Data

Alignments were performed using HISAT2, a fast and sensitive alignment program for mapping next-generation sequencing reads to a reference genome (Mortazavi *et al.*, 2008). HISAT2, which succeeds HISAT and TOPHAT2, employs a graph-based alignment method. It utilizes a global FM index along with a large set of small FM indexes, collectively covering the entire genome. These small indexes, or local indexes, combined with multiple alignment strategies, allow for effective alignment of RNA-seq reads, particularly those spanning multiple exons.

The HISAT2 algorithm operates in three stages:

- Aligning the entire sequence to a single exon.
- Piecewise aligning the sequence to two exons of the genome.
- Segmenting and aligning the sequence to more than three exons of the genome.

To assess the quality and efficiency of RNA-seq data, the reads from all samples were aligned to the reference genome *L. gibba* 7742a (Evan Ernst *et al.*, 2023) using HISAT2 (Mortazavi *et al.*, 2008). The total number of reads and mapping percentages for RNA from clones grown at control (20°C) and heat stress (35°C) temperatures are summarized in Table 5.3. Across all RNA samples, the total number of reads ranged from approximately 40 to 60 million per sample, with alignment rates varying depending on the clone and temperature condition.

Table 5.2. Sequencing quality statistics for RNA samples. For each sample (with a specific sample ID), the temperature (°C), the clone name, total base count of raw data (in gigabases, G), total base count of clean reads (in gigabases, G), the percentage of clean reads in relation to the raw data (in brackets) the average sequencing error rate (calculated by Qphred = $-10\log_{10}(e)$) and the GC percentage were presented.

Sample ID	T ^a (°C)	Clones	Raw bases	Clean bases	Error rate	GC (%)	Sample ID	T ^a (°C)	Clones	Raw bases	Clean bases	Error rate	GC (%)
s31	35	Manor	6.2G	6.08G (98.1%)	0.01	52.68	s46	20	Manor	7.17G	7.05G (98.29%)	0.01	54.18
s32	35	Manor	7.57G	7.4G (97.77%)	0.01	52.76	s47	20	Manor	7.7G	7.56G (98.26%)	0.01	54.11
s33	35	Manor	7.08G	6.93G (97.89%)	0.01	52.66	s48	20	Manor	8.22G	8.11G (98.64%)	0.01	54.19
s34	35	6861	8.95G	8.76G (97.82%)	0.01	54.24	s49	20	6861	7.56G	7.45G (98.55%)	0.01	54.85
s35	35	6861	8.25G	8.11G (98.3%)	0.01	53.95	s50	20	6861	8.5G	8.35G (98.28%)	0.01	54.91
s36	35	6861	8.86G	8.73G (98.54%)	0.01	53.94	s51	20	6861	7.27G	7.16G (98.46%)	0.01	54.77
s37	35	7763	9.13G	8.96G (98.22%)	0.01	54.54	s52	20	7763	8.57G	8.44G (98.52%)	0.01	55.38
s38	35	7763	7.31G	7.17G (98.15%)	0.01	54.15	s53	20	7763	7.76G	7.65G (98.58%)	0.01	55.27
s39	35	7763	8.19G	8.06G (98.33%)	0.01	54.32	s54	20	7763	8.01G	7.89G (98.47%)	0.01	55.42
s40	35	7796	7.83G	7.67G (97.99%)	0.01	54.51	s55	20	7796	7.84G	7.71G (98.41%)	0.01	55.83
s41	35	7796	7.79G	7.64G (98.09%)	0.01	54.48	s56	20	7796	9.45G	9.29G (98.26%)	0.01	55.27
s42	35	7796	6.56G	6.43G (98%)	0.01	54.13	s57	20	7796	9.29G	9.13G (98.28%)	0.01	55.28
s43	35	8703	7.89G	7.76G (98.27%)	0.01	52.55	s58	20	8703	8.89G	8.75G (98.35%)	0.01	53.48
s44	35	8703	7.17G	7.01G (97.75%)	0.01	52.46	s59	20	8703	8.41G	8.27G (98.36%)	0.01	53.68
s45	35	8703	7.88G	7.72G (97.96%)	0.01	52.81	s60	20	8703	8.68G	8.57G (98.68%)	0.01	54.1

For RNA samples from clones grown at the control condition (20°C), the mapping percentages of reads ranged from 8.24% to 91.14%. Those RNA samples from clones grown under heat stress (35°C), mapping percentages varied from 4.45% to 93.54%. Notably, RNA samples from the heat tolerance clones, particularly 7796, exhibited the highest percentage of mapped reads compared to the reference genome, with values exceeding 90% in both temperature conditions. RNA from clones 6861 and 7763 also showed high mapping percentages, further supporting their classification as heat-tolerant clones. In contrast, the RNA from the control Manor as well as the clone classified as heat-sensitive, 8703, showed significantly lower mapping percentages, particularly when those clones grew under heat stress (35°C), indicating a greater genetic divergence from the reference genome.

Regarding the quality of alignment, unique mapping rates (reads mapped to a single location in the genome) ranged from 3.21% to 86.21% at 35°C and from 5.22% to 85.85% at 20°C. Once again, RNA from the clone 7796 showed the highest unique mapping percentages, followed closely by RNA from clones 7763 and 6861. On the other hand, the RNA from the clones Manor and 8703 showed lower unique mapping percentages, particularly when they grew at under heat stress conditions (35°C). Multi-mapped reads (reads mapped to multiple locations) remained consistently low across all RNA samples, with percentages ranging from 1.24% to 4.65% and from 2.96% to 5.29% when clones grew at 35°C and 20°C, respectively.

These results suggest that the heat sensitive clones have more genetic divergence, which may explain their reduced capacity to handle heat stress compared to the heat-tolerant clones. This genetic divergence becomes more evident at higher temperatures, highlighting the relationship between the reference genome and the heat-tolerant clone in genetic similarity.

5.3.4. Gene Expression Profile Analysis

Gene expression level analysis is a fundamental aspect of RNA-seq experiments, as it provides insight into the biological activity of genes by quantifying the level of their expression. This was determined based on the number of reads that successfully mapped to the reference genome *L. gibba* 7742a (Ernst *et al.*, 2023).

Table 5.3. RNA-seq read counts and mapping statistics for different clones grown at 20 °C and 35 °C. Summary of the total read counts and mapping statistics for RNA-seq data from clones grown under control (20 °C) and heat stress (35 °C) conditions. It presents the number of sequenced reads and the percentage of reads mapped to the reference genome (7742, (Evan Ernst et al., 2023)) for each sample.

Sample ID	T ^a (°C)	Clone	Total reads	Total mapped	Sample ID	T ^a (°C)	Clone	Total reads	Total mapped
s31	35	MANOR	40539398	2758104(6.8%)	s46	20	MANOR	46972566	4226969(9.0%)
s32	35	MANOR	49355942	3181923(6.45%)	s47	20	MANOR	50428542	4516317(8.96%)
s33	35	MANOR	46213524	3174519(6.87%)	s48	20	MANOR	54081122	4666736(8.63%)
s34	35	6861	58388870	31491702(53.93%)	s49	20	6861	49648820	26219989(52.81%)
s35	35	6861	54094288	29008668(53.63%)	s50	20	6861	55669016	29236598(52.52%)
s36	35	6861	58214374	31828688(54.67%)	s51	20	6861	47715408	25012180(52.42%)
s37	35	7763	59752380	41455390(69.38%)	s52	20	7763	56298144	38283101(68.0%)
s38	35	7763	47821122	32601315(68.17%)	s53	20	7763	51009684	34616804(67.86%)
s39	35	7763	53705028	36170967(67.35%)	s54	20	7763	52581076	35473077(67.46%)
s40	35	7796	51149494	47846469(93.54%)	s55	20	7796	51407174	46852336(91.14%)
s41	35	7796	50932294	45683022(89.69%)	s56	20	7796	61910680	53174782(85.89%)
s42	35	7796	42869806	40007348(93.32%)	s57	20	7796	60844562	52787764(86.76%)
s43	35	8703	51701142	3027679(5.86%)	s58	20	8703	58309246	5113794(8.77%)
s44	35	8703	46748546	2526712(5.4%)	s59	20	8703	55122822	4544829(8.24%)
s45	35	8703	51487572	2289988(4.45%)	s60	20	8703	57112326	5515167(9.66%)

5.3.4.1. Gene Expression Quantification and Distribution Levels

The level of gene expression is directly reflected by the abundance of transcripts. In RNA-seq experiments, gene expression is estimated by the number of sequencing reads mapped to the genome or exons (Goldstein *et al.*, 2016). This count is influenced by factors such as gene expression level, gene length, and sequencing depth (Liao *et al.*, 2014). To account for these variables, FPKM (Fragments Per Kilobase of transcript sequence per Million base pairs sequenced) is commonly used (Trapnell *et al.*, 2010). FPKM corrects for differences in sequencing depth and gene length, providing a more accurate estimate of gene expression levels (Mortazavi *et al.*, 2008).

To compare gene expression across different conditions, the distribution of gene expression levels, represented, by FPKM values (Bray *et al.*, 2016), is displayed using boxplots as shown in Figure 5.3. For biological replicates, the mean FPKM value was used to represent the overall expression level. This method provides a visual comparison of gene expression levels across samples and treatments.

The distribution of gene expression levels across the samples shows distinct patterns between heat-tolerant and heat-sensitive clones under different temperature conditions. For the heat-tolerant clones (e.g., 7796, 7763, and 6861), there is a noticeable higher median gene expression, particularly in the samples grown at 35°C (represented by the upper part of the plot, with $\log_2(\text{FPKM}+1)$). These clones exhibit relatively low variation in gene expression, as reflected by the narrow interquartile range and consistent distribution of data points. This indicates a more stable and robust gene expression profile in response to heat stress.

In contrast, the heat-sensitive clones (e.g., Manor and 8703) show a lower median gene expression, often approaching 0, suggesting reduced overall expression levels. The heat-sensitive clones appear to have less stable gene expression under heat stress, which may be indicative of a weaker or less adaptive response to the heat treatment compared to the heat-tolerant clones.

Overall, the boxplot provides clear evidence that heat-tolerant clones maintain higher and more consistent gene expression levels, whereas heat-sensitive clones exhibit more variability and lower expression. This could suggest that heat-tolerant clones have more efficient or regulated transcriptional responses to heat stress.

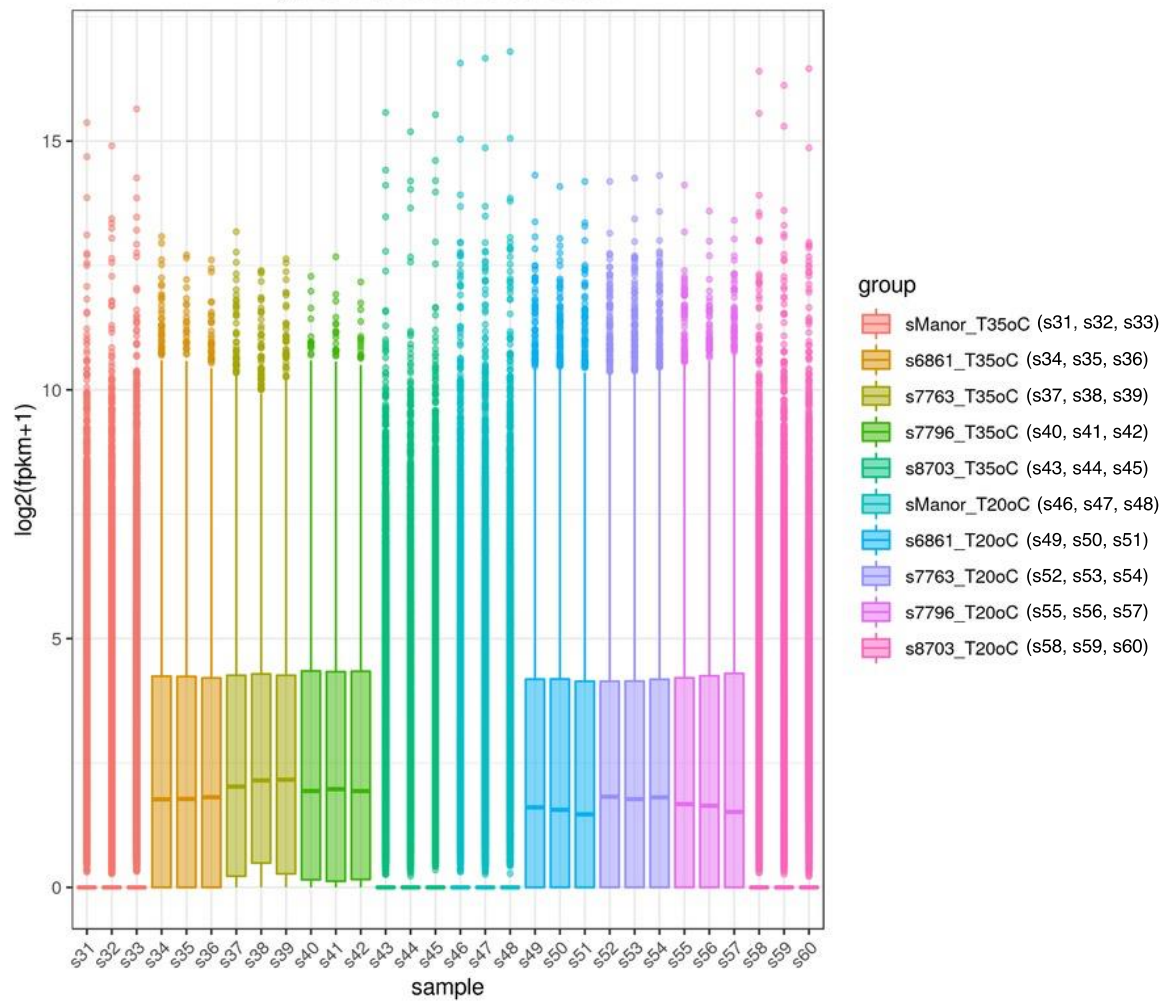


Figure 5.3. Distribution of gene expression levels across clones and temperature conditions. This boxplot illustrates the distribution of gene expression levels, represented as $\log_2(\text{FPKM}+1)$, across different clones (Manor, 6861, 7763, 7796, and 8703) under two temperature conditions (20 and 35°C). Each colour corresponds to a distinct clone. The boxplots show the median, interquartile range, and overall distribution of gene expression levels within each sample group.

5.3.4.2. Evaluation of Sample Consistency Using Pearson Correlation Analysis

In RNA-seq experiments, analysing the correlation of gene expression levels between samples is crucial for confirming the experiment's reproducibility and assessing sample suitability for differential expression analysis. High correlation coefficients suggest strong agreement between samples. According to ENCODE guidelines, a squared Pearson correlation coefficient above 0.92 and an R^2 greater than 0.8 are recommended benchmark for quality replication (Feingold *et al.*, 2004).

In this study, correlation coefficients were calculated using FPKM values across all genes in each sample. The results were visualized as a heatmap (Figure 5.4), where the darker blue areas indicate higher correlations, signifying greater similarity in expression profiles between samples.

For most samples, particularly replicates from heat-tolerant clones, strong intra-group correlations were observed. This consistent pattern suggests the RNA-seq experiment was reliable, as biological replicates demonstrated similar expression profiles within each group. These findings align with ENCODE's quality standards, reinforcing the validity of the experimental data.

However, one sample, *s60*, displayed an anomalous correlation pattern. Unlike other replicates, *s60* exhibited an unexpectedly uniform correlation level across all samples, failing to align closely with its own group. This deviation from expected behaviour indicates potential issues with *s60*, which could stem from experimental or technical factors, such as sequencing errors or sample contamination.

The unusual behaviour of *s60* raises concerns about its reliability and suitability for downstream analyses. While other samples meet the quality benchmarks recommended by ENCODE, *s60* may need further investigation. Depending on subsequent findings, it might be necessary to exclude this sample from differential expression analysis to ensure the accuracy and robustness of the study's conclusions.

Pearson correlation between samples

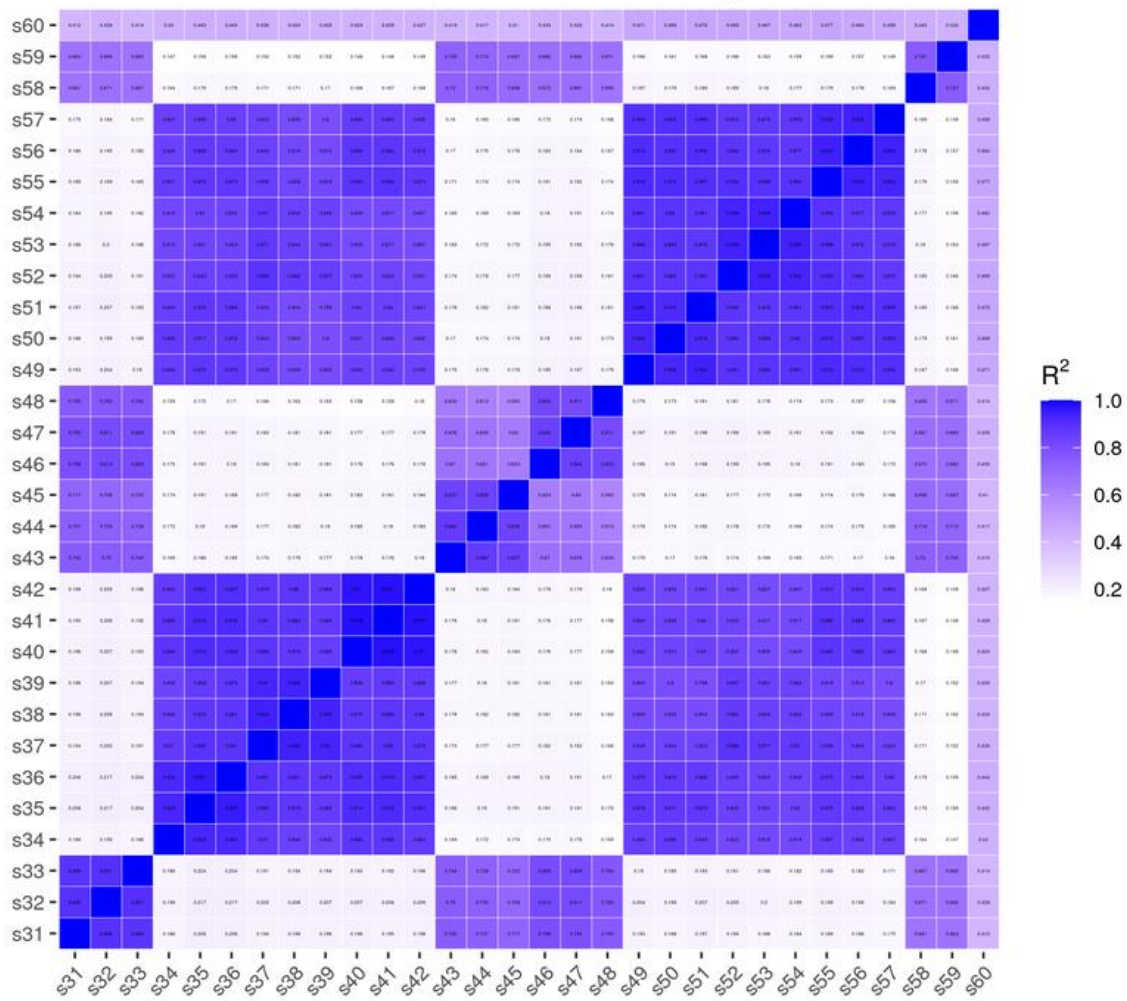


Figure 5.4. Pearson correlation heat map of gene expression levels. The heat map displays Pearson correlation coefficients between samples based on gene expression levels (FPKM values). Darker shades of blue indicate higher correlation values, with coefficients closer to 1 reflecting stronger similarity in gene expression profiles between samples. Lighter shades represent lower correlation values, suggesting greater differences in expression.

5.3.4.3. Principal Component Analysis (PCA) for Assessing Sample Variation and Group Differentiation

Principal Component Analysis (PCA) is a robust method used to evaluate intergroup differences and assess the consistency of samples within each group. By reducing high-dimensional gene expression data into principal components, PCA simplifies complex patterns and highlights the primary sources of variation across samples.

As shown in the Figure 5.5, the first two principal components, PCA1 and PCA2, explain 68.94% and 5.08% of the variance, respectively. The plot reveals a distinct separation between heat-sensitive and heat-tolerant clones: the heat-sensitive clones cluster on the left side of the plot, while the heat-tolerant clones are positioned on the right. This clear separation underscores the marked differences in gene expression profiles between the two groups.

Notably, while PCA2 accounts for only 5.08% of the variance, it captured a clear grouping of the heat-tolerant samples by treatments (temperature), reflecting their differential responses to heat stress. In contrast, the separation of heat-sensitive clones (Manor and 8703) was driven by genetic variance rather than by treatments, emphasizing inherent differences between these samples not from treatment effects.

Within each group, samples form tight cluster, reflecting strong consistency among biological replicates. However, sample s60 aligns with earlier observations from the correlation analysis, raising concerns about data quality and suggesting that it may require further investigation or exclusion from downstream analysis.

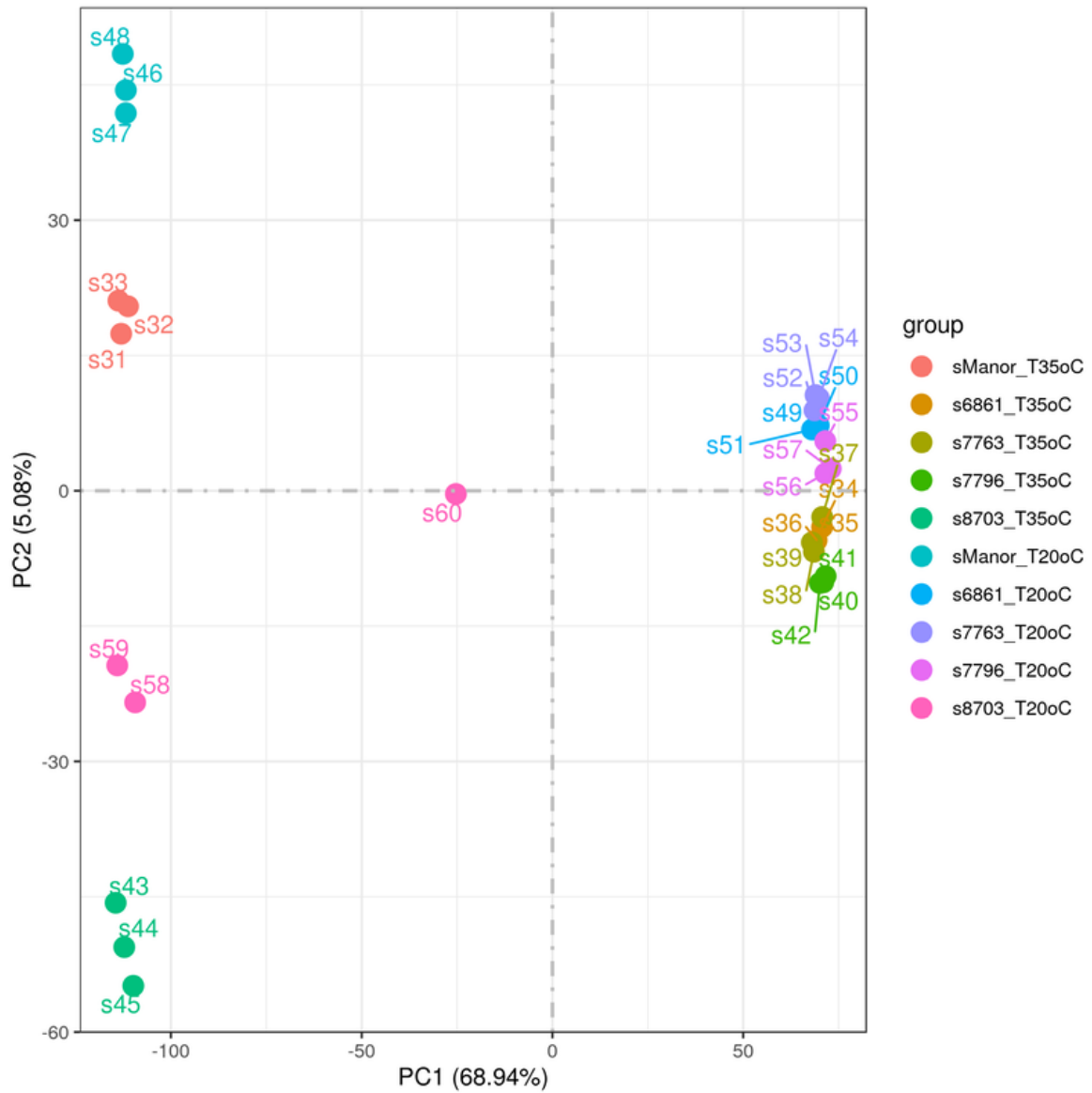


Figure 5.5. Principal Component Analysis of gene expression profiles. The PCA plot illustrates the variance in gene expression profiles across samples, with PCA1 and PCA2 accounting for 68.94% and 5.08% of the variance, respectively.

5.3.4.4. Coexpression Venn Diagram

The coexpression Venn diagram illustrates the number of genes uniquely expressed within each clone under each temperature condition, with overlapping regions representing the genes co-expressed across different groups. In this Venn diagram analysis, each clone was examined for gene expression patterns at two temperatures, 20°C and 35°C, to highlight the unique and shared genes under each condition. As can be seen in Table 5.4, each clone displayed distinct patterns of gene expression across the two temperatures. Notably, 6861, 7763 and 7796 exhibit a high percentage of genes expressed at both 20°C and 35°C, with over 80% of their total expressed genes shared across conditions. This high overlap suggests a stable expression profile under temperature stress, which may relate to their thermotolerant behaviour. Conversely, 8703 stands out for having a substantial portion of its gene expression uniquely at 20°C, with fewer genes shared between the two temperatures, further indicating a more temperature-sensitive response. However, the s60 sample exhibited unusual behaviour in the previous quality controls, which may have contributed to this variation. These differences provide insight into each clone's adaptive mechanisms to thermal variations.

After this individual analysis, a global Venn diagram was created to compare all clones under both temperature conditions, allowing us to identify genes that were commonly expressed across all samples at 20°C and 35°C. This comparison revealed differences in gene expression among the clones, suggesting possible mechanisms of heat-tolerance based on the unique and shared genes expressed under heat stress.

The Venn diagram analysis for the five clones at 20°C and 35°C (Figure 5.6) revealed some key observations. Firstly, gene expression was generally higher in the heat-tolerant clones at both temperatures. A larger number of genes expressed in the area where the three heat-tolerant clones overlapped: 7,547 genes were expressed at 20°C, while 10,543 were expressed at 35°C. In the area where all five clones converged, gene expression was consistent across temperatures, with 3,685 genes expressed at 20°C and 3,692 genes at 35°C. However, in the region where the heat-sensitive clones (8703 and Manor) overlapped with the heat-tolerant clones, a significant drop was observed: 3,671 genes were expressed at 20°C, but only 849 genes at 35°C. This notable decrease may be due to the unusual behaviour seen in sample s60.

Table 5.4. Summary of gene expression across individual clones (Manor, 6861, 7763, 7796, and 8703) at 20°C and 35°C. The total number of genes expressed, the number of genes co-expressed at both temperatures, and those uniquely expressed at either 20°C or 35°C.

Clones	Total N° of genes expressed	N° of genes expressed at both temperatures	N° of genes expressed at 20 °C	N° of genes expressed at 35 °C
Manor	5498	3993 (72.63%)	523 (9.51%)	982 (17.86%)
6861	18731	15997 (85.4%)	1084 (5.79%)	1650 (8.81%)
7763	20872	16982 (81.36%)	1197 (5.73%)	2693 (12.9%)
7796	19127	16215 (84.78%)	913 (4.77%)	1999 (10.45%)
8703	8428	4010 (47.58%)	3654 (43.36%)	764(9.07%)

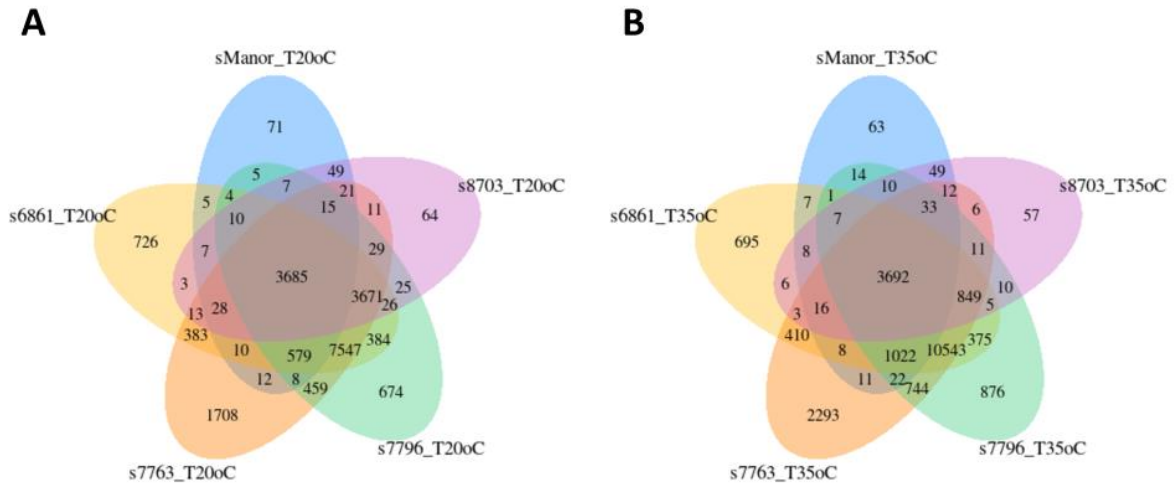


Figure 5.6. Venn diagram displaying the distribution of gene expression across five duckweed clones under two temperature conditions. (A) the number of genes expressed at 20°C, and (B) the gene expression at 35°C. Overlapping areas indicate genes that co-expressed among the clones.

5.3.5. Differential Gene Expression Analysis Under Heat Stress Conditions

5.3.6. Gene expression levels were quantified and normalized to account for sequencing depth. A statistical model was then applied to identify significant differences between growing conditions. To ensure accuracy, p-values were calculated, and multiple testing corrections were performed to determine false discovery rate (FDR) values (Anders & Huber, 2010).

The differential gene expression analysis between 35°C and 20°C in the five clones revealed a higher number of differentially expressed genes in heat-tolerant clones compared to heat-sensitive ones (Figure 5.7). This greater level of differential expression is likely due to the superior mapping quality in the heat-tolerant clones, facilitating more precise detection of gene expression changes under temperature variations.

Among the heat-tolerant clones, clone 7796 showed the highest number of differentially expressed genes, with 5,297 genes affected (2,947 upregulated and 2,350 downregulated). Followed by clone 7763 with 4,603 differentially expressed genes (2,446 upregulated and 2,157 downregulated), while clone 6861 showed 3,376 differentially expressed genes (1,690 upregulated and 1,686 downregulated) (Figure 5.7).

In contrast, the heat-sensitive clones displayed substantially fewer differentially expressed genes. Clone 8703 only had 436 genes showing changes in expression (180 upregulated and 256 downregulated), while the Manor clone showed 567 differentially expressed genes (271 upregulated and 296 downregulated).

Despite the differences in the total number of differentially expressed genes between heat-tolerant and heat-sensitive clones, the proportion of upregulated and downregulated genes remained remarkably similar across both groups. For the heat-tolerant clones, clone 7796 showed 55.6% of its differentially expressed genes upregulated and 44.4% downregulated. Similarly, clone 7763 displayed 53.1% upregulated and 46.9% downregulated genes, while the clone 6861 had an almost even split, with 50.1% upregulated and 49.9% downregulated. A comparable pattern was observed in the heat-sensitive clones: clone 8703 had 41.3% of its differentially expressed genes upregulated and 58.7% downregulated, and the Manor clone had 47.8% upregulated versus 52.2% downregulated.

This consistency in the proportion of upregulated and downregulated genes across both heat-tolerant and heat-sensitive clones suggests that, while the magnitude of transcriptional response (number of genes) differs significantly, the overall balance of changes in gene expression remains stable between the groups. This could indicate a fundamental similarity in the regulatory mechanisms governing gene expression under heat stress, irrespective of the clones' heat tolerance levels.

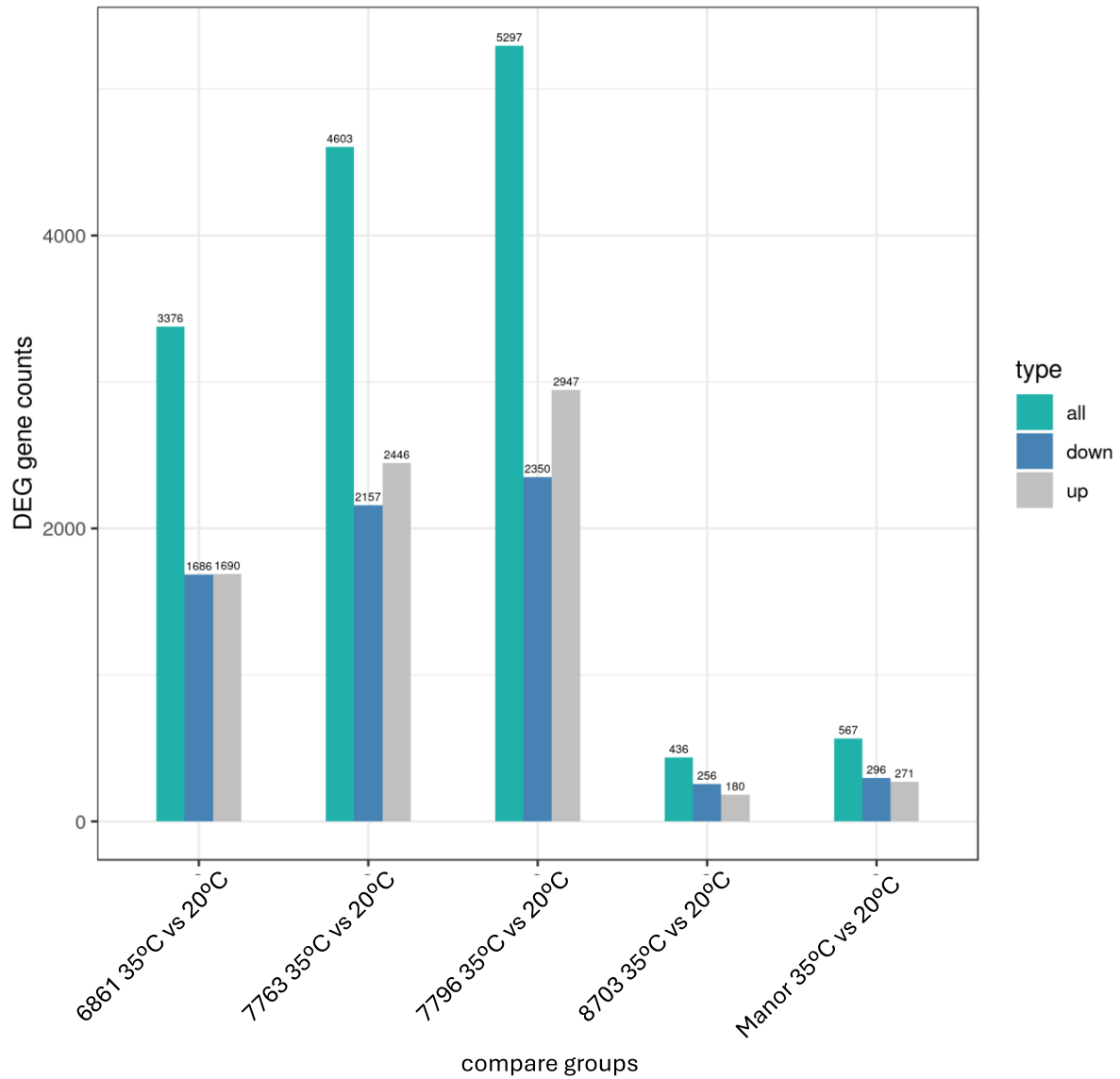


Figure 5.7. Differential gene expression counts across clones between 35°C and 20°C. The bar graph illustrates the number of differentially expressed genes (DEGs) across five *Lemna gibba* clones grown at 35°C vs 20°C. The y-axis represents the total DEG counts, while the x-axis displays the clones analysed. Each bar is divided into total (green), upregulated (grey) and downregulated (blue) gene counts.

5.3.6.1. Cluster Analysis of Differentially Expressed Genes Across Clones

To explore gene expression patterns, all differentially expressed genes (DEGs) were pooled for clustering analysis. Genes with similar expression profiles were grouped to reveal shared regulatory mechanisms. Hierarchical clustering, based on FPKM values standardized to Z-scores, enabled comparison across samples. This approach visualized expression trends, highlighting similarities and differences in gene expression under varying conditions.

The hierarchical clustering heat map (Figure 5.8), based on FPKM values, revealed distinct gene expression patterns among *Lemna* clones grown under control (20°C) and heat stress (35°C) conditions. Clustering analysis clearly separated the clones into two primary groups: heat-tolerant and heat-sensitive clones. Within each group, further sub-clustering aligned with the temperature. Heat-sensitive clones grown at 35°C clustered together, distinct from the same clones grown at 20°C, which formed a separate subgroup. This divergence emphasizes the substantial transcriptional changes induced by heat stress in heat-sensitive clones. Similarly, heat-tolerant clones exhibited consistent clustering at 20°C, reflecting uniform gene expression under non-stress conditions. However, clones grown at 35°C within the heat-tolerant group showed more variations, with some not aligning perfectly within the same subgroup. This suggests different transcriptional responses to heat stress among heat-tolerant clones, possibly reflecting diverse mechanisms of thermotolerance.

Interestingly, one heat-sensitive sample, S60, deviated from its technical replicates and failed to cluster within its expected subgroup. This discrepancy was also evident in the PCA analysis, where S60 appeared as an outlier. Upon closer inspection, some genes in S60 exhibited expression values of 0, which likely resulted from sequencing artefacts or issues with sequence quality. Despite this anomaly, the clustering of other heat-sensitive clones remained robust and unaffected, supporting the reliability of the clustering analysis in capturing the broader transcriptional patterns of heat-sensitive clones. The outlier highlights the importance of stringent quality checks in sequencing data to avoid potential misinterpretations while underscoring the robustness of the overall clustering methodology.

Two major gene clusters revealed opposing transcriptional responses to heat stress. The first cluster contained genes downregulated in heat-sensitive clones but upregulated in heat-tolerant ones, suggesting a role in promoting heat tolerance. The second cluster included genes upregulated in heat-sensitive clones but downregulated in heat-tolerant ones, potentially contributing to stress sensitivity. These clusters highlight distinct molecular responses, reflecting differences in heat tolerance mechanisms between clones.

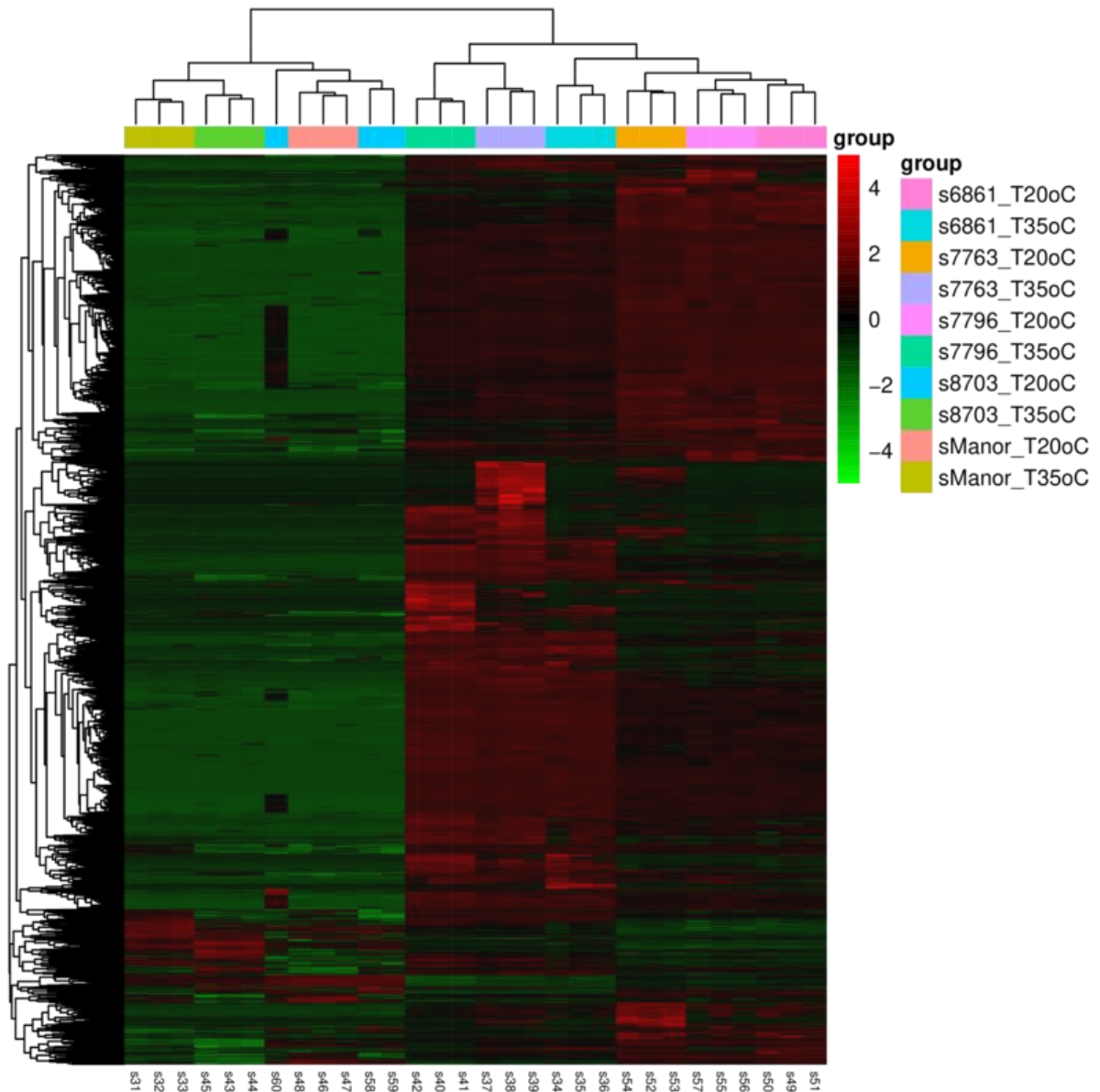


Figure 5.8. Hierarchical clustering heatmap of Differentially Expressed Genes (DEGs) in heat-sensitive and heat-tolerant duckweed clones at 20°C and 35°C. The heat map displays hierarchical clustering of gene expression data, with rows representing gene clusters (y-axis) and columns representing sample groups (x-axis). Heat-sensitive and heat-tolerant clones are distinctly clustered, with subgroups corresponding to growth at 20°C and 35°C. Genes are grouped into two primary clusters: those upregulated in heat-tolerant clones but downregulated in heat-sensitive clones, and the inverse. The colour gradient indicates the relative expression levels of genes, with red representing upregulation and green representing downregulation.

5.3.7. Functional Analysis of Differentially Expressed Genes in Duckweed Clones

Functional analysis of differentially expressed genes (DEGs) was performed to identify the biological functions and pathways significantly associated with gene expression changes in *Lemna* clones under control (20°C) and heat stress (35°C) conditions. Enrichment Analysis was conducted using ClusterProfiler (Young *et al.*, 2010), focusing on Gene Ontology (GO) and Kyoto Encyclopaedia of Genes and Genomes (KEGG) enrichment. These analyses revealed insights into the molecular mechanism underlying heat tolerance and sensitivity in duckweed clones.

5.3.7.1. GO Enrichment Analysis

The Gene Ontology (GO) framework (<http://www.geneontology.org/>) is a widely-used bioinformatics classification system aimed at standardizing gene properties across species. It comprises three main categories: biological process (BP), cellular component (CC), and molecular function (MF). In this study, GO terms with a p-adj value below 0.05 were considered significantly enriched. The top 30 most significant GO terms across five clones were presented in Figure 5.9.

In the biological process category, GO enrichment analysis highlighted photosynthesis-related activities as a significant feature of the biological process category. Clones Manor, 6861, 7763, and 7796 all showed enrichment scores above 2 for the photosynthesis term, with associated gene counts varying across clones: Manor (14 genes), 6861 (22 genes), 7763 (30 genes), and 7796 (26 genes). Clone 8703, identified as heat-sensitive, exhibited a lower enrichment score for photosynthesis-related activity, below 2. Notably, the Manor clones showed strong enrichment for the oxidation-reduction process, with 52 genes contributing to this activity. Clone 7796 significantly exhibited genes associated with the response to stress, with 74 genes involved.

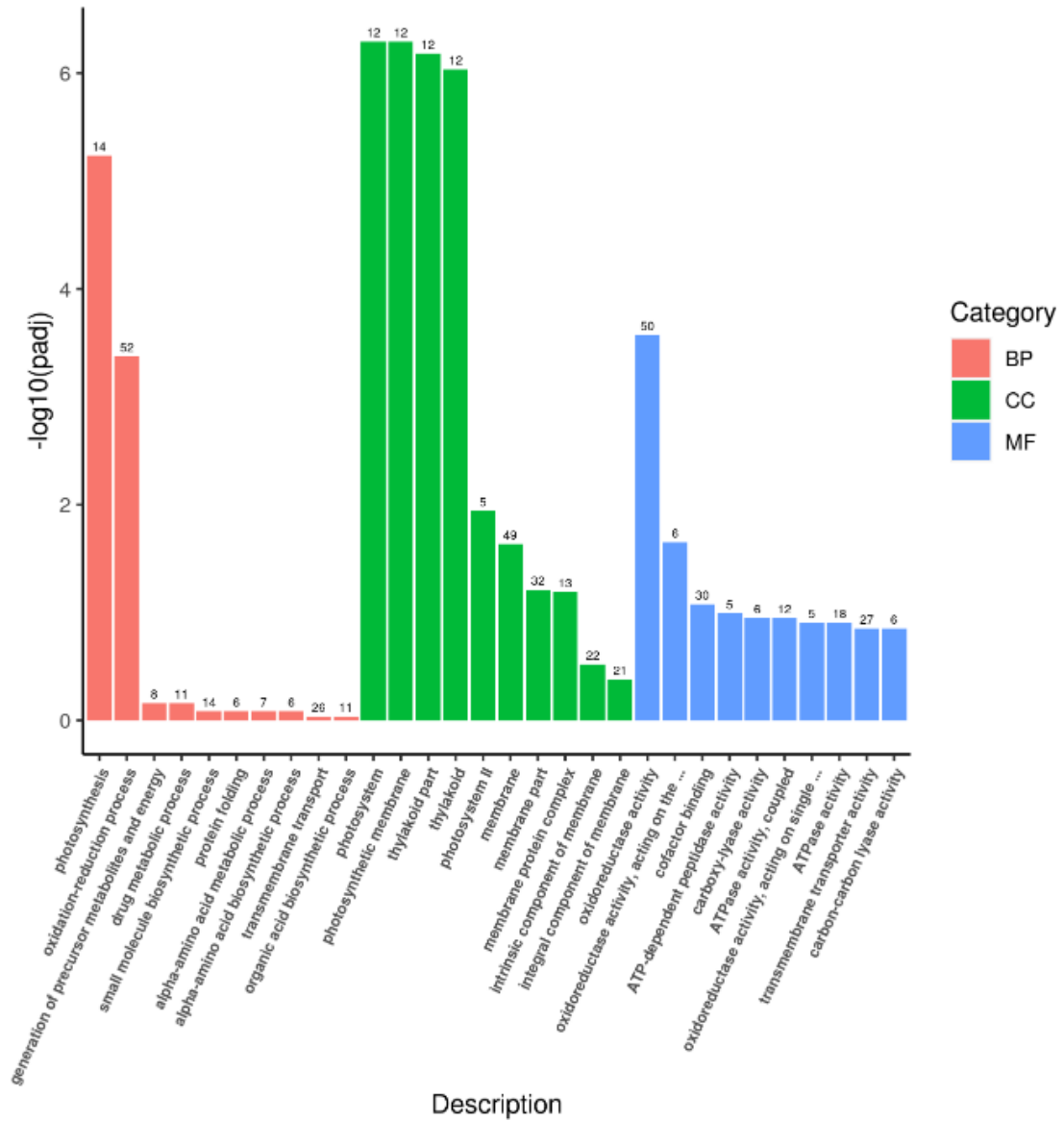
Enrichment in the cellular component category reflected a significant focus on photosynthesis structures. Terms such as photosystem, photosynthetic membrane, thylakoid part, and thylakoid were enriched across all five clones. These results highlight the centrality of the photosynthetic apparatus in the functional response of duckweed clones to environmental conditions.

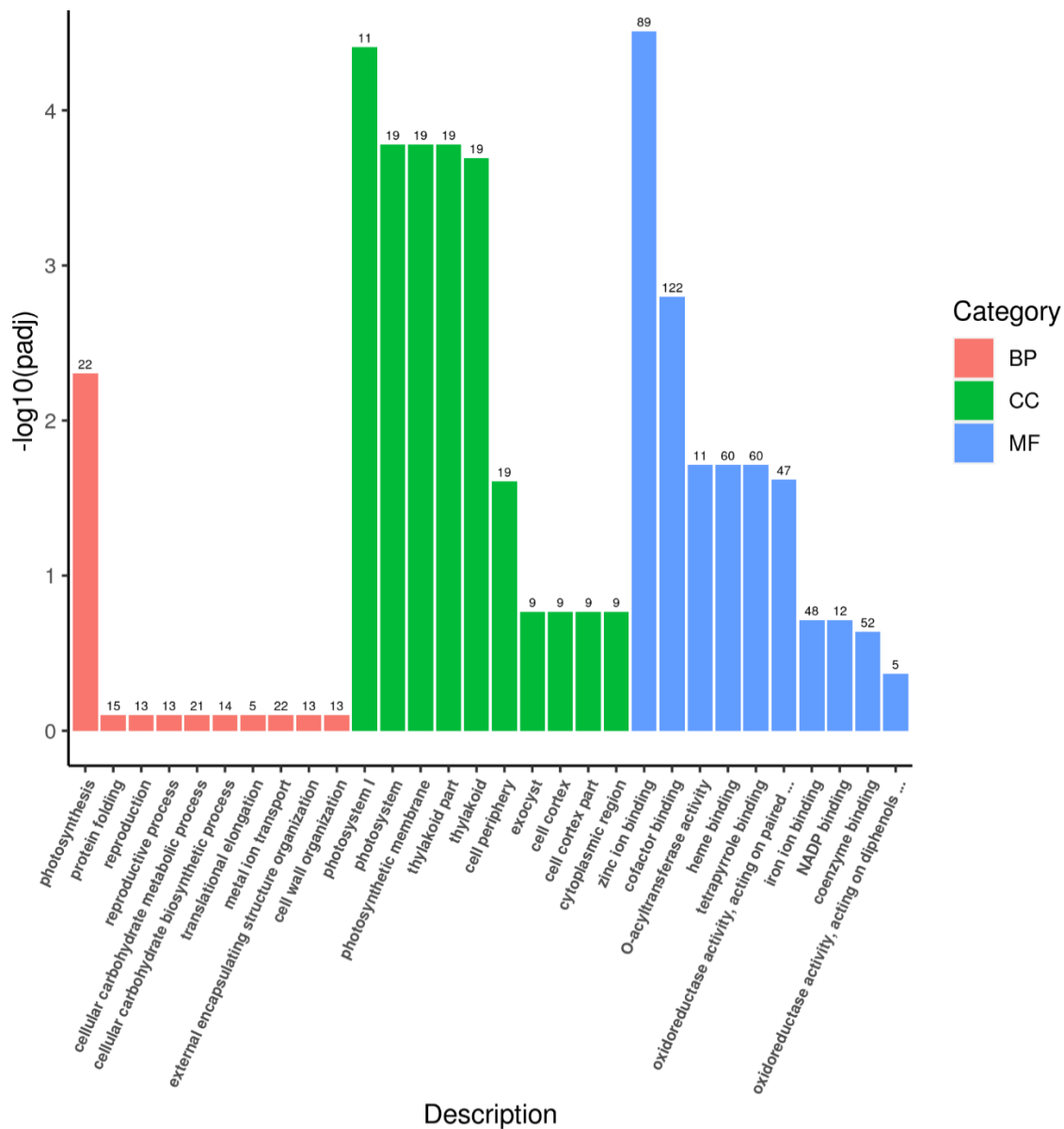
For molecular function category revealed marked differences between the heat-tolerant clones and heat sensitive clones. Heat-tolerant clones (6861, 7763, and 7796) showed substantial enrichment in zinc ion binding GO term, a feature absent in the heat-sensitive (8703) and control (Manor) clones. Gene counts for zinc ion binding were notably high, with 6861 showing 89 genes, 7763 with 100 genes, and 7796 with 122 genes. Clone 6861 also showed a significant enrichment in cofactor binding (122 genes), whereas 7763 had a significant enrichment in copper ion binding (100 genes). By contrast, the

Manor clone displayed high activity in oxidoreductase functions, whereas 8703 clone lacked notable enrichment in these molecular functions.

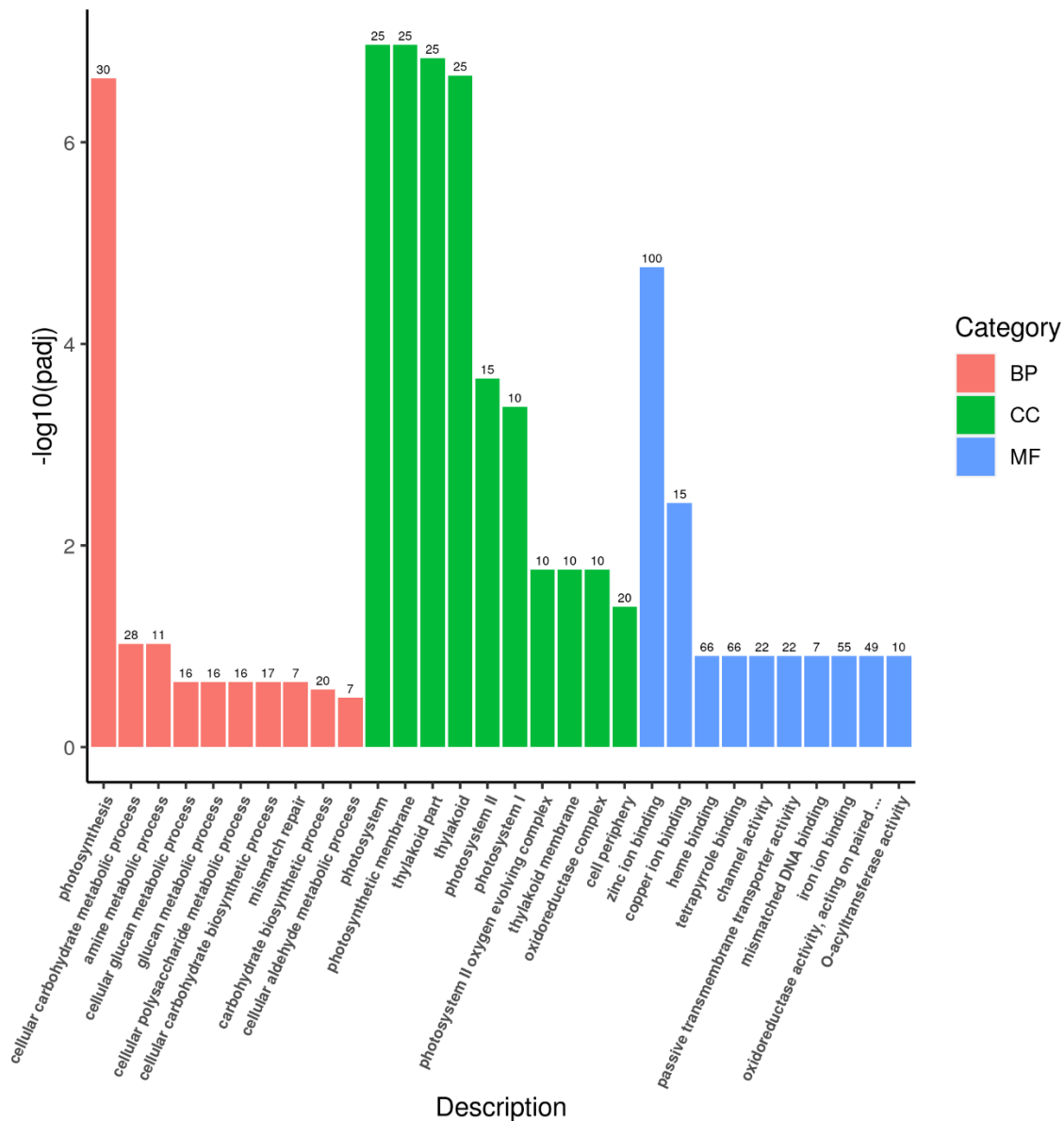
Differential regulation of genes across GO terms revealed intriguing patterns as can be seen in Figure 5.10. In the biological process category, photosynthesis-related genes were consistently downregulated across all clones, including the heat-sensitive clone 8703. However, 8703 exhibited fewer DEGs, contributing to a less pronounced downregulation in this category. Cellular component analysis also demonstrated a downregulation of DEGs related to photosynthetic structures, including the photosystem and thylakoid membrane. In molecular functions, zinc ion binding genes were upregulated exclusively in heat-tolerant clones (6861, 7763, and 7796), with no expression in 8703 or Manor. These patterns highlight a potential role of zinc ion binding in thermotolerance.

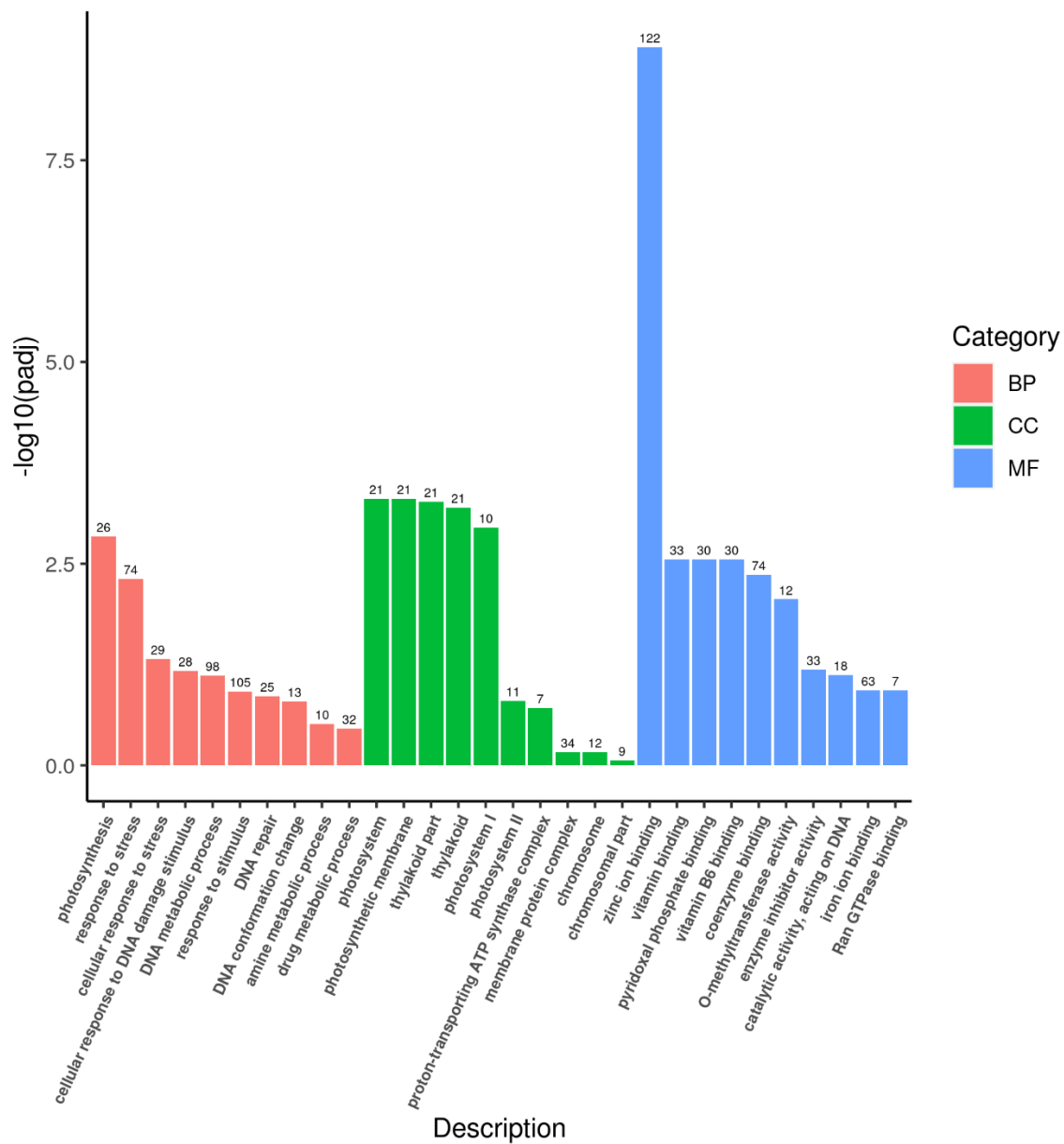
A



B

C



D

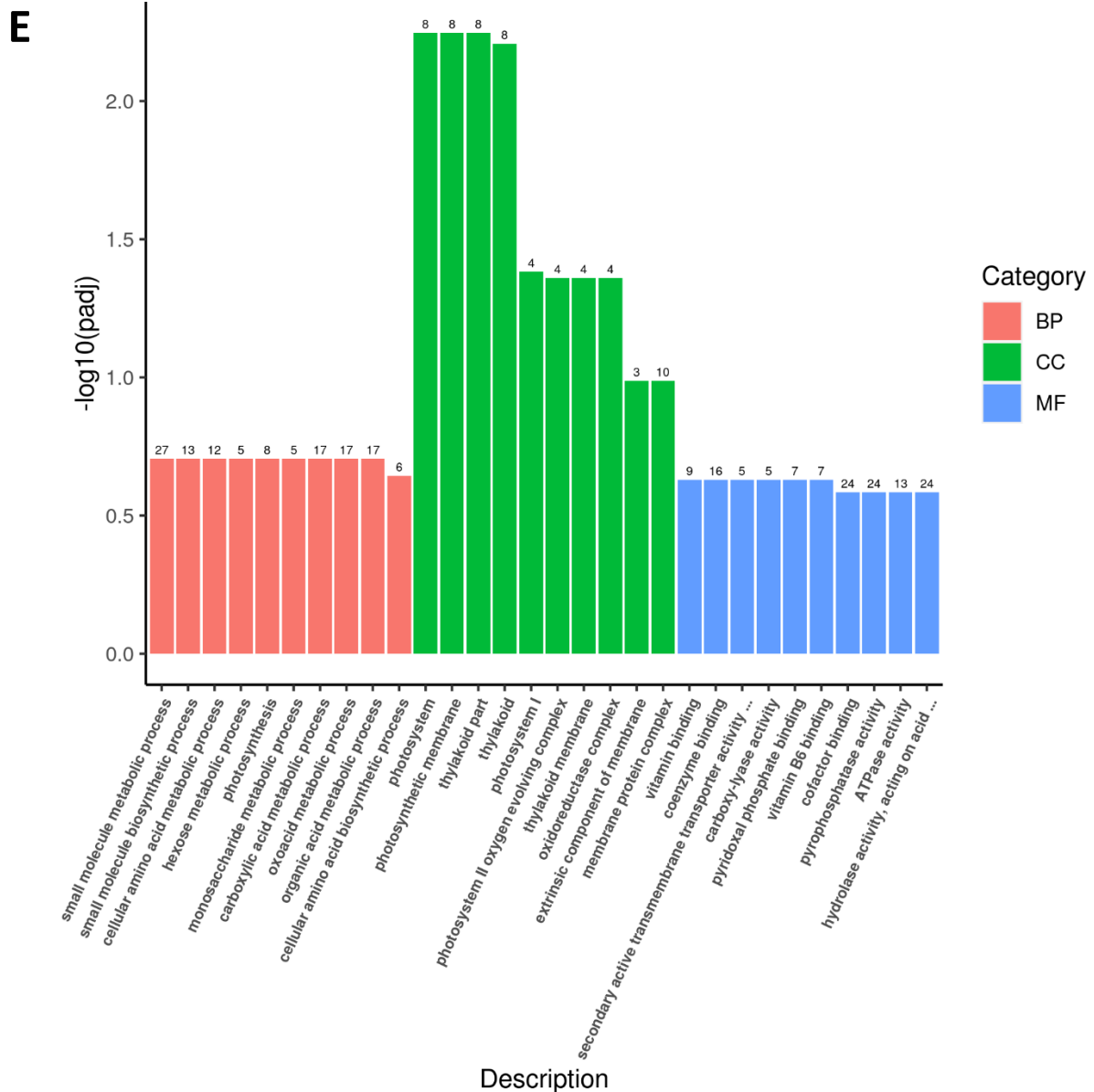
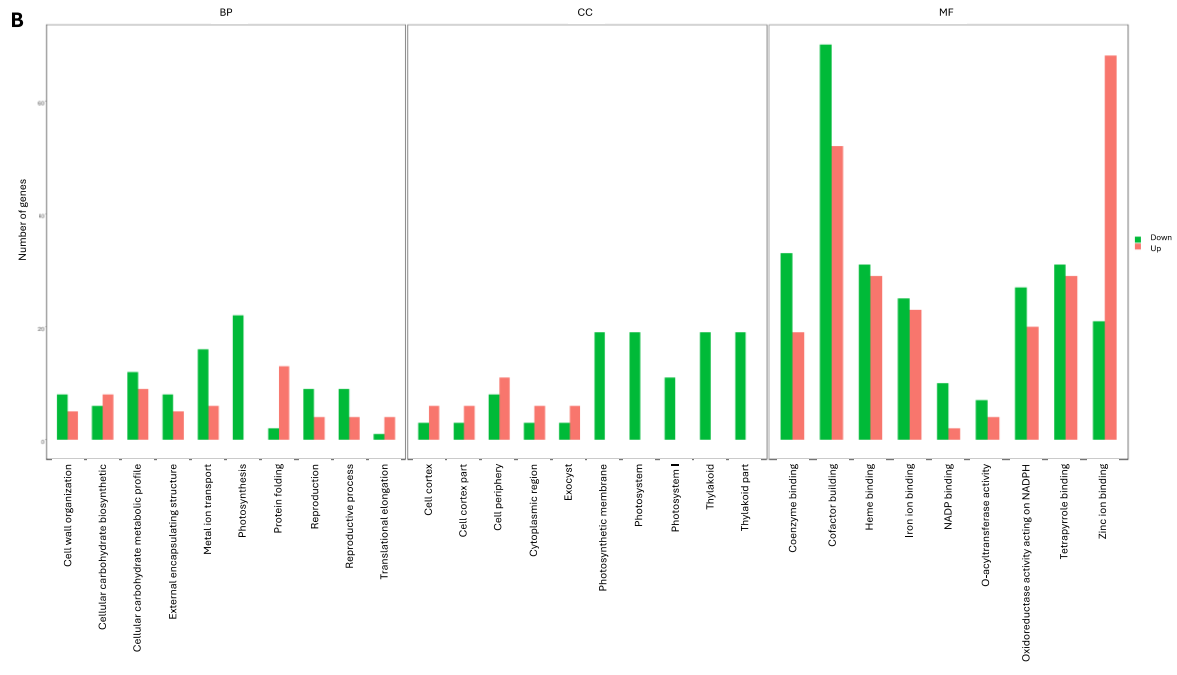
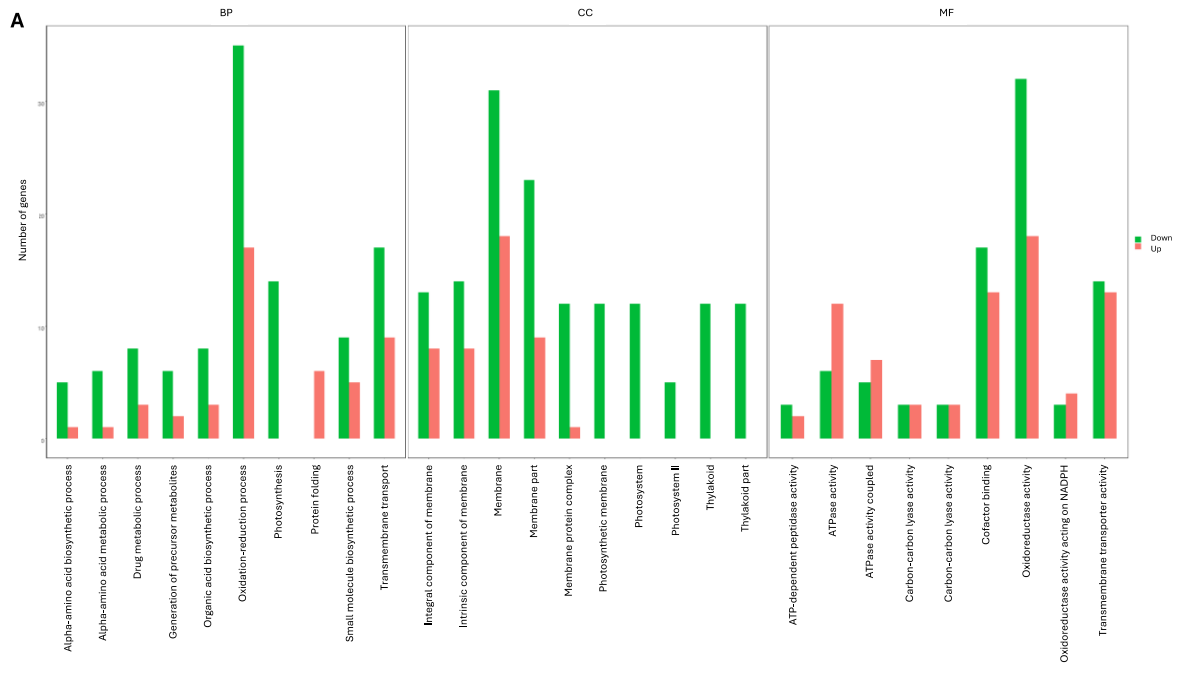
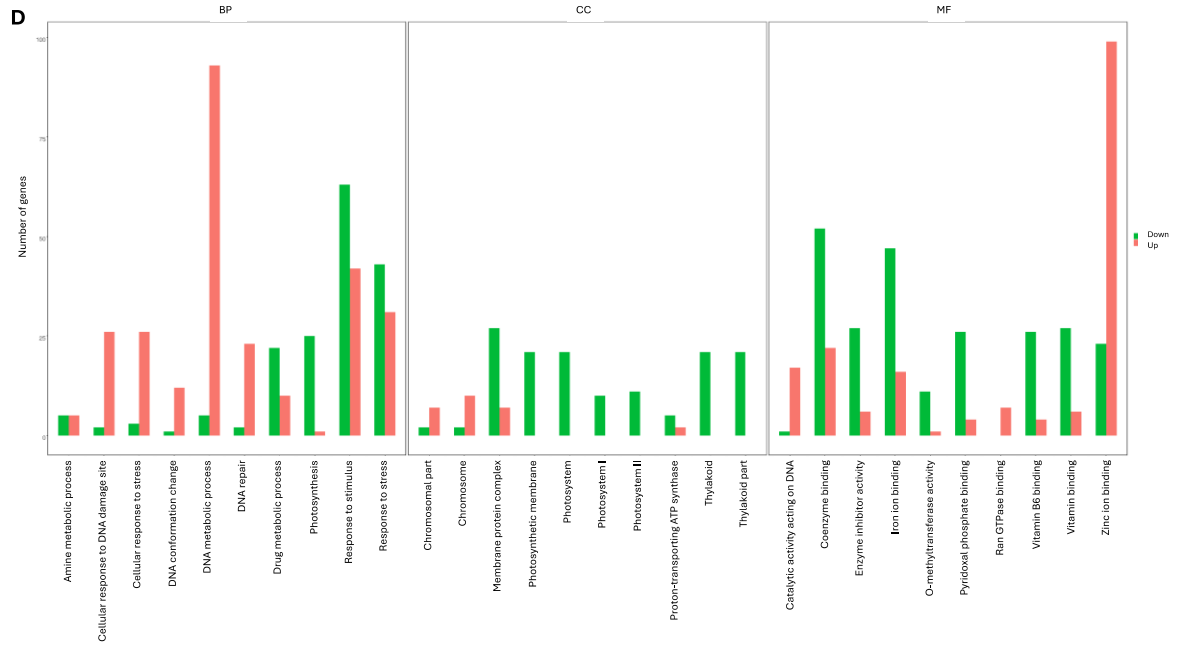
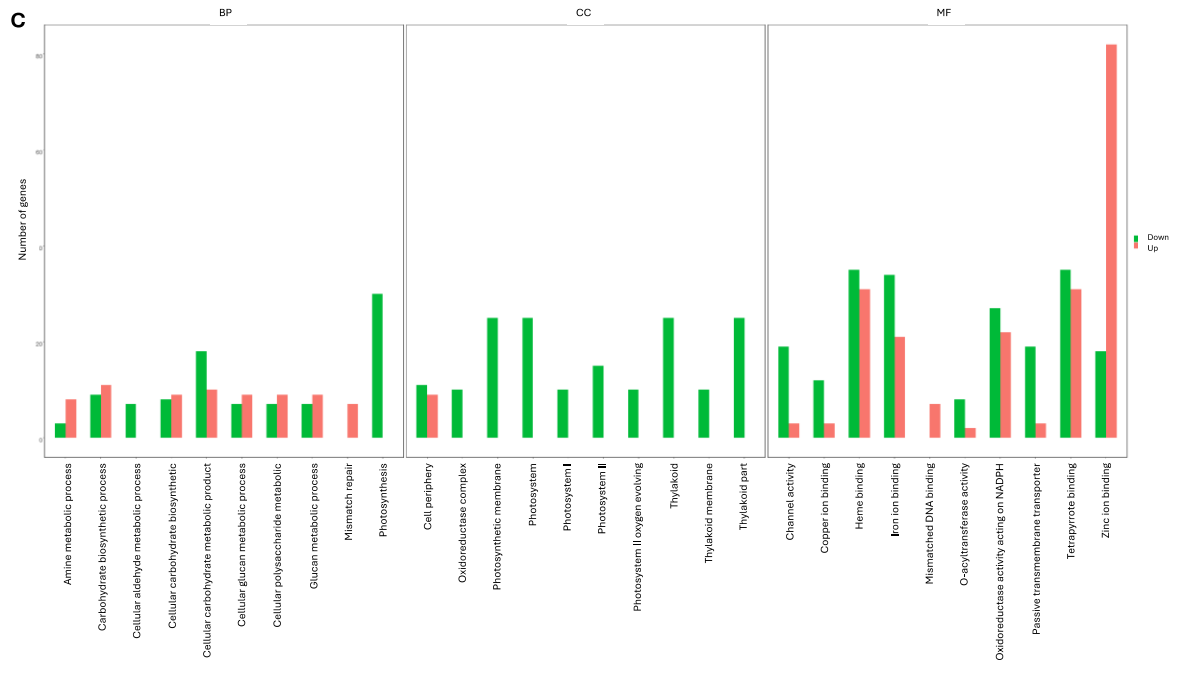


Figure 5.9. Enrichment analysis of GO terms for differentially expressed genes in five duckweed clones. Gene expression analysis was performed for five clones—Manor (A), 6861 (B), 7763 (C), 7796 (D), and 8703 (E)—comparing gene expression at 35°C (heat stress) with 20°C (control). Results are categorized by GO terms, with the x-axis displaying the GO term descriptions and the y-axis representing enrichment significance levels (-log10(padj)). Higher values on the y-axis indicate greater statistical significance. Bars are color-coded to distinguish GO categories: Biological Process (BP) in red, Cellular Component (CC) in green, and Molecular Function (MF) in blue. The number of DEGs associated with each GO term is indicated above the corresponding bar.





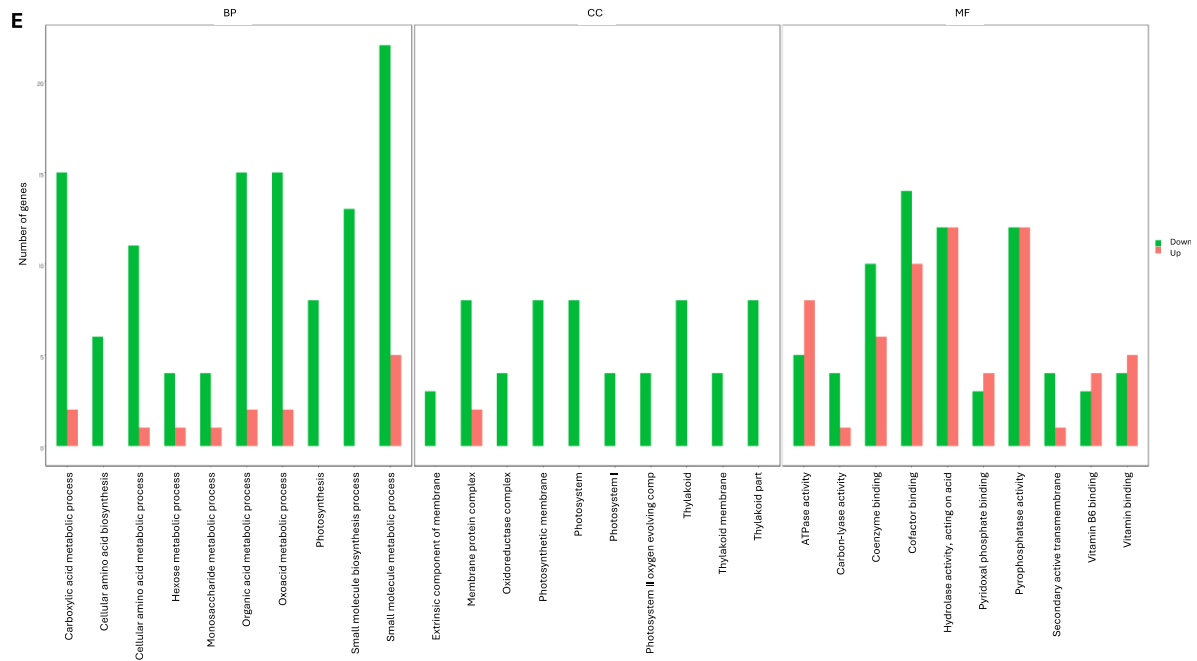


Figure 5.10. Classification of Differentially Expressed Genes (DEGs) by GO terms in five duckweed clones. Differential gene expression at 35°C (heat stress) versus 20°C (control) for five clones: Manor (A), 6861 (B), 7763 (C), 7796 (D), and 8703 (E). GO terms are categorized into Biological Process (BP), Cellular Component (CC), and Molecular Function (MF), displayed on the x-axis. Green bars representing down-regulated DEGs and red bars representing up-regulated DEGs. The y-axis shows the number of genes associated with each GO term for each clone.

5.3.7.2. Visualization with Directed Acyclic Graphs (DAGs)

The hierarchical relationships among enriched GO terms were explored using Directed Acyclic Graph (DAGs). DAGs provide a detailed visualization of enriched terms and their connections, where nodes represent GO terms, and branches indicate hierarchical relationships. Each DAG reflects one of the three GO categories: biological process, cellular component, and molecular function. The top five enriched terms were highlighted as main nodes, with darker shades representing higher enrichment levels.

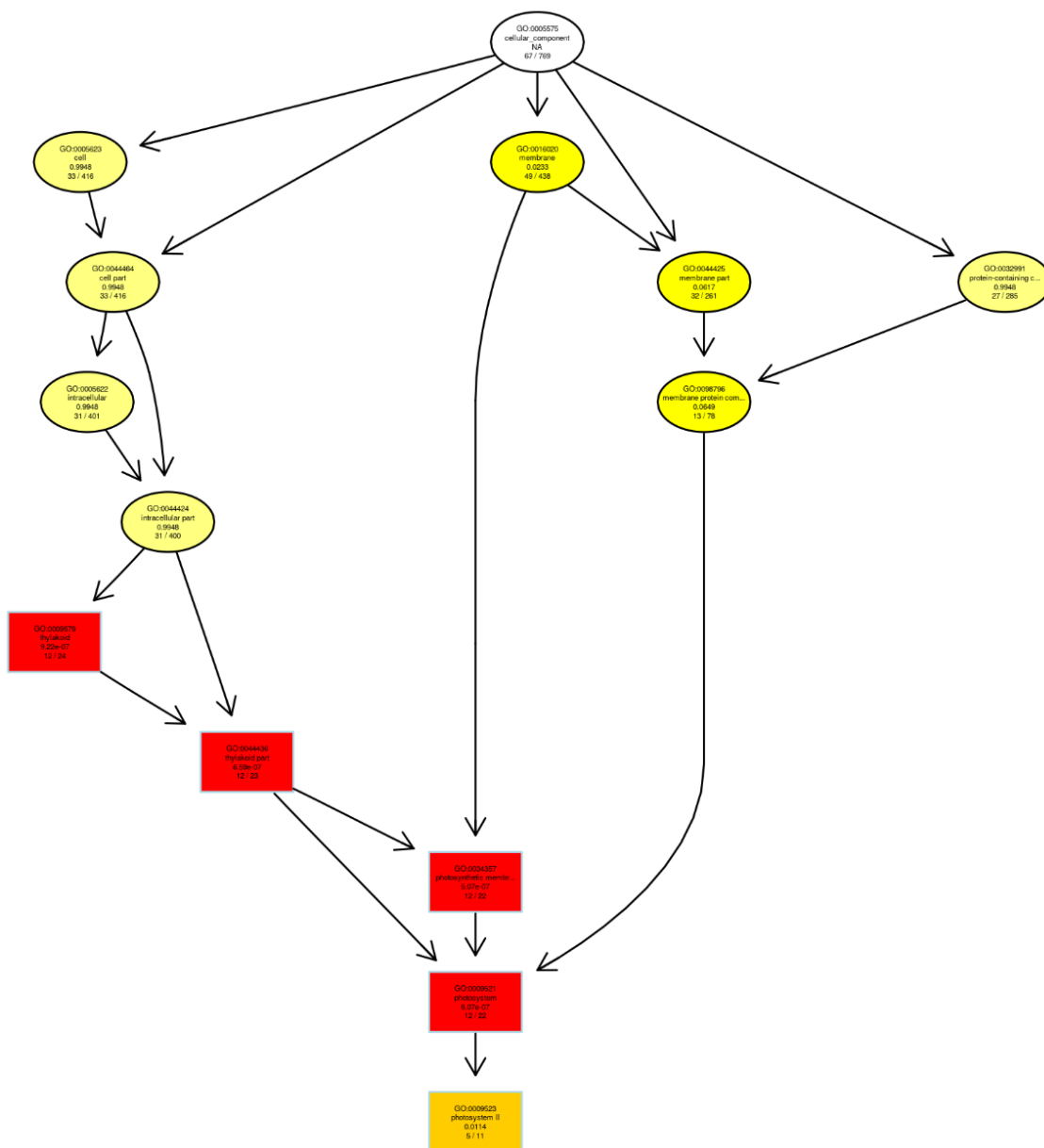
In the biological processes DAG, all clones showed notable enrichment in the GO:0015979 (photosynthesis), which aligns with the enrichment patterns shown in Figure 5.9, while photosystem-related terms displayed elevated enrichment scores. The Figure 5.10 illustrated a downregulation of DEGs associated with these processes under heat stress. This combination of enrichment and downregulation reflects the complex regulatory dynamics governing photosynthesis-related pathways during heat stress.

The cellular component DAG (Figure 5.11) emphasized significant enrichment in photosynthesis-related terms across all clones, including GO:0009579 (thylakoid), GO:0044436 (thylakoid part), GO:0034357 (photosynthetic membrane), and GO:0009521 (photosystem). Additionally, GO:0098796 (membrane protein complex) showed lower enrichment but maintained a close relationship with photosystem terms, indicating structural and functional links within the photosynthetic machinery.

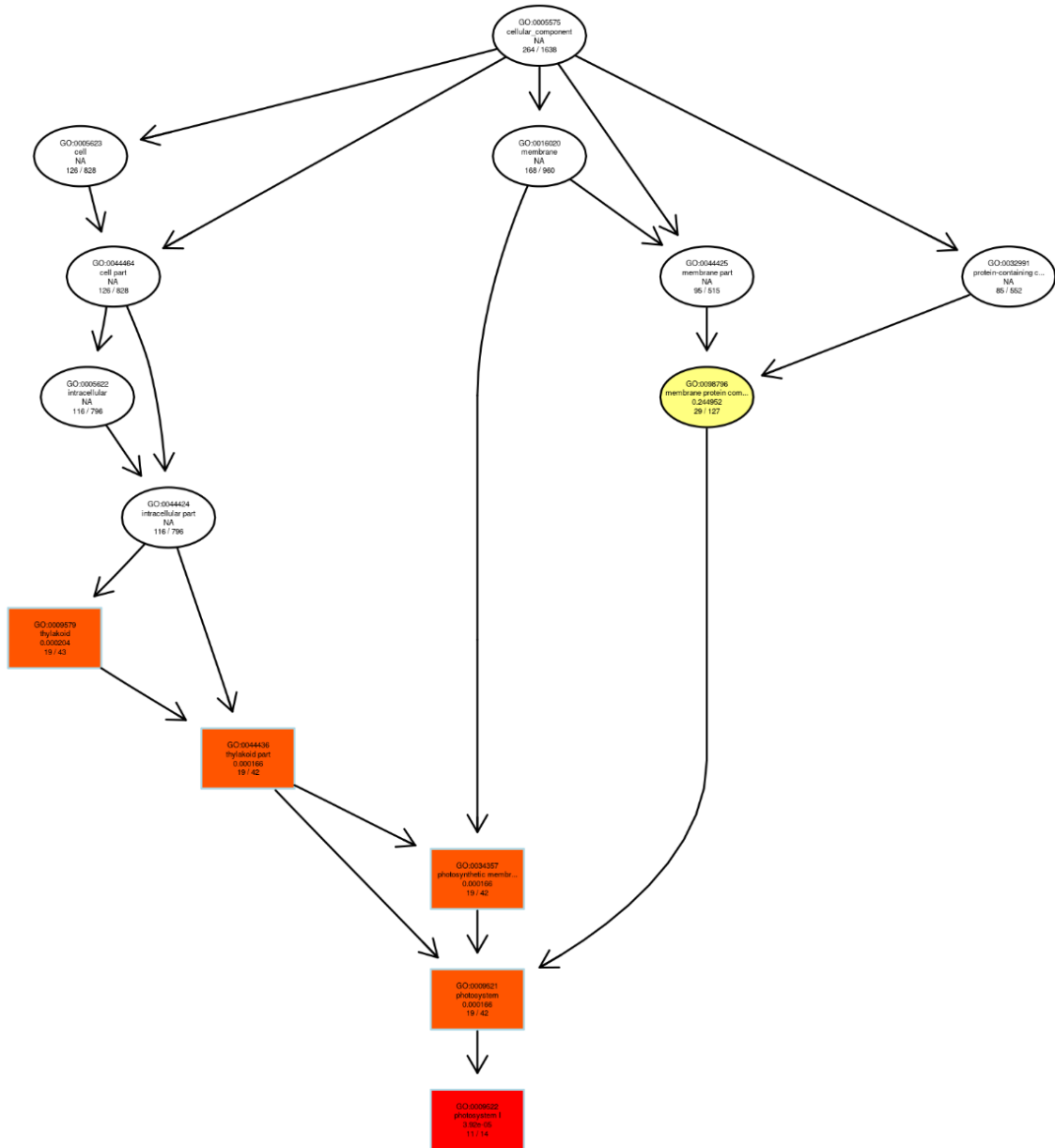
In the molecular function category, the DAG highlighted the upregulation of zinc ion binding (GO:0008270) in the heat-tolerant clones (6861, 7763, and 7796). This term was absent in the heat-sensitive (8703) and control (Manor) clones, reinforcing its potential role in thermotolerance. The DAGs also revealed connections to other metal ion binding functions, such as copper ion binding, further supporting the involvement of metal-associated pathways in the heat stress responses.

The functional analysis revealed distinct transcriptional strategies employed by duckweed clones to cope with heat stress. The enrichment of photosynthesis-related terms across biological processes and cellular components suggest that heat stress disrupts fundamental pathways related to energy production. The consistent downregulation of DEGs related to photosynthetic machinery across all clones highlights a universal stress response, albeit with varying intensity between heat-sensitive and heat-tolerant clones.

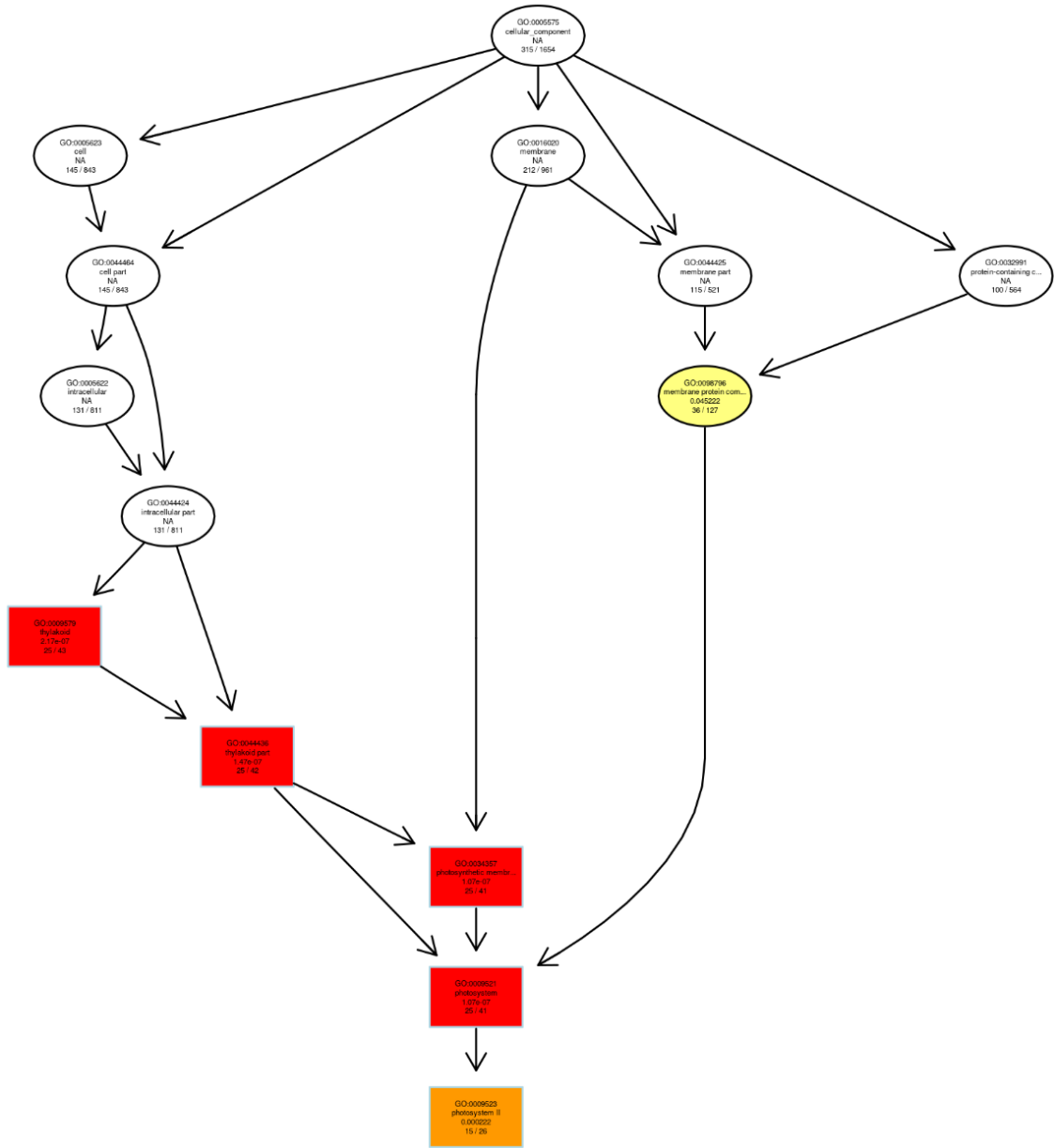
A



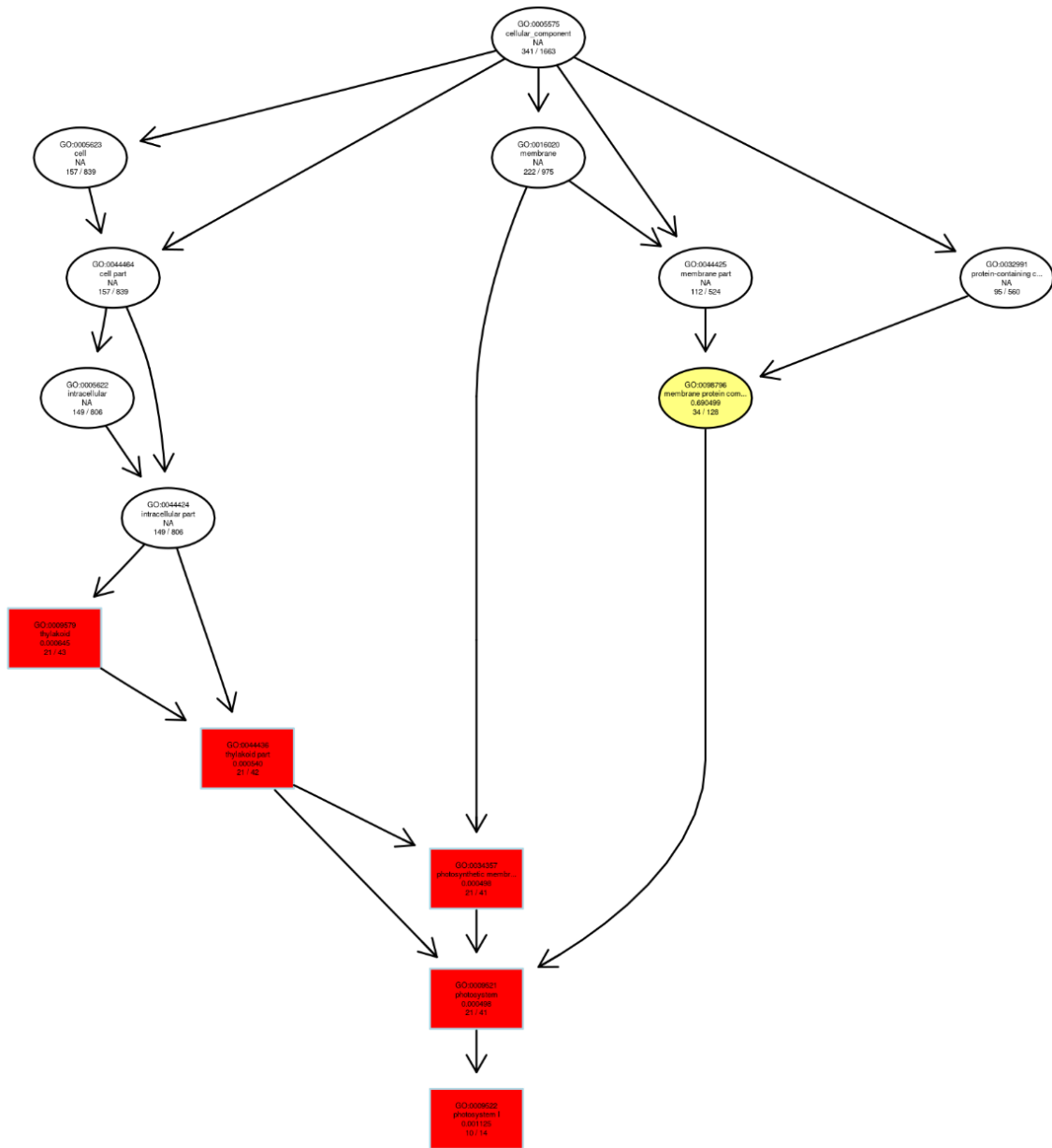
B



C



D



E

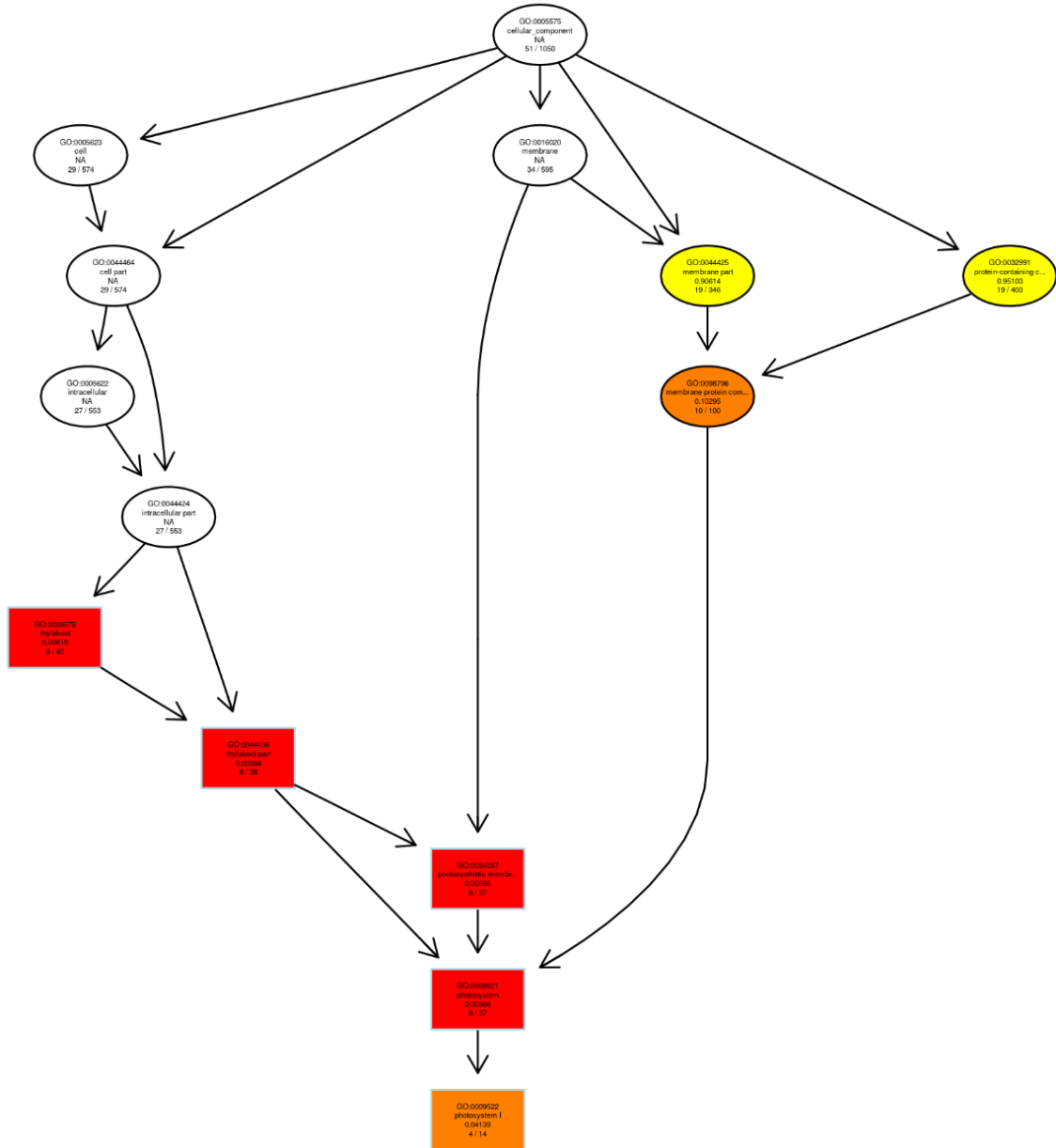


Figure 5.11. Directed Acyclic Graphs (DAGs) of cellular components for differentially expressed genes in duckweed clones. DAGs were generated for clones Manor (A), 6861 (B), 7763 (C), 7796 (D), and 8703 (E), showing the hierarchical relationships among cellular component GO terms. The top five enriched GO terms are highlighted as main nodes, with branches linking related terms. Colour intensity represents the degree of enrichment, with darker shades indicating higher enrichment levels.

5.3.7.3. KEGG Enrichment Analysis

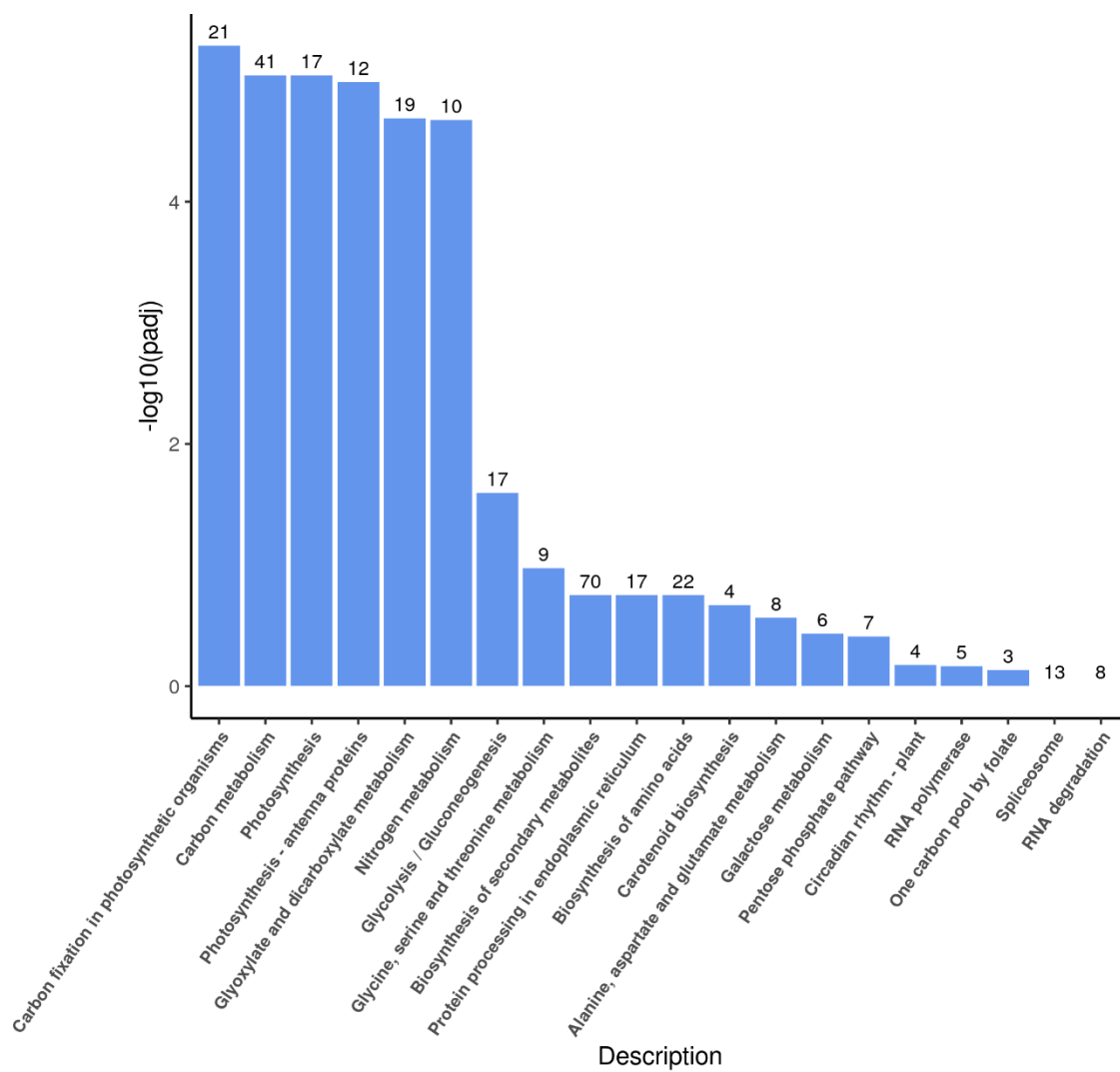
Biological functions often rely on interactions among multiple genes, which can be analysed through curated databases like KEGG (Kyoto Encyclopaedia of Genes and Genomes). KEGG provides detailed insights into metabolic pathways, signalling cascades, and disease associations (Kanehisa & Goto, 2000). By performing KEGG pathway enrichment analysis, biological processes most significantly associated with differentially expressed genes (DEGs), could be identified, using the entire genome as a reference background. Pathways with adjusted p-values (p_{adj}) below 0.05 were considered significantly enriched.

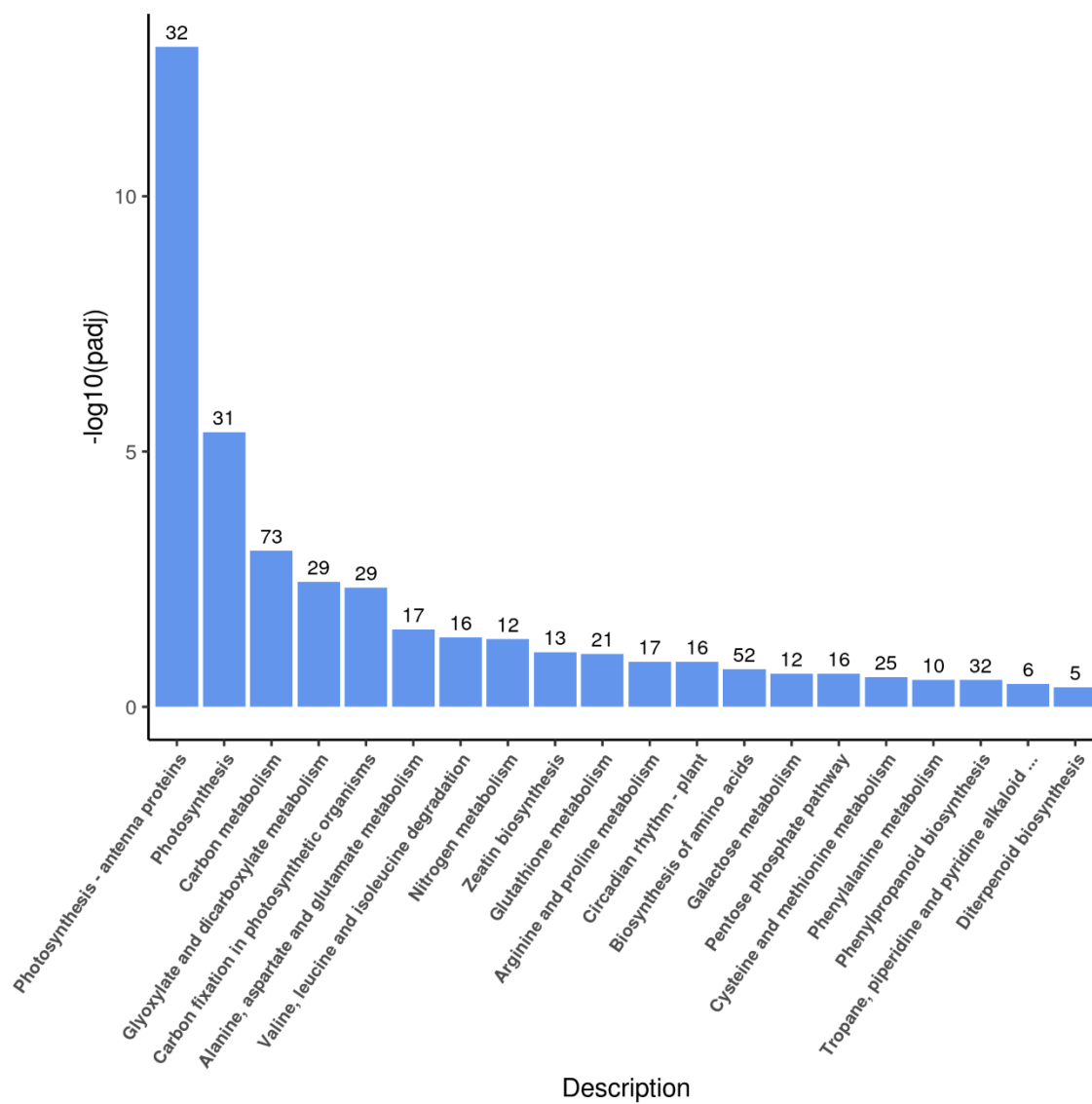
For this study, five *Lemna* clones were analysed by comparing gene expression profiles at 35°C (heat stress conditions) with those at 20°C. The 20 most significantly enriched KEGG pathways were selected for display, if less than 20 pathways were enriched, all significant pathways were included. The Figure 5.12 summarize these findings, where the x-axis lists the KEGG pathways, the y-axis reflects the enrichment significance level, and the number above each bar indicates the count of DEGs mapped to each pathway.

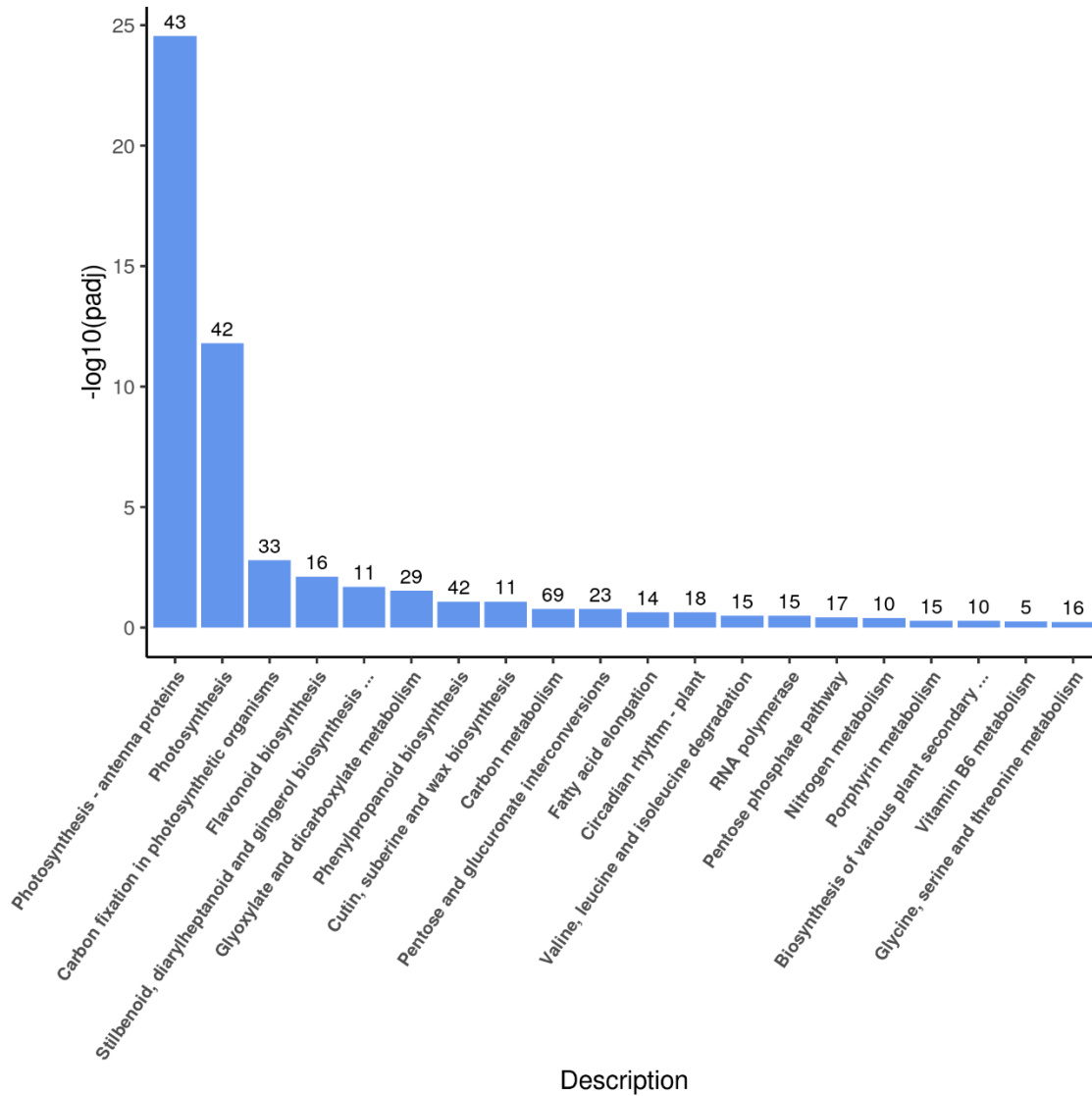
The KEGG enrichment analysis revealed pathways that were consistently enriched across all clones. Notably, pathways such as ath00710 (Carbon fixation in photosynthetic organisms), ath00196 (Photosynthesis - antenna proteins), ath00630 (Glyoxylate and dicarboxylate metabolism), and ath00195 (Photosynthesis) emerged as common features (Figure 5.12). These pathways highlight core metabolic processes integral to photosynthetic activity and energy production in *Lemna* under both control and heat-stressed conditions.

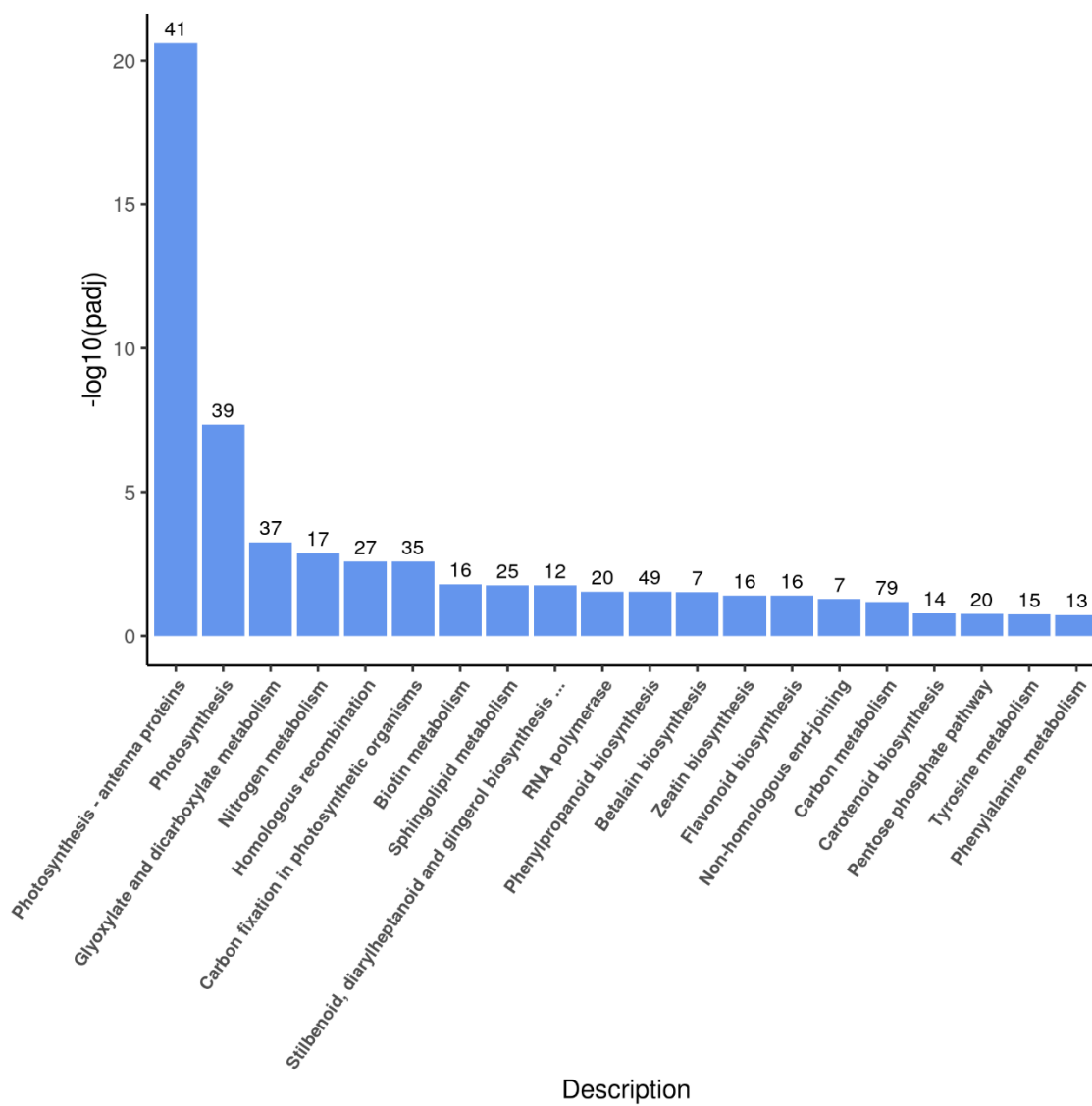
Interestingly, no single KEGG pathway was exclusively enriched in heat-tolerant, heat-sensitive, or control clones. This finding suggests that heat stress resistance, at least under the conditions analysed, does not correspond to specific KEGG-enriched pathways. Instead, the shared enrichment of photosynthesis and energy metabolism pathways across all clones suggest a general adaptive mechanism, possibly involving adjustments in basal metabolic processes rather than distinct stress-specific pathways.

A



B

C

D

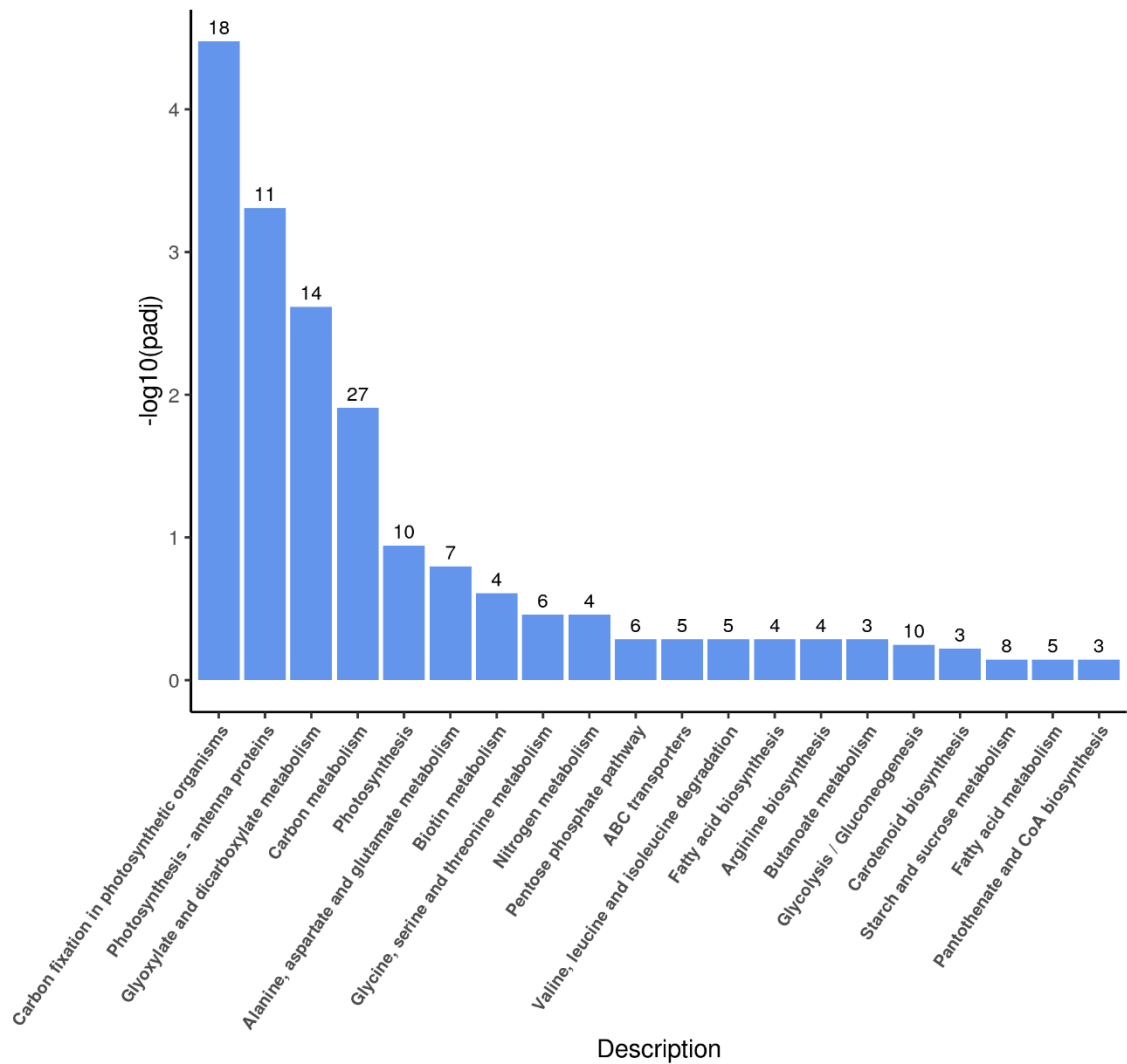
E

Figure 5.12. KEGG pathway enrichment analysis across clones under heat-stressed and control conditions. KEGG pathway enrichment analysis results for clones Manor (A), 6861 (B), 7763 (C), 7796 (D), and 8703 (E) grown at heat stress (35°C) compared to control (20°C) conditions. The x-axis represents the KEGG pathways with significant enrichment ($\text{padj} < 0.05$), and the y-axis indicates the enrichment significance level. Numbers displayed above each bar correspond to the count of differentially expressed genes (DEGs) associated with each KEGG pathway.

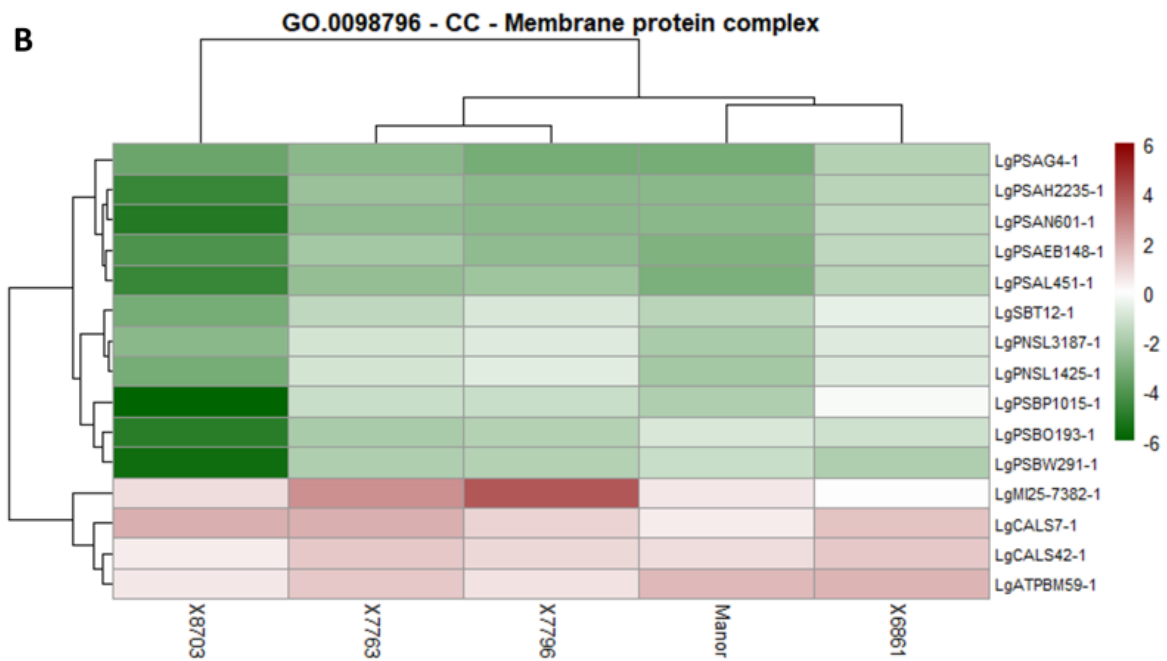
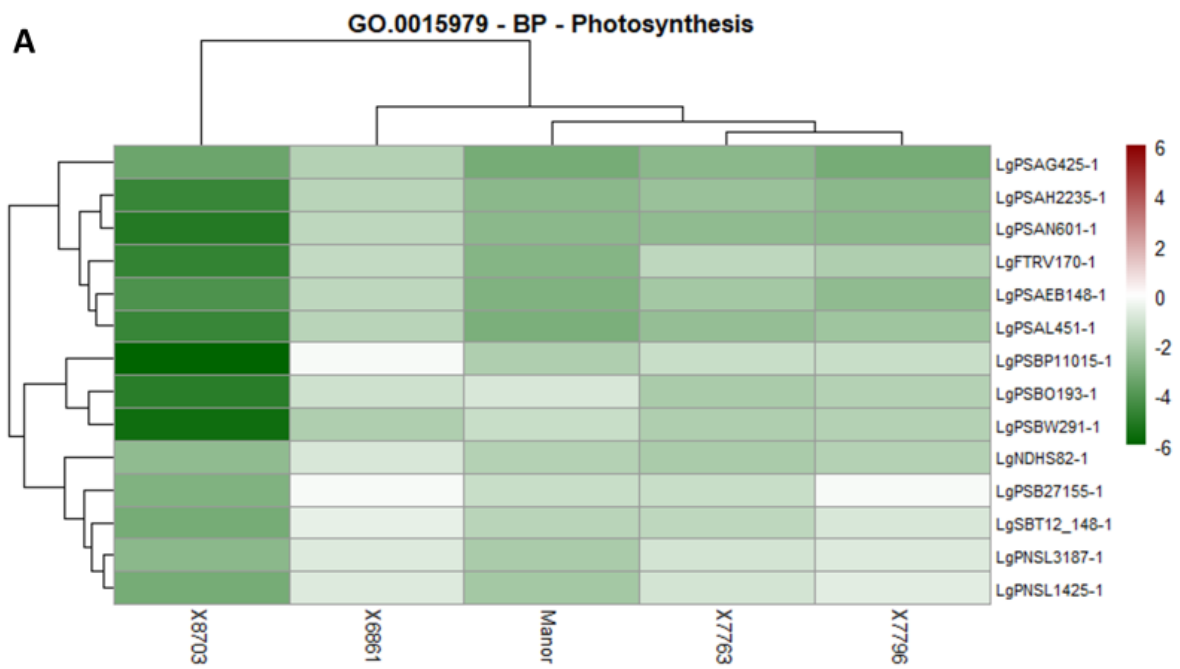
5.3.7.4. Selection and Cluster Analysis of Key Genes in GO and KEGG Pathways

Following GO and KEGG enrichment analyses, genes associated with specific pathways were identified and analysed to gain deeper insights into expression trends. The analysis focused on pathways and terms linked to photosynthesis, cellular components, and molecular functions, as well as metabolic pathways consistently enriched across clones. This approach enables us to explore potential relationships between gene expression profiles, treatment conditions, and heat tolerance.

In the GO analysis, genes associated with photosynthesis were prioritized. For Biological Processes (BP), the term GO:0015979 – photosynthesis was analysed (Figure 5.13(A)), revealing that the heat-sensitive clone (8703) consistently displayed lower expression levels across 14 photosynthesis-related genes compared to the other clones. This suggests a compromised ability to maintain photosynthetic activity under heat stress in the heat-sensitive clone.

Within Cellular Components (CC), terms related to photosynthesis including GO:0009579 (thylakoid), GO:0044436 (thylakoid part), GO:0034357 (photosynthetic membrane), and GO:0009521 (photosystem) were examined. These terms showed expression trends like those observed for GO:0015979 in the BP category, with uniformly lower expression in the heat-sensitive clone. However, GO:0098796 (Membrane protein complex) displayed distinct patterns of up- and down-regulation, with all clones following similar trends but varying by region, highlighting nuanced regulatory responses across clones (Figure 5.13(B)).

In the Molecular Functions (MF) category, GO:0008270 (Zinc ion binding) exhibited varying patterns of up- and down-regulation (Figure 5.13(C)). Four genes (LgPPR_40-1, LgPPR_568-1, LgUBP14_35-1, and LgGTF2H2_857-1) were consistently downregulated in the heat-sensitive clone but upregulated in the heat-tolerant clones, suggesting a correlation between zinc ion binding gene expression and heat tolerance. This finding suggests the potential role of zinc-binding proteins in managing stress-induced oxidative damage, particularly in heat-tolerant clones.



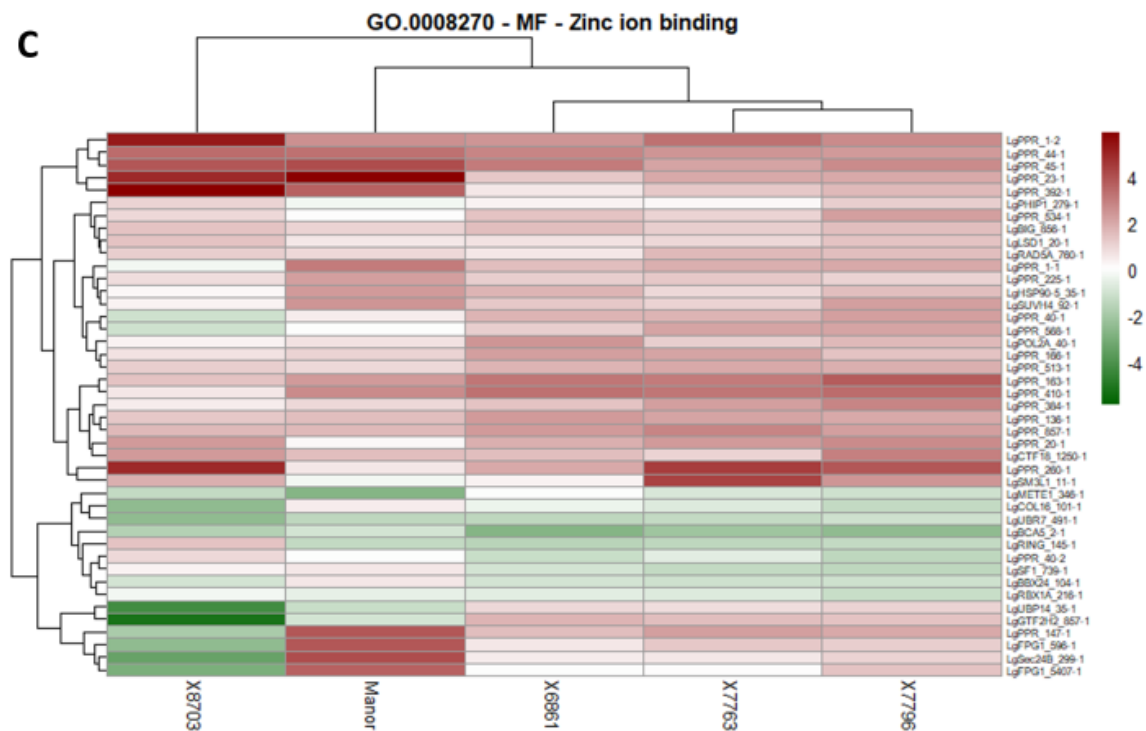
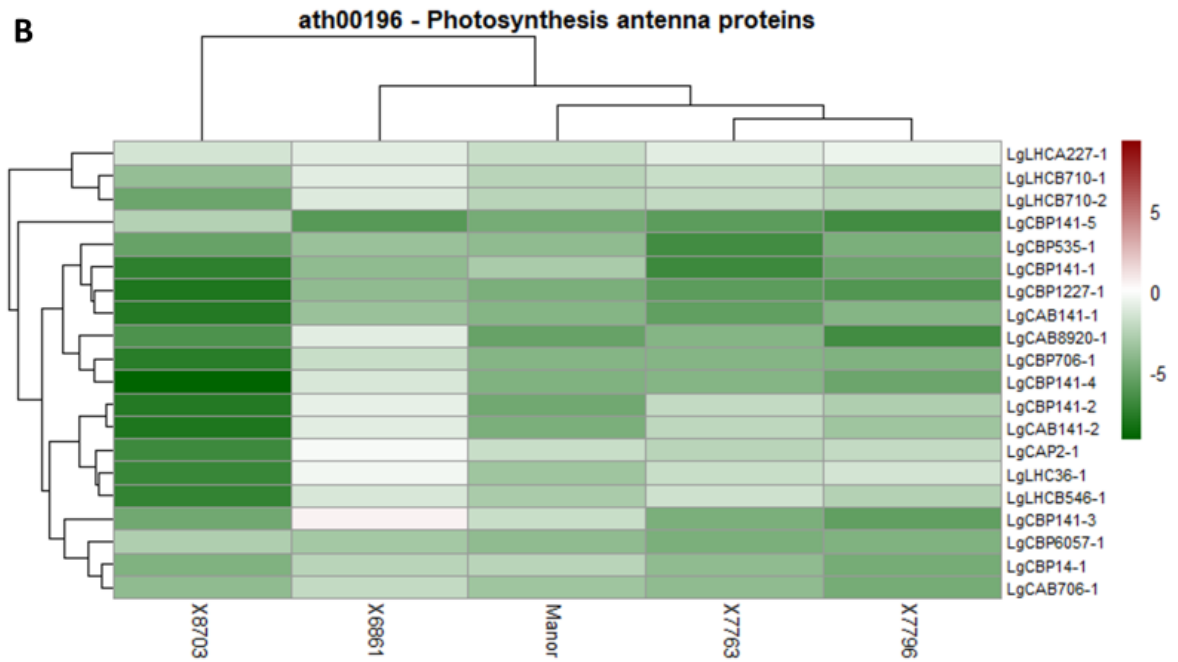
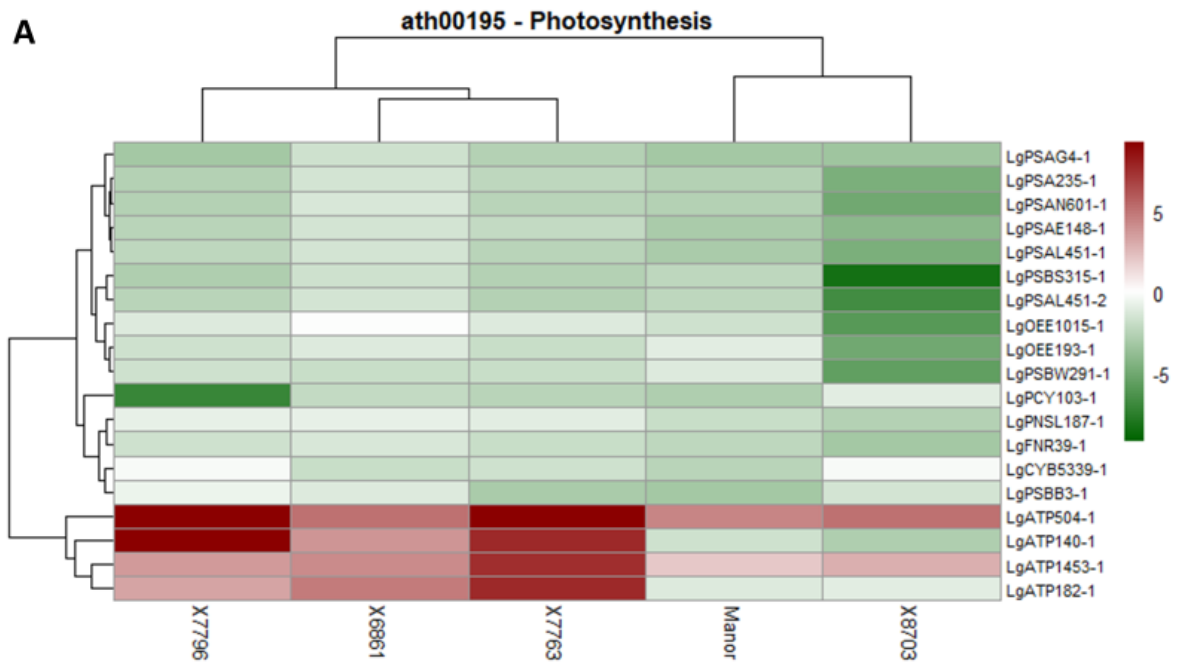


Figure 5.13. Cluster analysis of gene expression patterns for selected GO terms across five clones. Cluster analysis results for (A) GO:0015979 (Biological Process: Photosynthesis), (B) GO:0098796 (Cellular Component: Membrane Protein Complex), and (C) GO:0008270 (Molecular Function: Zinc Ion Binding). The x-axis represents the five clones (Manor, 6861, 7763, 7796, and 8703), while the y-axis lists the genes associated with each GO term. The upregulated genes highlighted in red and downregulated genes highlighted in green.

The KEGG analysis focused on pathways consistently overexpressed across clones. Pathways identified included ath00710 (Carbon fixation in photosynthetic organisms), ath00196 (Photosynthesis antenna proteins), ath00630 (Glyoxylate and dicarboxylate metabolism), and ath00195 (Photosynthesis) (Figure 5.14).

KEGG pathways predominantly exhibited downregulation across all clones under heat stress, with no distinct trend differentiating heat-tolerant from heat-sensitive clones. However, certain exceptions were noted. Within ath00195 – Photosynthesis (Figure 5.14(A)), specific genes (LgATP140-1 and LgATP182-1) displayed upregulation in heat-tolerant clones, contrasting with their downregulation in heat-sensitive and control clones. These observations suggest that these genes may play a role in conferring heat stress resistance, potentially through mechanisms such as enhanced photosynthetic efficiency or repair processes under stress conditions.

These findings will help to elucidate their potential contributions to heat stress resistance and provide a foundation for future investigations into the molecular mechanisms underlying thermal adaptation in *Lemna*.



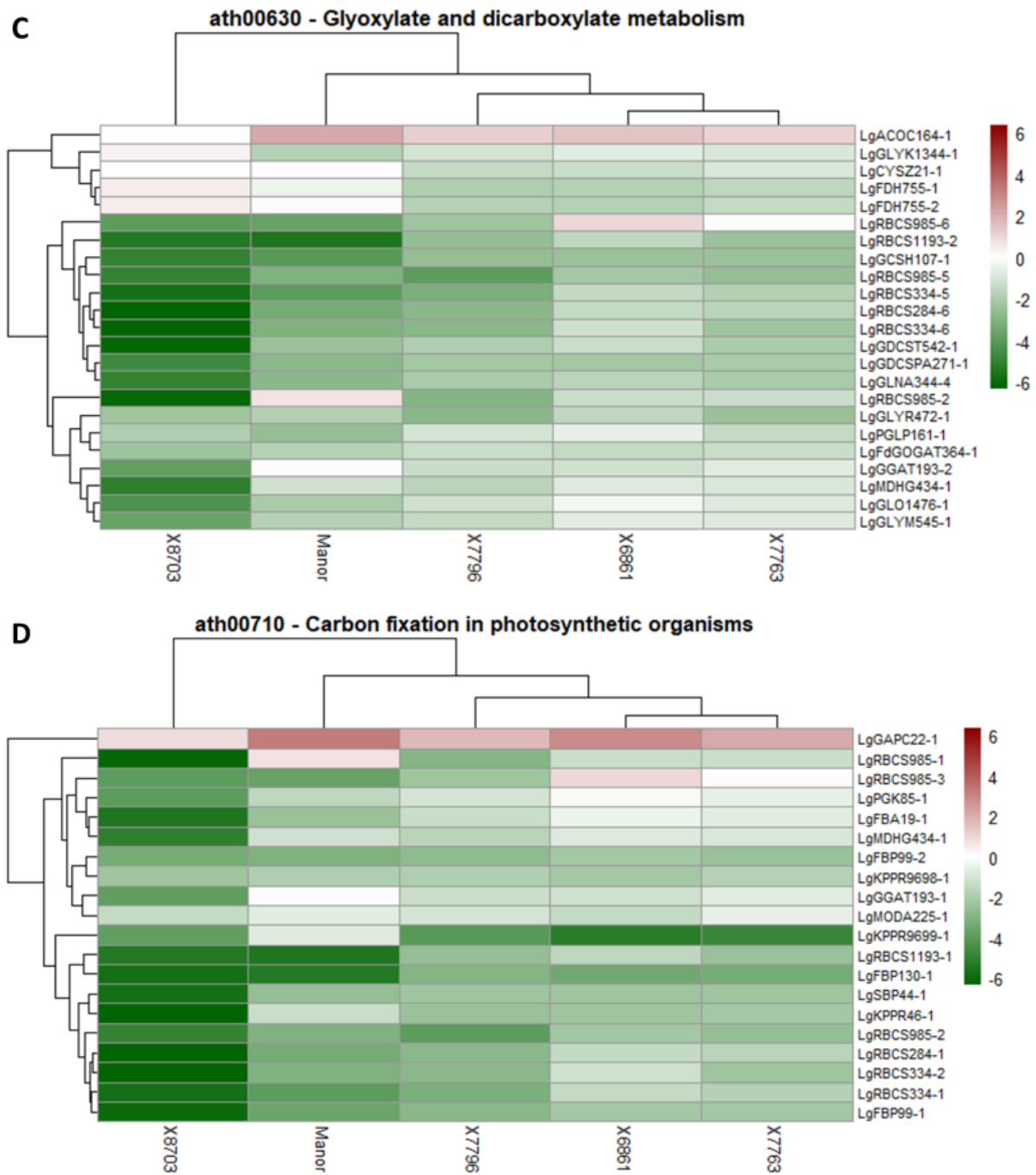


Figure 5.14. Cluster analysis of gene expression patterns for selected KEGG pathways across clones. Clustering results for (A) ath00195 – Photosynthesis, (B) ath00196 – Photosynthesis Antenna Proteins, (C) ath00630 – Glyoxylate and Dicarboxylate Metabolism, and (D) ath00710 – Carbon Fixation in Photosynthetic Organisms. The x-axis represents the analysed clones (Manor, 6861, 7763, 7796, and 8703), and the y-axis lists the genes associated with each KEGG pathway. Upregulated genes are shown in red, while downregulated genes are shown in green.

5.3.8. Identification and Annotation of Key Genes Associated with Heat Resistance

After analysing the gene expression profiles within the KEGG and GO pathways, we identified a set of genes that show potential involvement in heat resistance. For clarity and ease of reference, we have assigned simplified labels to these genes. Table 5.5 shows the original gene IDs, their assigned simplified labels, and descriptions. The simplified labels were used in subsequent analyses and discussion.

Genes LgATP140-1 and LgATP182-1, found in the ath00195 photosynthesis KEGG pathway, are described as ATP synthase protein YMF19 from *Helianthus annuus*. Enhanced ATP production can be critical under heat stress, as plants require increased energy to maintain cellular homeostasis. Additionally, genes LgPPR_40-1, LgPPR_568-1, LgUBP14_35-1, and LgGTF2H2_857-1, associated with GO:0008270 – zinc ion binding, are described as pentatricopeptide repeat proteins At2g27610 from *Arabidopsis thaliana* (LgPPR_40-1 and LgPPR_568-1), ubiquitin carboxyl-terminal hydrolase 14 from *Arabidopsis thaliana* (LgUBP14_35-1), and general transcription factor IIH subunit 2 from *Arabidopsis thaliana* (LgGTF2H2_857-1). These proteins often play roles in stabilizing cellular structures and supporting stress responses. They may serve protective functions, helping to preserve cellular integrity under high temperatures.

These findings provide a basis for further exploration of the roles these genes play in heat tolerance. Understanding how each gene contributes to cellular stability and function under stress can help us interpret the adaptive strategies employed by heat-tolerant clones.

Table 5.5. Key genes associated with heat resistance identified in KEGG and GO pathway analyses.

Label	Original Gene ID	Pathway	Description
<i>LgATP140-1</i>	maker-scf140-pred_gff_GlimmerHMM-gene-2.38	ath00195	ATP synthase protein YMF19 from <i>Helianthus annuus</i>
<i>LgATP182-1</i>	maker-scf182-pred_gff_GlimmerHMM-gene-1.18	ath00195	ATP synthase protein YMF19 from <i>Helianthus annuus</i>
<i>LgPPR_40-1</i>	augustus_masked-scf40-processed-gene-1.13	GO:0008270	Pentatricopeptide repeat protein At2g27610, <i>Arabidopsis thaliana</i>
<i>LgPPR_568-1</i>	maker-scf568-augustus-gene-0.90	GO:0008270	Pentatricopeptide repeat protein At4g02750, <i>Arabidopsis thaliana</i>
<i>LgUBP14_35-1</i>	maker-scf35-snap-gene-1.59	GO:0008270	Ubiquitin carboxyl-terminal hydrolase 14, <i>Arabidopsis thaliana</i>
<i>LgGTF2H2_857-1</i>	maker-scf857-pred_gff_GlimmerHMM-gene-0.34	GO:0008270	General transcription factor IIH subunit 2, <i>Arabidopsis thaliana</i>

5.4. Discussion

This chapter provides significant insights into the genetic and molecular responses of *Lemna gibba* clones to heat stress, focusing on the intricate relationships between genetic variability, molecular mechanisms, and phenotypic traits. A key observation was the substantial genetic variability among the clones, as evidenced by differences in mapping results against the reference *Lemna gibba* genome (Evan Ernst et al., 2023). Heat-sensitive and control clones consistently exhibited lower mapping scores compared to heat-tolerant clones, suggesting distinct genetic architectures that may underlie thermotolerance. This genetic variation offers a foundational explanation for the differential responses of the clones to elevated temperatures, emphasizing that inherent genetic differences are pivotal to the ability of certain clones to thrive under heat stress. These findings align genetic distinctions with observed phenotypic thermotolerance, creating a robust framework for understanding the adaptive mechanisms of heat stress resilience in *Lemna gibba*.

The molecular response data combined with the physiological data presented in Chapter 3 and Chapter 4 suggest a clear interplay between molecular and phenotypic thermotolerance. Heat-tolerant clones selected based on their capacity to maintain stable protein content across a range of temperatures (15, 20, 25, 30, and 35°C), consistently demonstrated molecular adaptations to heat stress supporting their stability at increased temperature. For example, although growth rates declined under heat stress across all clones, heat-tolerant clones exhibited less pronounced declines compared to heat-sensitive and control clones. This pattern suggests that molecular mechanisms in heat-tolerant clones mitigate the detrimental effects of heat stress, allowing for better maintenance of physiological processes. Collectively, these findings highlight the integrative role of genetic, molecular, and physiological factors in thriving heat resilience in *L. gibba*.

Overall, the hierarchical clustering heatmap of Differentially Expressed Genes (DEGS) in heat-sensitive and heat-tolerant duckweed clones (Figure 5.8) provided valuable insights into the transcriptional dynamics of *Lemna* clones under heat stress and control conditions. The clear separation of heat-tolerant clones from heat-sensitive clones, coupled with the identification of temperature-specific sub-clustering, emphasizes the high impact of heat stress on gene expression. Despite the anomaly of the S60 sample, the clustering analysis remained consistent and robust, capturing key trends in the data. Besides, the identification of gene clusters with opposing expression patterns between heat-tolerant and heat-sensitive clones highlights potential targets for further investigation into the molecular mechanisms underlying heat tolerance. These findings contribute to an improved understanding of the transcriptional responses of *Lemna* clones to heat stress, offering a foundation for exploring adaptive mechanisms and identifying genetic markers for thermotolerance.

This study identified key molecular pathways critical to thermotolerance, with photosynthesis and zinc ion binding standing out as particularly significant. Photosynthetic pathways are essential for maintaining energy production and repair mechanisms during heat stress. Heat-tolerant clones demonstrated a stronger transcriptional response in photosynthesis-related genes, aligning with studies in other plants where the preservation of photosynthetic efficiency is linked to stress resilience (Lou *et al.*, 2018; Yue *et al.*, 2023). Additionally, zinc ion-binding proteins were significantly upregulated in heat-tolerant clones, suggesting a protective role in stabilizing cellular components and regulating genes involved in oxidative stress responses. These mechanisms enhance protein stability and mitigate oxidative damage, reflecting broader strategies that enable heat-tolerant clones to sustain cellular homeostasis and functional integrity under stress (Han *et al.*, 2020, 2021).

Results of this study suggest that photosynthesis and zinc ion binding may play an important role in plant survival under changing climates since they are identified as key heat stress related pathways. Previous study showed that photosynthesis, vital for energy production, is particularly sensitive to stresses like heat and drought, which disrupt crucial processes like photosystems activity and ATP generation (Nouri *et al.*, 2015). To cope with these stresses, plants adjust gene expression quickly, both in chloroplast and nuclear gene expression (Nouri *et al.*, 2015). Zinc also stabilizes proteins and activates stress-responsive mechanisms through zinc-finger proteins, which regulate genes involved in tolerance against salinity, drought, and oxidative stress (Han *et al.*, 2020, 2021; Kiełbowicz-Matuk, 2012). These molecular responses are essential for plant resilience under stress, providing valuable insights into enhancing crop adaptation to climate change.

Results of this study agree with previous study that zinc ion-binding proteins play essential roles in stress adaptation by maintaining cellular homeostasis and regulating gene expression (Han *et al.*, 2021). Pentatricopeptide repeat proteins (PPRs), for example, stabilize RNA molecules in chloroplasts and mitochondria, ensuring proper translation and efficient cellular function under stress conditions (Han *et al.*, 2020, 2021). Ubiquitin carboxyl-terminal hydrolases (UCHs) are critical in protein turnover, removing misfolded proteins to prevent cellular damage during abiotic stresses like salinity and drought (Parlak & Yilmaz, 2012; Zschiesche *et al.*, 2015). Additionally, the General Transcription Factor IIH (TFIIH) subunit 2 plays a pivotal role in activating genes necessary for environmental adaptation, enabling the synthesis of proteins required for survival under adverse conditions (Kiełbowicz-Matuk, 2012; Rom *et al.*, 2006). In *Arabidopsis thaliana* and related species, zinc-binding proteins are critical regulators of abiotic stress responses, influencing pathways involved in salinity tolerance and oxidative stress mitigation (Han *et al.*, 2020; Kiełbowicz-Matuk, 2012). However, aquatic plants as *L. gibba* exhibit unique strategies for managing zinc-induced oxidative stress, including highly efficient antioxidant systems involving enzymes such as catalase (CAT) and superoxide dismutase (SOD). These

adaptations help protect the photosynthetic machinery from oxidative damage, a feature that distinguishes them from terrestrial plants (Parlak & Yilmaz, 2012).

Studying non-model species such as *L. gibba*, researchers can uncover novel mechanisms of stress tolerance, potentially contributing to the development of crops with enhanced resilience to environmental challenges. These findings underscore the importance of exploring unique molecular adaptations in diverse plant systems to address global agricultural challenges posed by climate change.

The upregulation of ATP synthase-related genes in heat-tolerant *Lemna* clones observed in this study underscores the critical role of ATP synthase-related proteins in thermotolerance. By facilitating ATP production during photophosphorylation, a process highly sensitive to elevated temperatures, these proteins enable energy-intensive repair mechanisms, ensuring that the photosynthetic machinery remains operational under heat stress. These findings align with previous studies highlighting the significance of ATP synthase in maintaining photosynthetic efficiency under thermal stress. For instance, in *Arabidopsis thaliana*, the FtsH11 protein regulates ATP synthase assembly by degrading the assembly factor BFA3, stabilizing the proton gradient and preserving photosystem II activity during heat stress (Yue *et al.*, 2023). Similarly, mutations in ATP synthase subunits in *Synechococcus elongatus* have been shown to enhance ATP production and photosynthetic efficiency under stress conditions (Lou *et al.*, 2018).

Comparative studies further emphasize the universality of ATP synthase regulation in stress responses. In *Arabidopsis*, disruptions in mitochondrial ATP production due to the absence of UCP1 exacerbate oxidative stress and impair carbon assimilation (Sweetlove *et al.*, 2006). Conversely, introducing cyanobacterial ATP synthase proteins into *Arabidopsis* enhances ATP production, boosting growth and light-use efficiency (Tula *et al.*, 2020). These findings highlight the conserved role of ATP synthase in mitigating heat-induced damage across diverse taxa.

The consistent involvement of ATP synthase in thermotolerance observed in this study and others suggests its potential as a target for developing strategies to improve plant resilience to heat stress. Enhancing ATP synthase activity could serve as a broadly applicable approach to bolstering thermotolerance in crops, offering significant implications for agriculture in the context of climate change.

Results of this study suggest that the genetic variability across the duckweed clones plays a crucial role in shaping their responses to heat stress. Clones exhibiting heat tolerance showed distinct genetic profiles from heat sensitive clones in their transcriptomic data. This variability indicates that genetic

factors play a significant role in the ability of certain clones to withstand elevated temperatures, shedding light on the mechanisms driving their heat resilience. In heat-tolerant clones, transcriptomic analyses revealed the upregulation of genes involved in photosynthesis and stress-related pathways. These pathways help regulate energy production and protect cellular structures, enabling the clones to maintain homeostasis under stress conditions. This highlights the importance of genetic composition in determining the adaptive capacity of these clones.

Additionally, the genetic differences observed may reflect adaptation to environmental pressures over time. These heat tolerant clones may possess an evolutionary potential to survive and thrive under challenging climate conditions. Understanding such adaptative mechanism can inform future studies on plant adaptation and guide efforts to develop thermotolerant crops, which is particularly relevant in the context of climate change.

The limitation of this study was the relatively low mapping results for heat-sensitive and control clones. This restricted the analysis to genes shared across all clones, potentially overlooking unique genetic mechanisms present in these clones. Future studies should employ de novo transcriptome assembly to uncover diverse and clone-specific responses to heat stress. This approach would provide a more comprehensive understanding of the genetic landscape and identify previously undetected pathways contributing to thermotolerance.

Functional validation of these identified genes is also needed to confirm their roles in heat stress adaptation. Techniques such as qPCR can assess gene expression levels under various conditions, while CRISPR-Cas9 gene editing could directly test the roles of specific genes in thermotolerance. These advanced methods will strengthen the findings of this study and pave the way for developing thermotolerant crops with enhanced resilience to climate change.

The study highlights the critical roles of genes encoding ATP synthase and zinc ion-binding proteins in maintaining photosynthetic efficiency and cellular stability under high temperatures. These findings enhance our understanding of thermotolerance in *L. gibba* and provide a basis for exploring similar mechanisms in other plant species.

Results of this study have practical applications in agriculture by informing the development of heat-tolerant crop varieties through marker-assisted breeding or transgenic methods. The molecular adaptations identified in *L. gibba* can be used for improving agricultural practices and enhancing crop resilience to climate change, which have potential to improve food security by increasing productivity in extreme environmental conditions.

By integrating genetic, molecular, and physiological data, this study offers a comprehensive view of the mechanisms underlying heat tolerance in *L. gibba*. It also underscores the importance of further research to address current limitations, explore additional pathways, and translate these findings into practical solutions for agriculture.

6. Chapter 6: General Discussion

The primary aim of this project was to investigate the effects of nitrogen availability and temperature on growth and protein content of duckweed, for optimizing its use as a sustainable protein source for both human and animal consumption. To achieve this, firstly the impact of different nitrogen sources on growth rate, protein content, nitrate accumulation, and nitrogen assimilation gene expression in *Lemna minor* and *Lemna gibba* was assessed (Chapter 3). Secondly, heat-tolerant and heat-sensitive clones were identified by evaluating physiological traits such as biomass, chlorophyll content, total nitrogen, total protein, and nitrate accumulation under control (20°C) and heat stress (35°C) conditions (Chapter 4). Finally, differential gene expression, alongside changes in protein content and growth rate, was analysed in five selected clones under both control (20°C) and heat stress (35°C) conditions using transcriptomics (Chapter 5). The findings from these experiments and their implications for improving duckweed productivity and its resilience to environmental stresses were discussed in the following three areas.

6.1. Impacts of Different Nitrogen Sources on Growth Rate, Protein Content, and Gene Expression of Genes Involved in Nitrogen Assimilation in Different Duckweed Clones

The effects of four nitrogen sources (Nitrate, Nil Nitrogen, Ammonium-Nitrate, and Urea-Nitrate) on growth and nitrogen metabolism in four duckweed clones (three *Lemna minor* SD, DG4, DG8 and one *Lemna gibba* 7796) were investigated. The variations in relative growth rate (RGR), protein content, nitrate accumulation, and the different patterns of expression of genes involved in nitrogen assimilation suggest that there are genetic and physiological diversity among those clones. The highest total nitrogen and protein content across different treatments in the clone 7796 suggest that this clone is superior in nitrogen use. These results align with previous findings highlighting the genetic diversity and assimilation efficiency in duckweed species (Barbosa Neto et al., 2019; Xu et al., 2023).

Growth responses to nitrogen sources differed among the clones. Clones SD and DG4 displayed strong growth under Nitrate treatments, emphasizing their reliance on nitrate as primary nitrogen source. In contrast, clone 7796 exhibited a preference for Urea-Nitrate, maintain high growth and protein content. Ammonium-Nitrate treatments, however, suppressed growth across some clones by day 7 due to medium acidification (Körner *et al.*, 2001). Notably, high protein content in the clone 7796 irrespective of treatment, underscore its metabolic efficiency, consistent with previous studies on effective nitrate assimilation in diverse plants (Zhou *et al.*, 2022). Variability in nitrate accumulation

patterns further supported the dynamic interplay between nitrogen source availability and metabolic pathways, with Urea-Nitrate treatments (Garnica *et al.*, 2010).

Comparative phylogenetics provided additional insights into the evolutionary dynamics of nitrogen assimilation genes. The alignment of *NiR* genes with monocot species suggests shared evolutionary origins, while *NR* genes clustered with dicots, reflecting divergent ecological adaptations (Zhou *et al.*, 2022). The absence of *GS1-3* in *Lemna* species, compensated by the dominance of *GS1-1* and *GS1-2*, suggests streamlined nitrogen use strategies that optimize the efficiency in aquatic environments.

Gene expression analysis reinforced these physiological observations. Clone 7796 exhibited significant upregulation of *NiR* and *GS* genes under Urea-Nitrate conditions, indicating its capacity to efficiently assimilate organic nitrogen. This aligns with findings in other aquatic species that favour similar nitrogen assimilation strategies (Azab & Soror, 2020). Conversely, the reduced expression of *NR* across all clones under Ammonium-Nitrate conditions indicates the decreased demand for nitrate reduction in the presence of ammonium, which is consistent with patterns reported in *Spirodela polyrhiza* (Zhou *et al.*, 2022). Furthermore, differential expression of *GS* isoforms revealed clone-specific strategies for ammonium assimilation. Clones SD and DG4 predominantly upregulated cytosolic *GS1-2* supporting ammonium assimilation under stress conditions. Interestingly, clone 7796 exhibited reduced *GS1-1* expression while maintaining high protein content, suggesting a reliance on alternative pathways for nitrogen assimilation and highlighting its robust adaptability to varied nitrogen conditions (Goodall *et al.*, 2013).

These findings underscore the agricultural and environmental potential of duckweed for targeted applications. Clones like SD, which have efficient nitrate uptake, hold promise for nutrient remediation projects in wastewater treatment, as they can actively remove excess nitrogen compounds from aquatic ecosystems. This ability supports duckweed's role in denitrification and phytoremediation, mitigating eutrophication risks and improving water quality.

From a food security perspective, high-protein clones such as 7796 could serve as sustainable feedstocks for animal and human consumption. With its superior nitrogen use efficiency and protein content, clone 7796 represents an ideal candidate for large-scale cultivation aimed at producing alternative protein sources, reducing dependency on conventional crops. This aligns with global efforts to enhance food sustainability by utilizing fast-growing, nutrient-efficient plants.

In the context of climate change, nitrogen assimilation efficiency plays a crucial role in plant resilience. As global temperatures rise, the ability of heat-tolerant duckweed clones to maintain efficient nitrogen metabolism becomes increasingly relevant. If clone 7796 exhibits robust nitrogen

assimilation even under elevated temperatures, it could be a key species in sustaining aquatic plant-based food systems in future climatic conditions. Looking ahead 20, 50, or even 100 years, climate models predict increased nitrogen deposition and temperature fluctuations, making the selection of resilient, high-protein duckweed strains a strategic approach to food and environmental security.

Genetic modification offers another avenue for optimizing duckweed's nitrogen use efficiency. Existing protocols for genetic transformation, such as *Agrobacterium*-mediated transformation and CRISPR-Cas9 genome editing, have been applied in *Lemna* species (Liu et al., 2019; Wang et al., 2021). Potential targets for future research include enhancing nitrogen assimilation gene expression to improve nitrogen assimilation. However, regulatory challenges remain a significant hurdle. Legislative frameworks governing genetically modified organisms (GMOs) vary across regions, and the acceptance of GM duckweed as a food source may face regulatory and consumer resistance.

The results of the Chapter 3 provide knowledge and materials for subsequent chapters to explore the relationships between nitrogen assimilation genes and environmental stress responses. For instance, Chapter 3 identified key nitrogen assimilation genes in duckweed, which were further analysed in Chapter 5. In Chapter 5, the transcriptomic analysis revealed significant differences in the expression of nitrogen assimilation genes across heat-tolerant and heat-sensitive clones grown at 20°C (control) and 35°C (heat stress). Heat-tolerant clones (6861, 7763 and 7796) exhibited distinct upregulation of GS1-1 indicating their enhance ability to assimilate nitrogen efficiently under stress (Figure 6.1). This pattern suggests that nitrogen metabolism plays a critical role in mitigating the impacts of heat stress, supporting higher protein content and growth rates despite unfavourable conditions. In contrast, heat-sensitive clones demonstrated widespread downregulation of nitrogen assimilation genes, underscoring their vulnerability to heat stress and highlighting the role of genetic variability in stress resilience.

Overall, these findings emphasize the importance of nitrogen source availability, genetic diversity, and gene expression dynamics in shaping duckweed growth and metabolic efficiency. Understanding these factors provides a foundation of future research and practical applications, particularly in optimizing duckweed systems for agricultural, environmental and bioeconomic purposes.

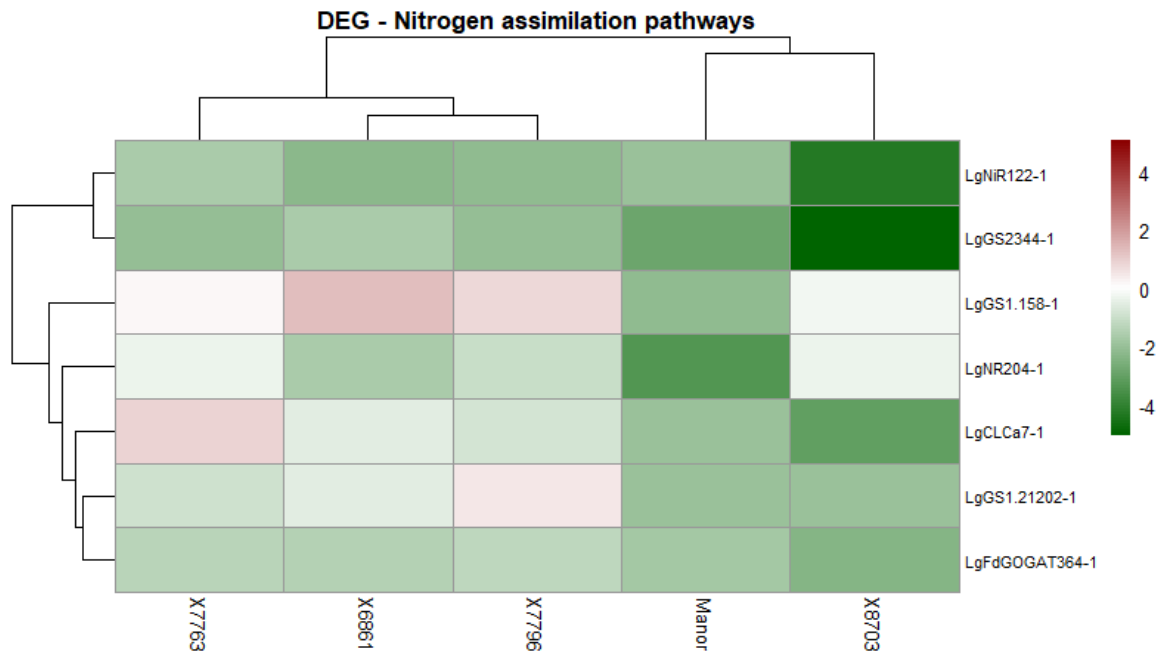


Figure 6.1. Cluster analysis of gene expression patterns for selected DEG in Nitrogen assimilation pathways. The x-axis represents the five clones (Manor, 6861, 7763, 7796, and 8703), while the y-axis lists the genes associated nitrogen assimilation genes. Gene expression levels are visualized with upregulated genes highlighted in red, indicating increased expression, and downregulated genes highlighted in green, indicating decreased expression.

6.2. Physiological Assessments on *Lemna* Growth Under Heat Stress

Specific *Lemna* clones exhibited greater heat tolerance were identified. It was hypothesized that distinct genotypes within *Lemna* species could exhibit variations in physiological responses to heat stress, a phenomenon widely reported in other plant species (Hu *et al.*, 2021; Z. Li *et al.*, 2021; Scafaro *et al.*, 2016). By testing 42 clones at control (20°C) and heat stress (35°C) conditions, heat-tolerant clones and heat-sensitive clones were identified. Specifically, clones 6861, 7763 and 7796 were identified as heat-tolerant, while clone 8703 as heat-sensitive.

The heat-sensitive clone 8703 exhibited significant reduction in protein content and relative growth rate (RGR) above 25°C, indicative of a compromised ability to withstand heat stress. This observation is consistent with previous studies showing protein denaturation and metabolic disruption under elevated temperature (Wahid *et al.*, 2007). Conversely, clones 6861, 7763, and 7796 maintained stable or slightly increased protein levels across the temperatures 15°C to 35°C. This suggests the presence of physiological mechanisms that preserve protein stability and cellular function under heat stress, potentially through the activation of protective pathways, such as heat shock protein response (Amano *et al.*, 2012; B. Huang & Xu, 2008).

Interestingly, the control clone Manor displayed growth trends similar to the clone 8703 at lower temperatures but maintained consistent growth rate at 35°C. This highlights the diversity of thermal responses within *Lemna*, underscoring the species' genetic variability and adaptability to changing environmental conditions (Strzałek & Kufel, 2021). The good growth rates of clones 6861, 7763, and 7796 under heat stress may be linked to enhanced protein synthesis, stabilization, and efficient cellular maintenance. Similar mechanisms have been reported in other plant species; for example, wild rice relies on proteins like Rubisco activase to maintain photosynthetic activity under heat stress (Bita & Gerats, 2013; Scafaro *et al.*, 2016).

The geographic origins of the clones did not show a good correlation with their thermal resilience, for example both Italian (6861, 7796) and UK (7763) clones exhibited robust heat tolerance. This finding underscores the genetic plasticity of *Lemna* and aligns with observations in other aquatic plants, such as *Potamogeton* species, where physiological traits often transcend geographic boundaries due to adaptive flexibility (Amano *et al.*, 2012). This genetic and physiological plasticity enables *Lemna* to thrive in diverse environmental conditions, offering significant potential for applications in agriculture and environmental management.

The global rise in temperature could increase the invasion potential of duckweed in different ecosystems since its optimal growth temperature is around 25°C. Additionally, its ability to grow in

flooded conditions makes it an attractive candidate for integration into rice paddies, providing potential benefits for sustainable agriculture. Furthermore, understanding the molecular mechanisms behind heat tolerance in these clones can contribute to the development of climate-resilient crops, reducing the negative impacts of heat stress on agricultural productivity.

The identification of heat-tolerant clones are valuable for addressing challenges posed by global warming, particularly in the context of sustainable biomass production, nutrient cycling, and water purification systems. The clones 6861, 7763, and 7796 maintained stable protein content and growth rates at elevated temperatures, they can be used to enhance productivity under heat-stress conditions, supporting the development of resilient agricultural and environmental systems.

6.3. Gene Expression Kinetics on *Lemna* Growth Under Heat Stress

The genetic and molecular responses of heat tolerant and heat sensitive *Lemna gibba* clones were investigated. The genetic variability among these clones was revealed by mapping results against the *Lemna gibba* reference genome (Ernst *et al.*, 2023), with heat-sensitive and control clones showing lower mapping scores compared to their heat-tolerant counterparts. These results suggest that heat-tolerant clones possess unique genetic traits that contribute to their ability to thrive under elevated temperatures. Such genetic variability and the observed phenotypic differences in heat-tolerant are essential for understanding the mechanisms driving heat tolerance. By integrating these genetic findings with physiological data, the molecular mechanisms underpinning physiological resilience under heat stress were revealed.

Crucial molecular pathways associated with thermotolerance were identified, particularly those related to photosynthesis and zinc ion binding. Heat-tolerant clones exhibited stronger transcriptional responses in photosynthesis-related genes, supporting the notion that maintaining photosynthetic efficiency is a cornerstone of thermotolerance (Lou *et al.*, 2018; Yue *et al.*, 2023). Efficient photosynthesis under stress ensures sustained energy production and carbon assimilation, which are vital for plant survival under elevated temperatures. Additionally, the upregulation of zinc ion-binding proteins in heat-tolerant clones suggests their role in stabilizing cellular components and regulating oxidative stress responses. Zinc-binding proteins are known to mitigate oxidative damage by maintaining cellular homeostasis, a mechanism consistent with findings in other stress-adapted plant species (Han *et al.*, 2020, 2021; Parlak & Yilmaz, 2012).

The upregulation of ATP synthase-related proteins in heat-tolerant clones, further confirmed the importance of ATP synthesis in sustaining photosynthetic efficiency under heat stress. ATP synthesis

is critical for energy production, which in turn supports the repair and stabilization of the photosynthetic machinery during thermal stress. These findings corroborate earlier studies demonstrating that efficient energy production is a hallmark of heat tolerance in various plant systems (Sweetlove *et al.*, 2006; Tula *et al.*, 2020).

Genetic variability across the clones was found to play a pivotal role in shaping their differential responses to heat stress. The heat-tolerant clones displayed distinct genetic profiles characterized by the upregulation of stress-related genes, which are likely integral to their ability to maintain homeostasis under adverse conditions. This suggests that these clones possess adaptive mechanisms enabling them to survive and thrive in fluctuating environmental conditions, offering valuable insights into plant resilience to climate change.

Despite the significant findings, a notable limitation of this study was the low mapping efficiency observed for heat-sensitive and control clones, which constrained the analysis to genes common across all clones. To overcome this limitation, future studies could employ *de novo* transcriptome assembly to capture clone-specific responses to heat stress. Moreover, functional validation of the identified genes through approaches such as qPCR or genetic modifications would provide stronger evidence for their roles in thermotolerance, further advancing our understanding of the genetic basis of heat resilience.

The findings of this study highlight the potential of *Lemna gibba* as a resilient species capable of withstanding heat stress, which has important implications for climate change adaptation and ecological sustainability. The observed genetic variability among clones suggests that natural selection may favour heat-tolerant variants, potentially influencing the species' distribution and ecosystem function over the coming decades. As global temperatures rise, resilient duckweed strains could play a crucial role in maintaining aquatic ecosystem stability by sustaining primary productivity and contributing to biogeochemical cycles such as nitrogen and carbon sequestration. Additionally, their capacity for phytoremediation, particularly in nitrogen-rich environments, suggests promising applications for mitigating nutrient pollution in freshwater bodies, thereby improving water quality and ecosystem health.

The genetic and molecular insights gained from this study also underscore the potential for biotechnological advancements through genetic modification. Existing protocols for duckweed transformation make it an attractive candidate for targeted genetic enhancement, allowing for the optimization of traits such as heat tolerance, biomass accumulation, and nutrient assimilation. Potential targets for modification include genes involved in photosynthetic efficiency, oxidative stress response, and nutrient metabolism, which could enhance *Lemna's* application in sustainable

agriculture, biofuel production, and wastewater treatment. By leveraging its rapid growth rate and ability to thrive in diverse environmental conditions, genetically engineered duckweed could serve as a valuable tool for addressing global challenges related to food security and environmental sustainability.

However, the expansion of genetically modified *Lemna* into commercial and ecological applications raises important legislative and ethical considerations. Regulatory frameworks governing genetically modified organisms (GMOs) vary widely across different countries, and the potential risks associated with the uncontrolled spread of modified duckweed in natural ecosystems must be carefully assessed. Concerns regarding biodiversity, gene flow, and ecological balance necessitate stringent containment and monitoring strategies before large-scale implementation. Additionally, ethical debates surrounding genetic modification in food and environmental applications highlight the need for transparent research, public engagement, and evidence-based policymaking to ensure that biotechnological advancements align with societal and ecological interests.

6.4. Conclusions

In conclusion, this study has provided significant insights into the factors influencing the growth, protein content, and stress resilience of duckweed, with a particular emphasis on nitrogen availability and heat stress. Through comprehensive assessments across physiological, molecular, and transcriptomic levels, this research has improved our understanding of the adaptive responses of *Lemna* species to environmental stressors, shedding light on their potential for sustainable agricultural applications and environmental remediation.

- The investigation into different nitrogen sources revealed genetic and physiological diversity among *Lemna* clones, with nitrogen availability significantly influencing growth rates, protein content, and nitrogen assimilation gene expression. Clone 7796 demonstrated superior nitrogen use efficiency and protein accumulation, particularly under Urea-Nitrate treatments, underscoring its potential for nutrient remediation and sustainable biomass production. These findings highlight the importance of tailoring nitrogen management strategies to specific clones to optimize their productivity and maximize their ecological and commercial applications.
- The assessment of *Lemna* growth under heat stress identified heat-tolerant clones (6861, 7763, and 7796) capable of maintaining stable protein content and growth rates under elevated temperatures. These clones exhibited key physiological adaptations, such as

enhanced protein stabilization, which mitigate the detrimental effects of heat stress. The identification of heat-tolerant clones holds significant promise for applications in biomass production and nutrient cycling in regions increasingly affected by climate change, supporting the development of climate-resilient agricultural systems.

- The transcriptomic analysis of heat stress responses in *L. gibba* revealed key molecular pathways associated with heat tolerance, including the upregulation of photosynthesis-related genes, zinc ion-binding proteins, and ATP synthase pathways. These molecular mechanisms support the physiological resilience of heat-tolerant clones, emphasizing the role of genetic variability in heat stress adaptation. These findings provide valuable insights for future efforts to enhance plant resilience and productivity through targeted genetic approaches, ultimately improving the efficiency of plant-based solutions for environmental and agricultural challenges.

The integration of physiological and molecular analyses has provided an understanding of how nitrogen availability and heat stress interact to influence *Lemna* growth and productivity. The identification of key genetic pathways associated with nitrogen assimilation, photosynthetic maintenance, and cellular stress responses provide new opportunities to optimize duckweed for both agricultural and environmental applications. Future research focusing on functional validation of these pathways, by using advanced molecular tools such as genetic transformation (overexpression, genome editing with CRISPR-Cas9), could further enhance our ability to develop stress-resilient and high-yielding duckweed varieties.

Overall, results of this study provide evidence for using *Lemna* as a versatile and sustainable resource capable of addressing critical challenges in agriculture, such as food security and climate adaptation. By exploiting the genetic diversity, nitrogen efficiency, and stress resilience, promising duckweed clones can be selected and used as a valuable protein source, which can contribute to nutrient cycling, and offer innovative solutions for sustainable agriculture facing global climate change. The findings from this study lay a strong foundation for future advancements in the utilization of duckweed, positioning it as a key crop for enhancing environmental sustainability and agricultural productivity.

References

- Acosta, K., Appenroth, K. J., Borisjuk, L., Edelman, M., Heinig, U., Jansen, M. A. K., Oyama, T., Pasaribu, B., Schubert, I., Sorrels, S., Sowjanya Sree, K., Xu, S., Michael, T. P., & Lam, E. (2021). Return of the Lemnaceae: duckweed as a model plant system in the genomics and postgenomics era. In *Plant Cell* 33(10).
- Acosta, K., Xu, J., Gilbert, S., Denison, E., Brinkman, T., Lebeis, S., & Lam, E. (2020). Duckweed hosts a taxonomically similar bacterial assemblage as the terrestrial leaf microbiome. *PLoS ONE*, 15(2).
- Ahammad, M. U., . M. S. R. S., . T. Y., . M. S. R., & . M. S. A. (2003). Replacement of Sesame Oil Cake by Duckweed (*Lemna minor*) in Broiler Diet. *Pakistan Journal of Biological Sciences*, 6(16).
- Akter, N., & Rafiqul Islam, M. (2017). Heat stress effects and management in wheat. A review. In *Agronomy for Sustainable Development* 37(5).
- Aleem, S., Sharif, I., Tahir, M., Najeebullah, M., Nawaz, A., Khan, M. I., Batool, A., & Arshad, W. (2021). Impact of Heat Stress on Cauliflower (*Brassica Oleracea* var. Botrytis): A Physiological Assessment. *Pakistan Journal of Agricultural Research*, 34(3).
- Almeida, J., Perez-Fons, L., & Fraser, P. D. (2021). A transcriptomic, metabolomic and cellular approach to the physiological adaptation of tomato fruit to high temperature. *Plant Cell and Environment*, 44(7).
- Amano, M., Iida, S., & Kosuge, K. (2012). Comparative studies of thermotolerance: Different modes of heat acclimation between tolerant and intolerant aquatic plants of the genus *Potamogeton*. *Annals of Botany*, 109(2).
- Amy-Sagers, C., Reinhardt, K., & Larson, D. M. (2017). Ecotoxicological assessments show sucralose and fluoxetine affect the aquatic plant, *Lemna minor*. *Aquatic Toxicology*, 185.
- Anders, S., & Huber, W. (2010). Differential expression analysis for sequence count data. *Genome Biology*, 11(10).
- Anderson, K. E., Lowman, Z., Stomp, A. M., & Chang, J. (2011). Duckweed as a feed ingredient in laying hen diets and its effect on egg production and composition. *International Journal of Poultry Science*, 10(1), 4–7.
- Appenroth, K.-J., Cheng, J. J., Fakhoorian, T., Mercovich, E., Morikawa, M., & Hai, Z. (2015, July). *ISCDRA International Steering Committee on Duckweed Research and Applications Issue #9*. 90–91.

- Appenroth, K. J., Sowjanya Sree, K., Bog, M., Ecker, J., Seeliger, C., Böhm, V., Lorkowski, S., Sommer, K., Vetter, W., Tolzin-Banasch, K., Kirmse, R., Leiterer, M., Dawczynski, C., Liebisch, G., & Jahreis, G. (2018). Nutritional value of the duckweed species of the Genus *Wolffia* (Lemnaceae) as human food. *Frontiers in Chemistry*, 6(483).
- Appenroth, K. J., Sree, K. S., Böhm, V., Hammann, S., Vetter, W., Leiterer, M., & Jahreis, G. (2017). Nutritional value of duckweeds (Lemnaceae) as human food. *Food Chemistry*, 217, 266–273.
- Ara, N., Nakkanong, K., Lv, W., Yang, J., Hu, Z., & Zhang, M. (2013). Antioxidant enzymatic activities and gene expression associated with heat tolerance in the stems and roots of two cucurbit species (“*Cucurbita maxima*” and “*Cucurbita moschata*”) and their interspecific inbred line “Maxchata.” *International Journal of Molecular Sciences*, 14(12).
- Ardenghi, N. M. G., Armstrong, W. P., & Paganelli, D. (2017). *Wolffia columbiana* (Araceae, Lemnoideae): First record of the smallest alien flowering plant in southern Europe and Italy. *Botany Letters*, 164(2).
- Ashby, E. (1948). Studies in the Morphogenesis of Leaves: I. An Essay on Leaf Shape. *New Phytologist*, 47(2).
- Ashraf, M. A., Iqbal, M., Rasheed, R., Hussain, I., & ... (2018). Environmental stress and secondary metabolites in plants: an overview. *Plant Metabolites and Regulation Under Environmental Stress*, 153-167.
- Ayasan, T., Okan, F., & Hizli, H. (2009). Threonine requirement of broiler from 22-42 days. *International Journal of Poultry Science*, 8(9), 862–865.
- Azab, E., & Soror, A. F. S. (2020). Physiological behavior of the aquatic plant *Azolla* sp. In response to organic and inorganic fertilizers. *Plants*, 9(7).
- Babayemi, O. J., Bamikole, M. A., & Omojola, A. B. (2006). Evaluation of the nutritive value and free choice intake of two aquatic weeds (*Nephrolepis biserrata* and *Spirodela polyrhiza*) by West African dwarf goats. *Tropical and Subtropical Agroecosystems*, 6(1).
- Baker, D. H. (2006). Comparative species utilization and toxicity of sulfur amino acids. *Journal of Nutrition*, 136(6), 1670–1675.
- Barbosa Neto, A. G., Morais, M. B., Dutra, E. D., & Calsa Junior, T. (2019). Biological diversity of *Lemna aequinoctialis* Welw. isolates influences biomass production and wastewater phytoremediation. *Bioresource Technology Reports*, 6.

- Bassioni, N., Allam, N., & Abaido, Y. (1980). Effect of Nitrogen Fertilization and Season of Growth on Nitrate Content of Spinach Plants (*Spinacia oleracea*, L.). *Zeitschrift Für Pflanzenernährung Und Bodenkunde*, 143(6).
- Baxter, A., Mittler, R., & Suzuki, N. (2014). ROS as key players in plant stress signalling. In *Journal of Experimental Botany*, 65(5).
- Ben-Asher, J., Garcia Y Garcia, A., & Hoogenboom, G. (2008). Effect of high temperature on photosynthesis and transpiration of sweet corn (*Zea mays* L. var. rugosa). *Photosynthetica*, 46(4).
- Ben Mrid, R., Benmrid, B., Hafsa, J., Boukcim, H., Sobeh, M., & Yasri, A. (2021). Secondary metabolites as biostimulant and bioprotectant agents: A review. In *Science of the Total Environment*, 777.
- Benchling [Biology Software]*. (2024). Retrieved from <https://benchling.com>.
- Benjamini, Y., & Hochberg, Y. (1995). Controlling the False Discovery Rate: A Practical and Powerful Approach to Multiple Testing. *Journal of the Royal Statistical Society Series B: Statistical Methodology*, 57(1).
- Bennett, M. D., Leitch, I. J., Price, H. J., & Johnston, J. S. (2003). Comparisons with *Caenorhabditis* (~100 Mb) and *Drosophila* (~175 Mb) using flow cytometry show genome size in *Arabidopsis* to be ~157 Mb and thus ~25% larger than the *Arabidopsis* genome initiative estimate of ~125 Mb. *Annals of Botany*, 91(5).
- Bernard, S. M., & Habash, D. Z. (2009). The importance of cytosolic Glutamine Synthetase in nitrogen assimilation and recycling. In *New Phytologist*, 182(3).
- Bhanthumnavin, K., & MCGarry, M. G. (1971). *Wolffia arrhiza* as a possible source of inexpensive protein. In *Nature*, 232(5311), 495.
- Billen, G., Garnier, J., & Lassaletta, L. (2013). The nitrogen cascade from agricultural soils to the sea: Modelling nitrogen transfers at regional watershed and global scales. *Philosophical Transactions of the Royal Society B: Biological Sciences*, 368(1621).
- Bitá, C. E., & Gerats, T. (2013). Plant tolerance to high temperature in a changing environment: Scientific fundamentals and production of heat stress-tolerant crops. In *Frontiers in Plant Science*, 4(JUL).
- Blackburn, K. (1933). Notes on the chromosomes of the duckweeds (Lemnaceae) introducing the question of chromosome size.
- Bloom, A. J. (2015). The increasing importance of distinguishing among plant nitrogen sources. In

Current Opinion in Plant Biology, 25.

- Bog, M., Sree, K. S., Fuchs, J., Hoang, P. T. N., Schubert, I., Kuever, J., Rabenstein, A., Paolacci, S., Jansen, M. A. K., & Appenroth, K. J. (2020). A taxonomic revision of *Lemna* sect. *Uninerves* (Lemnaceae). *Taxon*, 69(1), 56–66.
- Bolger, a. M., Lohse, M., & Usadel, B. (2014). Trimmomatic: A flexible read trimming tool for Illumina NGS data. *Bioinformatics*, 30(15).
- Borisjuk, N., Chu, P., Gutierrez, R., Zhang, H., Acosta, K., Friesen, N., Sree, K. S., Garcia, C., Appenroth, K. J., & Lam, E. (2015). Assessment, validation and deployment strategy of a two-barcode protocol for facile genotyping of duckweed species. *Plant Biology*, 17(s1), 42–49.
- Borisjuk, Nikolai, Peterson, A. A., Lv, J., Qu, G., Luo, Q., Shi, L., Chen, G., Kishchenko, O., Zhou, Y., & Shi, J. (2018). Structural and biochemical properties of duckweed surface cuticle. *Frontiers in Chemistry*, 6(JUL).
- Bray, N. L., Pimentel, H., Melsted, P., & Pachter, L. (2016). Near-optimal probabilistic RNA-seq quantification. *Nature Biotechnology*, 34(5).
- Britto, D. T., & Kronzucker, H. J. (2013). Ecological significance and complexity of N-source preference in plants. *Annals of Botany*, 112(6).
- Camargo, J. A., & Alonso, Á. (2006). Ecological and toxicological effects of inorganic nitrogen pollution in aquatic ecosystems: A global assessment. In *Environment International*, 32(6).
- Campanella, A., & Harold, M. P. (2012). Fast pyrolysis of microalgae in a falling solids reactor: Effects of process variables and zeolite catalysts. *Biomass and Bioenergy*, 46.
- Campanella, A., Muncrief, R., Harold, M. P., Griffith, D. C., Whitton, N. M., & Weber, R. S. (2012). Thermolysis of microalgae and duckweed in a CO₂-swept fixed-bed reactor: Bio-oil yield and compositional effects. *Bioresource Technology*, 109.
- Campbell, E. (2013). Response to embodied energy and energy analyses of a concentrating solar power (CSP) system (2012). In *Energy Policy*, 60.
- Cataldo, D. A., Haroon, M. H., Schrader, L. E., & Youngs, V. L. (1975). Rapid colorimetric determination of nitrate in plant tissue by nitration of salicylic acid. *Communications in Soil Science and Plant Analysis*, 6(1).
- Cedergreen, N., & Vindbæk Madsen, T. (2002). Nitrogen uptake by the floating macrophyte *Lemna minor*. In *New Phytologist*, 155(2), 1323–1334.

- Ceschin, S., Abati, S., Ellwood, N. T. W., & Zuccarello, V. (2018). Riding invasion waves: Spatial and temporal patterns of the invasive *Lemna minuta* from its arrival to its spread across Europe. *Aquatic Botany*, 150.
- Chaddad, Z., Kaddouri, K., Smouni, A., Missbah El Idrissi, M., Taha, K., Hayah, I., & Badaoui, B. (2023). Meta-analysis of *Arabidopsis thaliana* microarray data in relation to heat stress response. *Frontiers in Plant Science*, 14.
- Chalanika De Silva, H. C., & Asaeda, T. (2018). Stress response and tolerance of the submerged macrophyte *Elodea nuttallii* (Planch) St. John to heat stress: a comparative study of shock heat stress and gradual heat stress. *Plant Biosystems*, 152(4).
- Chen, G., Zhao, K., Li, W., Yan, B., Yu, Y., Li, J., Zhang, Y., Xia, S., Cheng, Z., Lin, F., Li, L., Zhao, H., & Fang, Y. (2022). A review on bioenergy production from duckweed. In *Biomass and Bioenergy* (Vol. 161).
- Chen, L., Fang, Y., Jin, Y., Chen, Q., Zhao, Y., Xiao, Y., & Zhao, H. (2013). Biosorption of Pb²⁺ by dried powder of duckweed (*Lemna aequinoctialis*). *Chinese Journal of Applied and Environmental Biology*, 19(6).
- Chen, Q., Jin, Y., Zhang, G., Fang, Y., Xiao, Y., & Zhao, H. (2012). Improving production of bioethanol from duckweed (*Landoltia punctata*) by pectinase pretreatment. *Energies*, 5(8), 3019–3032.
- Chen, S., & Li, H. (2017). Heat stress regulates the expression of genes at transcriptional and post-transcriptional levels, revealed by RNA-seq in *Brachypodium distachyon*. *Frontiers in Plant Science*, 7.
- Cheng, J. J., & Stomp, A. M. (2009). Growing Duckweed to recover nutrients from wastewaters and for production of fuel ethanol and animal feed. *Clean - Soil, Air, Water*, 37(1), 17–26.
- Chowdhury, S. D., & Akter, Y. (2011). Effect of duckweed (*Lemna minor*) meal in the diet of laying hen and their performance. *Bangladesh Research Publications Journal*, 5(3), 252–261.
- Chu, P., Wilson, G. M., Michael, T. P., Vaiciunas, J., Honig, J., & Lam, E. (2018). Sequence-guided approach to genotyping plant clones and species using polymorphic NB-ARC-related genes. *Plant Molecular Biology*, 98(3).
- Collard, F. X., & Blin, J. (2014). A review on pyrolysis of biomass constituents: Mechanisms and composition of the products obtained from the conversion of cellulose, hemicelluloses and lignin. In *Renewable and Sustainable Energy Reviews*, 38.

- Conley, D. J., Paerl, H. W., Howarth, R. W., Boesch, D. F., Seitzinger, S. P., Havens, K. E., Lancelot, C., & Likens, G. E. (2009). Ecology - Controlling eutrophication: Nitrogen and phosphorus. In *Science*, 323(5917).
- Coskun, D., Britto, D. T., Shi, W., & Kronzucker, H. J. (2017). Nitrogen transformations in modern agriculture and the role of biological nitrification inhibition. In *Nature Plants*, 3.
- Crump, S. P., Heier, J. S., & Rozzell, J. D. (1990). *The production of amino acids by transamination, in Biocatalysis*, 115–133.
- Cui, W., & Cheng, J. J. (2015). Growing duckweed for biofuel production: A review. In *Plant Biology*.
- Damry, Nolan, J. V., Bell, R. E., & Thomson, E. S. (2001). Duckweed as a Protein Source for Fine-Wool Merino Sheep: Its Edibility and Effects on Wool Yield and Characteristics. *Asian-Australasian Journal of Animal Sciences*, 14(4).
- De Angeli, A., Monachello, D., Ephritikhine, G., Frachisse, J. M., Thomine, S., Gambale, F., & Barbier-Brygoo, H. (2006). The nitrate/proton antiporter AtCLCa mediates nitrate accumulation in plant vacuoles. *Nature*, 442(7105).
- Del Buono, D., Bartucca, M. L., Ballerini, E., Senizza, B., Lucini, L., & Trevisan, M. (2022). Physiological and Biochemical Effects of an Aqueous Extract of *Lemna minor* L. as a Potential Biostimulant for Maize. *Journal of Plant Growth Regulation*, 41(7).
- Devlamynck, R., Fernandes de Souza, M., Bog, M., Leenknecht, J., Eeckhout, M., & Meers, E. (2020). Effect of the growth medium composition on nitrate accumulation in the novel protein crop *Lemna minor*. *Ecotoxicology and Environmental Safety*, 206.
- Dhaliwal, S. S., Singh, J., Taneja, P. K., & Mandal, A. (2020). Remediation techniques for removal of heavy metals from the soil contaminated through different sources: a review. In *Environmental Science and Pollution Research*, 27(2).
- Dhote, S., & Dixit, S. (2009). Water quality improvement through macrophytes - A review. In *Environmental Monitoring and Assessment*, 152(1–4).
- Docauer, D. M. (1983). A nutrient basis for the distribution of the Lemnaceae. *Dissertations Abstracts International, B Sciences and Engineering*, 44(6).
- Doemel, K. (2013). Mayan medicine: rituals and plant use by mayan ah-men.
- Du, T. H. (1998). Ensiled cassava leaves and duckweed as protein sources for fattening pigs on farms in Central Vietnam. *Livestock Research for Rural Development*, 10(3).

- Duangjarus, N., Chaiworapuek, W., Rachtanapun, C., Ritthiruangdej, P., & Charoensiddhi, S. (2022). Antimicrobial and Functional Properties of Duckweed (*Wolffia globosa*) Protein and Peptide Extracts Prepared by Ultrasound-Assisted Extraction. *Foods*, 11(15).
- Duarte, K. F., Junqueira, O. M., Filardi, R. da S., de Siqueira, J. C., Garcia, E. A., & de Laurentiz, A. C. (2012). Exigências em treonina para frangos de corte de 22 a 42 dias de idade. *Revista Brasileira de Zootecnia*, 41(1), 72–79.
- Duong, T. P., & Tiedje, J. M. (1985). Nitrogen fixation by naturally occurring duckweed–cyanobacterial associations. *Canadian Journal of Microbiology*, 31(4).
- Dutta, S., Mohanty, S., & Tripathy, B. C. (2009). Role of temperature stress on chloroplast biogenesis and protein import in pea. *Plant Physiology*, 150(2).
- Edelman, M., Appenroth, K. J., Sree, K. S., & Oyama, T. (2022). Ethnobotanical History: Duckweeds in Different Civilizations. In *Plants*, 11(16).
- Edelman, M., & Colt, M. (2016). Nutrient value of leaf vs. seed. *Frontiers in Chemistry*, 4(32).
- Effiong, B. N., Sanni, A., & Fakunle, J. . (2009). Effect of partial replacement of fishmeal with duckweed (*Lemna pauciscostata*) meal on the growth performance of *Heterobranchus longifilis* fingerlings. *Report and Opinion*, 1(3).
- Ekperusi, A. O., Sikoki, F. D., & Nwachukwu, E. O. (2019). Application of common duckweed (*Lemna minor*) in phytoremediation of chemicals in the environment: State and future perspective. In *Chemosphere* (Vol. 223).
- El-Shafai, S. A., El-Gohary, F. A., Verreth, J. A. J., Schrama, J. W., & Gijzen, H. J. (2004). Apparent digestibility coefficient of duckweed (*Lemna minor*), fresh and dry for Nile tilapia (*Oreochromis niloticus* L.). *Aquaculture Research*, 35(6).
- Ellis, R. J. (1979). The most abundant protein in the world. In *Trends in Biochemical Sciences*.
- Elsanosi, H. A., Zhu, T., Zhou, G., & Song, L. (2024). Genomic organization and expression profiles of nitrogen assimilation genes in *Glycine max*. *PeerJ*, 12(6), e17590.
- Ernst, E., & Martienssen, R. (2016). Status of the *Lemna gibba* 7742a and *Lemna minor* 8627 genomes. *ISCDRA*, 3, 9–10.
- Ernst, Evan, Abramson, B., Acosta, K., Hoang, P. T. N., Mateo-Elizalde, C., Schubert, V., Pasaribu, B., Hartwick, N., Colt, K., Aylward, A., Ramu, U., Birchler, J. A., Schubert, I., Lam, E., Michael, T. P., & Martienssen, R. A. (2023). The genomes and epigenomes of aquatic plants (Lemnaceae) promote

triploid hybridization and clonal reproduction. *BioRxiv*.

Espinosa-Montiel, J., Hernandez-Allica, J., Mashanova, A., Blachez, A., Haefele, S., Barrero-Sicilia, C., & McGrath, S. (2022, July). FT-MIR-PLSR simultaneous determination of total nitrogen and nitrate in duckweeds. *6th International Conference On Duckweed Research And Applications*.

Fahad, S., Bajwa, A. A., Nazir, U., Anjum, S. A., Farooq, A., Zohaib, A., Sadia, S., Nasim, W., Adkins, S., Saud, S., Ihsan, M. Z., Alharby, H., Wu, C., Wang, D., & Huang, J. (2017). Crop production under drought and heat stress: Plant responses and management options. In *Frontiers in Plant Science*, 8.

Fang, Y., Guo, L., Wang, S., Xiao, Y., Ding, Y., Jin, Y., Tian, X., Du, A., Liao, Z., He, K., Chen, S., Zhao, Y., Tan, L., Yi, Z., Che, Y., Chen, L., Li, J., Zhao, L., Zhang, P., ... Zhao, H. (2023). Artificially cultivated duckweed: a high-efficiency starch producer. *BioRxiv*.

FAO. (2004). Poultry Development Review. In *Revisión del desarrollo avícola*.

FAO. (2020). *FAO: Nutritional requirements Nile Tilapia*.

Fasolin, L. H., Pereira, R. N., Pinheiro, A. C., Martins, J. T., Andrade, C. C. P., Ramos, O. L., & Vicente, A. A. (2019). Emergent food proteins – Towards sustainability, health and innovation. In *Food Research International*, 125.

Feingold, E. A., Good, P. J., Guyer, M. S., Kamholz, S., Liefer, L., Wetterstrand, K., Collins, F. S., Gingeras, T. R., Kampa, D., Sekinger, E. A., Cheng, J., Hirsch, H., Ghosh, S., Zhu, Z., Patel, S., Piccolboni, A., Yang, A., Tammana, H., Bekiranov, S., ... Harvey, S. C. (2004). The ENCODE (ENCyclopedia of DNA Elements) Project. In *Science*, 306(5696).

Ferreira, S., Moreira, E., Amorim, I., Santos, C., & Melo, P. (2019). *Arabidopsis thaliana* mutants devoid of chloroplast glutamine synthetase (GS2) have non-lethal phenotype under photorespiratory conditions. *Plant Physiology and Biochemistry*, 144.

Feuchtmayr, H., Moran, R., Hatton, K., Connor, L., Heyes, T., Moss, B., Harvey, I., & Atkinson, D. (2009). Global warming and eutrophication: Effects on water chemistry and autotrophic communities in experimental hypertrophic shallow lake mesocosms. *Journal of Applied Ecology*, 46(3).

Finkelstein, J. D. (1990). Methionine metabolism in mammals. In *The Journal of Nutritional Biochemistry*, 1(5), 228–237.

Flores-Miranda, Ma del C., Luna-González, A., Cortés-Espinosa, D. V., Álvarez-Ruiz, P., Cortés-Jacinto, E., Valdez-González, F. J., Escamilla-Montes, R., & González-Ocampo, H. A. (2014). Bacterial

- fermentation of *Lemna* sp. as a potential substitute of fish meal in shrimp diets. *African Journal of Microbiology Research*, 8(14).
- Flores-Miranda, Ma del Carmen, Luna-González, A., Cortés-Espinosa, D. V., Álvarez-Ruiz, P., Cortés-Jacinto, E., Valdez-González, F. J., Escamilla-Montes, R., & González-Ocampo, H. A. (2015). Effects of diets with fermented duckweed (*Lemna* sp.) on growth performance and gene expression in the Pacific white shrimp, *Litopenaeus vannamei*. *Aquaculture International*, 23(2).
- Fu, L., Huang, M., Han, B., Sun, X., Sree, K. S., Appenroth, K. J., & Zhang, J. (2017). Flower induction, microscope-aided cross-pollination, and seed production in the duckweed *Lemna gibba* with discovery of a male-sterile clone. *Scientific Reports 2017 7:1*, 7(1), 1–13.
- Garnica, M., Houdusse, F., Zamarreño, A. M., & Garcia-Mina, J. M. (2010). Nitrate modifies the assimilation pattern of ammonium and urea in wheat seedlings. *Journal of the Science of Food and Agriculture*, 90(3).
- Gaur, R. Z., & Suthar, S. (2017). Nutrient scaling of duckweed (*Spirodela polyrhiza*) biomass in urban wastewater and its utility in anaerobic co-digestion. *Process Safety and Environmental Protection*, 107.
- Ge, X., Zhang, N., Phillips, G. C., & Xu, J. (2012). Growing *Lemna minor* in agricultural wastewater and converting the duckweed biomass to ethanol. *Bioresource Technology*, 124.
- Geber, G. (1989). *Zur Karyosystematik der Lemnaceae*.
- Geelen, D., Lurin, C., Bouchez, D., Frachisse, J. M., Lelièvre, F., Courtial, B., Barbier-Brygoo, H., & Maurel, C. (2000). Disruption of putative anion channel gene AtCLC-a in *Arabidopsis* suggests a role in the regulation of nitrate content. *Plant Journal*, 21(3).
- Giri, A., Heckathorn, S., Mishra, S., & Krause, C. (2017). Heat stress decreases levels of nutrient-uptake and -assimilation proteins in tomato roots. *Plants*, 6(1).
- Goldstein, L. D., Cao, Y., Pau, G., Lawrence, M., Wu, T. D., Seshagiri, S., & Gentleman, R. (2016). Prediction and quantification of splice events from RNA-seq data. *PLoS ONE*, 11(5).
- Goodall, A. J., Kumar, P., & Tobin, A. K. (2013). Identification and expression analyses of cytosolic glutamine synthetase genes in barley (*Hordeum vulgare* L.). *Plant and Cell Physiology*, 54(4).
- Green, D. I. G., Agu, R. C., Bringhurst, T. A., Brosnan, J. M., Jack, F. R., & Walker, G. M. (2015). Maximizing alcohol yields from wheat and maize and their co-products for distilling or bioethanol production. *Journal of the Institute of Brewing*, 121(3).

- Grossmann, L., & Weiss, J. (2021). Alternative Protein Sources as Technofunctional Food Ingredients. *Annual Review of Food Science and Technology*, 12.
- Guan, Q., Yue, X., Zeng, H., & Zhu, J. (2014). The protein phosphatase RCF2 and its interacting partner NAC019 Are Critical for heat stress-responsive gene regulation and thermotolerance in *Arabidopsis*. *Plant Cell*, 26(1).
- Guilherme, E. A., Carvalho, F. E. L., Daloso, D. M., & Silveira, J. A. G. (2019). Increase in assimilatory nitrate reduction and photorespiration enhances CO₂ assimilation under high light-induced photoinhibition in cotton. *Environmental and Experimental Botany*, 159.
- Guo, L., Jin, Y., Xiao, Y., Tan, L., Tian, X., Ding, Y., He, K., Du, A., Li, J., Yi, Z., Wang, S., Fang, Y., & Zhao, H. (2020). Energy-efficient and environmentally friendly production of starch-rich duckweed biomass using nitrogen-limited cultivation. *Journal of Cleaner Production*, 251.
- Guo, R., Wang, X., Han, X., Chen, X., & Wang-Pruski, G. (2020). Physiological and transcriptomic responses of water spinach (*Ipomoea aquatica*) to prolonged heat stress. *BMC Genomics*, 21(1).
- Gutiérrez, K., Sanginés, L., Pérez, F., & Martínez, L. (2001). Studies on the potential of the aquatic plant *Lemna gibba* for pig feeding. *Cuban Journal of Agricultural Science*, 35(4).
- Haider, S., Iqbal, J., Naseer, S., Yaseen, T., Shaukat, M., Bibi, H., Ahmad, Y., Daud, H., Abbasi, N. L., & Mahmood, T. (2021). Molecular mechanisms of plant tolerance to heat stress: current landscape and future perspectives. In *Plant Cell Reports*, 40(12).
- Hammann, M., Wang, G., Boo, S. M., Aguilar-Rosas, L. E., & Weinberger, F. (2016). Selection of heat-shock resistance traits during the invasion of the seaweed *Gracilaria vermiculophylla*. *Marine Biology*, 163(5).
- Han, G., Lu, C., Guo, J., Qiao, Z., Sui, N., Qiu, N., & Wang, B. (2020). C₂H₂ Zinc Finger Proteins: Master Regulators of Abiotic Stress Responses in Plants. In *Frontiers in Plant Science*, 11.
- Han, G., Qiao, Z., Li, Y., Wang, C., & Wang, B. (2021). The roles of CCCH zinc-finger proteins in plant abiotic stress tolerance. In *International Journal of Molecular Sciences*, 22(15).
- Hasanuzzaman, M., Nahar, K., Alam, M. M., Roychowdhury, R., & Fujita, M. (2013). Physiological, biochemical, and molecular mechanisms of heat stress tolerance in plants. In *International Journal of Molecular Sciences*, 14(5).
- Haustein, A. T., Gilman, R. H., Skillicorn, P. W., Guevara, V., Díaz, F., Vergara, V., Gastañaduy, A., & Gilman, J. B. (1992). Compensatory growth in broiler chicks fed on *Lemna gibba*. *British Journal*

of Nutrition, 68(2).

- Haustein, A. T., Gilman, R. H., Skillicorn, P. W., Hannan, H., Díaz, F., Guevara, V., Vergara, V., Gastañaduy, A., & Gilman, J. B. (1994). Performance of Broiler Chickens Fed Diets Containing Duckweed (*Lemna gibba*). *The Journal of Agricultural Science*, 122(2).
- Hedhly, A., Hormaza, J. I., & Herrero, M. (2009). Global warming and sexual plant reproduction. In *Trends in Plant Science*, 14(1).
- Hewitt, E. J. (1966). Sand and Water Culture Methods Used in the Study of Plant Nutrition. *Experimental Agriculture*, 3(2), 547.
- Hillman, W. S. (1976). Calibrating duckweeds: Light, clocks, metabolism, flowering. In *Science* 193(4252).
- Hilton, J., O'Hare, M., Bowes, M. J., & Jones, J. I. (2006). How green is my river? A new paradigm of eutrophication in rivers. *Science of the Total Environment*, 365(1–3).
- Hoang, P. T. N., Schubert, V., Meister, A., Fuchs, J., & Schubert, I. (2019). Variation in genome size, cell and nucleus volume, chromosome number and rDNA loci among duckweeds. *Scientific Reports*, 9(1).
- Hodin, J., Lind, C., Marmagne, A., Espagne, C., Bianchi, M. W., De Angeli, A., Abou-Choucha, F., Bourge, M., Chardon, F., Thomine, S., & Filleur, S. (2023). Proton exchange by the vacuolar nitrate transporter CLCa is required for plant growth and nitrogen use efficiency. *Plant Cell*, 35(1).
- Hofmann, L. C., Straub, S., & Bischof, K. (2013). Elevated CO₂ levels affect the activity of nitrate reductase and carbonic anhydrase in the calcifying rhodophyte *Corallina officinalis*. *Journal of Experimental Botany*, 64(4).
- Hort, A., T. (1917). Theophrastus: Enquiry into Plants. *Nature*, 99(2484).
- Hörtensteiner, S., & Feller, U. (2002). Nitrogen metabolism and remobilization during senescence. *Journal of Experimental Botany*, 53(370).
- Hou, W., Chen, X., Song, G., Wang, Q., & Chi Chang, C. (2007). Effects of copper and cadmium on heavy metal polluted waterbody restoration by duckweed (*Lemna minor*). *Plant Physiology and Biochemistry*, 45(1).
- Hovden, E. (2006). *Rainwater harvesting cisterns and local water management*. University of Bergen.
- Hozain, M., Abdelmageed, H., Lee, J., Kang, M., Fokar, M., Allen, R. D., & Holaday, A. S. (2012).

- Expression of AtSAP5 in cotton up-regulates putative stress-responsive genes and improves the tolerance to rapidly developing water deficit and moderate heat stress. *Journal of Plant Physiology*, 169(13).
- Hu, Yamin, Wang, S., Li, J., Wang, Q., He, Z., Feng, Y., Abomohra, A. E. F., Afonaa-Mensah, S., & Hui, C. (2018). Co-pyrolysis and co-hydrothermal liquefaction of seaweeds and rice husk: Comparative study towards enhanced biofuel production. *Journal of Analytical and Applied Pyrolysis*, 129.
- Hu, Yangjie, Fragkostefanakis, S., Schleiff, E., & Simm, S. (2020). Transcriptional basis for differential thermosensitivity of seedlings of various tomato genotypes. *Genes*, 11(6).
- Hu, Yangjie, Mesihovic, A., Jiménez-Gómez, J. M., Röth, S., Gebhardt, P., Bublak, D., Bovy, A., Scharf, K. D., Schleiff, E., & Fragkostefanakis, S. (2020). Natural variation in HsfA2 pre-mRNA splicing is associated with changes in thermotolerance during tomato domestication. *New Phytologist*, 225(3).
- Hu, Yanping, Zhang, T., Liu, Y., Li, Y., Wang, M., Zhu, B., Liao, D., Yun, T., Huang, W., Zhang, W., & Zhou, Y. (2021). Pumpkin (*Cucurbita moschata*) HSP20 Gene Family Identification and Expression Under Heat Stress. *Frontiers in Genetics*, 12.
- Huang, B., & Xu, C. (2008). Identification and characterization of proteins associated with plant tolerance to heat stress. In *Journal of Integrative Plant Biology*, 50(10).
- Huang, L., Lu, Y., Gao, X., Du, G., Ma, X., Liu, M., Guo, J., & Chen, Y. (2013). Ammonium-induced oxidative stress on plant growth and antioxidative response of duckweed (*Lemna minor* L.). *Ecological Engineering*, 58.
- Huque, K. S., Chowdhury, S. A., & Kibria, S. S. (1996). Study on the potentiality of duckweeds as a feed for cattle. *Asian-Australasian Journal of Animal Sciences*, 9(2).
- Iatrou, E. I., Kora, E., & Stasinakis, A. S. (2019). Investigation of biomass production, crude protein and starch content in laboratory wastewater treatment systems planted with *Lemna minor* and *Lemna gibba*. *Environmental Technology (United Kingdom)*, 40(20).
- Iberite, M., Iamónico, D., Abati, S., & Abbate, G. (2011). *Lemna valdiviana* phil. (Araceae) as a potential invasive species in Italy and Europe: Taxonomic study and first observations on its ecology and distribution. *Plant Biosystems*, 145(4).
- Illumina, I. (2024). *Complete Secondary Analysis Workflow for the Genome Analyzer*.
- Ishizawa, H., Kuroda, M., Morikawa, M., & Ike, M. (2017). Evaluation of environmental bacterial

- communities as a factor affecting the growth of duckweed *Lemna minor*. *Biotechnology for Biofuels*.
- ISO 20079. (2005). (E) *Water quality – Determination of the toxic effect of water constituents and waste water on duckweed (Lemna minor) – Duckweed growth inhibition test*.
- Jacobs, D. L. (1947). An Ecological Life-History of Spirodela Polyrhiza (Greater Duckweed) with Emphasis on the Turion Phase. *Ecological Monographs*, 17(4).
- Jagtap, A. B., Yadav, I. S., Vikal, Y., Praba, U. P., Kaur, N., Gill, A. S., & Johal, G. S. (2023). Transcriptional dynamics of maize leaves, pollens and ovules to gain insights into heat stress-related responses. *Frontiers in Plant Science*, 14.
- Jahreis, G., Brese, M., Leiterer, M., Schäfer, U., & Böhm, V. (2016). Legume flours: Nutritionally important sources of protein and dietary fiber. *Ernahrungs Umschau*, 63(2), 36–42.
- James, D., Borphukan, B., Fartyal, D., Achary, V. M. M., & Reddy, M. K. (2018). Transgenic manipulation of glutamine synthetase: A target with untapped potential in various aspects of crop improvement. In *Biotechnologies of Crop Improvement, Volume 2: Transgenic Approaches*.
- Kabir, J., Islam, M. A., Ahammad, M. U., & Howlider, M. A. R. (2005). Use of Duckweed (*Lemna minor*) in the Diet of Broiler. *Indian J. Anim.*, 39, 31–35.
- Kanehisa, M., & Goto, S. (2000). KEGG: Kyoto Encyclopedia of Genes and Genomes. In *Nucleic Acids Research*, 28(1).
- Kaplan, A., Zelicha, H., Tsaban, G., Yaskolka Meir, A., Rinott, E., Kovsan, J., Novack, L., Thiery, J., Ceglarek, U., Burkhardt, R., Willenberg, A., Tirosh, A., Cabantchik, I., Stampfer, M. J., & Shai, I. (2019). Protein bioavailability of *Wolffia globosa* duckweed, a novel aquatic plant – A randomized controlled trial. *Clinical Nutrition*, 38(6).
- Kawashima, N., & Wildman, S. G. (1970). A model of the subunit structure of fraction I protein. *Biochemical and Biophysical Research Communications*, 41(6).
- Khanum, J., Chwalibog, A., & Huque, K. S. (2005). Study on digestibility and feeding systems of duckweed in growing ducks. *Livestock Research for Rural Development*, 17(5).
- Kiełbowicz-Matuk, A. (2012). Involvement of plant C₂H₂-type zinc finger transcription factors in stress responses. In *Plant Science*, 185–186.
- Kim, I. (2011). Features of Plastids within Reduced *Spirodela polyrhiza*. *Korean J. Microscopy*, 41(1), 55–60.

- Kim, I. (2013). Cellular Features of the Fronds and Turions in *Spirodela polyrhiza*. *Applied Microscopy*, 43(4).
- Kim, I. (2016). Structural Differentiation of the Connective Stalk in *Spirodela polyrhiza* (L.) Schleiden. *Applied Microscopy*, 46(2).
- Knowlton, T. W. (2018). Flame, icons and healing: a colonial Maya ontology. *Colonial Latin American Review*, 27(3).
- Kojima, S., Konishi, N., Beier, M. P., Ishiyama, K., Maru, I., Hayakawa, T., & Yamaya, T. (2014). NADH-dependent glutamate synthase participated in ammonium assimilation in *Arabidopsis* root. *Plant Signaling and Behavior*, 9(8).
- Körner, S., Das, S. K., Veenstra, S., & Vermaat, J. E. (2001). The effect of pH variation at the ammonium/ammonia equilibrium in wastewater and its toxicity to *Lemna gibba*. *Aquatic Botany*, 71(1), 71–78.
- Kotak, S., Larkindale, J., Lee, U., von Koskull-Döring, P., Vierling, E., & Scharf, K. D. (2007). Complexity of the heat stress response in plants. In *Current Opinion in Plant Biology*, 10(3).
- Krapp, A. (2015). Plant nitrogen assimilation and its regulation: A complex puzzle with missing pieces. In *Current Opinion in Plant Biology*, 25.
- Kung, S. D., & Tso, T. C. (1978). Tobacco as a Potential Food Source and Smoke Material: Soluble Protein Content, Extraction, and Amino Acids Composition. *Journal of Food Science*, 43(6).
- Kwak, M., & Kim, I. (2008). Turion as dormant structure in *Spirodela polyrhiza*. *Korean J. Microscopy*, 38(4), 307–314.
- Lam, H. M., Coschigano, K. T., Oliveira, I. C., Melo-Oliveira, R., & Coruzzi, G. M. (1996). The molecular-genetics of nitrogen assimilation into amino acids in higher plants. *Annual Review of Plant Physiology and Plant Molecular Biology*, 47(1).
- Landolt, E., & Kandeler, R. (1987). The family of Lemnaceae—a monographic study, 2. Biosystematic Investigations in the Family of Duckweeds (Lemnaceae). *Veröffentlichungen Des Geobotanischen Institutes Der ETH. Stiftung Rübli, Zurich*.
- Landolt, Elias. (1986). The family of Lemnaceae—A monographic study—Vol.1. *Folia Geobotanica & Phytotaxonomica*, 28(1), 566.
- Laghari, S. J., Wahocho, N. A., Laghari, G. M., Laghari, A. H., Bhabhan, G. M., K.H.Talpur, Lashari., & A.A. (2016). Role of nitrogen for plant growth and development: A review. *Advances in*

Environmental Biology, 10(9).

- Li, N., Euring, D., Cha, J. Y., Lin, Z., Lu, M., Huang, L. J., & Kim, W. Y. (2021). Plant Hormone-Mediated Regulation of Heat Tolerance in Response to Global Climate Change. In *Frontiers in Plant Science*, 11.
- Li, Y., Zhang, F., Daroch, M., & Tang, J. (2016). Positive effects of duckweed polycultures on starch and protein accumulation. *Bioscience Reports*, 36(5).
- Li, Z., Tang, M., Hassan, M. J., Zhang, Y., Han, L., & Peng, Y. (2021). Adaptability to High Temperature and Stay-Green Genotypes Associated With Variations in Antioxidant, Chlorophyll Metabolism, and γ -Aminobutyric Acid Accumulation in Creeping Bentgrass Species. *Frontiers in Plant Science*, 12.
- Liang, G., & Zhang, Z. (2020). Reducing the Nitrate Content in Vegetables Through Joint Regulation of Short-Distance Distribution and Long-Distance Transport. In *Frontiers in Plant Science*, 11.
- Liao, Y., Smyth, G. K., & Shi, W. (2014). FeatureCounts: An efficient general purpose program for assigning sequence reads to genomic features. *Bioinformatics*, 30(7).
- Lippmann, R., Babben, S., Menger, A., Delker, C., & Quint, M. (2019). Development of Wild and Cultivated Plants under Global Warming Conditions. In *Current Biology*, 29(24).
- Liu, B., Kong, L., Zhang, Y., & Liao, Y. (2021). Gene and metabolite integration analysis through transcriptome and metabolome brings new insight into heat stress tolerance in potato (*Solanum tuberosum* L.). *Plants*, 10(1).
- Liu, Can, Ma, H., Zhou, J., Li, Z., Peng, Z., Guo, F., & Zhang, J. (2019). TsHD1 and TsNAC1 cooperatively play roles in plant growth and abiotic stress resistance of *Thellungiella halophila*. *Plant Journal*, 99(1).
- Liu, Changqi, Zhao, J., Gupta, S., & Carrillo, M. (2025). *Quantification of Crude and Soluble Protein Content*. 107–122.
- Liu, H. C., Liao, H. T., & Charng, Y. Y. (2011). The role of class A1 heat shock factors (HSFA1s) in response to heat and other stresses in *Arabidopsis*. *Plant, Cell and Environment*, 34(5).
- Liu, J., Zhang, R., Xu, X., Fowler, J. C., Miller, T. E. X., & Dong, T. (2020). Effect of summer warming on growth, photosynthesis and water status in female and male *Populus cathayana*: Implications for sex-specific drought and heat tolerances. *Tree Physiology*, 40(9).
- Liu, X., Hu, B., & Chu, C. (2022). Nitrogen assimilation in plants: current status and future prospects. In

Journal of Genetics and Genomics, 49(5).

- Liu, Y., Wang, Y., Xu, S., Tang, X., Zhao, J., Yu, C., He, G., Xu, H., Wang, S., Tang, Y., Fu, C., Ma, Y., & Zhou, G. (2019). Efficient genetic transformation and CRISPR/Cas9-mediated genome editing in *Lemna aequinoctialis*. *Plant Biotechnology Journal*, 17(11).
- Liu, Y., Xu, H., Yu, C., & Zhou, G. (2021). Multifaceted roles of duckweed in aquatic phytoremediation and bioproducts synthesis. In *GCB Bioenergy*, 13(1).
- López-Martínez, M. I., Miguel, M., & Garcés-Rimón, M. (2022). Protein and Sport: Alternative Sources and Strategies for Bioactive and Sustainable Sports Nutrition. In *Frontiers in Nutrition*, 9.
- Lou, W., Tan, X., Song, K., Zhang, S., Luan, G., Li, C., & Lu, X. (2018). A specific single nucleotide polymorphism in the ATP synthase gene significantly improves environmental stress tolerance of *Synechococcus elongatus* PCC 7942. *Applied and Environmental Microbiology*, 84(18).
- Love, M. I., Huber, W., & Anders, S. (2014). Moderated estimation of fold change and dispersion for RNA-seq data with DESeq2. *Genome Biology*, 15(12).
- Lucey, J. (2003). *Lemna minuta* Kunth (Least Duckweed) in E. Cork (VC H5). *Irish Botanical News*, 13, 5–8.
- Lyons, E., & Freeling, M. (2008). How to usefully compare homologous plant genes and chromosomes as DNA sequences. *Plant Journal*, 53(4).
- Lyons, E., Pedersen, B., Kane, J., Alam, M., Ming, R., Tang, H., Wang, X., Bowers, J., Paterson, A., Lisch, D., & Freeling, M. (2008). Finding and comparing syntenic regions among *Arabidopsis* and the outgroups papaya, poplar, and grape: CoGe with rosids. *Plant Physiology*, 148(4).
- Ma, C., Liu, J., Ye, M., Zou, L., Qian, G., & Li, Y. Y. (2018). Towards utmost bioenergy conversion efficiency of food waste: Pretreatment, co-digestion, and reactor type. In *Renewable and Sustainable Energy Reviews*, 90).
- Maeda, S. I., Konishi, M., Yanagisawa, S., & Omata, T. (2014). Nitrite transport activity of a novel HPP family protein conserved in cyanobacteria and chloroplasts. *Plant and Cell Physiology*, 55(7).
- Martínez-Dalmau, J., Berbel, J., & Ordóñez-Fernández, R. (2021). Nitrogen fertilization. A review of the risks associated with the inefficiency of its use and policy responses. In *Sustainability (Switzerland)*, 13(10).
- Masclaux-Daubresse, C., Daniel-Vedele, F., Dechorgnat, J., Chardon, F., Gaufichon, L., & Suzuki, A. (2010). Nitrogen uptake, assimilation and remobilization in plants: Challenges for sustainable

- and productive agriculture. In *Annals of Botany*, 105(7).
- Masclaux, C., Valadier, M. H., Brugière, N., Morot-Gaudry, J. F., & Hirel, B. (2000). Characterization of the sink/source transition in tobacco (*Nicotiana tabacum* L.) shoots in relation to nitrogen management and leaf senescence. *Planta*, 211(4).
- Mbagwu, I. G., & Adeniji, H. A. (1988). The nutritional content of duckweed (*Lemna paucicostata* hegel.) in the Kainji Lake area, Nigeria. *Aquatic Botany*, 29(4).
- McCormac, D. J., & Greenberg, B. M. (1992). Differential synthesis of photosystem cores and light-harvesting antenna during proplastid to chloroplast development in *Spirodela oligorrhiza*. *Plant Physiology*, 98(3).
- McLaren, J. S., & Smith, H. (1976). The Effect of Abscisic Acid on Growth, Photosynthetic Rate and Carbohydrate Metabolism in *Lemna minor* L. *New Phytologist*, 76(1).
- Miazek, K., & Ledakowicz, S. (2013). Chlorophyll extraction from leaves, needles and microalgae: A kinetic approach. *International Journal of Agricultural and Biological Engineering*, 6(2), 107–115.
- Mifsud, S. (2010). First occurrences of *Lemna minuta* Kunth (Fam: Lemnaceae) in the Maltese Islands. *Cent Medit Nat*, 5, 1–4.
- Mijatović, D., Van Oudenhoven, F., Eyzaguirre, P., & Hodgkin, T. (2013). The role of agricultural biodiversity in strengthening resilience to climate change: Towards an analytical framework. *International Journal of Agricultural Sustainability*, 11(2).
- Mishima, D., Kuniki, M., Sei, K., Soda, S., Ike, M., & Fujita, M. (2008). Ethanol production from candidate energy crops: Water hyacinth (*Eichhornia crassipes*) and water lettuce (*Pistia stratiotes* L.). *Bioresource Technology*, 99(7).
- Mishra, S. K., Tripp, J., Winkelhaus, S., Tschiersch, B., Theres, K., Nover, L., & Scharf, K. D. (2002). In the complex family of heat stress transcription factors, HsfA1 has a unique role as master regulator of thermotolerance in tomato. *Genes and Development*, 16(12).
- Mishra, S., Spaccarotella, K., Gido, J., Samanta, I., & Chowdhary, G. (2023). Effects of Heat Stress on Plant-Nutrient Relations: An Update on Nutrient Uptake, Transport, and Assimilation. In *International Journal of Molecular Sciences*, 24(21).
- Mortazavi, A., Williams, B. A., McCue, K., Schaeffer, L., & Wold, B. (2008). Mapping and quantifying mammalian transcriptomes by RNA-Seq. *Nature Methods*, 5(7).
- Moss, M. E. (1999). *Economics and feed value of integrating duckweed production with a swine*

operation.

- Moura, M. A. F. e., Martins, B. de A., Oliveira, G. P. d., & Takahashi, J. A. (2022). Alternative protein sources of plant, algal, fungal and insect origins for dietary diversification in search of nutrition and health. In *Critical Reviews in Food Science and Nutrition*, 63(31).
- Muradov, N., Fidalgo, B., Gujar, A. C., & T-Raissi, A. (2010). Pyrolysis of fast-growing aquatic biomass - *Lemna minor* (duckweed): Characterization of pyrolysis products. *Bioresource Technology*, 101(21).
- National Center for Biotechnology Information. (n.d.). Retrieved January 25, 2024, from <https://www.ncbi.nlm.nih.gov/>
- Ngamsaeng, A., Thy, S., & Preston, T. R. (2004). Duckweed (*Lemna minor*) and water spinach (*Ipomoea aquatica*) as protein supplements for ducks fed broken rice as the basal diet. *Livestock Research for Rural Development*, 16(3).
- Nie, X. Q., Dong, F. Q., Liu, N., Zhang, D., Liu, M. X., Yang, J., & Zhang, W. (2015). Biosorption and biomineralization of uranium(VI) from aqueous solutions by *Landoltia punctata*. *Guang Pu Xue Yu Guang Pu Fen Xi/Spectroscopy and Spectral Analysis*, 35(9).
- Nosaka, Y., & Nosaka, A. Y. (2017). Generation and Detection of Reactive Oxygen Species in Photocatalysis. In *Chemical Reviews*, 117(17).
- Nouri, M. Z., Moumeni, A., & Komatsu, S. (2015). Abiotic stresses: Insight into gene regulation and protein expression in photosynthetic pathways of plants. In *International Journal of Molecular Sciences*, 16(9).
- Ochieng', I. O., Gitari, H. I., Mochoge, B., Rezaei-Chiyaneh, E., & Gweyi-Onyango, J. P. (2021). Optimizing Maize Yield, Nitrogen Efficacy and Grain Protein Content under Different N Forms and Rates. *Journal of Soil Science and Plant Nutrition*, 21(3).
- Ohama, N., Sato, H., Shinozaki, K., & Yamaguchi-Shinozaki, K. (2017). Transcriptional Regulatory Network of Plant Heat Stress Response. In *Trends in Plant Science* 22(1), 53–65.
- Okamoto, A., Koyama, K., & Bhusal, N. (2022). Diurnal Change of the Photosynthetic Light-Response Curve of Buckbean (*Menyanthes trifoliata*), an Emergent Aquatic Plant. *Plants*, 11(2).
- Oláh, V., Lakatos, G., Bertók, C., Kanalas, P., Szollosi, E., Kis, J., & Mészáros, I. (2010). Short-term chromium(VI) stress induces different photosynthetic responses in two duckweed species, *Lemna gibba* L. and *Lemna minor* L. *Photosynthetica*, 48(4).

- Opiyo, M., Mbogo, K., Obiero, K., Orina, P., & Muendo, P. (2023). Nutritional Composition of Duckweed (*Lemna minor*) Cultured with Inorganic Fertilizer and Organic manure in Earthen Ponds. *Journal of Limnology and Freshwater Fisheries Research*, 9(3).
- Pagliuso, D., Grandis, A., Igarashi, E. S., Lam, E., & Buckeridge, M. S. (2018). Correlation of apiose levels and growth rates in duckweeds. *Frontiers in Chemistry*, 6(JUL).
- Panfili, I., Bartucca, M. L., & Del Buono, D. (2019). The treatment of duckweed with a plant biostimulant or a safener improves the plant capacity to clean water polluted by terbuthylazine. *Science of the Total Environment*, 646.
- Pasos-Panqueva, J., Baker, A., & Camargo-Valero, M. A. (2024). Unravelling the impact of light, temperature and nutrient dynamics on duckweed growth: A meta-analysis study,. *Journal of Environmental Management*, 366(121721).
- Peeters, E. T. H. M., van Zuidam, J. P., van Zuidam, B. G., Van Nes, E. H., Kosten, S., Heuts, P. G. M., Roijackers, R. M. M., Netten, J. J. C., & Scheffer, M. (2013). Changing weather conditions and floating plants in temperate drainage ditches. *Journal of Applied Ecology*, 50(3).
- Perdomo, J. A., Capó-Bauçà, S., Carmo-Silva, E., & Galmés, J. (2017). Rubisco and rubisco activase play an important role in the biochemical limitations of photosynthesis in rice, wheat, and maize under high temperature and water deficit. *Frontiers in Plant Science*, 8.
- Pertea, M., Pertea, G. M., Antonescu, C. M., Chang, T. C., Mendell, J. T., & Salzberg, S. L. (2015). StringTie enables improved reconstruction of a transcriptome from RNA-seq reads. *Nature Biotechnology*, 33(3).
- Petersen, F., Demann, J., Restemeyer, D., Ulbrich, A., Olf, H. W., Westendarp, H., & Appenroth, K. J. (2021). Influence of the nitrate-n to ammonium-n ratio on relative growth rate and crude protein content in the duckweeds *Lemna minor* and *Wolffiella hyalina*. *Plants*, 10(8).
- Pfaffl, M. W. (2001). A new mathematical model for relative quantification in real-time RT-PCR. *Nucleic Acids Research*, 29(9).
- Phylogeny.fr*. (n.d.). Retrieved from <https://www.phylogeny.fr/>
- Qu, A. L., Ding, Y. F., Jiang, Q., & Zhu, C. (2013). Molecular mechanisms of the plant heat stress response. In *Biochemical and Biophysical Research Communications*, 432(2).
- Regni, L., Buono, D. Del, Miras-Moreno, B., Senizza, B., Lucini, L., Trevisan, M., Venturi, D. M., Costantino, F., & Proietti, P. (2021). Biostimulant effects of an aqueous extract of duckweed

- (*Lemna minor* L.) on physiological and biochemical traits in the olive tree. *Agriculture (Switzerland)*, *11*(12).
- Reid, W. S. J. (2004). Exploring Duckweed (*Lemna gibba*) as a Protein Supplement for Ruminants Using the Boer Goat (*Capra hircus*) as a Model. <http://www.lib.ncsu.edu/resolver/1840.16/2576>
- Reinhold, D., Vishwanathan, S., Park, J. J., Oh, D., & Michael Saunders, F. (2010). Assessment of plant-driven removal of emerging organic pollutants by duckweed. *Chemosphere*, *80*(7).
- Rimon, D., & Galun, E. (1968). Morphogenesis of *Wolffia microscopica*-Fronde and Flower Development. *Phytomorphology*, *18*, 364–372.
- Robertson, G. P., & Vitousek, P. M. (2009). Nitrogen in agriculture: Balancing the cost of an essential resource. *Annual Review of Environment and Resources*, *34*.
- Rojas, O. J., Liu, Y., & Stein, H. H. (2014). Concentration of metabolizable energy and digestibility of energy, phosphorus, and amino acids in *Lemna* protein concentrate fed to growing pigs. *Journal of Animal Science*, *92*(11).
- Rom, S., Gilad, A., Kalifa, Y., Konrad, Z., Karpasas, M. M., Goldgur, Y., & Bar-Zvi, D. (2006). Mapping the DNA- and zinc-binding domains of ASR1 (abscisic acid stress ripening), an abiotic-stress regulated plant specific protein. *Biochimie*, *88*(6).
- RStudio Team. (2022). *RStudio: Integrated Development for R*.
- Ru, C., Hu, X., Chen, D., Song, T., Wang, W., Lv, M., & Hansen, N. C. (2022). Nitrogen Modulates the Effects of Short-Term Heat, Drought and Combined Stresses after Anthesis on Photosynthesis, Nitrogen Metabolism, Yield, and Water and Nitrogen Use Efficiency of Wheat. *Water (Switzerland)*, *14*(9).
- Rutgers Duckweed Stock Cooperative - Home*. (n.d.). Retrieved February 12, 2021, from <http://www.rduckweed.org/>
- Sah, N., & Sherpa, D. (2020). Tolerance Mechanism Against Impact of Heat Stress on Wheat : A Review. *Environmental Contaminants Reviews*, *4*(2).
- Santiago, C. B., & Lovell, R. T. (1988). Amino acid requirements for growth of Nile tilapia. *Journal of Nutrition*, *118*(12), 1540–1546.
- Sato, H., Mizoi, J., Tanaka, H., Maruyama, K., Qin, F., Osakabe, Y., Morimoto, K., Ohori, T., Kusakabe, K., Nagata, M., Shinozaki, K., & Yamaguchi-Shinozaki, K. (2014). *Arabidopsis* DPB3-1, A DREB2A Interactor, Specifically Enhances Heat Stress-Induced Gene Expression by Forming a Heat Stress-

- Specific Transcriptional Complex with NF-Y Subunits. *Plant Cell*, 26(12).
- Sawicka, B., Umachandran, K., Nasir, N. A., & Skiba, D. (2020). Alternative and New Protein Sources. In *Functional Foods and Nutraceuticals*.
- Scafaro, A. P., Gallé, A., Van Rie, J., Carmo-Silva, E., Salvucci, M. E., & Atwell, B. J. (2016). Heat tolerance in a wild *Oryza* species is attributed to maintenance of Rubisco activation by a thermally stable Rubisco activase ortholog. *New Phytologist*, 211(3).
- Schenk, R. U., & Hildebrandt, A. C. (1972). Medium and techniques for induction and growth of monocotyledonous and dicotyledonous plant cell cultures. *Canadian Journal of Botany*, 50(1).
- Scherr, C., Simon, M., Spranger, J., & Baumgartner, S. (2007). Duckweed (*Lemna gibba* L.) as a test organism for homeopathic potencies. *Journal of Alternative and Complementary Medicine*, 13(9).
- Segraves, K. A. (2017). The effects of genome duplications in a community context. In *New Phytologist*, 215(1).
- Shang, S., Zhang, Z., Li, L., Chen, J., Zang, Y., Liu, X., Wang, J., & Tang, X. (2022). Transcriptome analysis reveals genes expression pattern of *Spirodela polyrhiza* response to heat stress. *International Journal of Biological Macromolecules*.
- Silva, G. G., Green, A. J., Weber, V., Hoffmann, P., Lovas-Kiss, Stenert, C., & Maltchik, L. (2018). Whole angiosperms *Wolffia columbiana* disperse by gut passage through wildfowl in South America. *Biology Letters*, 14(12).
- Simon Andrews. (2020). Babraham Bioinformatics - FastQC A Quality Control tool for High Throughput Sequence Data. *Soil*, 5(1).
- Soltis, P. S., Marchant, D. B., Van de Peer, Y., & Soltis, D. E. (2015). Polyploidy and genome evolution in plants. In *Current Opinion in Genetics and Development*, 35.
- Song, Y., Chen, Q., Ci, D., Shao, X., & Zhang, D. (2014). Effects of high temperature on photosynthesis and related gene expression in poplar. *BMC Plant Biology*, 14(1).
- Soñta, M., Rekiel, A., & Batorska, M. (2019). Use of Duckweed (*Lemna* L.) in Sustainable Livestock Production and Aquaculture - A Review. *Annals of Animal Science*, 19(2).
- Sree, K. S., & Appenroth, K. (2014). Increase of starch accumulation in the duckweed *Lemna minor* under abiotic stress. *Albanian Journal of Agriculture Science, Special Edition*.
- Sree, K. S., Sudakaran, S., & Appenroth, K. J. (2015). How fast can angiosperms grow? Species and

- clonal diversity of growth rates in the genus *Wolffia* (Lemnaceae). *Acta Physiologiae Plantarum*, 37(10).
- Stewart, J. J., Adams, W. W., López-Pozo, M., Doherty Garcia, N., McNamara, M., Escobar, C. M., & Demmig-Adams, B. (2021). Features of the duckweed *Lemna* that support rapid growth under extremes of light intensity. *Cells*, 10(6).
- Strzałek, M., & Kufel, L. (2021). Light intensity drives different growth strategies in two duckweed species: *Lemna minor* L. and *Spirodela polyrhiza* (L.) Schleiden. *PeerJ*, 9.
- Su, C., Jiang, Y., Yang, Y., Zhang, W., & Xu, Q. (2019). Responses of duckweed (*Lemna minor* L.) to aluminum stress: Physiological and proteomics analyses. *Ecotoxicology and Environmental Safety*, 170.
- Sun, Q., Nan, C., Dai, L., Ji, N., & Xiong, L. (2014). Effect of sugar alcohol on physicochemical properties of wheat starch. *Standardization News*, 66(9–10).
- Suzuki, N., & Mittler, R. (2006). Reactive oxygen species and temperature stresses: A delicate balance between signaling and destruction. In *Physiologia Plantarum*, 126(1).
- Sweetlove, L. J., Lytovchenko, A., Morgan, M., Nunes-Nesi, A., Taylor, N. L., Baxter, C. J., Eickmeier, I., & Fernie, A. R. (2006). Mitochondrial uncoupling protein is required for efficient photosynthesis. *Proceedings of the National Academy of Sciences of the United States of America*, 103(51).
- Tan, X., Chen, S., Fang, Y., Liu, P., Hu, Z., Jin, Y., Yi, Z., He, K., Li, X., Zhao, L., Wang, H., & Zhao, H. (2022). Rapid and Highly Efficient Genetic Transformation and Application of Interleukin-17B Expressed in Duckweed as Mucosal Vaccine Adjuvant. *Biomolecules*, 12(12).
- Tavares, F. D. A., Rodrigues, J. B. R., Fracalossi, D. M., Esquivel, J., & Roubach, R. (2008). Dried duckweed and commercial feed promote adequate growth performance of tilapia fingerlings. *Biotemas*, 21(3).
- Taylor, L., Nunes-Nesi, A., Parsley, K., Leiss, A., Leach, G., Coates, S., Wingler, A., Fernie, A. R., & Hibberd, J. M. (2010). Cytosolic pyruvate,orthophosphate dikinase functions in nitrogen remobilization during leaf senescence and limits individual seed growth and nitrogen content. *Plant Journal*, 62(4).
- Tesseraud, S., Peresson, R., Lopes, J., & Chagneau, A. M. (1996). Dietary lysine deficiency greatly affects muscle and liver protein turnover in growing chickens. *British Journal of Nutrition*, 75(6), 853–865.

- Thu, P. T. L., Huong, P. T., Tien, V. Van, Ham, L. H., & Khanh, T. D. (2015). Regeneration and Transformation of Gene Encoding the Hemagglutinin Antigen of the H5N1 Virus in Frond of Duckweed (*Spirodela polyrhiza* L.). *Journal of Agricultural Studies*, 3(1).
- Tian, X., Fang, Y., Jin, Y., Yi, Z., Li, J., Du, A., He, K., Huang, Y., & Zhao, H. (2021). Ammonium detoxification mechanism of ammonium-tolerant duckweed (*Landoltia punctata*) revealed by carbon and nitrogen metabolism under ammonium stress. *Environmental Pollution*, 277.
- Tippery, N. P., Les, D. H., & Crawford, D. J. (2015). Evaluation of phylogenetic relationships in Lemnaceae using nuclear ribosomal data. *Plant Biology*, 17(s1), 50–58.
- Trapnell, C., Williams, B. A., Pertea, G., Mortazavi, A., Kwan, G., Van Baren, M. J., Salzberg, S. L., Wold, B. J., & Pachter, L. (2010). Transcript assembly and quantification by RNA-Seq reveals unannotated transcripts and isoform switching during cell differentiation. *Nature Biotechnology*, 28(5).
- Tula, S., Shahinnia, F., Melzer, M., Rutten, T., Gómez, R., Lodeyro, A. F., von Wirén, N., Carrillo, N., & Hajirezaei, M. R. (2020). Providing an Additional Electron Sink by the Introduction of Cyanobacterial Flavodiirons Enhances Growth of *A. thaliana* Under Various Light Intensities. *Frontiers in Plant Science*, 11.
- Ullah, H., Gul, B., Khan, H., Akhtar, N., Rehman, K. U., & Zeb, U. (2022). Effect of growth medium nitrogen and phosphorus on nutritional composition of *Lemna minor* (an alternative fish and poultry feed). *BMC Plant Biology*, 22(1).
- Ullah, H., Gul, B., Khan, H., & Zeb, U. (2021). Effect of salt stress on proximate composition of duckweed (*Lemna minor* L.). *Heliyon*, 7(6).
- Uruç Parlak, K., & Demirezen Yilmaz, D. (2012). Response of antioxidant defences to Zn stress in three duckweed species. *Ecotoxicology and Environmental Safety*, 85.
- Van, B. H., Men, L. T., Son, V. Van, & Preston, T. R. (1997). Duckweed (*Lemna* spp) as protein supplement in an ensiled cassava root diet for fattening pigs. *Livestock Research for Rural Development*, 9(1).
- Van De Peer, Y., Mizrachi, E., & Marchal, K. (2017). The evolutionary significance of polyploidy. In *Nature Reviews Genetics*, 18(7).
- Van Der Heide, T., Roijackers, R. M. M., Peeters, E. T. H. M., & Van Nes, E. H. (2006). Experiments with duckweed-moth systems suggest that global warming may reduce rather than promote herbivory. *Freshwater Biology*, 51(1).

- Van Der Heijden, I., Monteyne, A. J., Stephens, F. B., & Wall, B. T. (2023). Alternative dietary protein sources to support healthy and active skeletal muscle aging. In *Nutrition Reviews*, 81(2).
- Van Hoeck, A., Horemans, N., Monsieurs, P., Cao, H. X., Vandenhove, H., & Blust, R. (2015). The first draft genome of the aquatic model plant *Lemna minor* opens the route for future stress physiology research and biotechnological applications. *Biotechnology for Biofuels*.
- Von Bingen, H. (1933). *Ursachen und Behandlung der Krankheiten (Causa et Curae). (Reasons and Treatment of Diseases)*.
- Von Der Fecht-Bartenbach, J., Bogner, M., Dynowski, M., & Ludewig, U. (2010). CLC-b-Mediated NO₃⁻/H⁺ Exchange Across the Tonoplast of *Arabidopsis* Vacuoles. *Plant and Cell Physiology*, 51(6).
- Vunsh, R., Heinig, U., Malitsky, S., Aharoni, A., Avidov, A., Lerner, A., & Edelman, M. (2015). Manipulating duckweed through genome duplication. *Plant Biology*, 17(1).
- Wahid, A., Gelani, S., Ashraf, M., & Foolad, M. R. (2007). Heat tolerance in plants: An overview. In *Environmental and Experimental Botany*, 61(3).
- Wang, K. T., Hong, M. C., Wu, Y. S., & Wu, T. M. (2021). Agrobacterium-mediated genetic transformation of taiwanese isolates of *lemna aequinoctialis*. *Plants*, 10(8).
- Wang, Q. L., Chen, J. H., He, N. Y., & Guo, F. Q. (2018). Metabolic reprogramming in chloroplasts under heat stress in plants. In *International Journal of Molecular Sciences*, 19(3).
- Wang, W., Haberer, G., Gundlach, H., Gläßer, C., Nussbaumer, T., Luo, M. C., Lomsadze, A., Borodovsky, M., Kerstetter, R. A., Shanklin, J., Byrant, D. W., Mockler, T. C., Appenroth, K. J., Grimwood, J., Jenkins, J., Chow, J., Choi, C., Adam, C., Cao, X. H., ... Messing, J. (2014). The *Spirodela polyrhiza* genome reveals insights into its neotenus reduction fast growth and aquatic lifestyle. *Nature Communications*.
- Wang, Wenguo, Li, R., Zhu, Q., Tang, X., & Zhao, Q. (2016). Transcriptomic and physiological analysis of common duckweed *Lemna minor* responses to NH₄⁺ toxicity. *BMC Plant Biology*.
- Wang, Wenlei, Teng, F., Lin, Y., Ji, D., Xu, Y., Chen, C., & Xie, C. (2018). Transcriptomic study to understand thermal adaptation in a high temperature-tolerant strain of *Pyropia haitanensis*. *PLoS ONE*, 13(4).
- Wang, Wenqin, Kerstetter, R. A., & Michael, T. P. (2011). Evolution of Genome Size in Duckweeds (Lemnaceae). *Journal of Botany*.
- Wang, Wenqin, & Messing, J. (2011). High-Throughput sequencing of three Lemnoideae (duckweeds)

- chloroplast genomes from total DNA. *PLoS ONE*, 6(9).
- Wang, Wenqin, Wu, Y., Yan, Y., Ermakova, M., Kerstetter, R., & Messing, J. (2010). DNA barcoding of the Lemnaceae, a family of aquatic monocots. *BMC Plant Biology*, 10(1), 205.
- Wang, Xiao, Xin, C., Cai, J., Zhou, Q., Dai, T., Cao, W., & Jiang, D. (2016). Heat priming induces trans-generational tolerance to high temperature stress in wheat. *Frontiers in Plant Science*, 7.
- Wang, Xiaoli, Xu, C., Cai, X., Wang, Q., & Dai, S. (2017). Heat-responsive photosynthetic and signaling pathways in plants: Insight from proteomics. In *International Journal of Molecular Sciences*, 18(10).
- Ward, D. B., & Hall, D. W. (2010). Keys to the flora of Florida --25, Lemnaceae. *Phytologia*, 92(2), 241–248.
- Welfle, A., Thornley, P., & Röder, M. (2020). A review of the role of bioenergy modelling in renewable energy research & policy development. *Biomass and Bioenergy*, 136.
- White, S. L., & Wise, R. R. (1998). Anatomy and ultrastructure of *Wolffia columbiana* and *Wolffia borealis*, two nonvascular aquatic angiosperms. *International Journal of Plant Sciences*, 159(2).
- WHO. (2007). Protein and amino acid requirements in human nutrition. In *World Health Organization technical report series* (935).
- Wilson, P. C., & Koch, R. (2013). Influence of exposure concentration and duration on effects and recovery of *Lemna minor* exposed to the herbicide norflurazon. *Archives of Environmental Contamination and Toxicology*, 64(2).
- Witkowska, Z., Saeid, A., Chojnacka, K., Dobrzański, Z., Górecki, H., Michalak, I., Korczyński, M., & Opaliński, S. (2012). New biological dietary feed supplement for laying hens with microelements based on duckweed (*Lemna minor*). *American Journal of Agricultural and Biological Science*, 7(4).
- WormWeb.org - Welcome - by nikhil bhatla. (n.d.). Retrieved February 29, 2024, from <http://wormweb.org/>
- Xu, G., Fan, X., & Miller, A. J. (2012). Plant nitrogen assimilation and use efficiency. In *Annual Review of Plant Biology*, 63.
- Xu, Jiele, Cui, W., Cheng, J. J., & Stomp, A. M. (2011). Production of high-starch duckweed and its conversion to bioethanol. *Biosystems Engineering*. 110(2), 67-72.
- Xu, Jingwen, Shen, Y., Zheng, Y., Smith, G., Sun, X. S., Wang, D., Zhao, Y., Zhang, W., & Li, Y. (2023).

- Duckweed (Lemnaceae) for potentially nutritious human food: A review. In *Food Reviews International*, 39(7).
- Xu, Shuqing, Stapley, J., Gablenz, S., Boyer, J., Appenroth, K. J., Sree, K. S., Gershenzon, J., Widmer, A., & Huber, M. (2019). Low genetic variation is associated with low mutation rate in the giant duckweed. *Nature Communications*, 10(1).
- Xu, Siyu, Chen, J., Peng, H., Leng, S., Li, H., Qu, W., Hu, Y., Li, H., Jiang, S., Zhou, W., & Leng, L. (2021). Effect of biomass type and pyrolysis temperature on nitrogen in biochar, and the comparison with hydrochar. *Fuel*, 291.
- Yamaya, T., & Kusano, M. (2014). Evidence supporting distinct functions of three cytosolic glutamine synthetases and two NADH-glutamate synthases in rice. In *Journal of Experimental Botany*, 65(19).
- Yang, G. L., Feng, D., Liu, Y. T., Lv, S. M., Zheng, M. M., & Tan, A. J. (2021). Research progress of a potential bioreactor: Duckweed. In *Biomolecules*, 11(1).
- Yin, X. M., Luo, W., Wang, S. W., Shen, Q. R., & Long, X. H. (2014). Effect of Nitrogen Starvation on the Responses of Two Rice Cultivars to Nitrate Uptake and Utilization. *Pedosphere*, 24(5).
- Yin, Y., Yu, C., Yu, L., Zhao, J., Sun, C., Ma, Y., & Zhou, G. (2015). The influence of light intensity and photoperiod on duckweed biomass and starch accumulation for bioethanol production. *Bioresource Technology*, 187.
- Yoshida, T., Ohama, N., Nakajima, J., Kidokoro, S., Mizoi, J., Nakashima, K., Maruyama, K., Kim, J. M., Seki, M., Todaka, D., Osakabe, Y., Sakuma, Y., SchöZ, F., Shinozaki, K., & Yamaguchi-Shinozaki, K. (2011). Arabidopsis HsfA1 transcription factors function as the main positive regulators in heat shock-responsive gene expression. *Molecular Genetics and Genomics*, 286(5–6).
- Young, M. D., Wakefield, M. J., Smyth, G. K., & Oshlack, A. (2010). Gene ontology analysis for RNA-seq: accounting for selection bias. *Genome Biology*, 11(2).
- Yousefi, S., Marchese, A., Salami, S. A., Benny, J., Giovino, A., Perrone, A., Caruso, T., Gholami, M., Sarikhani, H., Buti, M., & Martinelli, F. (2022). Identifying conserved genes involved in crop tolerance to cold stress. *Functional Plant Biology*, 49(10).
- Yu, J., Li, R., Fan, N., Yang, Z., & Huang, B. (2017). Metabolic pathways involved in carbon dioxide enhanced heat tolerance in bermudagrass. *Frontiers in Plant Science*, 8.
- Yue, X., Ke, X., Shi, Y., Li, Y., Zhang, C., Wang, Y., & Hou, X. (2023). Chloroplast inner envelope protein

- FtsH11 is involved in the adjustment of assembly of chloroplast ATP synthase under heat stress. *Plant Cell and Environment*, 46(3).
- Zha, Q., Yin, X., Xi, X., & Jiang, A. (2023). Heterologous VvDREB2c Expression Improves Heat Tolerance in *Arabidopsis* by Inducing Photoprotective Responses. *International Journal of Molecular Sciences*, 24(6).
- Zhang, Haizhen, Yang, J., Li, D., Wei, M., & Li, C. (2019). PtHSFA4a gene play critical roles in the adaptation of *Arabidopsis thaliana* plants to high-Zinc stress. *Plant Signaling and Behavior*, 14(10).
- Zhang, Hengfeng, Wang, X. C., Zheng, Y., & Dzakpasu, M. (2023). Removal of pharmaceutical active compounds in wastewater by constructed wetlands: Performance and mechanisms. In *Journal of Environmental Management*, 325.
- Zhang, X., Cai, J., Wollenweber, B., Liu, F., Dai, T., Cao, W., & Jiang, D. (2013). Multiple heat and drought events affect grain yield and accumulations of high molecular weight glutenin subunits and glutenin macropolymers in wheat. *Journal of Cereal Science*, 57(1).
- Zhao, L., & Wang, Y. (2017). Nitrate Assay for Plant Tissues. *BIO-PROTOCOL*, 7(2).
- Zhou, Y., Chen, G., Peterson, A., Zha, X., Cheng, J., Li, S., Cui, D., Zhu, H., Kishchenko, O., & Borisjuk, N. (2018). Biodiversity of Duckweeds in Eastern China and Their Potential for Bioremediation of Municipal and Industrial Wastewater. *Journal of Geoscience and Environment Protection*, 6(03).
- Zhou, Y., Kishchenko, O., Stepanenko, A., Chen, G., Wang, W., Zhou, J., Pan, C., & Borisjuk, N. (2022). The dynamics of NO_3^- and NH_4^+ uptake in duckweed are coordinated with the expression of major nitrogen assimilation genes. *Plants*, 11(1).
- Zhou, Y., Stepanenko, A., Kishchenko, O., Xu, J., & Borisjuk, N. (2023). Duckweeds for Phytoremediation of Polluted Water. In *Plants*, 12(3).
- Ziegler, P., Adelman, K., Zimmer, S., Schmidt, C., & Appenroth, K. J. (2015). Relative in vitro growth rates of duckweeds (Lemnaceae) - the most rapidly growing higher plants. *Plant Biology*, 17(1).
- Zifarelli, G., & Pusch, M. (2009). Conversion of the 2 $\text{Cl}^-/1 \text{H}^+$ antiporter CIC-5 in a NO_3^-/H^+ antiporter by a single point mutation. *EMBO Journal*, 28(3).
- Zimmo, O. R., Van Der Steen, N. P., & Gijzen, H. J. (2004). Nitrogen mass balance across pilot-scale algae and duckweed-based wastewater stabilisation ponds. *Water Research*, 38(4).
- Zschiesche, W., Barth, O., Daniel, K., Böhme, S., Rausche, J., & Humbeck, K. (2015). The zinc-binding

nuclear protein HIPP3 acts as an upstream regulator of the salicylate-dependent plant immunity pathway and of flowering time in *Arabidopsis thaliana*. *New Phytologist*, 207(4).

Appendices

Appendix 1 – Supplementary Materials

Page 1 7796_psbK-psbI, DG4_psbK-psbI, DG8_psbK-psbI, L.gibba_psbK-psbI, SD_psbK-psbI

```
1
L.minor_p... ttagcatttggttggcaagctgctgtaagttttcgataaagttattaaaaactctactgaaaaaattcatgatttatttgata 82
DG4_psbK-... TTAGCAITTTGTTGGCAAGCTGCTGTAAGTTTCGATAAAGTTATTAAAACCTCTACTGAAAAAATTCATGATTTATTGATA
DG8_psbK-... TTAGCAITTTGTTGGCAAGCTGCTGTAAGTTTCGATAAAGTTATTAAAACCTCTACTGAAAAAATTCATGATTTATTGATA
SD_psbK-psbI TTAGCAITTTGTTGGCAAGCTGCTGTAAGTTTCGATAAAGTTATTAAAACCTCTACTGAAAAAATTCATGATTTATTGATA
L.gibba_p... TTAGCAITTTGTTGGCAAGCTGCTGTAAGTTTCGATAAAGTTATTAAAACCTCTACTGAAAAAATTCATGATTTATTGATA
7796_psbK... TTAGCAITTTGTTGGCAAGCTGCTGTAAGTTTCGATAAAGTTATTAAAACCTCTACTGAAAAAATTCATGATTTATTGATA
.....

83
L.minor_p... aaaaagatttctaataaaaaattgataacgtagtgcgaatcttagtttatcacatcctcatasaaaattttgaattcttctgtata 164
DG4_psbK-... AAAAAAGATTCTAATAAAAAATTGATAACGTAGTAGCAATCTTAGTTTATACATCCCTATAAAAAATATTGAAITCTTGTGATA
DG8_psbK-... AAAAAAGATTCTAATAAAAAATTGATAACGTAGTAGCAATCTTAGTTTATACATCCCTATAAAAAATATTGAAITCTTGTGATA
SD_psbK-psbI AAAAAAGATTCTAATAAAAAATTGATAACGTAGTAGCAATCTTAGTTTATACATCCCTATAAAAAATATTGAAITCTTGTGATA
L.gibba_p... AAAAAAGATTCTAATAAAAAATTGATAACGTAGTAGCAATCTTAGTTTATACATCCCTATAAAAAATATTGAAITCTTGTGATA
7796_psbK... AAAAAAGATTCTAATAAAAAATTGATAACGTAGTAGCAATCTTAGTTTATACATCCCTATAAAAAATATTGAAITCTTGTGATA
.....

165
L.minor_p... ttggataaaaaagagcgataaagtttggatcagtcacatttgcgcttctggcgcctcttccagtgaggaagtactttattttatt 246
DG4_psbK-... TTGGATAAAAAGAGCGATAAGTTTGGATCAGTCCATTTGCGCGTTCGGCCGCTCTCCAGTGAGGAAGTACTTTATTATT
DG8_psbK-... TTGGATAAAAAGAGCGATAAGTTTGGATCAGTCCATTTGCGCGTTCGGCCGCTCTCCAGTGAGGAAGTACTTTATTATT
SD_psbK-psbI TTGGATAAAAAGAGCGATAAGTTTGGATCAGTCCATTTGCGCGTTCGGCCGCTCTCCAGTGAGGAAGTACTTTATTATT
L.gibba_p... TTGGATAAAAAGAGCGATAAGTTTGGATCAGTCCATTTGCGCGTTCGGCCGCTCTCCAGTGAGGAAGTACTTTATTATT
7796_psbK... TTGGATAAAAAGAGCGATAAGTTTGGATCAGTCCATTTGCGCGTTCGGCCGCTCTCCAGTGAGGAAGTACTTTATTATT
.....

247
L.minor_p... tattagcttttggttttacacaatactttattgtaaatattagagttatattagaataaacctttttggtaaacgaaacagtc 328
DG4_psbK-... TATTAGCTTTTGGTTTACACAATACITTTATTGTTAATATTAGAGTTAATATTAGAATAAACCTTTTGGTAACGAACAAGTCA
DG8_psbK-... TATTAGCTTTTGGTTTACACAATACITTTATTGTTAATATTAGAGTTAATATTAGAATAAACCTTTTGGTAACGAACAAGTCA
SD_psbK-psbI TATTAGCTTTTGGTTTACACAATACITTTATTGTTAATATTAGAGTTAATATTAGAATAAACCTTTTGGTAACGAACAAGTCA
L.gibba_p... TATTAGCTTTTGGTTTACACAATACITTTATTGTTAATATTAGAGTTAATATTAGAATAAACCTTTTGGTAACGAACAAGTCA
7796_psbK... TATTAGCTTTTGGTTTACACAATACITTTATTGTTAATATTAGAGTTAATATTAGAATAAACCTTTTGGTAACGAACAAGTCA
.....

329
L.minor_p... taactttaatttaaaatgcatttcagtttgaaaaatcagtttttggtagaaaaaacactaaacttaatactatacttaata 410
DG4_psbK-... TAATCTTAATTTAAAATGCATTCATGAGTTTGAAAATTCAGTTTTGTAGAAAAAACACTAAACTTAATACTATACTTAAT
DG8_psbK-... TAATCTTAATTTAAAATGCATTCATGAGTTTGAAAATTCAGTTTTGTAGAAAAAACACTAAACTTAATACTATACTTAAT
SD_psbK-psbI TAATCTTAATTTAAAATGCATTCATGAGTTTGAAAATTCAGTTTTGTAGAAAAAACACTAAACTTAATACTATACTTAAT
L.gibba_p... TAATCTTAATTTAAAATGCATTCATGAGTTTGAAAATTCAGTTTTGTAGAAAAAACACTTAACTTAACTAT====AA
7796_psbK... TAATCTTAATTTAAAATGCATTCATGAGTTTGAAAATTCAGTTTTGTAGAAAAAACACTTAACTTAACTAT====AA
.....

411
L.minor_p... aaaaataaagaattgtcttttatttttcatagtttttttcttggcatgcccaataatacatgtgttacataactcaaatg 492
DG4_psbK-... AAAATAAAGAATTGTCTTTTATTITTCATAGTTTTTTTTCTTGGCATGCCCAATAATAACATGTGTACATAACTCAAATG
DG8_psbK-... AAAATAAAGAATTGTCTTTTATTITTCATAGTTTTTTTTCTTGGCATGCCCAATAATAACATGTGTACATAACTCAAATG
SD_psbK-psbI AAAATAAAGAATTGTCTTTTATTITTCATAGTTTTTTTTCTTGGCATGCCCAATAATAACATGTGTACATAACTCAAATG
L.gibba_p... AAAATAAAGAATTGTCTTTTATTITTCATAGTTTTTTTTCTTGGCATGCCCAATAATAATAATGTGTACATAACTCAAATG
7796_psbK... AAAATAAAGAATTGTCTTTTATTITTCATAGTTTTTTTTCTTGGCATGCCCAATAATAATAATGTGTACATAACTCAAATG
.....

493
L.minor_p... gataatctattcccttttaaccccaaaaatgatcctatcttggagatttggtaaatgctta 551
DG4_psbK-... GATAATCTATTCCCTTTTAAACCCAAAAATGATCCTATCTTGGAGATTGGTAATGCTTA
DG8_psbK-... GATAATCTATTCCCTTTTAAACCCAAAAATGATCCTATCTTGGAGATTGGTAATGCTTA
SD_psbK-psbI GATAATCTATTCCCTTTTAAACCCAAAAATGATCCTATCTTGGAGATTGGTAATGCTTA
L.gibba_p... GATAATCTATTCCCTTTTAAACCCAAAAATGATCCTATCTTGGAGATTGGTAATGCTTA
7796_psbK... GATAATCTATTCCCTTTTAAACCCAAAAATGATCCTATCTTGGAGATTGGTAATGCTTA
.....
```

Figure S.1. Identification and barcoding of four *Lemna* clones used in the study through *psbK-psbI* intergenic spacers. The clones DG4, DG8, and SD were identified as *Lemna minor*, and clone 7796 was identified as *Lemna gibba*. Identification was performed by sequencing the *psbK-psbI* intergenic spacers and comparing them with the CoGe sequence database.

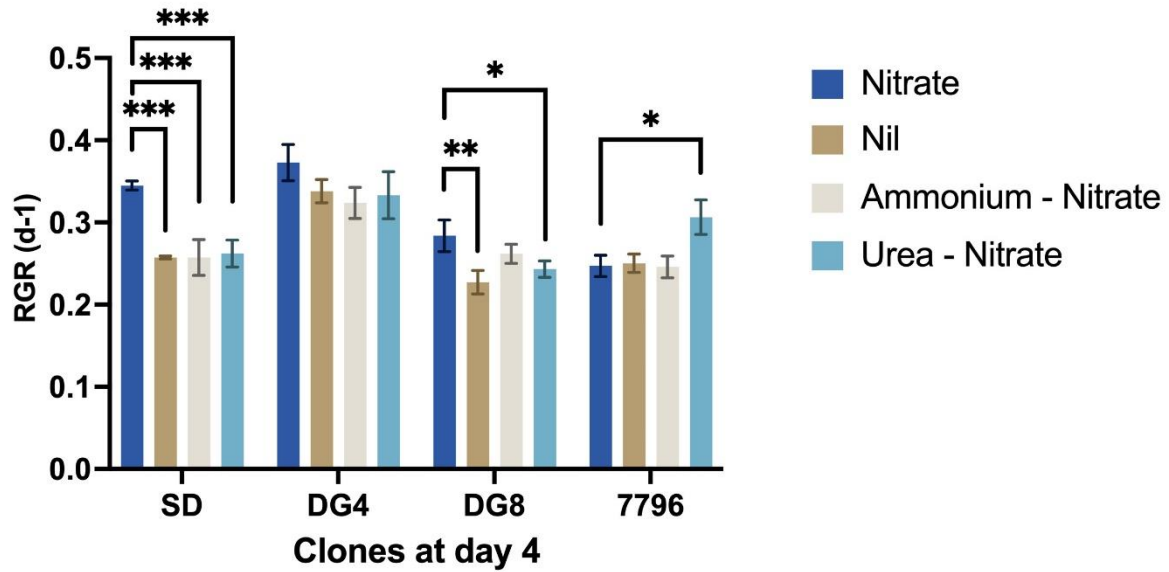


Figure S.3. Relative Growth Rate (RGR) of duckweed clones (SD, DG4, DG8, 7796) grown under different Nitrogen sources at day 4. Bars represent the mean RGR of three biological replicates, with standard errors shown. Asterisks denote significant differences compared to the control (Nitrate), as determined by student t-test analysis: * $p < 0.05$, ** $p < 0.01$, *** $p < 0.001$, **** $p < 0.0001$. The four nitrogen conditions tested were Nitrate (control), Nil (negative control with no nitrogen), Ammonium-Nitrate, and Urea-Nitrate.

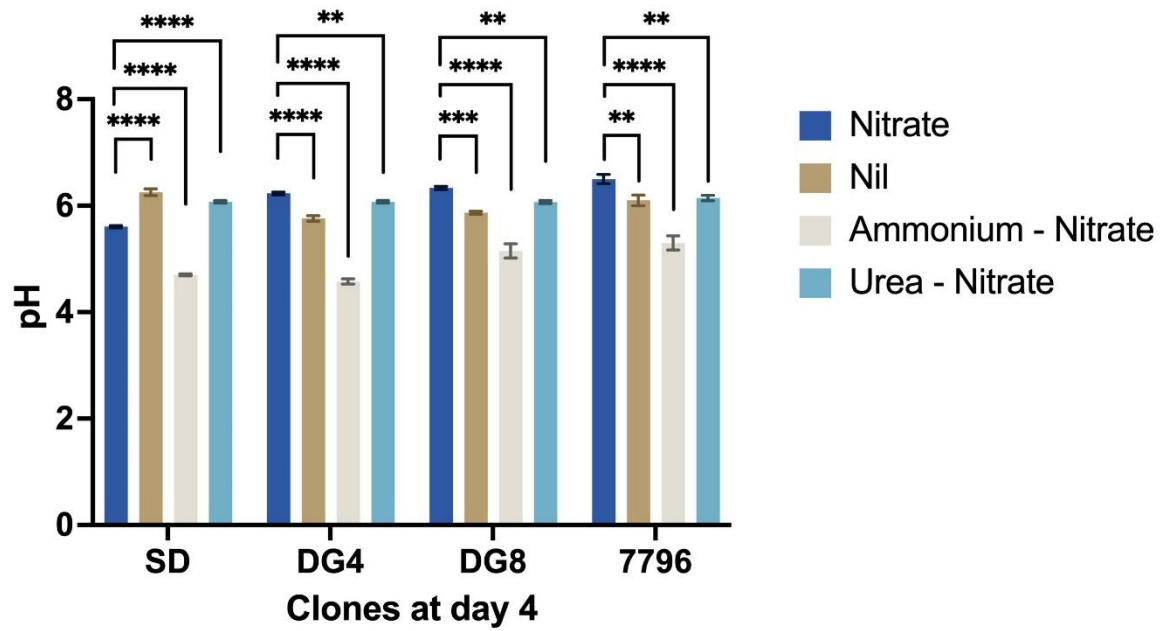


Figure S.4. Variation in medium pH for duckweed clones (SD, DG4, DG8, 7796) grown under different Nitrogen sources on day 4. Bars represent the mean pH values of the growth medium from three biological replicates, with standard error (SE) shown. Asterisks denote significant differences compared to the control (Nitrate), as determined by student t-test analysis: * $p < 0.05$, ** $p < 0.01$, *** $p < 0.001$, **** $p < 0.0001$. The four nitrogen conditions tested were Nitrate (control), Nil (negative control with no nitrogen), Ammonium-Nitrate, and Urea-Nitrate.

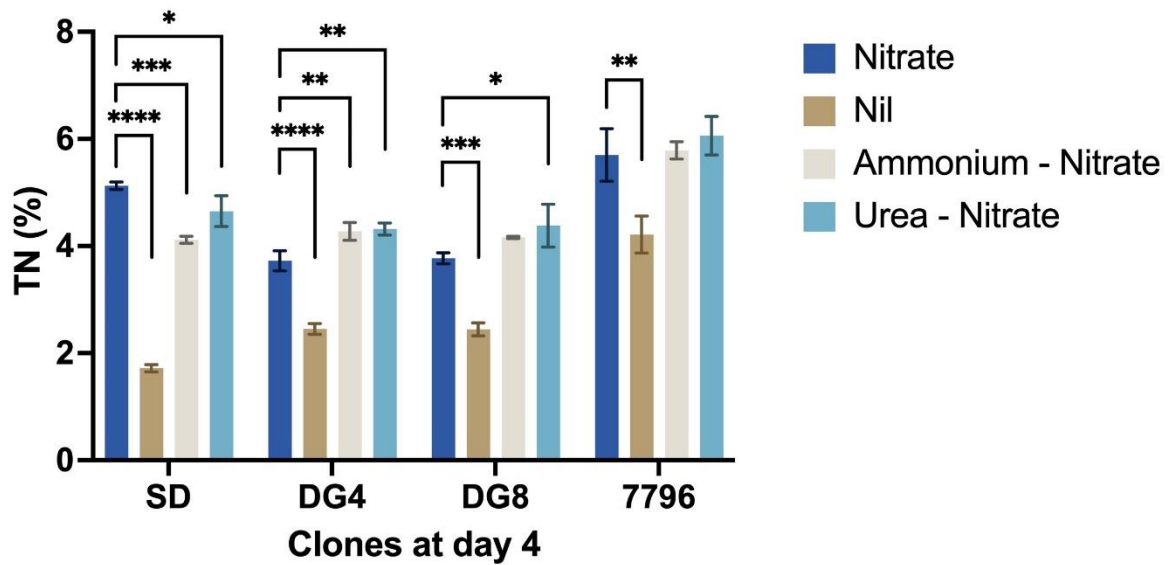


Figure S.5. Total Nitrogen content (%) in duckweed clones (SD, DG4, DG8, 7796) grown under different Nitrogen sources on day 4. Bars represent the mean total nitrogen content from three biological replicates, with standard error (SE) shown. Asterisks denote significant differences compared to the control (Nitrate), as determined by student t-test analysis: * $p < 0.05$, ** $p < 0.01$, *** $p < 0.001$, **** $p < 0.0001$. The four nitrogen conditions tested were Nitrate (control), Nil (negative control with no nitrogen), Ammonium-Nitrate, and Urea-Nitrate.

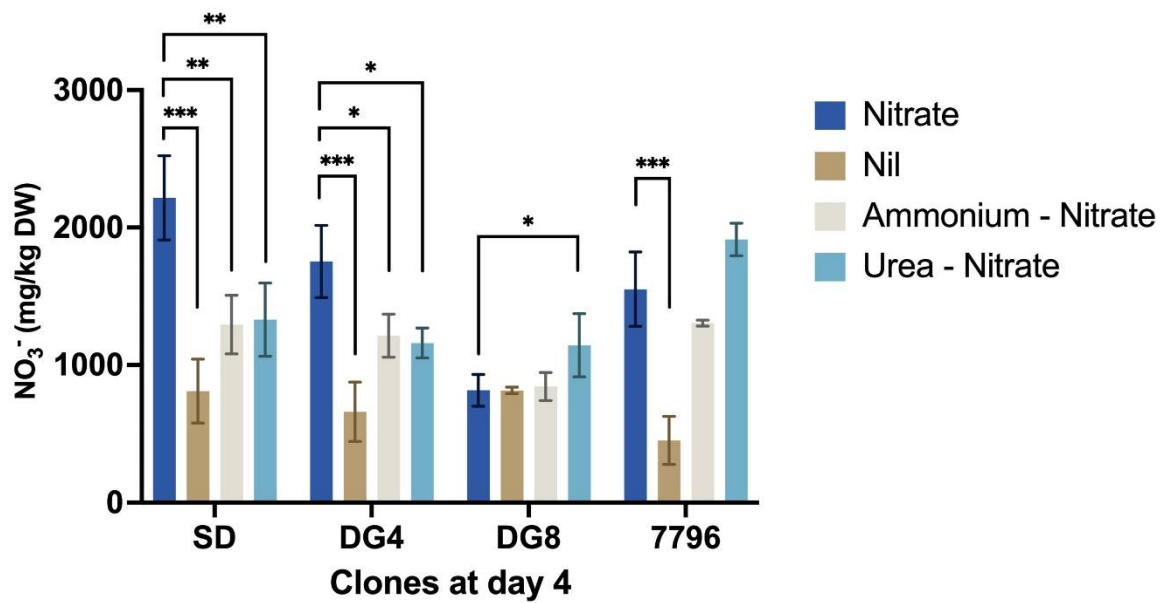


Figure S.6. Total Nitrate content (mg NO₃⁻/kg DW) in duckweed clones (SD, DG4, DG8, 7796) grown under different Nitrogen sources at day 4. Bars represent the mean total nitrate content from three biological replicates, with standard error (SE) shown. Asterisks denote significant differences compared to the control (Nitrates), as determined by student t-test analysis: *p < 0.05, **p < 0.01, ***p < 0.001, ****p < 0.0001. The four nitrogen conditions tested were Nitrates (control), Nil (negative control with no nitrogen), Ammonium-Nitrate, and Urea-Nitrate.

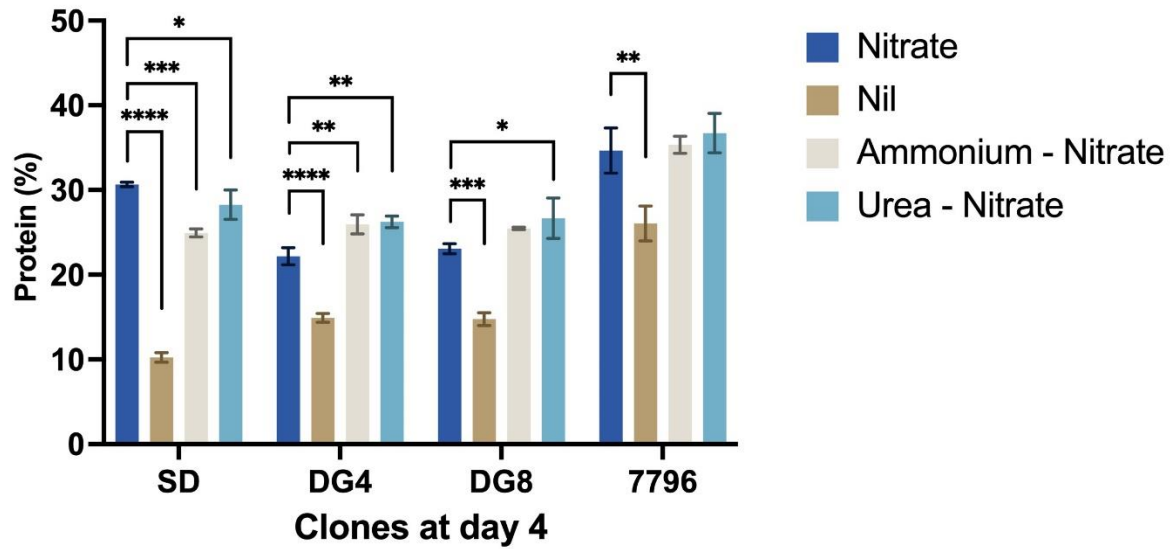


Figure S.7. Total Protein content (%) in duckweed clones (SD, DG4, DG8, 7796) grown under different Nitrogen sources at day 4. Bars represent the mean total protein content from three biological replicates, with standard error (SE) shown. Asterisks denote significant differences compared to the control (Nitrate), as determined by student t-test analysis: * $p < 0.05$, ** $p < 0.01$, *** $p < 0.001$, **** $p < 0.0001$. The four nitrogen conditions tested were Nitrate (control), Nil (negative control with no nitrogen), Ammonium-Nitrate, and Urea-Nitrate.

Table S.1. List of species, nitrogen assimilation proteins, and their accession numbers. This table presents the species analysed (*A. thaliana*, *B. distachyon*, *N. nucifera*, *O. sativa*, *S. bicolor*, and *S. polyrhiza*), the nitrogen assimilation-related proteins (NR, NiR, GS1, GS2, Fd-GOGAT, NADH-GOGAT, and CLCA), and their corresponding accession numbers.

Species	Proteins	Accession number	Species	Proteins	Accession number
<i>A. thaliana</i>	AtNR1	NP_177899.1	<i>S. bicolor</i>	SbGS1;3	XP_021306978.1
<i>A. thaliana</i>	AtNR2	NP_174901.1	<i>S. polyrhiza</i>	SpGS1;1	UJI64963.1
<i>B. distachyon</i>	BdNR1	XP_003570548.1	<i>S. polyrhiza</i>	SpGS1;2	UJI64964.1
<i>B. distachyon</i>	BdNR2	XP_003574607.1	<i>S. polyrhiza</i>	SpGS1;3	UJI64965.1
<i>N. nucifera</i>	NnNR1	XP_010246478	<i>A. thaliana</i>	AtGS2	NP_001031969.1
<i>N. nucifera</i>	NnNR2	XP_010245911	<i>B. distachyon</i>	BdGS2	XP_003580719.1
<i>O. sativa</i>	OsNR1	XP_015622710.1	<i>H. vulgare</i>	HvGS2	P13564.2
<i>O. sativa</i>	OsNR2	XP_015650300.1	<i>N. nucifera</i>	NnGS2	XP_010255852.1
<i>O. sativa</i>	OsNR3	XP_015650643.1	<i>O. sativa</i>	OsGS2	XP_015635322.1
<i>S. bicolor</i>	SbNR1	XP_002454625.1	<i>S. bicolor</i>	SbGS2	XP_021319069.1
<i>S. bicolor</i>	SbNR2	XP_002444490.1	<i>S. polyrhiza</i>	SpGS2	UJI64966.1
<i>S. bicolor</i>	SbNR3	XP_002454083.1	<i>A. thaliana</i>	AtFd-GOGAT1	NP_850763.1
<i>S. polyrhiza</i>	SpNR	UJH94654.1	<i>A. thaliana</i>	AtFd-GOGAT2	NP_181655.1
<i>A. thaliana</i>	AtNiR	NP_179164	<i>B. distachyon</i>	BdFd-GOGAT	XP_003559858.1
<i>B. distachyon</i>	BdNiR	XP_003570568	<i>N. nucifera</i>	NnFd-GOGAT	XP_010276670
<i>N. nucifera</i>	NnNiR	XP_010263547	<i>O. sativa</i>	OsFd-GOGAT	XP_015646712.1
<i>O. sativa</i>	OsNiR	NP_001388488.1	<i>S. bicolor</i>	SbFd-GOGAT	XP_002463318.2
<i>S. bicolor</i>	SbNiR	XP_002454602	<i>S. polyrhiza</i>	SpFd-GOGAT	UJI64967.1
<i>S. polyrhiza</i>	SpNiR	UJH94655.1	<i>A. thaliana</i>	AtNADH-GOGAT	NP_200158.2
<i>A. thaliana</i>	AtGS1;1	NP_198576.1	<i>B. distachyon</i>	BdNADH-GOGAT1	XP_003566997.1
<i>A. thaliana</i>	AtGS1;2	NP_176794.1	<i>B. distachyon</i>	BdNADHGOGAT2	XP_024315185.1
<i>A. thaliana</i>	AtGS1;3	NP_188409.1	<i>N. nucifera</i>	NnNADH-GOGAT1	XP_010261570.1
<i>A. thaliana</i>	AtGS1;4	NP_001331815.1	<i>N. nucifera</i>	NnNADH-GOGAT 2	XP_010266511.1
<i>A. thaliana</i>	AtGS1;5	NP_175280.1	<i>O. sativa</i>	OsNADH-GOGAT1	XP_015649242.1
<i>B. distachyon</i>	BdGS1;1	XP_010236151.1	<i>O. sativa</i>	OsNADH-GOGAT2	XP_015640407.1
<i>B. distachyon</i>	BdGS1;2	XP_003560727.2	<i>S. bicolor</i>	SbNADH-GOGAT1	XP_002458326.1
<i>B. distachyon</i>	BdGS1;3	XP_003558466.1	<i>S. bicolor</i>	SbNADH-GOGAT2	XP_021302649.1
<i>N. nucifera</i>	NnGS1;1	XP_010271383.1	<i>S. polyrhiza</i>	SpNADH-GOGAT	UJH94656.1
<i>N. nucifera</i>	NnGS1;2	XP_010271347.1	<i>A. thaliana</i>	AtCLCa1	NP_198905.1
<i>N. nucifera</i>	NnGS1;3	XP_010250142.1	<i>A. thaliana</i>	AtCLCa2	NP_001031990.1
<i>O. sativa</i>	OsGS1;1	XP_015626102.1	<i>B. distachyon</i>	BdCLCa	XP_003576525.1
<i>O. sativa</i>	OsGS1;2	XP_015631679.1	<i>N. nucifera</i>	NnCLCa	XP_010276208
<i>O. sativa</i>	OsGS1;3	XP_015628694.1	<i>O. sativa</i>	OsCLCa	XP_015620662.1
<i>S. bicolor</i>	SbGS1;1	XP_021313946.1	<i>S. bicolor</i>	SbCLCa	XP_002438781.1
<i>S. bicolor</i>	SbGS1;2	XP_002465624.1	<i>S. polyrhiza</i>	SpCLCa	Spipo7G0046500

Table S.2. Summary of clone characteristics and physiological data: Overview of 42 duckweed clones, including their name, species (36 *L. gibba* and 6 *L. minor*), country of origin, and physiological measurements recorded at 20°C and 35°C. Physiological parameters include chlorophyll content (µg/mL), RGR (d⁻¹), total nitrogen (TN, %), total nitrate (NO₃⁻, mg/kg DW), and total protein (%). The gradient provides a visual representation of the significance levels for each parameter comparison. The clones selected for transcriptomic analysis are marked as bold format in the "Clone" column. These include Manor as the control, 6861, 7763, and 7796 as heat-tolerant clones, and 8703 as the heat-sensitive clone.

Clone	Species	Country	Chlorophyll (µg/mL)		RGR (d ⁻¹)		TN (%)		NO ₃ ⁻ (mg/kg DW)		Protein (%)		
			20 °C	35 °C	20 °C	35 °C	20 °C	35 °C	20 °C	35 °C	20 °C	35 °C	
7021	<i>L. gibba</i>	Spain	601.71 ± 10.27	280.1 ± 25.56	0.25 ± 0.004	0.08 ± 0.007	6.81 ± 0.048	4.85 ± 0.01	3547.67 ± 212.11	1146.57 ± 239.02	40.32 ± 0.31	29.63 ± 0.38	ns
7245	<i>L. gibba</i>	South Africa	521.51 ± 51.16	229.54 ± 29.46	0.17 ± 0.009	0.12 ± 0.013	6.62 ± 0.054	4.8 ± 0.06	3813.15 ± 291.61	1204.95 ± 127	39.1 ± 0.17	29.22 ± 0.33	*
7263	<i>L. gibba</i>	Greece	500.02 ± 26.54	150.46 ± 33.61	0.25 ± 0.001	0.1 ± 0.021	6.68 ± 0.025	6.14 ± 0.17	4896.33 ± 92.2	1768.83 ± 200.7	38.67 ± 0.1	37.25 ± 1.16	***
7749	<i>L. gibba</i>	Belgium	691.23 ± 9.4	332.49 ± 70.99	0.2 ± 0.005	0.07 ± 0.023	6.74 ± 0.095	4.65 ± 0.03	5014.98 ± 143.18	1965.77 ± 123.37	38.98 ± 0.63	27.84 ± 0.25	****
8738	<i>L. gibba</i>	Argentina	517.46 ± 66.06	142.42 ± 60.11	0.26 ± 0.005	0.09 ± 0.034	6.75 ± 0.23	5.85 ± 0.25	4130.33 ± 293.47	2034.35 ± 255.15	39.58 ± 1.59	35.26 ± 1.73	****
9481	<i>L. gibba</i>	Denmark	567.35 ± 24.51	324.73 ± 35.58	0.26 ± 0.006	0.1 ± 0.017	6.75 ± 0.116	4.43 ± 0.15	4589.07 ± 332.4	1413.78 ± 260.41	39.29 ± 0.68	26.77 ± 0.76	****
7784	<i>L. gibba</i>	Ethiopia	634.33 ± 6.79	276.01 ± 111.92	0.23 ± 0.005	0.05 ± 0.007	6.8 ± 0.031	3.99 ± 0.22	4287.17 ± 164.83	1908.47 ± 165.18	39.85 ± 0.26	23.74 ± 1.46	
8124	<i>L. gibba</i>	USA	590.4 ± 37.59	291.22 ± 138.68	0.23 ± 0.007	0.07 ± 0.019	6.78 ± 0.024	4.3 ± 0.11	3941 ± 424.93	1859.05 ± 93.07	39.9 ± 0.38	25.69 ± 0.66	
8655	<i>L. gibba</i>	Argentina	580.44 ± 20.93	239.51 ± 82.23	0.24 ± 0.003	0.08 ± 0.009	6.81 ± 0.058	4.72 ± 0.2	3727.22 ± 200.1	1206.84 ± 278.53	40.24 ± 0.3	28.74 ± 1.41	
8682	<i>L. gibba</i>	Saudi-Arabia	485.82 ± 27.03	135.72 ± 49.11	0.25 ± 0.004	0.06 ± 0.012	6.55 ± 0.038	4.94 ± 0.48	4803.42 ± 304.33	1834.77 ± 637.99	37.92 ± 0.33	29.73 ± 2.62	
9248	<i>L. gibba</i>	Italy	533.04 ± 35.95	321.97 ± 53.75	0.23 ± 0.005	0.06 ± 0.015	6.53 ± 0.065	4.4 ± 0.15	4975.23 ± 578.97	1352.1 ± 121.43	37.72 ± 0.53	26.62 ± 0.88	
9255	<i>L. gibba</i>	Finland	580.8 ± 41.01	319.89 ± 20.15	0.23 ± 0.008	0.08 ± 0.01	6.41 ± 0.071	4.27 ± 0.31	4196.63 ± 136.58	1713.67 ± 38.51	37.45 ± 0.42	25.63 ± 1.97	
9583	<i>L. gibba</i>	Poland	550.32 ± 21.47	307.28 ± 26.41	0.27 ± 0.013	0.07 ± 0.023	6.59 ± 0.066	4.09 ± 0.11	3590.72 ± 250.45	843.37 ± 173.67	38.96 ± 0.42	25.03 ± 0.75	
7537	<i>L. gibba</i>	Spain	560.98 ± 7.72	306.98 ± 21.17	0.22 ± 0.013	0.08 ± 0.017	6.97 ± 0.089	5.43 ± 0.28	4799.45 ± 233.76	2133.27 ± 279.64	40.59 ± 0.18	32.6 ± 1.87	
7641	<i>L. gibba</i>	Israel	539.2 ± 19.96	276.56 ± 23.87	0.23 ± 0.025	0.07 ± 0.02	7.07 ± 0.071	5.32 ± 0.47	5179.4 ± 354.11	2069.5 ± 112.97	40.95 ± 0.32	31.99 ± 2.96	
7805	<i>L. gibba</i>	France	546.76 ± 16.13	203.49 ± 30.23	0.2 ± 0.006	0.07 ± 0.016	6.72 ± 0.06	6.26 ± 0.27	4366.65 ± 189.65	1851.33 ± 42.32	39.28 ± 0.36	37.97 ± 1.73	
9532	<i>L. gibba</i>	Germany	544.6 ± 5.91	327.84 ± 73.75	0.21 ± 0.005	0.07 ± 0.013	7.08 ± 0.049	4.94 ± 0.42	5733.4 ± 90.43	2006.47 ± 195.02	40.69 ± 0.25	29.64 ± 2.73	
9591	<i>L. gibba</i>	Hungary	598.01 ± 10.39	457.09 ± 37.94	0.23 ± 0.011	0.11 ± 0.005	7.26 ± 0.034	5.99 ± 0.06	4467.75 ± 225.78	1492.13 ± 151.58	42.6 ± 0.07	36.55 ± 0.4	
Manor	<i>L. gibba</i>	UK	562.87 ± 16.06	403.84 ± 66.79	0.24 ± 0.009	0.1 ± 0.005	7 ± 0.061	5.46 ± 0.19	4577.07 ± 315.43	1317.07 ± 97.97	37.94 ± 0.37	29.61 ± 2.14	
SD	<i>L. minor</i>	UK	527.81 ± 1.62	389.23 ± 74.43	0.23 ± 0.005	0.08 ± 0.005	6.81 ± 0.165	5.42 ± 0.07	5152.27 ± 293.06	1111.06 ± 213.37	39.36 ± 0.91	33.2 ± 0.55	
DG4	<i>L. minor</i>	Ireland	571.36 ± 10.05	341.08 ± 75.96	0.24 ± 0.003	0.09 ± 0.022	6.57 ± 0.019	4.86 ± 0.33	5009.8 ± 506.57	1233.1 ± 131.98	37.94 ± 0.37	29.61 ± 2.14	
DG8	<i>L. minor</i>	Germany	550.08 ± 18.92	256.36 ± 61.85	0.24 ± 0.005	0.05 ± 0.025	6.62 ± 0.149	4.35 ± 0.08	4425.03 ± 57.8	940.18 ± 148.56	38.59 ± 0.89	26.62 ± 0.39	
DG9	<i>L. minor</i>	Iran	568.87 ± 33.95	359.89 ± 52.45	0.25 ± 0.014	0.06 ± 0.008	6.64 ± 0.084	4.71 ± 0.25	3320.97 ± 142.64	673.14 ± 127.12	39.43 ± 0.46	28.99 ± 1.58	
DG10	<i>L. minor</i>	New Zealand	575.55 ± 7.15	221.8 ± 48.64	0.25 ± 0.014	0.06 ± 0.008	6.46 ± 0.197	3.88 ± 0.18	3301.15 ± 386.75	416 ± 185.86	38.29 ± 1	23.98 ± 1.22	
DG12	<i>L. minor</i>	UK	527.31 ± 25.28	332.64 ± 25.18	0.25 ± 0.008	0.1 ± 0.014	6.71 ± 0.007	5.55 ± 0.19	3662.4 ± 283.14	35.15 ± 0.05	39.67 ± 0.13	34.68 ± 1.2	
Colour	<i>L. gibba</i>	UK	612.41 ± 11.56	361.52 ± 14.41	0.24 ± 0.015	0.06 ± 0.005	6.66 ± 0.029	4.61 ± 0.14	3725.77 ± 260.91	711.51 ± 208.61	39.31 ± 0.25	28.34 ± 0.98	
Jen	<i>L. gibba</i>	UK	582.7 ± 6.11	352.72 ± 30.69	0.23 ± 0.008	0.09 ± 0.003	6.44 ± 0.051	5.27 ± 0.11	4373.02 ± 106.74	512.98 ± 474.76	37.52 ± 0.39	32.64 ± 0.38	
Oxley	<i>L. gibba</i>	UK	580.99 ± 38.37	409.16 ± 49.77	0.25 ± 0.01	0.07 ± 0.016	6.62 ± 0.068	5.06 ± 0.39	3580.5 ± 168.39	476.27 ± 243.01	39.15 ± 0.33	31.33 ± 2.57	
Sailor	<i>L. gibba</i>	UK	533.4 ± 19.68	234.61 ± 40.16	0.26 ± 0.003	0.07 ± 0.011	6.9 ± 0.034	3.77 ± 0.02	2889.52 ± 473.87	500.34 ± 382.94	41.29 ± 0.47	23.26 ± 0.3	
Pond	<i>L. gibba</i>	UK	580.3 ± 34.88	249.17 ± 19.08	0.25 ± 0.007	0.05 ± 0.013	6.78 ± 0.088	3.95 ± 0.22	3694.07 ± 613.21	1140.69 ± 361.67	40.04 ± 0.94	23.97 ± 1.46	
5615	<i>L. gibba</i>	Israel	536.86 ± 17.64	130.52 ± 3.79	0.23 ± 0.006	0.1 ± 0.019	6.49 ± 0.071	5.66 ± 0.13	2935.13 ± 444.78	207.5 ± 474.99	38.71 ± 0.62	34 ± 1.11	
6861	<i>L. gibba</i>	Italy	606.61 ± 16.65	449.53 ± 106.79	0.23 ± 0.014	0.15 ± 0.024	6.77 ± 0.082	6.73 ± 0.3	3318.68 ± 91.34	1559.4 ± 189.92	40.24 ± 0.53	41.1 ± 1.88	
7532	<i>L. gibba</i>	Ireland	553.49 ± 13.45	119.05 ± 11.97	0.19 ± 0.006	0.08 ± 0.02	6.47 ± 0.096	4.61 ± 0.01	3162.63 ± 136.76	2200.15 ± 158.85	38.47 ± 0.51	27.43 ± 0.84	
7798	<i>L. gibba</i>	Peru	520.66 ± 34.78	96.6 ± 41.4	0.19 ± 0.017	0.09 ± 0.018	6.34 ± 0.2	4.51 ± 0.21	3165.2 ± 433.57	2586.17 ± 26.76	37.62 ± 1.09	26.6 ± 1.3	
8428	<i>L. gibba</i>	Switzerland	517.74 ± 4.6	416.69 ± 83.17	0.22 ± 0.012	0.12 ± 0.01	6.75 ± 0.052	4.77 ± 0.46	2890.52 ± 144.14	1199.06 ± 261	40.37 ± 0.41	35.32 ± 2.74	
8678	<i>L. gibba</i>	India	495.4 ± 19.33	441.77 ± 63.67	0.24 ± 0.005	0.1 ± 0.013	6.79 ± 0.043	6.15 ± 0.09	3362.92 ± 663.78	1956.1 ± 477.8	40.32 ± 0.35	37.23 ± 0.38	
9435	<i>L. gibba</i>	Albania	484.97 ± 64.64	206.26 ± 30.63	0.24 ± 0.002	0.09 ± 0.009	6.59 ± 0.209	5.2 ± 0.18	2196.53 ± 323.66	1470.67 ± 159.93	39.83 ± 1.1	31.6 ± 1.15	
9619	<i>L. gibba</i>	Albania	502.9 ± 16.62	405.83 ± 61.28	0.26 ± 0.007	0.13 ± 0.015	6.71 ± 0.094	6.6 ± 0.32	3641.85 ± 189.13	2181.83 ± 558.48	39.68 ± 0.47	39.87 ± 2.37	
7705	<i>L. gibba</i>	India	594.38 ± 19.35	275.07 ± 43.16	0.24 ± 0.005	0.07 ± 0.003	6.64 ± 0.026	3.41 ± 0.42	3816.33 ± 53.09	1297.97 ± 341.29	39.12 ± 0.19	20.51 ± 2.75	
7763	<i>L. gibba</i>	UK	589.05 ± 9.21	311.95 ± 44.1	0.18 ± 0.002	0.11 ± 0.023	6.57 ± 0.013	6.32 ± 0.37	4142.47 ± 21.47	1854.33 ± 165.6	38.48 ± 0.07	41.21 ± 1.75	
7796	<i>L. gibba</i>	Italy	372.35 ± 15.86	324.62 ± 22.6	0.2 ± 0.019	0.11 ± 0.001	6.01 ± 0.114	6.78 ± 0.3	4099 ± 288.96	1848.67 ± 241.15	35.02 ± 0.59	38.37 ± 2.48	
8703	<i>L. gibba</i>	Japan	546.34 ± 37.02	61.09 ± 37.6	0.25 ± 0.002	0.07 ± 0.01	6.79 ± 0.045	3.99 ± 0.25	3117.62 ± 96.55	1522.35 ± 105.69	40.46 ± 0.3	24.02 ± 1.61	

Appendix 2 – Poster Presentations

A) SRUK Annual General Assembly 2022 – Ponds to Pounds: Maximising the Potential of Duckweeds to Convert Nitrogen to Protein – Jul 3rd, 2022 – Oxford, United Kingdom



Ponds to Pounds: Maximising the Potential of Duckweeds to Convert Nitrogen to Protein.

Javier Espinosa-Montiel¹, Javier Hernandez-Allica², Alyssa Blachez³, Yongju Huang¹, Cathy Thomas², Steve McGrath², Cristina Barrero-Sicilia¹

¹ Clinical, Pharmaceutical & Biological Science Department. University of Hertfordshire ² Department of Sustainable Agriculture Sciences. Rothamsted Research ³ DryGro Ltd

Introduction.

Several studies have demonstrated the need to reduce the impact of meat and dairy production/ consumption to stop the climate change. Duckweeds are one of the most promising alternatives as sustainable protein source for feed and food. In optimum conditions, these tiny aquatic plants can yield more than 30 ton/ha/year with up to 40% of protein content in dry matter. To reach the optimum conditions with the lowest production cost, the source of nitrogen is the most important parameter to consider. In this work we investigated the effect of different nitrogen sources on duckweeds yield and protein content.

Materials and Methods.

Lemna japonica (named as DG8) and *Lemna gibba* (named as clone SD) clones were grown in a glasshouse with controlled temperature (21/18°C day/night) and light supplement (16h, LED), in containers with 20L of Rorison medium that was renewed every week. After 30 days, 5 g of fresh weight duckweed were transferred to individual trays of 22 x 16 cm. Three different N sources (nitrate, ammonium nitrate and urea-nitrate) were applied at 2 different N doses (4 and 12 mM N) making a total of 6 different N treatments (3 sources x 2 doses) with 3 replicates for 14 days. After 2 days the medium of each tray was topped up to compensate for evaporation and at day 7 the medium was renewed. After 14 days, the pH of the medium was measured and all the samples were collected, weighed for fresh weight, dried, milled and scanned by FT-MIR (Tensor II, Bruker). Total nitrogen (TN) and nitrate nitrogen (NO₃-N) were predicted using OPUS-QUANTII software (Bruker). Total protein % (TP) was calculated using the formula TP = (TN – NO₃-N) x 6.25.

Results.

The ammonium nitrate treatment showed a substantial decrease of the pH with both N doses at harvest (Figure1). At the same time, a decrease in the biomass production was observed for ammonium nitrate treatments at both N doses, although more significant in *L. gibba*, where the biomass production was more than 25 % less than the respective nitrate and urea-nitrate treatments (Figure2).

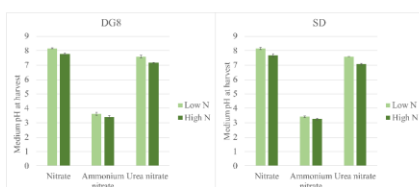


Figure 1. Medium pH data in DG8 and SD clone under different N source and concentration after 14 days treatment.

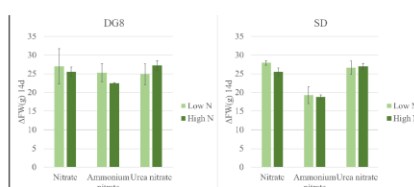


Figure 2. Growth rate in DG8 and SD clone under different N source and concentration after 14 days treatment.

The SD clone showed a higher NO₃-N accumulation than DG8, and for both clones, increasing the nitrate dose produced a significant increase of NO₃-N. The maximum NO₃-N level observed in the SD clone supplied with 12 mM nitrate (5614 mg NO₃-N/kg DW) would exceed the maximum NO₃-N level allowed by the EU for human consumption. Despite differences in NO₃-N, no significant effects of N sources were found in duckweed TN and TP % (see table above).

[N]	N source	Nitrate (%)		Total nitrogen (%)		Total protein (%)	
		DG8	SD	DG8	SD	DG8	SD
4 mM	Nitrate	0.23 ± 0.02	0.31 ± 0.02	5.33 ± 0.21	5.13 ± 0.09	31.82 ± 1.25	30.12 ± 0.64
	Ammonium nitrate	0.13 ± 0.01	0.11 ± 0.01	5.44 ± 0.15	4.86 ± 0.17	33.21 ± 0.96	29.67 ± 1.03
	Urea nitrate	0.11 ± 0.01	0.22 ± 0.03	5.32 ± 0.1	5.38 ± 0.07	32.51 ± 0.58	32.23 ± 0.45
12 mM	Nitrate	0.39 ± 0.04	0.56 ± 0.04	5.62 ± 0.08	5.41 ± 0.08	32.72 ± 0.52	30.29 ± 0.63
	Ammonium nitrate	0.23 ± 0.03	0.17 ± 0.02	5.92 ± 0.11	5.68 ± 0.1	35.59 ± 0.69	34.43 ± 0.53
	Urea nitrate	0.36 ± 0.02	0.37 ± 0.04	5.89 ± 0.14	5.84 ± 0.18	34.54 ± 0.87	34.19 ± 1.32

Conclusion.

These results show that the N source does not have a significant impact on the total protein concentration of representative duckweed species (i.e. *L. japonica* and *L. gibba*). Ammonium as a N source needs to be carefully managed, as it can affect duckweed growth. NO₃-N should be routinely analysed in duckweeds. Also, we propose Rorison medium for duckweed experiments regarding N uptake.

Acknowledgments.

This work is funded by European Research Development Fund (ERDF), Hertfordshire Local Enterprise Partnership's Single Local Growth Fund, for Hertfordshire Knowledge Exchange Partnership Project.



B) Sixth International Conference on Duckweed Research and Applications – FT-MIR-PLSR simultaneous determination of total nitrogen and nitrate in duckweeds - May 29th to Jun 1st, 2022 – Gatersleben, Germany



FT-MIR-PLSR simultaneous determination of total nitrogen and nitrate in duckweeds

Javier Espinosa-Montiel¹, Javier Hernandez-Allica², Alla Mashanova¹, Alyssa Blachez³, Stephan Haefele², Cristina Barrero-Sicilia¹, Steve McGrath²

¹Clinical, Pharmaceutical & Biological Science Department, University of Hertfordshire, AL109AB, UK; ²Department of Sustainable Agriculture Sciences, Rothamsted Research, AL52JQ, UK; ³ CO2i Ltd (DryGro), HP178HE, UK.

Introduction

From both nutritional and sanitary perspectives, it is necessary to know the quality and safety of duckweeds as a novel protein-rich source by determining total nitrogen (TN) and nitrate (NO₃-N). An important constraint for the routine analysis of TN and NO₃-N is the high cost of analysis. Fourier Transformed Mid Infra-Red Spectroscopy (FT-MIR) has advanced rapidly as a new, fast, easy to operate, inexpensive and reliable method of analysis in plant science, to a great extent due to the introduction of chemometric predictive modelling using regression analysis and typically Partial Least Squares (PLS) algorithms. The objective of the present research was to investigate the feasibility of simultaneous determination of TN and NO₃-N in duckweeds by means of FT-MIR-PLSR.

Materials and Methods

A set of duckweed samples obtained from both field (Figure 1) and controlled environment (Figure 2A) was prepared to obtain the widest variation possible in TN and NO₃-N content. All the samples were dried, milled and analysed by both “reference” methods (i.e. Dumas combustion with LECO CN628 for TN and salicylic nitration with spectrophotometric determination at λ₄₁₀ for NO₃-N), and by FT-MIR-PLSR (Figure 2B; Tensor II and OPUS-QUANT II software, Bruker).

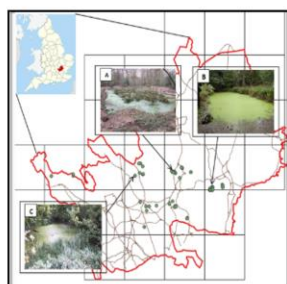


Figure 1. Ponds with duckweed in Hertfordshire county in United Kingdom.

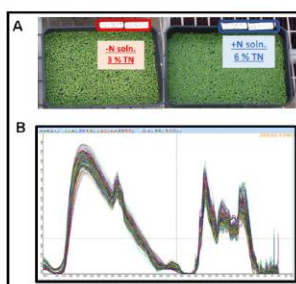


Figure 2. A) Duckweeds grown in greenhouse with low nitrogen (red) and high nitrogen nutrient solution (blue). B) Raw FT-MIR spectra of 155 duckweed samples.

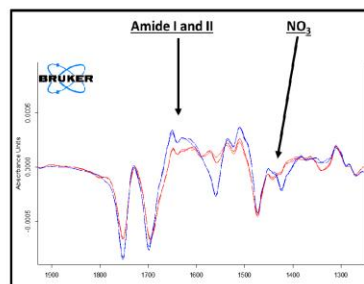


Figure 3. Amide and NO₃-N peak assignment in processed spectra of duckweed samples taken from trays in fig. 2A. High N (blue line) and low N (red line).

Results

Corrections of the raw spectra were made using the first derivative, with 17 smoothing points using the Savitsky–Golay algorithm. Assessment of the predictive performance of the chemometric models was made with the calculation of the coefficient of determination (R²), which gives the percentage of variance present in the true component values and is reproduced in the prediction; the Root Mean Squared Errors of Cross Validation (RMSECV); and the Residual Prediction Deviation for the rank (RPD = SD/SECV), which allows comparison of model performance across different data sets (See values in the Table below).

	Number of samples	Interval	Mean	Median	Rank	R ²	RMSECV	RPD
TN (%)	155	0.77 – 6.62	3.72	3.60	6	94.66	0.37	4.33
NO ₃ -N (%)	73	0.03 – 0.59	0.20	0.20	8	92.29	0.31	3.61

Conclusion

These results indicate that FT-MIR is a reliable technique to simultaneously predict the content of TN and NO₃-N in duckweeds (Figure 3). With this method, the cost of analysis is reduced dramatically allowing an affordable routine analysis of both TN and nitrate. This method could also allow to a more accurate nitrogen to protein conversion calculation in duckweeds. We propose the standardization of FT-MIR as the routine method of analysis for TN and NO₃-N in duckweeds.

This work was funded by European Research Development Fund for Agri-Tech Research Innovation Accelerator (AgRIA-CO2IRP10297-24).



C) Sixth International Conference on Duckweed Research and Applications – Biomass, protein and nitrate accumulation in duckweeds supplied with 3 different sources of nitrogen - May 29th to Jun 1st, 2022 – Gatersleben, Germany



Biomass, protein and nitrate accumulation in duckweeds supplied with 3 different sources of nitrogen

Javier Espinosa-Montiel¹, Javier Hernandez-Allica², Alyssa Blachez³, Yongju Huang¹, Cathy Thomas², Steve McGrath², Cristina Barrero-Sicilia¹

¹Clinical, Pharmaceutical & Biological Science Department, University of Hertfordshire, AL109AB, UK; ²Department of Sustainable Agriculture Sciences, Rothamsted Research, AL52JQ, UK; ³ CO2i Ltd (DryGro), HP178HE, UK.

Introduction

The selection of the nitrogen (N) source for duckweed cultivation can have a direct impact on productivity. Our objective was to investigate the effect of 3 different nitrogen sources (nitrate, ammonium nitrate and urea-nitrate) on the biomass, total protein % and nitrate content of 2 representative duckweed species (i.e. *Lemna japonica* and *Lemna gibba*).

Materials and Methods

Lemna japonica (clone 7868 RDSC Collection) was provided by DryGro Ltd and named as DG8. *Lemna gibba* was obtained from a local pond in Harpenden, (Hertfordshire, UK; 51.807793, -0.33942981) and named as clone SD. Both clones were grown in a glasshouse with controlled temperature (21/18 °C day/night) and light supplement (16h, LED), in containers with 20 L of Rorison medium that was renewed every week. After 30 days, 5g of fresh weight duckweed were transferred to individual trays of 22 x 16 cm. Three different N sources (nitrate, ammonium nitrate and urea-nitrate) were applied at 2 different N doses (4 and 12 mM N) making a total of 6 different N treatments (3 sources x 2 doses) with 3 replicates for 14 days. After 2 days the medium of each tray was topped up to compensate for evaporation and at day 7 the medium was renewed. After 14 days, the pH of the medium was measured and all the samples were collected, weighed for fresh weight, dried, milled and scanned by FT-MIR (Tensor II, Bruker). Total nitrogen (TN) and nitrate nitrogen (NO₃-N) were predicted using OPUS-QUANT II software (Bruker). Total protein % (TP) was calculated using the formula TP = (TN – NO₃-N) x 6.25.

Results

The ammonium nitrate treatment showed a substantial decrease of the pH with both N doses at harvest (Figure 1). At the same time, a decrease in the biomass production was observed for ammonium nitrate treatments at both N doses, although more significant in *L. gibba*, where the biomass production was more than 25% less than the respective nitrate and urea-nitrate treatments (Figure 2).

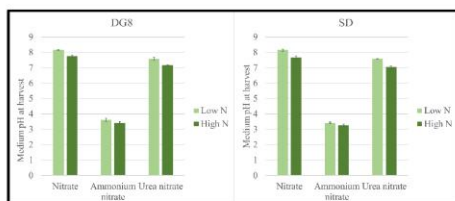


Figure 1. Medium pH data in DG8 and SD clone under different N source and concentration after 14 days treatment.

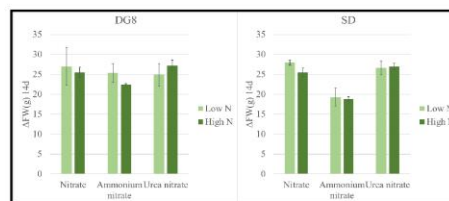


Figure 2. Medium pH data in DG8 and SD clone under different N source and concentration after 14 days treatment.

The SD clone showed a higher NO₃-N accumulation than DG8, and for both clones, increasing the nitrate dose produced a significant increase of NO₃-N. The maximum NO₃-N level observed in the SD clone supplied with 12mM nitrate (5614 mg NO₃-N/kg DW) would exceed the maximum NO₃-N level allowed by the EU for human consumption. Despite differences in NO₃-N, no significant effects of N sources were found in duckweed TN and TP % (see table above).

		NO ₃ -N				TN				Total Protein (TP)			
		DG8		SD		DG8		SD		DG8		SD	
		Average	Std. dev.	Average	Std. dev.	Average	Std. dev.	Average	Std. dev.	Average	Std. dev.	Average	Std. dev.
Low N (4 mM)	Nitrate	0.23	0.02	0.31	0.02	5.33	0.21	5.13	0.09	31.82	1.25	30.12	0.64
	Ammonium nitrate	0.13	0.01	0.11	0.01	5.44	0.15	4.86	0.17	33.21	0.96	29.67	1.03
	Urea nitrate	0.11	0.01	0.22	0.03	5.32	0.10	5.38	0.07	32.51	0.58	32.23	0.45
High N 12 mM	Nitrate	0.39	0.04	0.56	0.04	5.62	0.08	5.41	0.08	32.72	0.52	30.29	0.63
	Ammonium nitrate	0.23	0.03	0.17	0.02	5.92	0.11	5.68	0.10	35.59	0.69	34.43	0.53
	Urea nitrate	0.36	0.02	0.37	0.04	5.89	0.14	5.84	0.18	34.54	0.87	34.19	1.32

Conclusion

These results show that the N source does not have a significant impact on the total protein concentration of representative duckweed species (i.e. *L. japonica* and *L. gibba*). Ammonium as an N source needs to be carefully managed, as it can affect duckweed growth. NO₃-N should be routinely analysed in duckweeds. Also, we propose Rorison medium for duckweed experiments regarding N uptake.

This work is funded by European Research Development Fund (ERDF), Hertfordshire Local Enterprise Partnership's Single Local Growth Fund, for Hertfordshire Knowledge Exchange Partnership Project.



D) LMS Annual Research Conference 2021 – Unlocking rapid, inexpensive total nitrogen determination in *Lemna* using FTIR spectroscopy and PLSR analysis. – Jun 21st, 2021 – Hatfield, United Kingdom

University of Hertfordshire **UH**

Agriculture and Geography Department

Unlocking rapid, inexpensive total nitrogen determination in *Lemna* using FTIR spectroscopy and PLSR analysis.

Espinosa-Montiel, J.¹, Hernandez-Allica, J.², Mashanova, A.¹, Huang, Y.¹, Blachez, A.³, McGrath, S.P.², Barrero-Sicilia, C.¹.

¹School of Life and Medical Sciences, University of Hertfordshire, UK; ²Rothamsted Research, UK; ³DryGro, UK.

Introduction: Kjeldahl and Dumas methods are the standard analytical procedures for total nitrogen (TN) determination in food and plant samples. However, these methods have a number of disadvantages, such as the inability to measure actual protein, a big sample amount is needed and are long and complex methods (Tomé *et al.*, 2019). In this work, Fourier Transform Infrared (FTIR) was investigated as an alternative to traditional total nitrogen measurement methods using duckweed.

Materials and methods: A set of 155 duckweed samples and 7 plant certified standard samples were measured with Dumas method using a LECO CN628 Combustion Analyser. These samples were also measured with Bruker's benchtop TENSOR II FTIR spectrometer. Then, a calibration model was built up by Partial Least Squares Regression (PLSR) analysis.

Results: As shown in Figure 1 the samples measured showed a very wide distribution of TN values and the correlation coefficient between the Dumas combustion and FTIR methods was 0.948 and 0.9729 for the calibration and validation (Figure 2). The method was done with an optimum rank of 6 factors with a validation RPD of 4.33 and a bias of 0.006.

Figure 1: TN distribution of the samples measured by Dumas Combustion method.

Figure 2: FTIR cross validation for TN against Dumas Combustion method.

Conclusions: FTIR is an accurate and inexpensive method for total nitrogen measurements in duckweed samples.

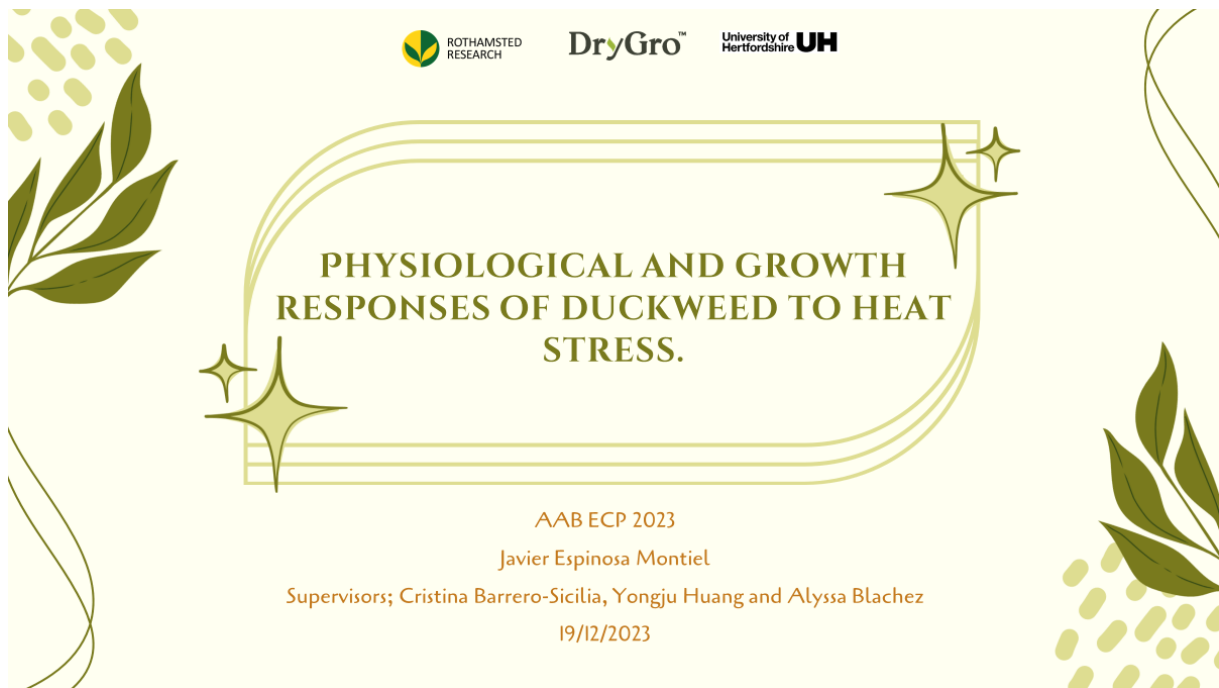
References: Tomé, D., Cordella, C., Dib, O., & Péron, C. (2019). Nitrogen and protein content measurement and nitrogen to protein conversion factors for dairy and soy protein-based foods: a systematic review and modelling analysis. In *Food and Agriculture Organization of the United Nations* (14–17).

Appendix 3 – Presentations

A) II Jornadas Jóvenes Investigadores Barrenos – Inspirando a las Nuevas Generaciones – Dec 5th, 2024 – Los Barrios, Spain



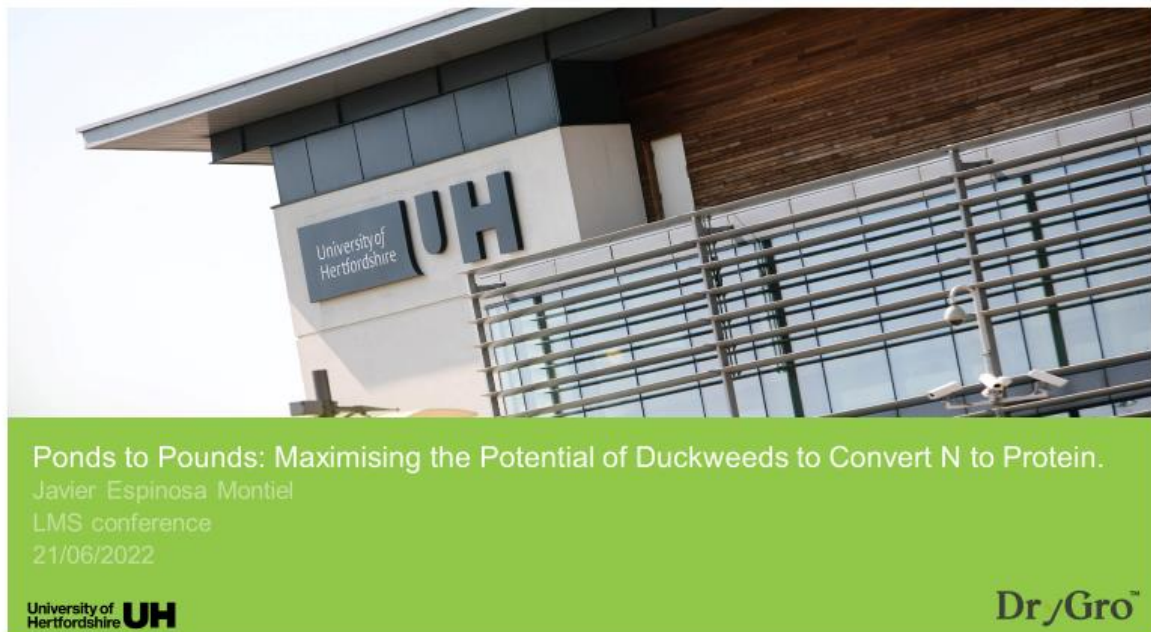
**B) Association of Applied Biologists Early Career Professional Skills and Science Workshop –
Physiological and Growth Responses of Duckweed to Heat Stress – Dec 18th and 19th, 2023 –
University of Leicester, United Kingdom**



C) I Jornada Jóvenes Investigadores Barreños – Inspirando a las Nuevas Generaciones – Oct 30th, 2023 – Los Barrios, Spain



D) LMS Annual Research Conference 2022 – Ponds to Pounds: Maximising the Potential of Duckweeds to Convert N to Protein. – Jun 21st, 2022 – Hatfield, United Kingdom



F) University of Hertfordshire Postgraduate Research Conference 2022 – Genetic Control of *Lemna* Growth Rate and Protein Content. – Feb 7th, 2022 – Hatfield, United Kingdom

GENETIC CONTROL OF *LEMNA* GROWTH RATE AND PROTEIN CONTENT.

PG SEMINARS

JAVIER ESPINOSA-MONTIEL

7TH FEBRUARY 2022



G) University of Hertfordshire Postgraduate Research Conference 2021 – Genetic Control of *Lemna* Growth Rate and Protein Content. – Jul 12th, 2021 – Hatfield, United Kingdom



Genetic control of *Lemna* growth rate and protein content.

PG seminars

Javier Espinosa-Montiel

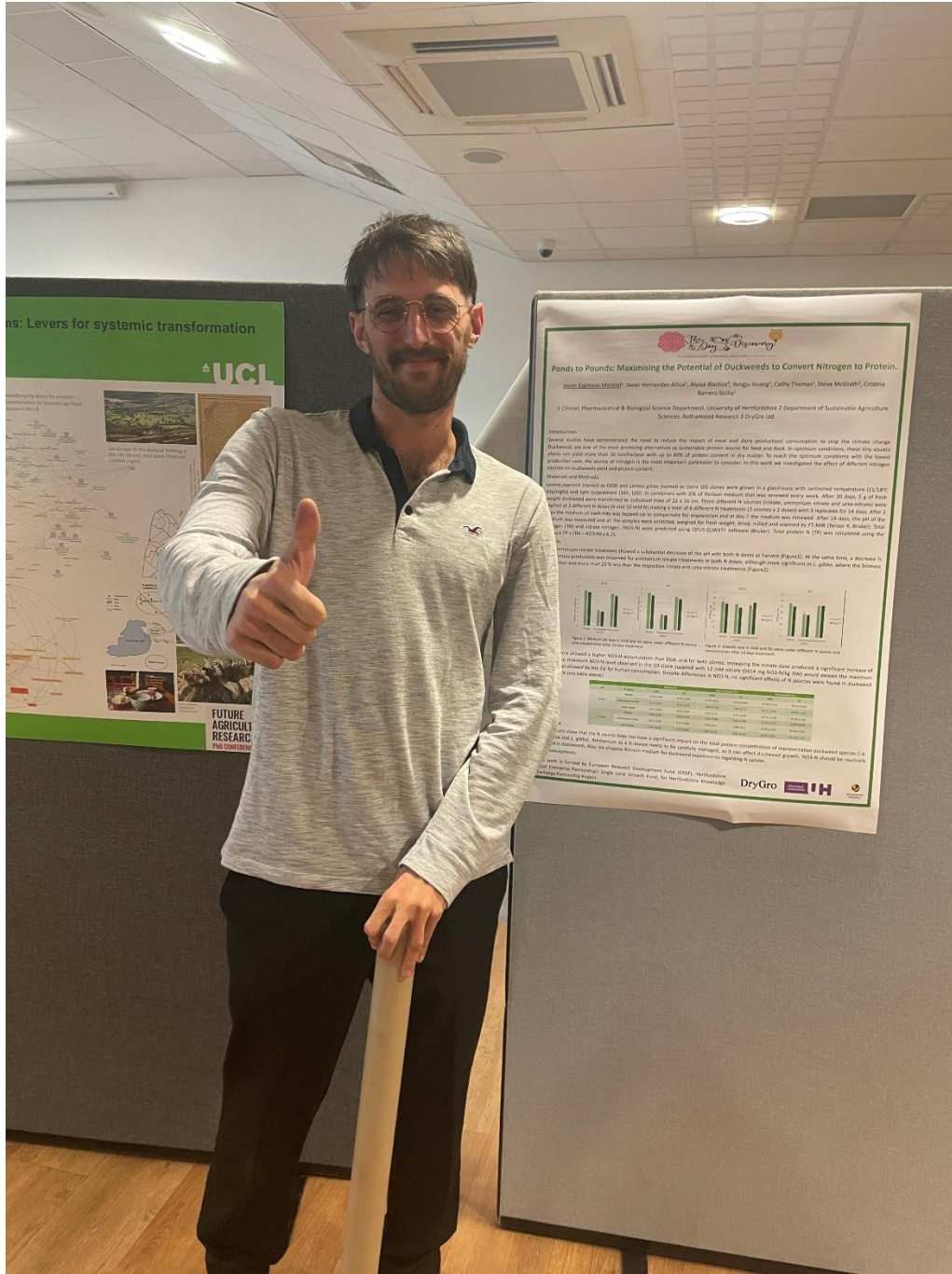
12th July 2021

University of Hertfordshire **UH**

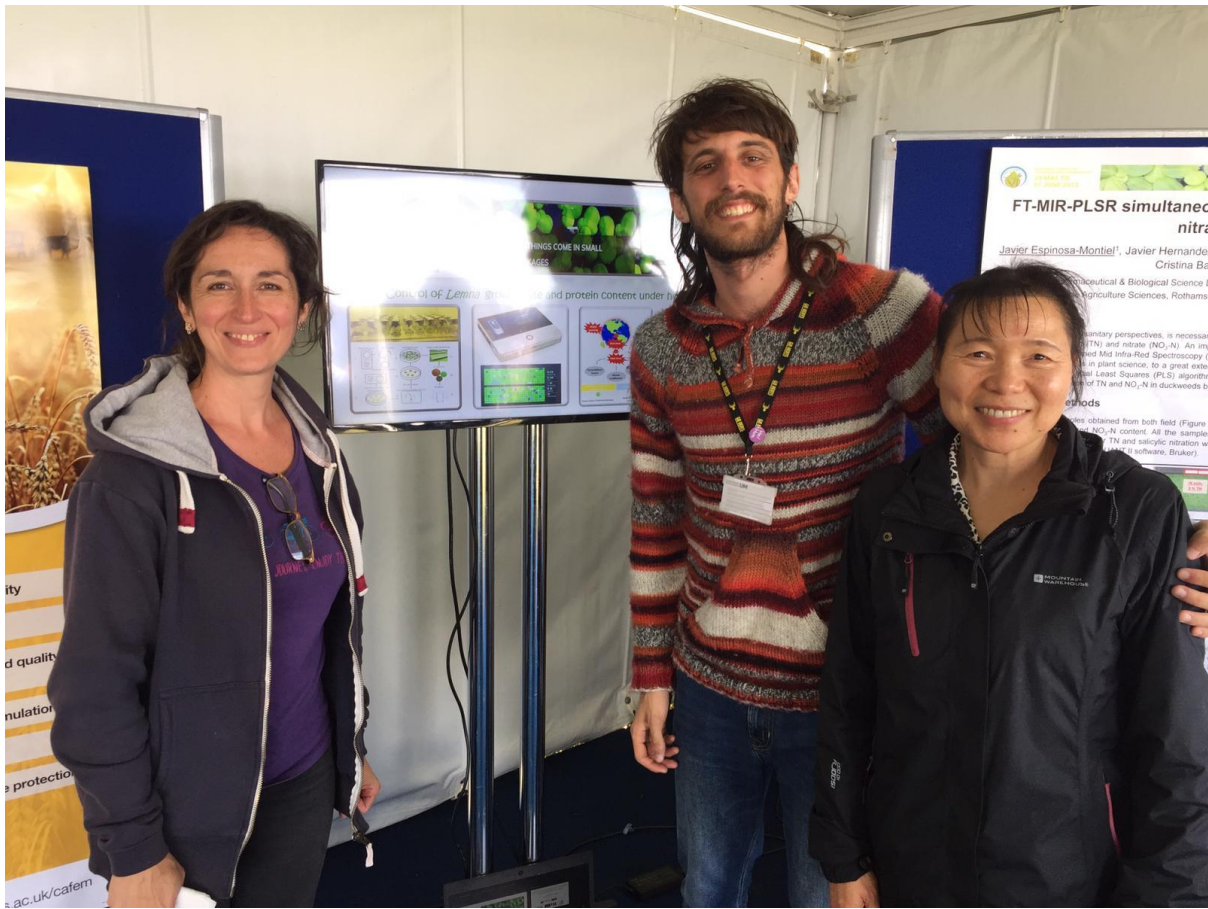
DryGro™

Appendix 4 – Events.

A) Future Agricultural Researchers PhD Conference 2023 – Nov 14th, 2023 – Exeter, United Kingdom



B) Cereals the Arable Event – Jun 8th, 2022 – Duxford, United Kingdom



C) Sixth International Conference on Duckweed Research and Applications – May 29th to Jun 1st, 2022 – Gatersleben, Germany



Publications

Fat Duckweed (*Lemna gibba*) Might Be Much More Widespread in Hertfordshire Than Previously Thought. Status: Published Co-Authors: Alla Mashanova, Javier Espinosa-Montiel, Cristina Barrero-Sicilia. Journal: Transactions of the Hertfordshire Natural History Society. 54 (1) 2022

Fat Duckweed (*Lemna gibba*) might be much more widespread in Hertfordshire than previously thought

Alla Mashanova, Javier Espinosa Montiel, Cristina Barrero Sicilia

Fat Duckweed, *Lemna gibba*, is one of three native species of duckweeds occurring in Hertfordshire. It is referred to as 'cover very common' by James (2009). According to iRecord, records of duckweeds in Hertfordshire are sparse with most records of duckweeds referring to Common Duckweed, *Lemna minor*. As checked on 8/02/20, from 29 accepted records of *Lemna*, 16 referred to *L. minor*, four to *L. trisulca* (three of them submitted by Alla Mashanova - AM), two to *L. minuta* and one to an unidentified *Lemna*.

The lack of Fat Duckweed records is likely to be attributed to difficulties in distinguishing it from Common Duckweed. Identifying Fat Duckweed in its 'fat' state, with thalli (leaves) swollen on the underside (Snee, 2019; OPAL, 2014) is straightforward but when it is 'flat' it is not readily distinguishable from Common Duckweed (Lansdown, Runsey and Crouch, 2019; Lansdown and Runsey, 2020). According to Polard & Clement (2009), Fat Duckweed is likely to be in its 'fat' state during the flowering season, it is advisable not to record duckweeds outside the growing season to avoid confusion or, alternatively, to grow plants to allow clearer investigation of their morphology.

In our experience, Fat Duckweed would not necessarily become 'fat' even when it is grown under favourable conditions, but there is a set of features distinguishing it from other duckweeds (Crouch and Runsey 2020; BSH 2016). Two readily observable features are the asymmetrical shape of the leaves and large air-spaces called lacunae (Figure 1). Another useful feature is the number of veins, as they are only visible after removal of chloroplast. We used immersion in alcohol to bleach thalli. Fat Duckweed has five veins (Figure 2). Common Duckweed has three and Least Duckweed has one. When thalli start to develop they have only one vein and so, seeing fewer than five veins does not exclude Fat Duckweed (pers. communication R. Lansdown).

As part of a bigger project studying properties of duckweeds as a potential protein supplement, we checked 22 sites (mostly ponds) in Hertfordshire between September 2020 and March 2021. Duckweeds were present at 37 localities where samples were taken (Figure 3). All samples were screened initially and



Figure 1. Asymmetrical shape of senescing thallus of *Lemna gibba* from Huntingly Park and features visible in a thallus from Verdunians Park (St. Albans). Scale bars were estimated from different images taken at the same magnification.

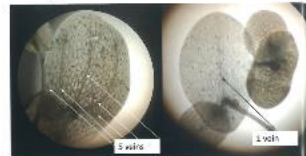


Figure 2. Thallus of *Lemna gibba* with chloroplast removed showing 5 veins (left) and 1 vein (right). Lacunae, which are visible in both images, help to identify the plant on the right as *Lemna gibba*. Length of the thallus are approximately 3.5 mm in the left image and 2.5 mm in the right image.

then, locat, partly at the University of Hertfordshire under controlled environment conditions and partly at AM's residences, to see whether individual plants would develop better to ease identification. In a few cases more samples were taken if the initial samples were lost due to senescing (aging). Fat Duckweed was convincingly identified in 31 samples suggesting that it is a common and widespread species in Hertfordshire.

We could allocate the name of Fat Duckweed when we saw the features of this species, but we could not identify Common Duckweed on the grounds of not seeing the features of Fat Duckweed. Therefore, we cannot compare distribution of these two species.

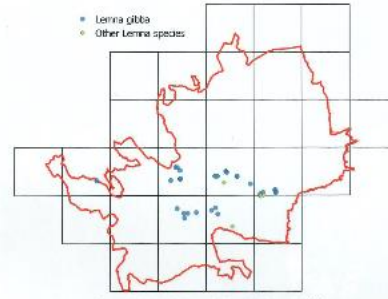


Figure 3. Map of sampling locations where any species of duckweeds were found. Locations where *Lemna gibba* was confirmed are marked as circles and other *Lemna* species as diamonds.

In a few cases, when duckweeds were left to grow, Fat Duckweed features became obvious after a few days even when the sample looked like Common Duckweed to begin with. It is very likely that a mixture of both species was present in most samples. Further molecular study is planned at the University of Hertfordshire to improve understanding of differences in distribution between Fat Duckweed and Common Duckweed. In this study, sampling was restricted to Central Hertfordshire. A wider area will be sampled in the future.

Acknowledgements. We thank Richard Lansdown for advice on identification of duckweeds, Ian Denholm for helpful discussions, a call for information within Heris Flora Group, arranging access to sites and commenting on the manuscript, and all naturalists who alerted us to duckweed presence in their local water bodies.

References
BSBI. (2016). *Lemna* Crb. Available at: https://bsbi.org/wp-content/uploads/dlm_uploads/Lemna_Crb.pdf [Accessed: 25 January 2022].
Crouch, H. & Runsey, F. (2019). Introduction to Duckweeds. Available at: https://bsbi.org/wp-content/uploads/dlm_uploads/Introduction-to-Duckweeds-Holma-Crouch.pdf [Accessed: 25 January 2022].

James, T.J. (2009). *Flora of Hertfordshire*. Welwyn Garden City: Hertfordshire Natural History Society.
Lansdown, R. and Runsey, F. (2020). Yes it is *Lemna gibba*, even if it is flat! Available at: <http://pondslawer.co.uk/nature/lemna-ohm-lansdown-runsey.jpg> [Accessed: 25 January 2022].
Lansdown, R., Runsey, F. & Crouch, H. (2019) ... yes – it is *Lemna gibba*, even if it is flat! Tackling common Duckweed dilemmas. Available at: <http://pondslawer.co.uk/nature/lemna-2019-bsh-acce-lansdown-runsey-crouch.pdf> [Accessed: 25 January 2022].
OPAL (2014). Guide to Duckweeds. Available at: <https://www.ngps.org.uk/media/10/petal-college/research-centre-research-ops/opal/water-survey-duckweed-guide-A5-2014.pdf> [Accessed: 25 January 2022].
Palani, J. and Clement, E.J. (2009). *The Vegetative Key to the British Flora*. Southampton: J. Palani in association with Botanical Society of the British Isles.
Runsey, F. Some under-recorded or misidentified taxa https://bsbi.org/wp-content/uploads/dlm_uploads/BSBI_RC_2016_FIR.pdf [25 January 2022].
Snee, C.A. (2019). *New Flora of the British Isles* (4th ed.). Mistlewood Green, Suffolk: C. and M. Floristics.